



Durham E-Theses

Functional soil release polymers for cellulosic surfaces

LOVATO, TATIANA

How to cite:

LOVATO, TATIANA (2016) *Functional soil release polymers for cellulosic surfaces*, Durham theses, Durham University. Available at Durham E-Theses Online: <http://etheses.dur.ac.uk/11572/>

Use policy

The full-text may be used and/or reproduced, and given to third parties in any format or medium, without prior permission or charge, for personal research or study, educational, or not-for-profit purposes provided that:

- a full bibliographic reference is made to the original source
- a [link](#) is made to the metadata record in Durham E-Theses
- the full-text is not changed in any way

The full-text must not be sold in any format or medium without the formal permission of the copyright holders.

Please consult the [full Durham E-Theses policy](#) for further details.

Functional Soil Release Polymers for Cellulosic Surfaces

A thesis submitted for the degree of

Doctor of Philosophy

by

Tatiana Lovato



Department of Chemistry

Durham University

February 2016

Functional soil release polymers for cellulosic surfaces

Abstract

Soil release polymers (SRPs) are additives components of washing detergents for synthetic fibres, as they are effective in removing stains from the fabric surface and in preventing re-deposition of the stain during a wash cycle. Currently, there are no SRPs which can be used to efficiently perform the same function for natural cellulose based textiles. In this work, the synthesis of functional carbohydrate-based materials for application as potential SRPs for cellulosic surfaces was discussed. Two strategies were developed, exploiting the affinity of polysaccharides to adsorb over cellulose surfaces. The first strategy involved the synthesis of a co-polymer between poly(ethylene glycol diacrylate) (PEGDA), ethylenediamine and maltose, through a three step procedure. During the first step, the co-polymer backbone was synthesised through the co-polymerisation of PEGDA with *N*-Boc-ethylenediamine in bulk at room temperature. Then, the second amine functionality was de-protected and reacted with maltose to yield the desired co-polymer. The structure was confirmed through ^1H and ^{13}C NMR spectroscopy in solution, and through diffusion studies. The second strategy aimed to tune the strong affinity of carboxymethyl cellulose (CMC) for cellulose surfaces through grafting of poly(ethylene glycol) (PEG) chains. A variety of co-polymers were synthesised comprising different proportions of PEG bound. The co-polymers were characterised through a series of techniques, such as ^{13}C solid state NMR, ^1H gel state NMR, pulse field gradient NMR spectroscopy (PFG NMR) and size exclusion chromatography (SEC) in DMF. The potential of the co-polymers for application as SRPs was evaluated through soil release and whiteness tests. Furthermore, a preliminary study on the adsorption of two fluorescently labelled CMC-g-PEG co-polymers over cotton surfaces was conducted by means of fluorescence measurement.

Table of Contents

List of Figures	i
List of Schemes	viii
List of Tables	x
List of Equations	xii
List of Abbreviations	xiii
Statement of Copyright	xvi
Acknowledgements	xvii
Thesis overview	xviii
1. Introduction	1
1.1. Cellulose: an important material	1
1.2. Functional polymers for cellulose modification	4
1.2.1. <i>Cellulosic functional polymers</i>	7
1.2.1.1. Carboxymethyl cellulose	8
1.2.2. <i>Oligo- and polysaccharide functional polymers</i>	15
1.2.2.1. Xyloglucan	15
1.3. Polymeric additives for laundry detergents	19
1.4. Aims and objectives	22
1.5. References	24

2. Synthesis of a soil release polymer from poly(ethylene glycol)diacrylate and maltose	28
2.1. Introduction	28
2.2. Experimental Section	32
2.2.1. <i>Materials</i>	32
2.2.2. <i>Analysis</i>	32
2.2.2.1. ^1H , ^{13}C and DOSY NMR spectroscopy	32
2.2.2.2. Size exclusion chromatography (SEC)	33
2.2.3. <i>Model reactions with hexylamine</i>	33
2.2.3.1. Model reactions with PEGDAs and hexylamine in bulk	33
2.2.3.2. Model reactions with PEGDAs and hexylamine in DMSO	34
2.2.3.3. Model reaction with PEGDA and hexylamine in DCM	35
2.2.4. <i>Synthesis of a PEGDA-ethylenediamine-maltose co-polymer</i>	36
2.2.4.1. Polymerization of PEGDA with N-Boc-ethylenediamine in DCM	36
2.2.4.2. Polymerization of PEGDA with N-Boc-ethylenediamine in bulk	36
2.2.4.3. De-protection of PEGDA-N-Boc-ethylenediamine poly(β -amino ester) co-polymer	37
2.2.4.4. Reductive amination between de-protected poly(β -amino ester) co-polymer and maltose	37
2.3. Results and Discussion	39
2.3.1. <i>Introduction</i>	39
2.3.2. <i>Model Michael addition reactions with hexylamine</i>	42
2.3.2.1. Polymerisation in bulk	43
2.3.2.2. Polymerisation in Solution	46

2.3.3.	<i>Synthesis of a PEGDA-ethylenediamine-maltose co-polymer</i>	49
2.3.3.1.	Polymerisation in DCM	52
2.3.3.2.	Reaction in bulk	55
2.3.3.3.	De-protection of PEGDA-N-Boc- ethylenediamine poly(β -amino ester) co-polymer	58
2.3.3.4.	Reductive amination between de-protected poly(β -amino ester) co-polymer and maltose	63
2.4.	Conclusions	71
2.5.	References	73
2.6.	Appendix A	74
3.	Functionalization of carboxymethyl cellulose	75
3.1.	Introduction	75
3.2.	Experimental section	78
3.2.1.	<i>Materials</i>	78
3.2.2.	<i>Analysis</i>	78
3.2.2.1.	Potentiometric titration	78
3.2.2.2.	^{13}C solid state NMR spectroscopy	79
3.2.2.3.	PFM NMR spectroscopy and ^1H gel state NMR spectroscopy	79
3.2.2.4.	^{13}C and ^1H NMR spectroscopy in solution	80
3.2.2.5.	Size exclusion chromatography (SEC)	80
3.2.2.6.	Fluorescence spectroscopy	81
3.2.3.	<i>Synthesis of poly(ethylene glycol) methyl ether bromide</i>	81
3.2.4.	<i>Synthesis of poly(ethylene glycol) methyl ether azide</i>	83

3.2.5.	<i>Synthesis of amino poly(ethylene glycol) methyl ether</i>	84
3.2.6.	<i>Synthesis of CMC-g-PEG co-polymers</i>	86
3.2.7.	<i>Labelling of CMC and CMC derivative</i>	89
3.3.	Results and Discussion	90
3.3.1.	<i>Synthesis of amino poly(ethylene glycol) methyl ether</i>	90
3.3.2.	<i>Synthesis of CMC-g-PEG co-polymers</i>	99
3.3.2.1.	Characterization of sodium carboxymethyl cellulose (CMC)	101
3.3.2.2.	Synthesis of CMC-g-PEG co-polymers	109
3.3.2.3.	Solid state NMR spectroscopy	117
3.3.2.4.	Size Exclusion Chromatography (SEC)	119
3.3.2.5.	Gel state NMR spectroscopy	123
3.3.2.6.	Pulse field gradient NMR analysis (PFG NMR)	128
3.3.3.	<i>Fluorescent Labelling of CMC-g-PEG co-polymers</i>	138
3.4.	Conclusions	142
3.5.	References	144
3.6.	Appendix B	146
4.	Evaluation of the washing properties of CMC-g-PEG co-polymers	150
4.1.	Introduction	150
4.2.	Experimental section	154
4.2.1.	<i>Material</i>	154
4.2.2.	<i>Instruments</i>	154
4.2.3.	<i>Analysis</i>	155

4.2.3.1.	Fluorescence Microscope -----	155
4.2.3.2.	¹³ C solid state NMR analysis-----	155
4.2.4.	<i>Soil release test</i> -----	155
4.2.5.	<i>Whiteness test</i> -----	156
4.2.6.	<i>Quantitative analysis of deposition using fluorescently labelled CMC</i>	157
4.2.6.1.	1% CMC-g-PEG co-polymer in weight in the laundry detergent composition -----	158
4.2.6.2.	0.5% CMC-g-PEG co-polymer in weight in the laundry detergent composition-----	159
4.2.6.3.	0.3% CMC-g-PEG co-polymer in weight in the laundry detergent composition-----	159
4.3.	Soil release and anti-redeposition properties of the CMC-g-PEG co- polymers-----	160
4.3.1.	<i>Possible shortcomings of soil release test and whiteness test</i> -----	163
4.3.2.	<i>Soil release and whiteness properties of CMC-g-PEG_2K_23.7, CMC-g- PEG_2K_9.5, CMC-g-PEG_2K_42.8 and CMC-g-PEG_5K_19.0</i> -----	165
4.3.3.	<i>Soil release and whiteness properties of CMC-g-PEG_2K_50.4, CMC-g- PEG_2K_56.1, CMC-g-PEG_5K_51.1 and CMC-g-PEG_5K_55.6</i> -----	172
4.3.4.	<i>Soil release and whiteness properties of CMC-g-PEG_2K_62.5, CMC-g- PEG_5K_63.7, CMC-g-PEG_10K_84.5, CMC-g-PEG_10K_85.8 and CMC-g- PEG_10K_76.5</i> -----	177
4.4.	Quantitative analysis of deposition using fluorescently labelled CMC-- -----	184
4.4.1.	<i>Fluorescence measurements</i> -----	186
4.4.2.	<i>Fluorescence microscopy</i> -----	194

4.4.3.	<i>¹³C solid state NMR spectroscopy analysis</i>	198
4.5.	Conclusions	200
4.6.	References	202
5.	Conclusions and future works	203
5.1.	Conclusions	203
5.2.	Future Work	209
5.3.	References	211

List of Figures

Figure 1.1. Structure of cellulose backbone. -----	4
Figure 1.2. H-bond network in cellulose backbone. -----	5
Figure 1.3. Commercial derivatives of cellulose. -----	7
Figure 1.4. Structure of carboxymethyl cellulose (CMC) sodium salt.-----	8
Figure 1.5. Commercial synthesis of carboxymethyl cellulose ^[31] . -----	9
Figure 1.6. Variation of the conformation of the CMC-g-PEG co-polymer adsorbed in water over a cellulosic surface in response to a change of pH of the solution. Above pH 4.5 (A) the conformation of CMC-g-PEG is swollen, as a result of electrostatic repulsive interactions between chains. Whilst below pH 4.5 (B) the conformation is contracted, due to the lack of charges. -----	13
Figure 1.7. Multi-step modification of a cellulosic surface through adsorption of an azide-modified CMC backbone (blue, picture A) and subsequent CuAAC click reaction with an alkyne derivative (yellow, picture B) to yield a functionalised cellulosic surface (C) ^[39] .-----	14
Figure 1.8. Structure of xyloglucan extracted from tamarind seed -----	16
Figure 1.9. Mechanism of action of a SRP. During the first wash cycle (top picture) the SRP additive (purple) contained in the laundry detergent is adsorbed over the textile surface (blue), forming a protective layer. Upon deposition of the stain (middle picture), the stain (brown) cannot penetrate into the fabric (blue) due to the presence of the SRP layer (purple). During the subsequent wash cycle (bottom picture) the stain (brown) is removed together with the SRP protective layer (purple).-----	20
Figure 1.10. Structure of PET-POET soil release polymer for polyester fibres.--	20
Figure 2.1. Chemical structure of cotton fibre. -----	29

Figure 2.2. Structure of maltose.-----	29
Figure 2.3. Structure of the SRP designed to interact with cotton fibre. The backbone (blue) is constituted from poly(ethylene glycol)diacrylate (PEGDA) units. The sugar moiety (red) is connected to the backbone via ethylenediamine linkers (black).-----	30
Figure 2.4. Structure of A) N-Boc-ethylenediamine and B) Fmoc-ethylenediamine.-----	50
Figure 2.5. Comparison between ^1H NMR spectra of PEGDA-N-Boc-ethylenediamine poly(β -amino ester) co-polymer synthesised in DCM and the starting materials N-Boc-ethylenediamine and PEGDA. Spectra recorded at 700 MHz in CDCl_3 .-----	54
Figure 2.6. Comparison between ^1H NMR spectra of PEGDA-N-Boc-ethylenediamine poly(β -amino ester) co-polymer synthesised in bulk and the starting materials N-Boc-ethylenediamine and PEGDA. Spectra recorded at 700 MHz in CDCl_3 .-----	57
Figure 2.7. Enlargement of ^1H NMR spectrum of PEGDA-N-Boc-ethylenediamine poly(β -amino ester) co-polymer (Figure 2.6).-----	59
Figure 2.8. ^1H NMR spectrum of PEGDA-N-Boc-ethylenediamine co-polymer end capped with N-Boc-ethylenediamine. Spectrum recorded at 700 MHz in CDCl_3 .-----	60
Figure 2.9. Progress of the de-protection of PEGDA-N-Boc-ethylenediamine co-polymer with TFA. Spectra recorded after (b) 3 hours, (c) 24 hours, (d) 48 hours and (e) 72 hours in CDCl_3 (a-b-c) and D_2O (d) at 700 MHz.-----	62
Figure 2.10. Equilibrium between open ring and closed ring forms of maltose in solution.-----	64
Figure 2.11. Imine intermediate of the reductive amination of de-protected poly(β -amino ester) co-polymer and maltose.-----	64

Figure 2.12. Comparison between ^1H NMR spectra of PEGDA-ethylenediamine-maltose co-polymer and the starting materials de-protected poly(β -amino ester) co-polymer and maltose. Spectra recorded in D_2O at 700 MHz. -----	65
Figure 2.13. DOSY plot of the PEGDA-ethylenediamine-maltose co-polymer. The red circle shows the enlarged section of the ^1H NMR spectrum of the PEGDA-ethylenediamine-maltose co-polymer containing the C1' signal. The green rectangle highlights the resonances of the protons that belong to the PEGDA-ethylenediamine-maltose co-polymer. The blue rectangle highlights the resonances of the protons that belong to the maltose-ethylenediamine dimer. Data recorded in D_2O at 700 MHz. -----	68
Figure 2.14. Structure of the dimer between ethylenediamine and maltose. ----	70
Figure 2.15. ^{13}C NMR spectrum of PEGDA-N-Boc-ethylenediamine poly(β -amino ester) co-polymer synthesised in bulk. Spectrum recorded at 700 MHz in CDCl_3 . -----	74
Figure 2.16. ^{13}C NMR spectrum of PEGDA-ethylenediamine-maltose co-polymer. Spectrum recorded in D_2O at 700 MHz. -----	74
Figure 3.1. Structure of the sodium salt of carboxymethyl cellulose. -----	76
Figure 3.2. ^1H NMR spectrum of PEG-OH2K. Spectrum recorded at 700 MHz in CDCl_3 . -----	92
Figure 3.3. ^{13}C NMR spectrum of PEG-OH2K. Spectrum recorded at 700 MHz in CDCl_3 . -----	92
Figure 3.4. SEC traces of PEG-OH starting materials in DMF. Data recorded using a refractive index (RI) detector. The value of M_n was determined against a conventional calibration based on PEG standards. -----	94
Figure 3.5. Comparison between ^1H NMR spectra of PEG-OH2K, PEG-Br2K, PEG-N ₃ 2K and PEG-NH ₂ 2K. Spectra recorded at 700 MHz in CDCl_3 . -----	95
Figure 3.6. Comparison between ^{13}C NMR spectra of PEG-OH2K, PEG-Br2K, PEG-N ₃ 2K and PEG-NH ₂ 2K. Spectra recorded at 700 MHz in CDCl_3 . -----	97

Figure 3.7. ^{13}C solid state NMR spectrum of CMC as sodium salt. Spectrum recorded at 100 MHz. -----	102
Figure 3.8. Titration profiles for the potentiometric titration of CMC with 0.1 M NaOH (blue curve) and 0.1 M HCl (black curve). Data recorded at 25 °C using a glass combined electrode. -----	104
Figure 3.9. Second derivative of the titration curve of the potentiometric titration of CMC with HCl in presence of an excess of NaOH (black). The first equivalence point is identified by the first instance of crossing of the data with the x-axis (green), while the second equivalent point is identified by the second crossing of the data with the x-axis (red).-----	106
Figure 3.10. Idealised picture showing formation of PEGylated area on to a CMC backbone with high DB upon reaction with PEG-NH ₂ . -----	108
Figure 3.11. Inter chain ester bond between CMC backbones. -----	111
Figure 3.12. Interference of the random coil conformation of PEG-NH ₂ in solution upon the speed of the amidation reaction. -----	114
Figure 3.13. Sterical hindrance of a grafted PEG chain on the grafting of a second PEG chain to the CMC backbone.-----	115
Figure 3.14. Comparison between ^{13}C solid state NMR of CMC-g-PEG_2K_62.5, CMC as TBA salt and PEG-NH ₂ 2K. The expanded region on the left highlights the presence of the resonance of the amide functionality. Spectra recorded at 100 MHz. -----	118
Figure 3.15. Calibration profile for PEG-NH ₂ 2K correlating the peak integral of the protons of the PEG chain with the weight percentage of PEG in the sample. -----	125
Figure 3.16. Example of the procedure to calculate the weight percentage of PEG bound of CMC-g-PEG_2K_50.4 co-polymer. -----	126

Figure 3.17. Plot of I/I_0 Vs the magnetic field-gradient applied (G) for the study of the self-diffusion behaviour of the PEG component of the CMC- <i>g</i> -PEG_2K co-polymers and unbound PEG. -----	130
Figure 3.18. Example of the percentage of unbound PEG in CMC- <i>g</i> -PEG_2K_9.5 determined by the software.-----	134
Figure 3.19. Plot of I/I_0 Vs the magnetic field-gradient applied (G) for the study of the self-diffusion behaviour of the PEG component of the CMC- <i>g</i> -PEG_5K co-polymers. -----	135
Figure 3.20. Plot of I/I_0 Vs the magnetic field-gradient applied (G) for the study of the self-diffusion behaviour of the PEG component of the CMC- <i>g</i> -PEG_10K co-polymers. -----	137
Figure 3.21. Labelling of CMC with DTAF in water at pH 8. -----	139
Figure 3.22. Steric hindrance of PEG grafted on to the CMC backbone to the reaction with DTAF. -----	141
Figure 3.23. Comparison between ^1H NMR spectra of PEG-OH5K, PEG-Br5K, PEG-N ₃ 5K and PEG-NH ₂ 5K. Spectra recorded at 700 MHz in CDCl ₃ . -----	154
Figure 3.24. Comparison between ^{13}C NMR spectra of PEG-OH5K, PEG-Br5K, PEG-N ₃ 5K and PEG-NH ₂ 5K. Spectra recorded at 700 MHz in CDCl ₃ . -----	155
Figure 3.25. Comparison between ^1H NMR spectra of PEG-OH10K, PEG-Br10K, PEG-N ₃ 10K and PEG-NH ₂ 10K. Spectra recorded at 700 MHz in CDCl ₃ . -----	155
Figure 3.26. Comparison between ^{13}C NMR spectra of PEG-OH10K, PEG-Br10K, PEG-N ₃ 10K and PEG-NH ₂ 10K. Spectra recorded at 700 MHz in CDCl ₃ . -----	156
Figure 3.27. ^{13}C solid state NMR spectra of CMC- <i>g</i> -PEG_2K co-polymers. Spectra recorded at 100 MHz.-----	156
Figure 3.28. ^{13}C solid state NMR spectra of CMC- <i>g</i> -PEG_5K co-polymers. Spectra recorded at 100 MHz.-----	157
Figure 3.29. ^{13}C solid state NMR spectra of CMC- <i>g</i> -PEG_10K co-polymers. Spectra recorded at 100 MHz.-----	157

Figure 3.30. Example of ¹ H solid state NMR spectra of CMC. Spectrum recorded at 100 MHz in cross-polarisation. -----	158
Figure 4.1. Soil release test stages. 1) Prewash stage. 2) Staining stage. 3) Rinsing stage.-----	151
Figure 4.2. Structure of 1-hydroxy-4-(p-tolylamino)-anthraquinone (SV13-DYE). -----	160
Figure 4.3. Steric interference of grafted PEG chains on adsorption of CMC-g-PEG co-polymer onto a cotton surface. -----	166
Figure 4.4 Comparison between soil release index (SRI) of unmodified CMC (sample V, DK and BDA) and CMC-g-PEG co-polymers (sample 2K_23.8, 2K_9.5, 2K_42.8 and 5K_19.0) as measured using the spectrophotometer at 460 nm. Error calculated as standard deviation.-----	168
Figure 4.5. Comparison between CIE whiteness (y-axis) of unmodified CMC (sample V, DK and BDA) and CMC-g-PEG co-polymers (sample 2K_23.8, 2K_9.5, 2K_42.8 and 5K_19.0) as measured by the spectrophotometer at 460 nm. Error calculated as standard deviation. -----	168
Figure 4.6. Comparison between soil release index (SRI) of unmodified CMC (sample V, DK and BDA) and CMC-g-PEG co-polymers (sample 2K_50.4, 2K_56.1, 5K_51.1 and 5K_55.6) as measured by the spectrophotometer at 460 nm. -----	173
Figure 4.7. Comparison between CIE whiteness (y-axis) of unmodified CMC (sample V, DK and BDA) and CMC-g-PEG co-polymers (sample 2K_50.4, 2K_56.1, 5K_51.1 and 5K_55.6) as measured by the spectrophotometer at 460 nm. -----	173
Figure 4.8. Comparison between soil release index (SRI) of unmodified CMC (sample V and DK) and CMC-g-PEG co-polymers (sample 2K_62.5, 5K_63.7, 10K_76.5, 10K_84.5 and 10K_85.8) as measured by the spectrophotometer at 460 nm. -----	179

Figure 4.9. Comparison between CIE whiteness (y-axis) of unmodified CMC (sample V and DK) and CMC-g-PEG co-polymers (sample 2K_62.5, 5K_63.7, 10K_76.5, 10K_84.5 and 10K_85.8) as measured by the spectrophotometer at 460 nm. -----	179
Figure 4.10. Fluorescence emission intensity of the wash liquor before and after wash cycle with 0.3% concentration of unmodified CMC* or CMC-g-PEG* co-polymers. -----	187
Figure 4.11. Fluorescence emission intensity of the wash liquor before and after wash cycle with 0.5% concentration of unmodified CMC* or CMC-g-PEG* co-polymers. -----	190
Figure 4.12. Fluorescence emission intensity of the wash liquor before and after wash cycle with 1% concentration of unmodified CMC* or CMC-g-PEG* co-polymers. -----	191
Figure 4.13. Calibration curve for DTAF fluorophore in water. -----	193
Figure 4.14. Microscope images of the swatches surfaces under transmitted light (1) and using a fluorescence filter (2). Scale Bar 27.2 μm . A) Finnifix V. B) Finnifix DK. C) CMC-g-PEG*_5K_19.0. D) CMC-g-PEG*_5K_51.1. $\lambda_{\text{ex}}= 495 \text{ nm}$, $\lambda_{\text{em}}= 516 \text{ nm}$. -----	195
Figure 4.15. Image of a 0.02% w/v solution of Finnifix V* in deionised water (left, washing liquor of the control experiment) and comparison between a swatch of unbrightened cotton (A) and the swatch washed in the control experiment (B). -----	196
Figure 4.16. ^{13}C solid state NMR spectra of an unbrightened cotton swatch, PEGNH ₂ , a swatch treated with CMC-g-PEG_5K_19.0* and a swatch treated with CMC-g-PEG_5K_51.1*. Data recorded at 100 MHz in cross-polarization. -----	198

List of Schemes

Scheme 2.1. Model Michael addition reaction between PEGDA and hexylamine. -----	42
Scheme 2.2. Step growth polymerization of PEGDA with N-Boc-ethylenediamine. -----	51
Scheme 2.3. End capping reaction of PEGDA-N-Boc-ethylenediamine co-polymer. -----	59
Scheme 2.4. De-protection of PEGDA-ethylenediamine poly(β -amino ester) under nitrogen flow.-----	61
Scheme 2.5. De-protection of PEGDA-ethylenediamine poly(β -amino ester) in presence of water. -----	61
Scheme 2.6. Reductive amination between de-protected poly(β -amino ester) and maltose. -----	63
Scheme 3.1. Multi-step procedure for the synthesis of amino poly(ethylene glycol) methyl ether. Step 1, yield >99%; step 2, yield >98 %; step 3, yield > 97%. Overall yield=94%. *Diethyl ether was used as solvent instead of dichloromethane (DCM) for poly(ethylene glycol) methyl ether azide M_n 2000 g/mol. -----	90
Scheme 3.2. Reaction scheme for the synthesis of CMC-g-PEG co-polymers using 2-chloromethylpyridinium iodide (CMP-I), tetrabutylammonium hydroxide (TBAOH), triethylamine and PEG-NH ₂ in DMF.-----	99
Scheme 3.3. Synthesis of CMCTBA -----	109
Scheme 3.4. Activation of the carboxymethyl group of CMCTBA with CMP-I in DMF.-----	110
Scheme 3.5. Reaction between the activated carboxymethyl groups of the CMC backbone with PEG-NH ₂ in presence of triethylamine in DMF. -----	111

List of Tables

Table 2-1. Reaction conditions for the model polymerisation of PEGDA and hexylamine in bulk.-----	34
Table 2-2. Reaction conditions for the model polymerisation of PEGDAs and hexylamine in DMSO.-----	35
Table 2-3. Reaction conditions for the model polymerisation of PEGDAs and hexylamine in DCM.-----	35
Table 2-4. SEC data for the polymerisation of PEGDA M_n 258 g/mol and hexylamine in bulk (absence of solvent).-----	44
Table 2-5. SEC data for the polymerisation of PEGDA and hexylamine in various solvents.-----	47
Table 2-6. SEC data for the polymerisation of PEGDA M_n 700 g/mol and N-Boc-ethylenediamine in DCM at 40 °C.-----	53
Table 2-7. SEC data for the polymerisation of PEGDA M_n 700 g/mol and N-Boc-ethylenediamine in bulk at room temperature. -----	56
Table 3-1. Reaction conditions for the synthesis of CMC-g-PEG co-polymers.--	87
Table 3-2. Average M_n of PEG-OH starting materials.-----	94
Table 3-3. List of CMC-g-PEG samples synthesised by amidation reaction in DMF between CMC and PEG-NH ₂ . -----	113
Table 3-4. Percentage of purity of the CMC-g-PEG co-polymers determined by SEC in DMF. -----	121
Table 3-5. Weight percentage of PEG bound in the CMC-g-PEG co-polymers.	127
Table 3-6. Self-diffusion coefficient (D) and purity of the CMC-g-PEG_2K co-polymers synthesised.-----	133

Table 3-7. Self-diffusion coefficient (D) and purity of the CMC- <i>g</i> -PEG_5K co-polymers synthesised.-----	136
Table 3-8. Self-diffusion coefficient (D) and purity of the CMC- <i>g</i> -PEG_10K co-polymers synthesised.-----	137
Table 3-9. Extent of labelling of the Finnifix V*, Finnifix DK* and CMC- <i>g</i> -PEG* co-polymers.-----	140
Table 4-1. Properties of the CMC- <i>g</i> -PEG analysed via soil release test and whiteness test.-----	167
Table 4-2. Properties of the CMC- <i>g</i> -PEG analysed via soil release test and whiteness test.-----	172
Table 4-3. Properties of the CMC- <i>g</i> -PEG analysed via soil release test and whiteness test.-----	178
Table 4-4. CMC- <i>g</i> -PEG* co-polymers analysed during the quantitative test.--	186
Table 4-5. Amount of CMC- <i>g</i> -PEG* co-polymer adsorbed in one wash cycle over cotton fabric.-----	193

List of Equations

Equation 1. -----	40
Equation 2. -----	40
Equation 3. -----	40
Equation 4. -----	67
Equation 1. -----	93
Equation 2. -----	93
Equation 3. -----	93
Equation 4. -----	106
Equation 5. -----	107
Equation 6. -----	107
Equation 7. -----	125
Equation 8. -----	126
Equation 9. -----	126
Equation 10. -----	129
Equation 1. -----	161
Equation 2. -----	161
Equation 3. -----	192

List of Abbreviations

A	Milli-equivalents of total carboxyl units per gram of carboxymethyl cellulose
b	Volume of titrant of the second equivalence point in potentiometric titration
c	Volume of titrant of the first equivalence point in potentiometric titration
CBr ₄	Tetrabromomethane
CEI	Parameter correlated with the brightness of the surface
CHCl ₃	Chloroform
CMC	Carboxymethyl cellulose
CMP-I	2-chloro-methylpyridinium iodide
Đ	Dispersity
DB	Degree of blockiness
DCM	Dichloromethane
DMF	Dimethylformamide
DMSO	Dimethylsulphoxide
DP _n	Degree of polymerisation
DS	Degree of substitution
DTAF	5-([4,6-dichlorotriazin-2-yl]amino)fluorescein
EHEC	Ethyl(hydroxyethyl)cellulose
IPA	Isopropanol
LAS	Linear alkylbenzene sulphonate
M	Concentration of titrant

M_n	Number average molecular weight
n	Amount of carboxymethyl cellulose used for the titration
N_A	number of the functional groups of A present at the end of the reaction
N_{A0}	number of the functional groups of A present at the beginning of the reaction
NaCNBH_3	Sodium cyanoborohydride
NaN_3	Sodium azide
p	Extent of reaction
PEG	Poly(ethylene glycol)
PEG-Br	Poly(ethylene glycol)methyl ether bromide
PEGDA	Poly(ethylene glycol) diacrylate
PEG- N_3	Poly(ethylene glycol)methyl ether azide
PEG- NH_2	Amino poly(ethylene glycol)methyl ether
PEG-OH	Poly(ethylene glycol)methyl ether
PEO	Poly(ethylene oxide)
PET-POET	Polyethylene terephthalate/polyoxyethylene terephthalate
PFG NMR	Pulse field gradient NMR spectroscopy
PPh_3	Triphenylphosphine
PPh_3O	Triphenylphosphine oxide
PS	Polystyrene
r	Ratio between the functional groups A and B
SEC	Size exclusion chromatography
SRI	Soil release index
SRP	Soil release polymer
TBAOH	Tetrabutylammonium hydroxide
TFA	Trifluoroacetic acid

THF	Tetrahydrofuran
W	Adhesion force
γ_{CF}	Interfacial tension between the cleaning solution and the fabric
γ_{CP}	Interfacial tension between the cleaning solution and the film
γ_{FP}	Interfacial tension between the film and the fabric
γ_{SC}	Interfacial tension between the stain and the cleaning solution
γ_{SF}	Interfacial tension between the stain and the fabric
γ_{SP}	Interfacial tension between the stain and the film

Statement of Copyright

The copyright of this thesis rests with the author. No quotation from it should be published without the author's prior written consent and information derived from it should be acknowledged."

Acknowledgements

First of all I would like to thank my supervisor Prof Lian Hutchings whose advice and support over the last few years have helped me to develop both as a chemist and as a person. I would like to thank P&G. and my industrial supervisor Dr Neil Lant for the opportunity to undertake this research. Furthermore, particular thanks go to Hester Sharpe for her kind help during my visits to P&G for sample testing. I would like to thank the Durham University NMR and MS services and Dr Eric Hughes for his assistance regarding gel state NMR and PFG NMR analysis. Thanks to Douglas Carswell for all the help throughout my time in Durham.

I cannot thank enough the members of the Hutchings group present and past in particular Brunella, Gabriele, Paul, Serena, Matthew, Roberto, Irina and Anne-Charlotte for making it such a pleasure to come to work every day. I would also like to thank Arin, Becky, Maria, as well as all the other members of CG156 past and present.

I owe a lot to my partner David for his endless patience and his relentless positivity throughout the time of writing this thesis. I would also like to thank Dave's family, in particular his grandma Dot for letting me stay over at her place anytime I needed to be in Durham. Finally for the support of my parents, brother and grandma. I will be forever grateful. Without their support I would not have reached this point today.

Thesis overview

This thesis will describe the development of a new soil release polymer (SRP) additive for modern laundry detergents. A SRP improves the detachment of stains from garments by modifying the textile surface during the wash cycle. The SRP adsorbs over the fabric surface during the first wash cycle and creates a protective layer. As a consequence of the presence of this polymeric film, any stain deposited over the fabric surface will not penetrate into the fabric itself. Moreover, with the subsequent wash cycle the SRP layer will then desorb from the fabric surface, simultaneously removing the stain. Whilst SRPs technology is already commercial available for synthetic fibres, such as polyester and polyester-blended fibres, no SRP has been developed for natural cellulosic fibres. Since the SRP must adsorb over the target textile surface, the ideal SRP for cellulosic surfaces will include a moiety with structural affinity for cellulose. Moreover, to ensure the desorption from the textile surface, the ideal SRP should also include a component with affinity for the washing liquor.

Chapter 1 will focus on the synthetic strategies reported in the literature to modify cellulose derivatives in order to tune the properties of the resulting material upon adsorption over cellulosic surfaces. Furthermore, a brief section describing the characteristics of SRP is reported and the aims and objectives of this work are outlined.

Chapters 2 and 3 contain a full description and discussion of the strategies investigated toward the synthesis of a potential SRP for cellulosic surfaces.

In particular, chapter 2 reports the synthesis and full characterisation of a SRP from poly(ethylene glycol)diacrylate, ethylenediamine and maltose (referred to as PEGDA-ethylenediamine-maltose co-polymer).

Chapter 3, describes the modification of the carboxymethyl cellulose (CMC) backbone with poly(ethylene glycol) (PEG), to yield a CMC-g-PEG co-polymer for application as SRP. An extensive characterisation of the resulting co-polymers through several different techniques (such as size exclusion chromatography, solid state NMR spectroscopy, pulse field gradient NMR spectroscopy and gel state NMR spectroscopy) is also reported.

Chapter 4 summarises the results of the tests performed on to the CMC-g-PEG co-polymers synthesised in chapter 3 to evaluate their efficacy as SRPs for cellulosic surfaces. Furthermore, a preliminary study on fluorescently labelled CMC-g-PEG co-polymers is described, in an attempt to quantify the amount of co-polymer adsorbed over cotton surfaces.

In chapter 5, conclusions are drawn and future perspectives are discussed.

1

Introduction

1.1. Cellulose: an important material

With a yearly natural production of around 10^{11} tons, cellulose is the most abundant natural polymer on earth. The main sources of cellulose are cotton plants and trees, although several bacteria (such as acetobacter, rhizobium and agrobacterium), algae and fungi have been shown to synthesise cellulose in minor quantities^[1].

Cellulose (as a material) has been part of human history for millennia. According to archaeological finds in China and south east of Asia, cellulose was used since 4500 BC in rope production^[2], and accounts of the use of cellulose-based fibres, such as cotton and linen, were found in Egypt and India dating back to 3000 BC^[2]. With the discovery of the chemical formula of cellulose in 1838 by the French chemist Anselm Payen^[3], cellulose fibres began to attract more interest as a possible starting material for the production of new textile

fibres. The textile fibres derived from modified natural fibres such as cotton, are referred to as “artificial fibres” or “man-made natural polymers”. This is because they are obtained from a natural fibre which undergoes a manufacturing process.

In 1855, George Audemars filed a patent entitled “Obtaining and Treating vegetable fibres”, in which he discussed the dissolution of cellulose into nitric acid to yield a viscous solution of nitro-cellulose, which can be spun into bobbins or converted into an explosive. This first patent was the beginning of both the explosive industry and the search for semi-synthetic fibres derived from cellulose to use as a textile substitute for cotton^[4]. Later, in 1885, Joseph Swan found a method to stabilise nitro-cellulose, allowing its use as a regenerated cellulose fibre in the textile industry as “artificial silk”. In 1904 Louis-Marie-Hilaire Bernigaud started the first regenerated cellulose industry ^[4].

An alternative process for the production of “artificial silk” was suggested by Matthias Edward Schweizer in 1857. According to his discovery, cellulose fibre derived from cotton plants could be dissolved in a copper salt/ammonia solution. The entire process of dissolution and regeneration was, however, patented by Luis Henri Despeissis in 1890 and it became known as the *cuprammonium process*, while the fibre obtained became commercially known as “Cupra”^[4].

In 1891, a third semi-synthetic fibre (viscose) was derived from the dissolution of cotton. Cotton fibres and wood cellulose were treated with a sodium hydroxide solution, then with carbon disulphide to yield sodium cellulose xanthate^[4]. The process resulted in a patent entitled “Improvements in Dissolving Cellulose and Allied Compounds” from Charles Cross and Edward Bevan.

Beside its use in the textile industry, cellulose and cellulose derivatives also find applications in paper^[1], cosmetics, food and the pharmaceutical industry^[5]. For example, cellulose ether and cellulose ester are both used in healthcare product as excipient, or in slow release drugs as matrices^[5]. While in food industry cellulose derivatives are used as thickening agent and stabiliser for emulsions.

1.2. Functional polymers for cellulose modification

Upon discovery of the chemical structure of cellulose, cellulose started to be seen not only as a material but also as potential functional material^[6].

Cellulose is a polysaccharide made of glucose units. The structure of cellulose was first proposed by Staudinger in 1920^[7]. Staudinger proved that, contrary to common opinion, the glucose units found in the cellulose structure are actually covalently bonded to each other, and not just aggregated to form a larger structure. In particular, the linkage between the D-glucose unit is a $\beta(1\rightarrow4)$ glycosidic bond, occurring between the hydroxyl group of the C1 (anomeric carbon) of the first glucose unit and the hydroxyl group at C4 of the second glucose unit, as shown in Figure 1.1^[8].

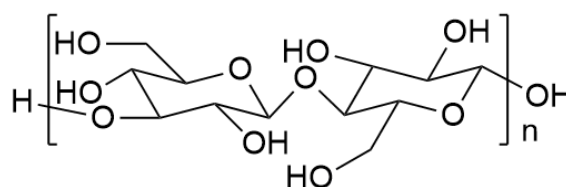


Figure 1.1. Structure of cellulose backbone.

The degree of polymerisation (DP) of the cellulose backbone varies according to the origin of the cellulose. For example, cellulose isolated from cotton plants can have a DP up to 15000, while cellulose extracted from wood has a lower DP (around 10000)^[8]. Cellulose is present in two forms: cellulose I and cellulose II. These two forms of cellulose are polymorphs, thus they differ only for the orientation of the polysaccharide chains in the macro structure (parallel in cellulose I and antiparallel in cellulose II).^[1]

The properties of cellulose are greatly influenced by its structure, in particular by the intra- and intermolecular network of H-bonding between the hydroxyl groups of the polymer chains. Intramolecular bonds can occur between the O5-OH3 and the OH2-O6, while intermolecular interactions are found between O6-OH3^[9] (Figure 1.2).

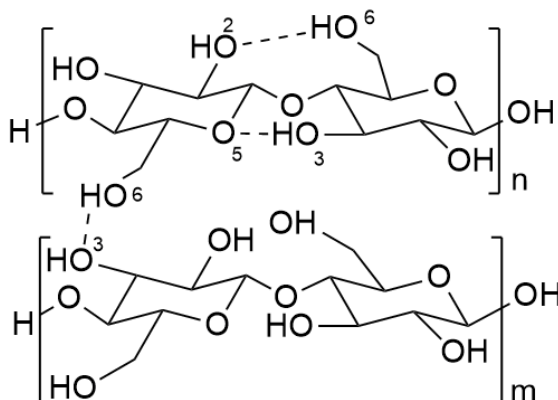


Figure 1.2. H-bond network in cellulose backbone.

The presence of these multiple interactions is the primary reason why cellulose is insoluble in water. When the degree of polymerisation (DP) of the polymer backbone is higher than 8, the affinity of the glucan chains for one another is higher than the affinity for the water, thus the solvent cannot penetrate within the structure and dissolve the polymer^[1]. In the solid state, the supramolecular structure of cellulose is characterised by areas of highly ordered chains (crystallinity) alternated with areas of low ordered chains (amorphous). The reactivity of the hydroxyl groups in amorphous and crystalline regions of cellulose are different. In particular, hydroxyl groups in the amorphous regions are found to be more reactive than the hydroxyl groups of the crystalline region as they are more accessible^{[6],[10]} since they are not involved in a crystalline structure. Moreover, hydroxyl groups within the same region also possess different reactivity, with the primary OH at C6 being the most reactive among

the three hydroxyl units in a glucose ring due to its decreased steric hindrance^[11].

The properties of cellulose can be tuned by both chemical and physical modifications.

The chemical modification of cellulose involves reaction between the hydroxyl groups present in the structure of the cellulose and a modifying agent. The modifying agent introduced can vary dramatically in nature, according to the properties to be imparted to the material. For example, the grafting of oligomers or polymers containing isocyanates or anhydride functionalities onto cellulose fibres was found to be an efficient way to improve the adhesion between a reinforcing agent and the polymeric matrix in composite materials^[12, 13]. Furthermore, the introduction of highly hydrophobic moieties (such as octadecanoyl or dodecanoyl chlorides) onto the cellulose backbone modifies dramatically the interaction on the polysaccharide with water, to the point at which the cellulose becomes hydrophobic^[14].

The modifying agent can also be introduced onto the surface of cellulose fibres via physical adsorption. In order to physically modify the surface of the cellulose fibre, the modifying agent must be able to interact with the substrate. Due to their structural affinity, polysaccharides (like xyloglucan and chitosan) and functionalised polysaccharides (such as carboxymethyl cellulose) are able to physically bind on to the cellulose surfaces^[15]. The nature of the interaction between polysaccharide and cellulose surfaces is not yet fully understood. Some studies support the importance of hydrogen bonding between the cellulose surface and the polysaccharide, to allow adsorption of the material over the surface^[15]. Others suggest that hydrogen bonding may not be the only reason for adsorption of the cellulose derivative^[16] stating that the presence of electric charges could also contribute to the physical binding of a polysaccharide onto a cellulose surface. During the last decade, the influence of hydrogen bonding upon adsorption has been deeply questioned^[17, 18]. The

results of ^{13}C NMR studies and molecular models conducted by Bootten et al.^[17] and Zhang et al.^[18] on the adsorption of xyloglucan (a branched polysaccharide comprising units of glucose joined through a $\beta(1\rightarrow4)$ bond) onto cellulose fibres seems to suggest that hydrogen bonding is not responsible for the adsorption over cellulose surfaces. Instead, it would appear that the adsorption process is greatly influenced by the type of surface targeted^[19-21]. For example, Kargl et al.^[19] reported on the adsorption of carboxymethyl cellulose (CMC) over cellulose, cellulose acetate, deacetylated cellulose acetate and poly(ethylene terephthalate) films. It was found that the adsorption of carboxymethyl cellulose is selective for cellulose film or surface possessing a partial cellulose character, such as deacetylated cellulose acetate film. The reason for this preference was due to the possibility to create electrostatic interactions between the CMC backbone and the cellulose surface, as a consequence of the similarity between the two polymer backbones.

1.2.1. Cellulosic functional polymers

Cellulose is often chemically modified via esterification or etherification reactions^[6] involving the hydroxyl groups of the cellulose backbone, to yield commercial cellulose derivatives, such as carboxymethyl cellulose, ethyl cellulose, hydroxyl ethyl cellulose and cellulose acetate (Figure 1.3).

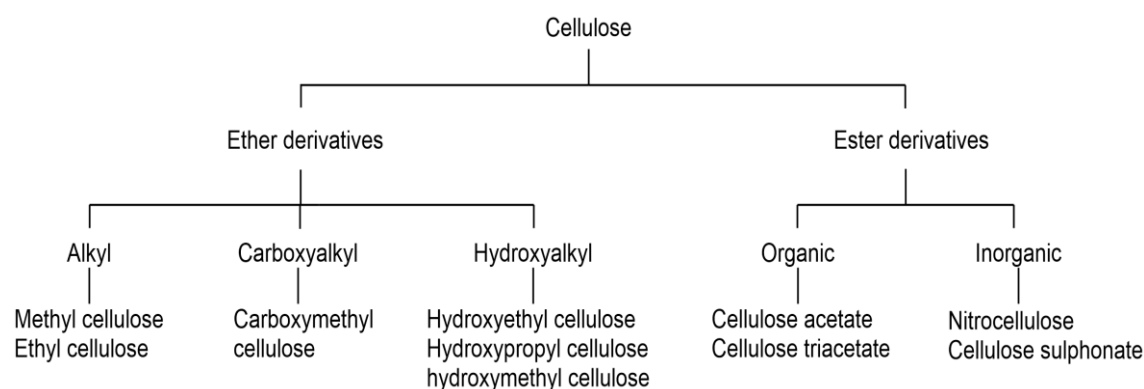


Figure 1.3. Commercial derivatives of cellulose.

The number of hydroxyl groups per glucose repeating unit modified is referred to as degree of substitution (DS). Commercial derivatives of cellulose find applications in several different areas, such as film^[22], fibres^[23] and thickening agents^[24]. Furthermore, cellulose derivatives are capable of physically adsorbing over (unmodified) cellulose fibres surfaces, allowing the creation of new materials^[21].

Ester derivatives of cellulose, such as cellulose acetate and triacetate, find their principal applications as membranes, film and fibres^[22, 23]. Whilst, ether derivatives of cellulose such as carboxymethyl cellulose and hydroxypropyl cellulose, are used as emulsion stabilisers, thermoplastic coating materials and films.

Among the cellulose derivatives, carboxymethyl cellulose (CMC) has been extensively studied as an additive to modify the surface of cellulosic substrates such as textile fibres, due to the presence of a carboxymethyl functionality which allows further tuning of the properties to be imparted to the new materials. The next paragraph will focus on the different modifications of carboxymethyl cellulose (CMC) and their applications.

1.2.1.1. Carboxymethyl cellulose

Carboxymethyl cellulose (CMC, Figure 1.4) is a water soluble derivative of cellulose in which the hydroxyl functionalities have been partially substituted with carboxymethyl groups^[19].

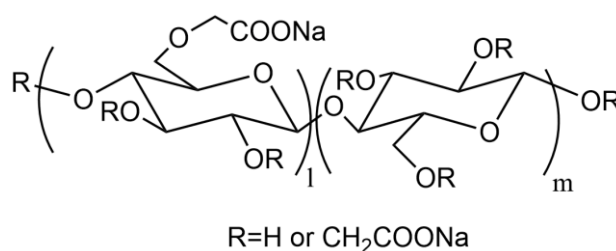


Figure 1.4. Structure of carboxymethyl cellulose (CMC) sodium salt.

The properties of CMC are dependent upon the molecular weight of the polymer backbone, the degree of substitution (proportion of hydroxyl groups converted into carboxymethyl per glucose unit, DS) and the distribution of the substituents^[6]. CMC possesses a high viscosity, high water absorption capability, biodegradability and biocompatibility^[6, 25, 26], and it is used predominantly within the paper, textile and food industries^[24, 27]. In the food industry CMC is commonly used as emulsion stabiliser additive for dairy products such as frozen yogurts and desserts, and as thickening agent for example in salad dressing^[24]. Whilst CMC is used as additive in both paper and textile industry, to enhance the strength of paper^[28, 29] and the wettability of textile surfaces^[30] respectively. The enhancement of the strength of paper sheets upon adsorption of a layer of CMC is due to the formation of a stronger interaction between fibres^[29]. Whilst the adsorption onto textiles results in the increased wettability of the surface, due the presence of a higher number of hydroxyl groups on the surface, allowing the binding of more water^[30].

The commercial synthesis of CMC is performed under heterogeneous conditions^[31]. The deprotonated form of cellulose is reacted with monochloroacetic acid in ethanol to yield CMC as sodium salt (Figure 1.5).

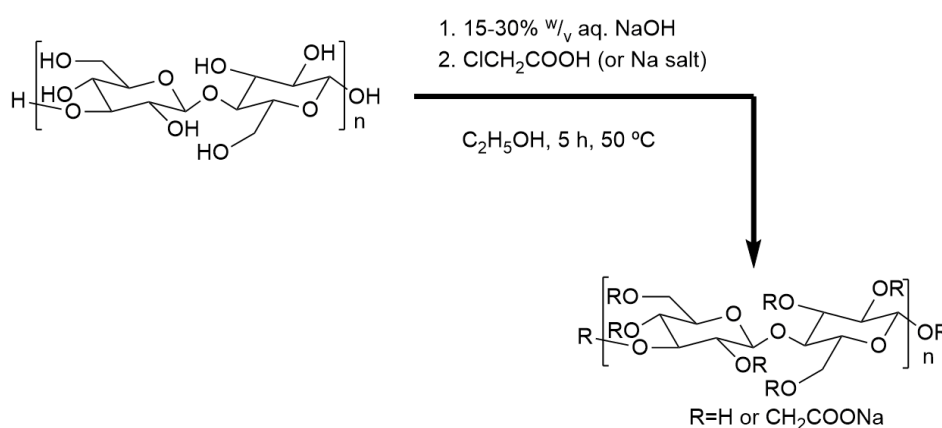


Figure 1.5. Commercial synthesis of carboxymethyl cellulose^[31].

Monochloroacetic acid is able to react with any of the hydroxyl groups of cellulose, although the order of preference for reaction is $O6 \geq O2 > O3$ within the same glucose unit. The distribution of the carboxymethyl groups in the backbone is statistical^[31], thus the substituted units are distributed randomly along the cellulose backbone.

The synthetic strategy illustrated in Figure 1.5 was first patented in Germany in 1918^[32]. Since then, the reactants used for the production of CMC have not changed, but the process has been developed to synthesise CMC material with a controlled distribution of the carboxymethyl groups along the polymer backbone^[33] or with a high proportion of substituted units^[32].

For example, CMC materials synthesised under heterogeneous conditions in *N,N*-dimethyl acetamide/lithium chloride (DMAc/LiCl) with solid particles of sodium hydroxide (NaOH) possess a non-statistical distribution of the carboxymethyl groups along the backbone^[31]. Ionic liquid solvents (ILs) have also been investigated as potential solvent systems for the synthesis of CMC. ILs are molten salt system used as solvents in organic synthesis. They possess a low toxicity, biodegradability and are extremely versatile due to the vast combinations of anions and cations available that allow modulation of the solvent system according to the reaction performed. Furthermore, ILs are known to be able to dissolve cellulose^[34]. Thus, the use of ILs during the synthesis of CMC favours the multiple reaction of hydroxyl groups of cellulose located upon the same glucose unit, creating a preferential (blocky) distribution of substituents^[31].

As a cellulose derivative, CMC possesses a structural affinity with the cellulose chain, thus it is capable of irreversibly adsorbing on to the surface of cellulose, creating a protective layer^[19]. The efficiency of the adsorption of CMC over a cellulosic surface depends upon the pH^[35], temperature and ionic strength of the medium^[19]. Low values of pH (2-4) and high ionic strength (10 mM) appear to be the most favourable conditions for the adsorption of CMC. Under these

conditions, CMC is devoid of charge^[36], thus the adsorption occurs due to hydrogen bonding between unmodified segments of CMC and the cellulose fibre surface^[37]. Furthermore, the uniformity of the adsorbed layer is strictly related to the hydrophobicity of the surface. For example, for a hydrophobic cellulosic film such as cellulose acetate, CMC adsorbs in large aggregates, thus the coverage is not uniform. On the contrary, on hydrophilic substrates such as cotton a uniform adsorption is observed^[19].

The adsorption of CMC over cellulose surface is used often in the textile industry as a non-invasive method to introduce acidic groups on the surface of fibres. The introduction of these charged functional groups allows the modification of the swelling, strength, hydrophobicity and adsorption capacity of the fibres^[30]. The adsorption of a layer of CMC results in an increase in the total charge on the surface of +50%, thus improving the water uptake, the wettability of the surface and the capacity to adhere to moist surfaces.

The adsorption capability of CMC combined with the presence of two different functionalities on the CMC backbone (carboxylic and hydroxyl groups) can be exploited to impart new properties to cellulosic surfaces, opening the possibility of using cellulose-derivatives as functional materials.

The CMC backbone has been modified with a variety of molecules, such as fatty acids^[27], epoxide derivatives^[38], alkyne and azide derivatives^[39, 40], peptides^[41], antibodies^[42] and polymer chains^[35], both prior to or after adsorption onto cellulosic surfaces.

Tomanová et al.^[27] described the derivatization of CMC with a fatty acid methyl ester from rapeseed oil. A variety of solvent systems were investigated for this modification, including dimethylformamide/4-toluenesulphonic acid (DMF/TSA) and water/dimethylformamide (H₂O/DMF). Furthermore, the possibility to carry out the reaction without the use of potassium carbonate as

catalyst, thus increasing the rate of esterification reaction using microwave radiation, was investigated.

The CMC-derivatives synthesised by Tomanová et al. contained low amounts of fatty acid chains and were capable of forming micelles in solution, thus they could act as potential polymeric surfactants for laundry detergents. Furthermore, the presence of aliphatic fatty-acid chains seemed to improve the washing properties of the CMC backbone, especially when compared with a sample of unmodified CMC.

The modification of the CMC backbone was also investigated by Pahimanolis et al.^[38] for potential application in cellulose nanocomposite films. The surface of a cellulose film was coated with a layer of CMC. The reactivity of the superficial carboxymethyl groups on the CMC backbone could then be exploited to graft glycidyltrimethylammonium chloride (GTMA), in order to improve the wet-strength of the material (i.e. the resistance of the wet material to rupture) allowing for potential application of the cellulose nanocomposite film as a wound dressing.

CMC can also be modified with polymer chains, in particular poly(ethylene glycol) (PEG), before adsorption onto cellulose surface in order to decrease the friction between fibres. An example of this was reported by Olszewka et al. ^[35]. The CMC backbone was first functionalised via an amidation reaction with methoxy poly(ethylene glycol) amine. The modified CMC (CMC-g-PEG) was adsorbed onto cellulose surfaces and the adsorption was studied at a range of pHs. The acidity of the reaction medium was shown to affect the amount of water retained, thus altering the friction, and reducing the performance of the adsorbed CMC-g-PEG. It was also found that the best friction reduction (-88% compared to untreated cellulose fibre) was obtained when the CMC co-polymer was adsorbed at a pH value above the pK_a of the carboxylic acid groups (4.5). Above pH 4.5, the carboxylic acid residues of the CMC backbone are in their deprotonated carboxylate form and the structure of the CMC-g-PEG co-

polymer is swollen, as shown in Figure 1.6 (A). Furthermore, the electrostatic repulsion between negatively charged adsorbed layers can lead to a higher amount of retained solvent, which contributed to lowering the friction between fibres.

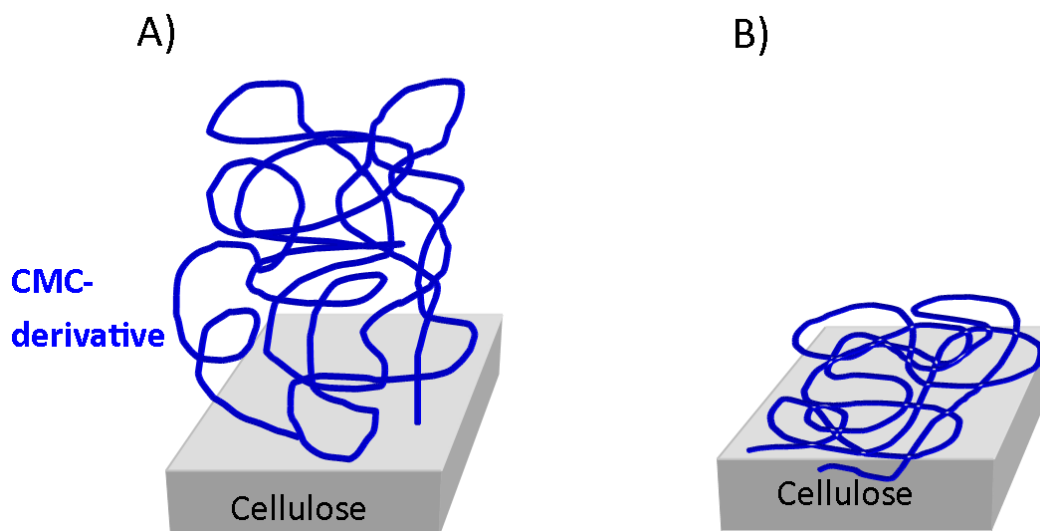


Figure 1.6. Variation of the conformation of the CMC-g-PEG co-polymer adsorbed in water over a cellulosic surface in response to a change of pH of the solution. Above pH 4.5 (A) the conformation of CMC-g-PEG is swollen, as a result of electrostatic repulsive interactions between chains. Whilst below pH 4.5 (B) the conformation is contracted, due to the lack of charges.

The carboxymethyl groups on the CMC backbone have been used by Filpponen et al.^[39] to introduce azide (and alkyne) groups. The introduction of azide or alkyne groups onto the CMC backbone prior to adsorption to cellulose substrates provides the possibility to modify the cellulose surface via copper(I)-catalysed azide-alkyne cycloaddition (CuAAC) reaction on the adsorbed CMC. An example of this approach was given by Filpponen et al.^[39] and Junka et al.^[40]. In their article, Filpponen et al. discussed the possibility of modifying a cellulose surface under heterogeneous conditions via adsorption of an azide or alkyne CMC derivative, followed by reaction between the azide (or alkyne functionality) with the respective complementary group located onto a different molecule, as shown in Figure 1.7.

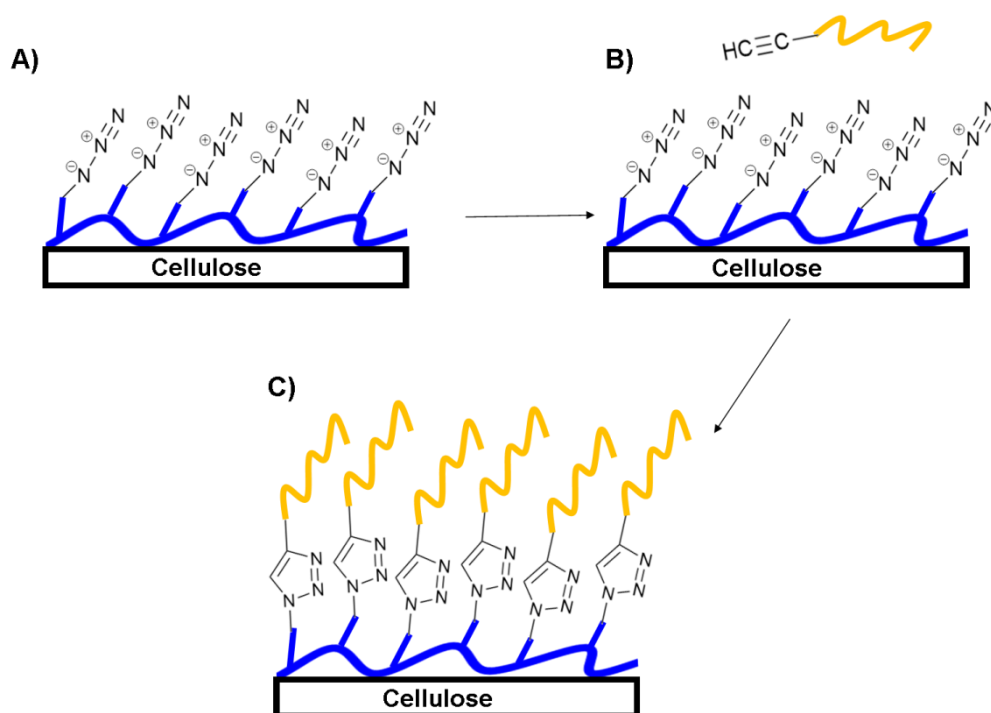


Figure 1.7. Multi-step modification of a cellulosic surface through adsorption of an azide-modified CMC backbone (blue, picture A) and subsequent CuAAC click reaction with an alkyne derivative (yellow, picture B) to yield a functionalised cellulosic surface (C)^[39].

The methodology suggested by Filpponen et al. is extremely versatile, as it allows the creation of materials with very specific properties due to the huge range of molecules which could be reacted with the CMC surface (provided that they possess the complementary functionality). Proteins, fluorescent dyes and polymer chains have all been attached via a CuAAC click reaction to CMC in order to modify different cellulose surfaces, such as cellulosic film and filter paper. The parameters affecting the adsorption of the azide/alkyne CMC-derivative onto cellulose surface are the degree of substitution (DS) of the CMC backbone and the ionic strength of the medium. Junka et al. ^[40] found that the CMC-derivative with a low degree of modification were adsorbed in higher quantities than the derivative with a high degree of modification under the same conditions due to the steric hindrance of the molecule grafted on to CMC. Moreover, increasing the ionic strength of the medium favoured the adsorption of the CMC-derivative onto cellulose, due to electrostatic interactions between

the hydroxyl groups of the cellulose backbone and the carboxymethyl functionalities of CMC.

The presence of CMC on a cellulose surface increases the biocompatibility and antimicrobial activity of the material, allowing for application in wound healing devices and dressings materials^[30, 41]. For example, collagen peptides are known to facilitate the healing process of wounds. Fan et al.^[41] optimised the synthesis of CMC-derivatives containing collagen peptides for subsequent adsorption over cellulose bandages. The influence of the quantity of collagen present in the material was investigated and it was concluded that a high amount of collagen bound (around 0.57 of the total proportion of carboxyl methyl groups reacted with collagen) to the adsorbed CMC was necessary for optimum antioxidant capability.

CMC was also investigated by Orelma et al. ^[42] to create new type of biomedical devices. In this work, the modification of CMC with antihemoglobin antibodies was reported. Using this versatile method, a range of antibodies were attached to the CMC backbone before adsorption on the cellulose surface. The ability to regenerate the cellulose surface using an acid treatment led to the suggested application of these materials for the diagnosis of illness.

1.2.2. *Oligo- and polysaccharide functional polymers*

Beside cellulose derivatives, polysaccharides such as xyloglucan and chitosan have demonstrated the ability to adsorb onto cellulosic surfaces.

1.2.2.1. Xyloglucan

The term “xyloglucan” (XG) refers to a family of branched polysaccharides containing a $\beta(1\rightarrow4)$ glucan backbone substituted at C6 with α -xylopyranosyl

residues.^[43] XG is found mainly in seeds and plant cell walls, usually combined with cellulose. In nature, XG exhibits a dual function, as both carbohydrate storage and cell support. The most commonly used XG is extracted from tamarind seeds (Figure 1.8), in which it comprises around 60% in mass^[43, 44].

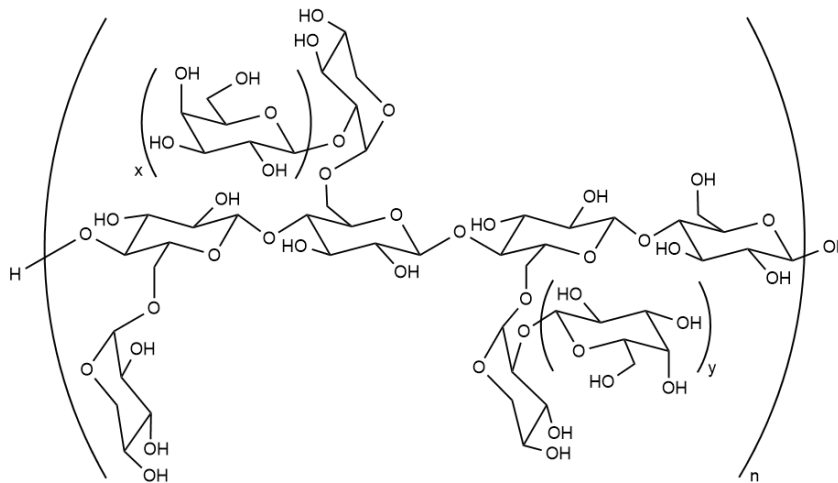


Figure 1.8. Structure of xyloglucan extracted from tamarind seed

XG is used for a range of applications, for example in the food industry as a stabiliser for emulsions and thickening/gelling agent, and in the pharmaceutical industry for drug delivery. XG is also used in the textile industry as a sizing agent (i.e. additive to increase the strength of the fibre) for cotton and jute fibres. Cotton and jute fibres treated with XG possess a higher strength, smoothness and stiffness as a result of the enhanced crosslinking between fibres. XG also finds applications also in the paper industry as a wet-end additive to strengthen the paper fibres again through enhanced crosslinking^[44]. Furthermore, high molecular weight XG (above 2.5 MDa) can be used as a film forming material^[45].

XG adsorbs irreversibly onto cellulose surfaces. Multiple studies have been conducted to understand the dynamics leading to the adsorption of XG onto cellulose^[46] and the factors that could influence such interactions^[44, 47], in order to widen the application areas of XG. The adsorption of XG onto cellulose

surface depends on the structure of both the xyloglucan and the particular surface involved. The formation of H-bonding between the end units of XG side chains and the cellulose surface is the key element that promotes the adsorption of XG and not, as previously hypothesised, the stacking of the XG backbone onto cellulose surface^[44].

The adsorption of XG is greatly impacted by the XG molecular weight, with xyloglucan oligomers (XGO) having been shown to possess a low affinity for cellulose surfaces^[44]. Furthermore, Hayashi et al. demonstrated that the adsorption of XGOs onto cellulose occurs only for XGOs with a degree of polymerisation of at least 8. The presence of a higher proportion of fucosylated residue at the side chain end promotes adsorption on to cellulose due to H-bonding^[48].

The interaction between XG and cellulose surfaces has been harnessed to develop new functional cellulose materials^[46] particularly via the introduction of modifying agents through reaction with the XG hydroxyl groups.

The modification of XG prior to adsorption onto cellulose surfaces could be an opportunity to overcome some of problems associated with the direct modification of cellulose, such as the loss of supramolecular structure (as a consequence of the modification reaction being performed under homogeneous reaction conditions) and disruption of the H-bonding network due to the presence of a substituent^[44].

The most popular strategy to modify XG involves the combined use of a chemical and enzymatic system. Through the use of enzymes, it is possible to hydrolyse (i.e. degrade) the structure of XG and obtain xyloglucan oligosaccharides (XGOs) with well-defined structures^[44]. XGOs can then be modified to introduce fluorescent dyes molecules^[49], thiols^[50], fatty acids^[51], initiators for polymerisation reaction^[52], peptides^[53] and cyclic peptides^[54], and

polymer chains^[55] for application in the paper industry, bio-composite materials and as scaffolds for tissue engineering.

In 2005 Zhou et al. ^[52], discussed the modification of cellulose surfaces through adsorption of XG in order to improve the affinity between the cellulose reinforcing agent and the polymeric matrix in bio-composite materials. In particular, XGOs were modified to include an initiator for atom transfer radical polymerisation (ATRP). Subsequently, the XGOs were incorporated with XG extracted from plants using an endo-transglycosylase enzyme (XET). The chemo-enzymatic approach allowed poly(methyl methacrylate) chains to be grown from the surface of the XG derivative. In a later work, the same group ^[55] reported the modification of cellulose nanocrystals through adsorption of a triblock co-polymer constituting XGOs, poly (ethylene glycol) and polystyrene. This specific modification was studied in order to prevent the nanocrystalline cellulose from aggregating in the polymer matrix solution, thus improving the compatibility between the reinforcing agent and the matrix in composite materials. The presence of XGO promoted the adsorption of the co-polymer onto cellulose, while the PS moiety favoured the interaction with the composite matrix. The PEG chain acts as anchor between the two components of the co-polymer.

XG can also be modified through an enzyme-only strategy. Gustavsson et al. ^[51], for example, reported a method for the modification of XGOs, in order to introduce fatty acid esters and thiol groups onto the surface of cellulose fibres using only enzymes. XGOs were acylated with vinyl stearate or γ -thiobutyrlactone to introduce hydrophobic chains or sulfidryl groups respectively in the presence of an enzyme. Then, the XGOs were combined with high molecular weight XG through XET enzyme and the resulting material was adsorbed onto a cellulose surface.

1.3. Polymeric additives for laundry detergents

Modern laundry detergents contain several ingredients such as surfactants to help remove stains (e.g. linear alkylbenzene sulphonate -LAS and alcohol sulphate), pH neutralisers (e.g. sodium hydroxide), builders to soften the water used for laundry (e.g. sodium carbonate and zeolites) and enzymes (e.g. protease and amylase) to improve the removal of protein and carbohydrate based stains. Moreover, modern laundry detergents also contain a series of additives to improve the smell and softness of the clothes and the brightness and cleanability of the textile surface. These additives can be simple organic molecules, such as disodium 4,4'-diaminostilbene-2,2'-disulphonate (used as an optical brightener), or polymers, such as sodium carboxymethyl cellulose (used to prevent the redeposition of stains during a wash cycle).

Among the polymeric additives found in modern laundry detergents are soil release polymers (SRPs). These SRPs improve the detachment of stains from a garments by modifying the textile surface. During the first wash cycle using a laundry detergent containing a SRP, the polymer additive is adsorbed over the fibre surface, creating a protective layer (Figure 1.9). The presence of the polymeric film prevents subsequent stains from penetrating into the fabric. In the subsequent wash cycle the SRP layer desorbs from the textile surface, simultaneously removing the stain as shown from Figure 1.9.

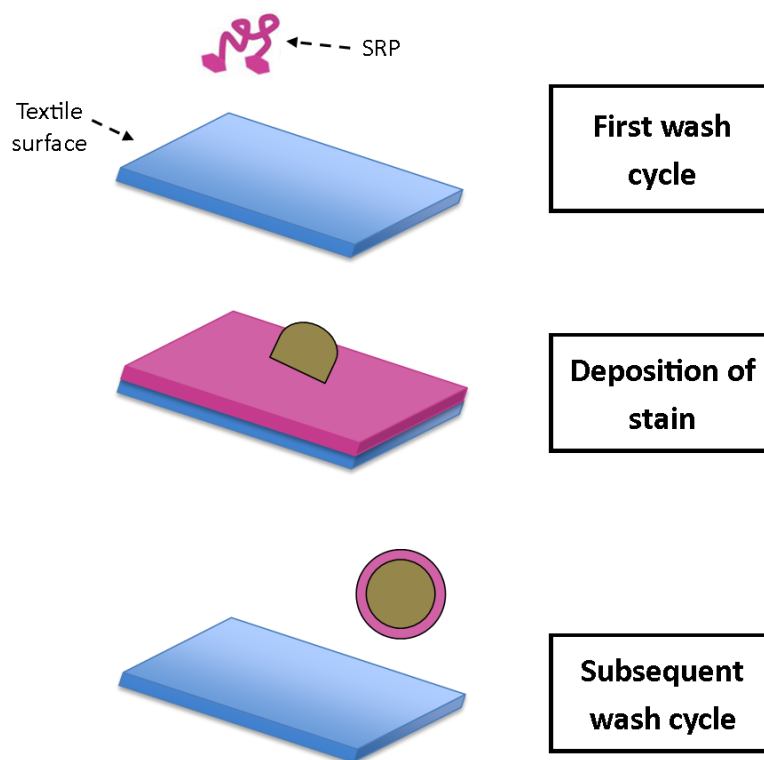


Figure 1.9. Mechanism of action of a SRP. During the first wash cycle (top picture) the SRP additive (purple) contained in the laundry detergent is adsorbed over the textile surface (blue), forming a protective layer. Upon deposition of the stain (middle picture), the stain (brown) cannot penetrate into the fabric (blue) due to the presence of the SRP layer (purple). During the subsequent wash cycle (bottom picture) the stain (brown) is removed together with the SRP protective layer (purple).

The adsorption of a SRP over the fabric surface is promoted by an affinity between the chemical structure of the SRP and the target fibre^[56]. For example, a SRP commonly used for polyester fibres is a PET-POET co-polymer, synthesised from terephthalic acid, ethylene glycol and oligoethylene oxide^[57]. (Figure 1.10)

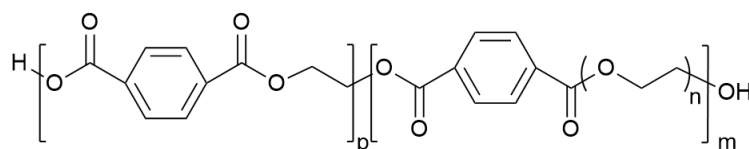


Figure 1.10. Structure of PET-POET soil release polymer for polyester fibres.

The adsorption of this co-polymer onto synthetic fibre surfaces is enhanced due to π - π interaction between the aromatic rings in the PET moiety and the ones on the surface of the polyester fibre. The presence of hydrophilic PEO segments then promotes desorption of the SRP layer due to the affinity of PEO for the washing liquor. If the SRP does not have a structure which is complementary to the target surface, it will not adsorb efficiently and hence the benefits deriving from the use of a laundry detergent containing SRP will be lost. The SRPs developed for synthetic fibres, like polyesters and polyester blended fibres, do not interact with natural fibres such as cotton or wool^[58], as the structure of cotton is very different from polyester. Therefore, a new class of SRPs must be developed to treat natural fibres.

1.4. Aims and objectives

The aim of this project is the development of functional carbohydrate-based materials to modify the surface of cotton fibres in order to improve the cleanability over a wash cycle at low temperature (below 30 °C). These materials will be present as additives (soil release polymers) in the laundry detergent composition and they will be designed to reversibly adsorb on to/desorb from cotton fibre surfaces during a wash cycle.

Two strategies have been developed for the synthesis of these materials, both based on the affinity of carbohydrate molecules for cellulosic surfaces.

Strategy one (Chapter 2) focuses on the synthesis of a co-polymer prepared from poly(ethylene glycol), ethylenediamine and maltose. The synthetic procedure will involve three steps. Firstly, the reaction between poly(ethylene glycol)diacrylate and a mono-protected ethylenediamine to grow the polymer backbone via Michael addition reaction. Polymerisation of the backbone was followed by deprotection of the ethylenediamine and the functionalisation with maltose via a reductive amination.

The second strategy (Chapter 3) will exploit the affinity of CMC, a commercial derivative of cellulose, for cotton fibres. The strong (irreversible) interaction between the CMC and the cotton fibre will be altered via chemical modification of the CMC backbone with poly(ethylene glycol) chains to yield CMC-g-PEG derivatives.

The efficacy of the CMC-derivatives synthesised as soil release polymers toward the removal of stains from cotton surfaces will be evaluated through the combined use of a soil release tests (using lard as the standard stain) and a whiteness test (using carbon black as the standard stain, Chapter 4). Furthermore, attempts to monitor the interaction of the functional carbohydrate-based material with cotton fibre surfaces involved labelling of the

CMC-g-PEG with a fluorophore and fluorescence measurements of the washing liquid. Moreover, the interaction of the CMC-g-PEG co-polymers with the cotton fibre surface will be monitored by means of fluorescence spectroscopy.

1.5. References

1. Brown Jr, R. M. *Journal of Polymer Science Part A: Polymer Chemistry* **2004**, 42, 487-495.
2. Hon, D. N. S. *Cellulose* **1994**, 1, 1-25.
3. O'Sullivan, C. *Journal of Chemical Society* **1872**, 25, 579-588.
4. Woodings, C., *Regenerated Cellulose Fibre*. Woodhead publishing limited: The textile institute, 1994.
5. Van de Ven, T.; Godbout, L., *Cellulose-medical, Pharmaceutical and Electronic Applications*. 2013.
6. Kamel, S. *eXPRESS Polymer Letters* **2008**, 2, (11), 758-778.
7. Klemm, D.; Heublein, B.; Fink, H. P.; Bohn, A. *Angewandte Chemie* **2005**, 44, (22), 3358-93.
8. O'Sullivan, A. C. *Cellulose* **1997**, 4, 173-207.
9. Bocek, A. M. *Russian Journal of Applied Chemistry* **2003**, 76, (11), 1711-1719.
10. Bullock, A. L.; Rowland, S. P.; Cirino, V. O. *Textile Research Journal* **1970**, 40, (4), 313-317.
11. Roy, D.; Semsarilar, M.; Guthrie, J. T.; Perrier, S. *Chemical Society reviews* **2009**, 38, (7), 2046-2064.
12. Trejo-O'Reilly, J. A.; Cavaille, J. Y. *Cellulose* **1997**, 4, 305-320.
13. Ly, E. h. B.; Bras, J.; Sadocco, P.; Belgacem, M. N.; Dufresne, A.; Thielemans, W. *Materials Chemistry and Physics* **2010**, 120, (2-3), 438-445.
14. Pasquini, D.; Belgacem, M. N.; Gandini, A.; Curvelo, A. A. *Journal of Colloid and Interface Science* **2006**, 295, (1), 79-83.
15. Laine, J.; Lindström, T.; Nordmark, G. G.; RIsinger, G. *Nordic Pulp and Paper Research Journal* **2002**, 17, (1), 50-57.
16. Eronen, P.; Junka, K.; Laine, J.; Osterberg, M. *BioResources* **2011**, 6, (4), 4200-4217.
17. Bootten, T. J.; Harris, P. J.; Melton, L. D.; Newman, R. H. *Biomacromolecules* **2009**, 10, 2961-2967.

18. Zhang, Q.; Brumer, H.; Agren, H.; Tu, Y. *Carbohydrate Research* **2011**, 346, (16), 2595-6002.
19. Kargl, R.; Mohan, T.; Bracic, M.; Kulterer, M.; Doliska, A.; Stana-Kleinschek, K.; Ribitsch, V. *Langmuir: The ACS Journal of Surface and Colloids* **2012**, 28, (31), 11440-11447.
20. Mohan, T.; Zarth, C. S.; Doliska, A.; Kargl, R.; Griesser, T.; Spirk, S.; Heinze, T.; Stana-Kleinschek, K. *Carbohydrate Polymers* **2013**, 92, (2), 1046-53.
21. Sundman, O. *Cellulose* **2013**, 21, (1), 115-124.
22. Sata, H.; Murayama, M.; Shimamoto, S. *Macromolecular Symposia* **2004**, 208, (1), 323-334.
23. Fischer, S.; Thümmeler, K.; Volkert, B.; Hettrich, K.; Schmidt, I.; Fischer, K. *Macromolecular Symposia* **2008**, 262, (1), 89-96.
24. Zorba, M.; Ova, G. *Food Hydrocolloids* **1999**, 13, 73-76.
25. Saake, B.; Horner, S.; Kruse, T.; Puls, J.; Liebert, T.; Heinze, T. *Macromolecular Chemistry and Physics* **2000**, 201, 1996-2002.
26. Han, B.; Zhang, D.; Shao, Z.; Kong, L.; Lv, S. *Desalination* **2013**, 311, 80-89.
27. Tomanová, V.; Pielichowski, K.; Sroková, I.; Žoldaková, A.; Sasinková, V.; Ebringerová, A. *Polymer Bulletin* **2008**, 60, 15-25.
28. Duker, E.; Lindström, T. *Nordic Pulp and Paper Research Journal* **2008**, 23, (1), 57-65.
29. Wu, T.; Farnood, R. *Carbohydrate Polymers* **2014**, 114, 500-5.
30. Zemlič, L. F.; Stenius, P.; Laine, J.; Stana-Kleinschek, K. *Cellulose* **2008**, 15, 315-321.
31. Heinze, T. *Macromolecular Chemistry and Physics* **1998**, 199, 2341-2364.
32. Qi, H.; Liebert, T.; Meister, F.; Heinze, T. *Reactive and Functional Polymers* **2009**, 69, (10), 779-784.
33. Varshney, V. K.; Gupta, P. K.; Naithani, S.; Khullar, R.; Bhatt, A.; Soni, P. L. *Carbohydrate Polymers* **2006**, 63, (1), 40-45.
34. Graenacher, C. Cellulose solution. patent number 1,934,176, 1934.
35. Olszewska, A.; Junka, K.; Nordgren, N.; Laine, J.; Rutland, M. W.; Österberg, M. *Soft Matter* **2013**, 9, (31), 7448.

36. Zhivkov, A. M., *Electric Properties of Carboxymethyl Cellulose*. 2013.
37. Zemljič, L. F.; Stenius, P.; Laine, J.; Kleinschek, K. S. *Cellulose* **2006**, 13, (6), 655-663.
38. Pahimanolis, N.; Salminen, A.; Penttilä, P. A.; Korhonen, J. T.; Johansson, L. S.; Ruokolainen, J.; Serimaa, R.; Seppälä, J. *Cellulose* **2013**, 20, (3), 1459-1468.
39. Filpponen, I.; Kontturi, E.; Nummelin, S.; Rosilo, H.; Kolehmainen, E.; Ikkala, O.; Laine, J. *Biomacromolecules* **2012**, 13, (3), 736-42.
40. Junka, K.; Filpponen, I.; Johansson, L. S.; Kontturi, E.; Rojas, O. J.; Laine, J. *Carbohydrate Polymer* **2014**, 100, 107-15.
41. Fan, L.; Peng, M.; Zhou, X.; Wu, H.; Hu, J.; Xie, W.; Liu, S. *Carbohydrate Polymers* **2014**, 112, 32-8.
42. Orelma, H.; Teerinen, T.; Johansson, L. S.; Holappa, S.; Laine, J. *Biomacromolecules* **2012**, 13, (4), 1051-8.
43. Hayashi, T.; Kaida, R. *Molecular Plant* **2011**, 4, (1), 17-24.
44. Zhou, Q.; Rutland, M. W.; Teeri, T. T.; Brumer, H. *Cellulose* **2007**, 14, (6), 625-641.
45. Kochumalayil, J.; Sehaqui, H.; Zhou, Q.; Berglund, L. A. *Journal of Materials Chemistry* **2010**, 20, (21), 4321.
46. Stiernstedt, J.; Brumer III, H.; Zhou, Q.; Teeri, T. T.; Rutland, M. W. *Biomacromolecules* **2006**, 7, 2147-2153.
47. Lopez, M.; Fort, S.; Bizot, H.; Buléon, A.; Driguez, H. *Carbohydrate Polymers* **2012**, 88, (1), 185-193.
48. Hayashi, T.; Ogawa, K.; Mitsuishi, Y. *Plant and Cell Physiology* **1994**, 35, (8), 1199-1205.
49. Zhou, Q.; Baumann, M.; Brumer, H.; Teeri, T. *Carbohydrate Polymers* **2006**, 63, (4), 449-458.
50. Brumer III, H.; Zhou, Q.; Baumann, M. J.; Carlsson, K.; Teeri, T. T. *Journal of American Chemical Society* **2004**, 126, 5715-5721.
51. Gustavsson, M. T.; Persson, P. V.; Iversen, T.; Martinelle, M.; Hult, K.; Teeri, T. T.; Brumer III, H. *Biomacromolecules* **2005**, 6, 196-203.
52. Zhou, Q.; Greffe, L.; Baumann, M. J.; Malmstrom, E.; Teeri, T. T.; Brumer III, H. *Macromolecules* **2005**, 38, 3547-3549.

53. Bodin, A.; Ahrenstedt, L.; Fink, H. P.; Brumer, H.; Risberg, B.; Gatenholm, P. *Biomacromolecules* **2007**, *8*, 3697-3704.
54. Araujo, A. C.; Nakhai, A.; Ruda, M.; Slattegard, R.; Gatenholm, P.; Brumer, H. *Carbohydrate Research* **2012**, *354*, 116-20.
55. Zhou, Q.; Brumer, H.; Teeri, T. T. *Macromolecules* **2009**, *42*, (15), 5430-5432.
56. Lang, F. P.; Morschhauser, R. *SOWT-Journal* **2006**, *132*, 24-34.
57. McIntyre, J. E.; Robertson, M. M. *Modifying Treatment of Shaped Articles Derived from Polyesters*. 1967.
58. Lang, F. P. *Chimica Oggi* **1998**, *16*, (9).

2

Synthesis of a soil release polymer from poly(ethylene glycol)diacrylate and maltose

2.1. Introduction

In order to apply the soil release concept (described in Chapter 1, section 1.3) to cotton fibres, a polymer (or co-polymer) is needed that has affinity for both the fabric, to promote adsorption, and the washing liquor, to favour the desorption.

Cotton is a natural fibre composed of 94% cellulose (Figure 2.1)^[1], a polysaccharide made of linear chains of glucose units linked via $\beta(1\rightarrow4)$ bonds.

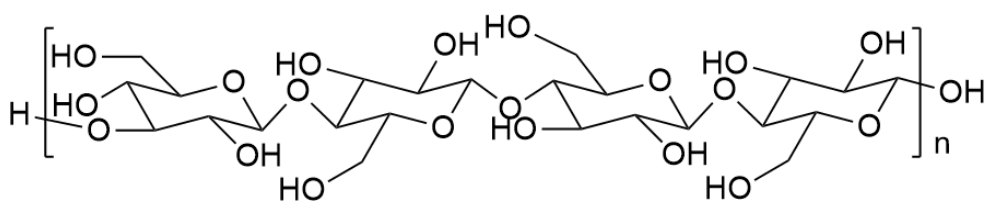


Figure 2.1. Chemical structure of cotton fibre.

When designing a polymer with soil release properties suitable for cotton fibres, a saccharide component may be useful to promote adsorption onto the cotton surface due to structural similarity.

Polysaccharides such as xyloglucan and carboxymethyl cellulose have previously demonstrated a very strong affinity for cotton fibres^[2, 3]. However, the interaction of xyloglucan and carboxymethyl cellulose with cotton fibres is too strong (irreversible) to allow them to be applied as a SRP for cotton fabrics without any modification. For effective soil release properties, the adsorption must be reversible and the polymer must be able to desorb from the target surface to promote stain removal.

Taking inspiration from the pre-existing SRPs for polyester fibres^[4], it was decided to design a co-polymer comprising of both saccharide units, with an affinity for the cotton substrate, and poly(ethylene glycol) units, with an affinity for the washing liquor. Maltose, a disaccharide composed of two units of glucose bonded with a $\alpha(1\rightarrow4)$ bond (Figure 2.2), was chosen as a candidate starting building block for this purpose.

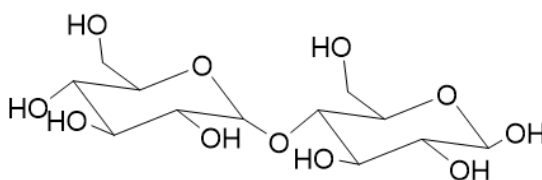


Figure 2.2. Structure of maltose.

In this chapter, the synthesis and characterisation of a potential SRP for cotton fibres from maltose and PEGDA will be discussed. The synthetic strategy investigated involves two steps. During the first stage, PEGDA is used as a starting material for the synthesis of the co-polymer backbone via step growth polymerisation with ethylenediamine. Then the resulting co-polymer is functionalised with maltose via an amination reaction during the second step.

2.2. Experimental Section

2.2.1. Materials

Dichloromethane (purity $\geq 99\%$), isopropanol (purity $\geq 99.8\%$), hexane (purity $\geq 99.7\%$), methanol (purity $\geq 99.5\%$) and tetrahydrofuran (purity $\geq 99\%$) were purchased from Fisher Scientific and used as received unless specified below. Dimethylformamide (anhydrous, purity $\geq 99.8\%$), dimethylsulphoxide (anhydrous, purity $\geq 99.9\%$), D-maltose monohydrate (purity $\geq 99.0\%$), N-Boc-ethylenediamine (purity $\geq 98.0\%$), poly(ethylene glycol)diacrylate (average M_n 258 g/mol and average M_n 700 g/mol), hexylamine (purity $\geq 99\%$), trifluoroacetic acid (purity $\geq 98.0\%$), sodium acetate (purity $\geq 99.5\%$), and sodium cyanoborohydride (purity $\geq 95\%$) were purchased from Sigma Aldrich and used as received unless specified below. Deuterated chloroform (purity $\geq 99.8\%$) and deuterated water (purity $\geq 99.9\%$) were supplied by Goss Scientific. Dichloromethane was dried over calcium hydride and stored under vacuum. Dimethylformamide and dimethylsulphoxide were dried over molecular sieves (pellets, pore size 3 Å) and stored under nitrogen. D-maltose monohydrate was dried over phosphorus pentoxide and stored in a desiccator. Poly(ethylene glycol) diacrylate (average M_n 258 g/mol and average M_n 700 g/mol) was dried over molecular sieves (pellets, pore size 3 Å).

2.2.2. Analysis

2.2.2.1. 1H , ^{13}C and DOSY NMR spectroscopy

The 1H , ^{13}C and DOSY NMR spectra were measured with Varian VNMRS 700 MHz or Bruker DRX-400 MHz spectrometer using deuterated chloroform ($CDCl_3$) or deuterated water (D_2O) as solvent.

2.2.2.2. Size exclusion chromatography (SEC)

The molecular weight of all the co-polymers synthesised was determined by a conventional calibration created using poly(ethylene glycol) (PEG) standards (Polymer Labs). The chromatograms were recorded using a refractive index detector. Two PLgel 5 μm mixed B columns were used. The solvent was dimethylformamide (DMF) with 0.1% of lithium bromide, the flow rate was 1.0 mL/min at a temperature of 70 °C.

2.2.3. Model reactions with hexylamine

2.2.3.1. Model reactions with PEGDAs and hexylamine in bulk

PEGDA (M_n 258 g/mol, 6.73 g, 26.1 mmol) and hexylamine (2.64 g, 26.0 mmol) in a ratio of 1:1 with respect to the reactive functionalities were added to a three-neck flask equipped with a condenser and a mechanical overhead stirrer. The reaction was carried out in bulk (without solvent) and the progress was followed by withdrawing small samples for analysis by size exclusion chromatography in DMF. The synthesised polymer was dissolved in tetrahydrofuran (THF) (10.0 mL) and recovered by precipitation with cold isopropanol (IPA) (100 mL). The same procedure was followed for different reaction conditions, as summarised in Table 2-1.

Table 2-1. Reaction conditions for the model polymerisation of PEGDA and hexylamine in bulk.

Time (h)	Temperature (°C)	M _n (g/mol)	Đ	Yield (%)
24	50	1220	3.0	39
24	60	1440	3.2	39
24	70	1650	3.0	40
24	100	1770	2.0	45
48	60	1770	2.8	48
48	70	2150	2.5	55
48	100	2550	2.1	63

2.2.3.2. Model reactions with PEGDAs and hexylamine in DMSO

PEGDA (M_n 258 g/mol, 5.55 g, 21.5 mmol) and hexylamine (2.18 g, 21.5 mmol) in a ratio 1:1 with respect to the reactive functionalities were added to a three-neck flask equipped with a condenser and a mechanical overhead stirrer. The reaction was carried out in dimethylsulphoxide (DMSO) (11 mL) under nitrogen flow and the progress was followed by withdrawing small samples for analysis by size exclusion chromatography in DMF. The solvent was removed through high vacuum distillation at 70 °C and the polymer was used as is.

The same procedure was followed for different reaction conditions, as summarised in Table 2-2.

Table 2-2. Reaction conditions for the model polymerisation of PEGDAs and hexylamine in DMSO.

M_n PEGDA (g/mol)	Time (h)	Temperature (°C)	M_n (g/mol)	\bar{D}	Yield (%)
258	24	40	1300	4.8	38
700	24	40	1030	2.0	32
700	24	80	2940	2.3	48

2.2.3.3. Model reaction with PEGDA and hexylamine in DCM

PEGDA (M_n 258 g/mol, 5.55 g, 21.5 mmol) and hexylamine (2.18 g, 21.5 mmol) in a ratio 1:1 with respect to the reactive functionalities were added to a three-neck flask equipped with a condenser and a mechanical overhead stirrer. The reaction was carried out in dichloromethane (DCM) (11 mL) at 40 °C under nitrogen flow and the progress was followed by withdrawing small samples for analysis by size exclusion chromatography in DMF. The synthesised polymer was precipitated with hexane (100 mL). The same procedure was followed for different reaction conditions, as summarised in Table 2-3.

Table 2-3. Reaction conditions for the model polymerisation of PEGDAs and hexylamine in DCM.

M_n PEGDA (g/mol)	Time (h)	Temperature (°C)	M_n (g/mol)	\bar{D}	Yield (%)
258	24	40	1040	3.1	43
700	24	40	6260	1.9	88

2.2.4. Synthesis of a PEGDA-ethylenediamine-maltose copolymer

2.2.4.1. Polymerization of PEGDA with N-Boc-ethylenediamine in DCM

PEGDA (M_n 700 g/mol, 11.38 g, 16.3 mmol) and N-Boc-ethylenediamine (2.60 g, 16.1 mmol) in a ratio 1:1 with respect to the reactive functionalities were added to a three-neck flask equipped with a condenser and a mechanical overhead stirrer. The reaction was carried out in DCM (22 mL) at 40 °C under nitrogen flow and the progress was followed by withdrawing small samples for analysis by size exclusion chromatography in DMF. After 192 hours the reaction was stopped and the polymer synthesised was precipitated in hexane (200 mL).

M_n 3820 g/mol; \bar{D} 2.0; yield 56%.

2.2.4.2. Polymerization of PEGDA with N-Boc-ethylenediamine in bulk

PEGDA (M_n 700 g/mol, 10.13 g, 14.7 mmol) and N-Boc-ethylenediamine (2.31 g, 14.3 mmol) in a ratio 1:1 with respect to the reactive functionalities were added to a three-neck flask equipped with a condenser and a mechanical overhead stirrer. The reaction was carried out for 30 days in bulk at 21 °C under nitrogen flow and the progress was followed by withdrawing small samples for analysis by size exclusion chromatography in DMF. The resulting poly(β -amino ester) was characterised by ^1H and ^{13}C NMR spectroscopy in CDCl_3 .

^1H NMR (CDCl_3 , 700 MHz): δ_{H} 1.43 (9H, s, H1', H1'' and H1'''), 2.40-2.44 (2H, m, H9' and H9''), 2.49-2.55 (2H, m, H6' and H6''), 2.73-2.78 (2H, m, H8' and H8''), 3.14-3.18 (2H, m, H5' and H5''), 3.63-4.19 (58H, m, H11', H11'', H12' and H12''), 5.10-5.15 (1H, m, H4), 5.78 (1H, d, H15', $J=1.4$ Hz), 6.09-6.13 (1H, m, H14), 6.36 (1H, d, H15'', $J=1.4$ Hz). ^{13}C NMR (CDCl_3 , 700 MHz): δ_{C} 28.6 (3C, s, C1', C1'' and C1'''), 28.9 (1C, s, C2), 32.6 (1C, s, C9), 38.8 (1C, s, C5), 49.1 (1C, s,

C8), 53.4 (1C, s, C6), 63.6-70.7 (28C, 2 x s overlapped, C11 and C12), 128.1 (1C, s, C14), 130.9 (1C, s, C15), 155.8 (1C, s, C3), 166.6 (1C, s, C13), 171.4 (1C, s, C10).

M_n 8500 g/mol; \bar{D} 2.0; yield 98%.

2.2.4.3. De-protection of PEGDA-N-Boc-ethylenediamine poly(β -amino ester) co-polymer

Poly(β -amino ester) (1.19 g, 1.38 mmol) was dissolved in dry DCM (25 mL) in a two neck flask under nitrogen flow. The reaction was cooled to 0 °C through the use of an ice bath. Upon addition of trifluoroacetic acid (TFA, 3.0 mL) the reaction was allowed to warm up to room temperature and then stirred for 48 h. The progress of the de-protection reaction was followed using ^1H NMR spectroscopy in CDCl_3 through the disappearance of the resonance of the tert-butyl group of Boc. Upon completion of the reaction, the solvent was evaporated under a flow of nitrogen. The unprotected poly(β -amino ester) was characterised by ^1H NMR spectroscopy in D_2O . Yield 95%.

^1H NMR (D_2O , 700 MHz): δ_{H} 1.40 (2H, s, H1' and H1''), 3.56-3.60 (2H, m, H3' and H3''), 3.74-3.77 (2H, m, H5' and H5''), 3.35-3.33 (2H, m, H2' and H2''), 3.65-3.69 (58H, m, H8', H8'', H9' and H9'').

2.2.4.4. Reductive amination between de-protected poly(β -amino ester) co-polymer and maltose

De-protected poly(β -amino ester) (2.68 g, 3.12 mmol) and maltose (9.17 g, 50.94 mmol) were added to a solution of sodium acetate (1 M, 120 mL) under a flow of nitrogen in a three-neck round bottom flask. With vigorous stirring, sodium cyanoborohydride (NaCNBH_3) was added to reach a final concentration of 1.03 M. The progress of the reaction was followed by TLC (DCM/methanol, 70:30)

using ninhydrin as indicator to visualise the disappearance of the primary amine functionality.

The reaction mixture was then concentrated via vacuum distillation (final volume 20 mL). The by-products, unreacted maltose and unreacted NaCNBH_3 were isolated by precipitation in methanol. The mother liquor containing the desired maltose functionalised co-polymer was concentrated via rotary evaporator, dried in vacuum oven and characterised by ^1H , ^{13}C , ^1H - ^1H COSY, ^1H - ^{13}C HSQC, ^1H - ^{13}C HMBC and 2D DOSY NMR spectroscopy in D_2O . Yield 85%.

^1H NMR (D_2O , 700 MHz): δ_{H} 3.74-3.72 (2H, m, H9' and H9''), 3.88-3.91 (2H, m, H11' and H11''), 3.80-4.40 (58H, m, H14', H14'', H15' and H15''), 5.24 (1H, d, H1', J=5.0 Hz). ^{13}C NMR (D_2O , 700 MHz): δ_{C} 100.5 (1C, s, C1'), 71.7 (1C, s, C9), 71.7 (1C, s, C11), 69.3-69.9 (28C, 2 x s overlapped, C14 and C15).

2.3. Results and Discussion

2.3.1. Introduction

Step growth polymerisation is a chemical process of polymer chain formation which does not require the presence of a specific activated centre (for example a radical or an anion) to drive the connection between the monomer units. In contrast to a chain growth technique, where polymerisation proceeds by the addition of one monomer at a time to the reactive chain-end, step-growth polymerisation proceeds by the reaction between bifunctional monomers with mutually reactive functional groups which combine to form dimer/trimers in the early stages of the reaction. As the reaction conversion increases and more active monomer units are consumed, the dimer/trimers then react with each other generating much longer polymer chains. The reaction occurring between monomers can be an addition or a condensation reaction. Step growth polymerisation via addition reaction leads only to the formation of a polymer backbone, while polymerisation via condensation reaction results in a side-product in addition to the polymer chain -usually a low molecular weight molecule. An example of step growth polymerisation via addition reaction is the synthesis of polyurethane from diisocyanate and polyol monomers. The hydroxyl groups of the polyol monomer react with the isocyanate groups to form dimers, then tetramers, and so on, and no side-products are formed. In contrast, the PET-POET polyester shown in is synthesised via step growth polymerisation, but the reaction occurring between the monomers is a condensation, since water is produced as side-product.

An understanding of the mechanism of step-growth polymerisations is fundamental to the effective synthesis of these materials. The progress of these reactions can be followed via the disappearance of one of the functional end groups. If one of the functional end groups is called generically A, the number of the functional groups of A present at the beginning of the reaction would be

N_{A0} , while the number of functional groups A remaining unreacted at a time t of the reaction would be N_A . Therefore, the extent of the reaction (p), i.e. the fraction of the functional groups A that have already reacted at a time t could be calculated as described by Equation 1.

$$p = \frac{N_{A0} - N_A}{N_{A0}}$$

Equation 1.

The extent of the reaction p multiplied by 100 expresses the conversion as a percentage of the monomer containing the functional group A. The degree of polymerisation, defined as the number of monomer units per polymer chain (DP_n), is correlated with the extent of the reaction as described by Equation 2, also called Carothers equation.

$$DP_n = \frac{1}{1 - p}$$

Equation 2.

Since the DP_n depends on the extent of the reaction, it is clear that in order to achieve high molecular weight polymers it is necessary to reach high percentages of conversion. Hence, not only must the chemical reactions be efficient but the stoichiometric ratio of the functional groups involved in the polymerisation must be equal. Therefore, the molar ratio (r) between the functional groups of the monomers involved in the step growth polymerisation must be 1. If the molar ratio is not equal to 1, i.e. one of the monomers is in excess, the equation predicting the DP_n can be modified as (Equation 3):

$$DP_n = \frac{1 + r}{1 + r - 2rp}$$

Equation 3.

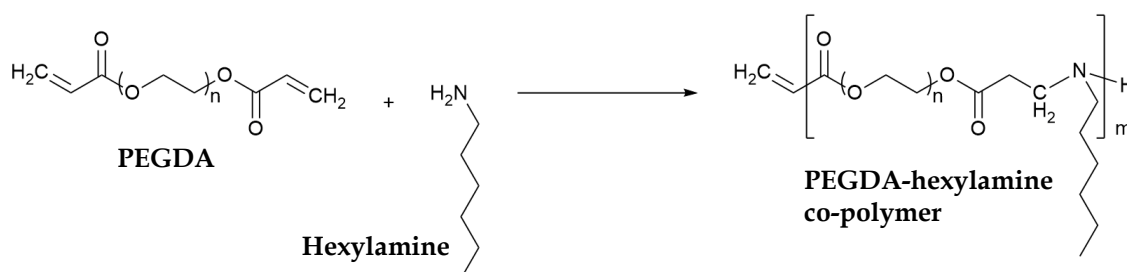
Where p is the extent of the reaction for the functional group present in deficit and r is the molar ratio between the functional groups calculated using the excess functional group as denominator. From Equation 3 it is possible to notice that a strict control of the stoichiometry of the reaction of polymerisation is fundamental to improve the DP_n . Indeed, the presence of a 0.1% excess of one of the monomers involved in the reaction could cause the DP_n to decrease by several orders of magnitude.

As a result of the multi-functionality of monomers used in step growth polymerisations, materials with a wide range of different architectures can be synthesised, such as hyperbranched polymers, dendrimers and polymer brushes^[5]. Linear^[6] as well as cross linked polymers^[7] can be achieved depending on the number of functional groups each monomer contains.

The aim of the current work was to synthesise a potential SRP via the step growth polymerisation of PEGDA and ethylenediamine, such that the pendant amine groups of the resulting copolymer could be functionalised with maltose groups. In order to avoid the formation of cross-linked structures and to retain the second amine functionality of ethylenediamine for the subsequent reaction with maltose, a mono-protected ethylenediamine was used for the step growth polymerisation with PEGDA. Due to the high cost of N-Boc-ethylenediamine, a series of optimisation reactions were conducted with a cheaper mono-functional amine in order to investigate the best conditions for the polymerisation reaction. Hexylamine was chosen as a substitute amine in a series of model reactions with PEGDA to analyse the influence of temperature and a variety of solvents on the polymerisation process.

2.3.2. Model Michael addition reactions with hexylamine

In a preliminary series of experiments, the polymerisation of PEGDA with hexylamine was carried out in a variety of solvents and in bulk without solvent (Scheme 2.1). This allowed an investigation of the influence of the type of solvent used on the molecular weight of the final co-polymer and establish whether a solvent is required at all. A second important parameter to consider is the reaction temperature, thus the model polymerisations were also carried out at various temperatures to investigate the influence of the temperature over the rate and extent of the reaction.



Scheme 2.1. Model Michael addition reaction between PEGDA and hexylamine.

Particular attention was paid towards the use of a stoichiometric amount of the monomers PEGDA and hexylamine. However, the focus of this work was not primarily to produce a high molecular weight co-polymer, but to investigate the influence of temperature and solvent on the molecular weight of the co-polymer. The adsorption properties of the final SRP, following the addition of maltose, could (in theory) be tuned by varying the chain length of the PEGDA. A higher molecular weight PEGDA should make the polymer more hydrophilic and promote desorption. Alternatively, changing the length of the sugar unit might be a strategy to promote adsorption, because a trisaccharide or oligosaccharide might be expected to enhance adsorption through stronger interaction with the cotton surface.

2.3.2.1. *Polymerisation in bulk*

High molecular weight co-polymers have been successfully synthesised from diacrylate monomers and primary amines in the absence of solvent and at high temperatures^[8-10]. Hence, an initial series of reactions were carried out in bulk, i.e. without any solvent, at different temperatures to investigate the effect of temperature over the step growth polymerization of PEGDA with hexylamine. These reactions can also be compared with those conducted in various solvents described in the following section. The reactions were performed under nitrogen flow to avoid possible hydrolysis of the ester bond in PEGDA by the humidity in the air. Moreover, the reagents were stored over molecular sieves to avoid the presence of water.

The molecular weight (M_n) of the PEGDA used for the polymerisation was 258 g/mol, hence the PEG chain contained only an average of 3 ethylene glycol repeating units. The use of a low molecular weight PEGDA should reduce the impact of steric hindrance on the accessibility of the acrylate end groups and reduce the viscosity of the reaction mixture. Since the PEG chain assumes a random coil conformation, a longer PEG chain is likely to reduce access to the chain end groups, thus slowing the rate of the polymerisation reaction, especially as the conversion increases.

As the polymerisation proceeds, both the formation of oligomers and the absence of solvent will contribute to a highly viscous reaction mixture. This could potentially be an obstacle to the increase of the molecular weight of the resulting co-polymer, because the remaining unreacted acrylate and amine functionalities will be less mobile and, therefore, likely to interact with each other. Furthermore, the molar ratio of monomers plays an important role in the molecular weight of the final co-polymer. As demonstrated from Equation 3, the excess of one monomer can cause the molecular weight to drop considerably, with the effect being higher as the conversion increases.

The polymerisation of PEGDA and hexylamine in bulk was repeated at different temperatures and the molecular weights of the resulting co-polymers are summarised in Table 2-4. The progress of each polymerisation reaction was followed using size exclusion chromatography (SEC) in DMF.

Table 2-4. SEC data for the polymerisation of PEGDA M_n 258 g/mol and hexylamine in bulk (absence of solvent).

Temperature (°C)	Time (h)	M_n^* (g/mol)	\bar{D}^*
50	24	1220	3.0
60	24	1440	3.2
	48	1770	2.8
70	24	1650	3.0
	48	2150	2.5
100	24	1770	2.0
	48	2550	2.1

*Data collected using a refractive index detector and a calibration based on PEG standard

Since the molecular weight of the co-polymer was calculated using a conventional calibration based on PEG standards, the value of molecular weight obtained is not an absolute value, however, it does allow the progress of the reaction to be followed. The calibration curve correlates the hydrodynamic volume of a PEG standard with its retention volume (i.e. the volume of solvent necessary to elute a species from the column). The hydrodynamic volume is directly related to the molecular weight of the polymer standard and a calibration curve is built to allow comparison of molecular weight with retention volume. The use of a conventional calibration based on PEG standards for the analysis of the PEGDA-hexylamine co-polymer means that

the molecular weight of the co-polymer backbone is relative, however, it allows for valid comparisons among similar co-polymers.

The results summarised in Table 2-4 seem to suggest that a change in the reaction temperature may have a slight influence on the molecular weight of the resulting co-polymer. When the reaction is conducted for 24 hours at 50 °C a M_n of 1220 g/mol is reached. This increases to 1440 g/mol as the temperature is raised to 60 °C for the same time. Despite the apparent increase in average molecular weight, the difference (200 g/mol) corresponds to less than one repeat unit. When the temperature was increased to 70 °C and 100 °C further increases in M_n were observed, to 1650 g/mol and 1770 g/mol respectively, and the DP_n increased from 3 (reaction in bulk at 50 °C) to approximately 5. The dispersity of the polymers synthesised after 24 h was high in each case, demonstrating a wide range of chain lengths in the mixture. This is to be expected for a step growth polymerisation at low conversion where a range of di-, tri- and oligomers will be present at one time.

When the reaction time was increased from 24 hours to 48 hours at 60 °C, an increase in M_n from 1440 g/mol to 1770 g/mol was observed. In addition the dispersity decreased slightly from 3.2 to 2.8. Again, this maybe be expected as the conversion increases and the smaller chains join together to give macromolecules of a more uniform size. Again, at 70 °C and 100 °C when the reaction time is increased to 48 hours the M_n is shown to increase giving 2150 g/mol and 2550 g/mol respectively. The DP_n also increased as consequence of the increase in the reaction temperature, from 5 for the reaction at 60 °C, to 6 and 7 for the reaction at 70 °C and 100 °C respectively.

The model reaction performed in bulk seems to be influenced by the temperature, namely an increase in temperature results in a higher M_n . However, the overall values of M_n achieved are not very high. It is possible that the increase in viscosity of the system may have been enough to considerably slow down the rate of the polymerisation, even if the molecular weight of the

final co-polymer was rather modest. Alternatively, the PEGDA starting material might have been contaminated with poly(ethylene glycol) monoacrylate, which would alter the amount of acrylates groups available for the reaction thus lowering the final DP_n .

In light of these results, it was decided to investigate the possibility to perform the step growth polymerisation of PEGDA and hexylamine in solution and determine whether the presence of a solvent has a positive impact on the molecular weight of the resulting co-polymer.

2.3.2.2. Polymerisation in Solution

In an attempt to achieve higher molecular weight, the step growth polymerization of PEGDA and hexylamine was conducted in a variety of dry solvents. The solvents chosen were dichloromethane^[6] (DCM) and dimethylsulphoxide^[11] (DMSO), as they allow full solubilisation of the reaction starting materials^[2]. Dry solvents and a nitrogen atmosphere were used for the reaction to avoid possible hydrolysis of the ester bond in the PEGDA at higher temperature.

Two PEGDA monomers with different molecular weights were used for the polymerisations in solution (M_n 258 g/mol and M_n 700 g/mol), with a view to modify the potential SRP properties of the resulting co-polymer. A higher PEGDA molecular weight should reduce access to the reactive PEG chain ends hence reducing reaction rate. However, the presence of the solvent should favour a more homogenous and less viscous reaction mixture compared to the viscous environment of the reactions in bulk, thus the steric hindrance of the PEG chain should have a smaller impact on the rate of the reaction. The use of a higher molecular weight PEGDA during the model reaction with hexylamine allows the potential use of longer PEGDA to be studied for the step growth polymerisation with N-Boc-ethylenediamine. The presence of long PEG chains

in the structure of a potential SRP should (in theory) improve the affinity for the washing liquor, and thus desorption from the fabric surface.

The results obtained from the polymerisation of PEGDA with hexylamine in the two solvents and at two temperatures are summarised in Table 2-5. All the reactions were performed for 24 h to allow a rapid screening of the solvent effect. The co-polymers synthesised in DCM were recovered by precipitation in hexane. The co-polymers synthesised in DMSO were recovered after evaporation of the solvent under reduced pressure at 70 °C, as precipitation was unsuccessful in a range of non-solvents.

Table 2-5. SEC data for the polymerisation of PEGDA and hexylamine in various solvents.

Solvent	M_n PEGDA (g/mol)	Temperature (°C)	M_n^* (g/mol)	\bar{D}^*
DMSO	258	40	1300	4.8
	700	40	1030	2.3
		80	2940	2.0
DCM	258	40	1040	3.1
	700	40	6260	1.9

* Data collected using a refractive index detector and a calibration based on PEG standard

Regarding the results obtained for the polymerisation of PEGDA M_n 258 g/mol and hexylamine in the presence of solvent (Table 2-5), no significant difference is observed when the reaction is performed in DMSO or DCM at 40 °C. The M_n of the resulting co-polymers are 1300 g/mol (DMSO at 40 °C) and 1040 g/mol (DCM at 40 °C) respectively. Using a PEGDA monomer with M_n 258 g/mol gives an average DP_n of between 3-4 repeating units. This result seems to suggest that at this lower temperature, a reaction time of 24 hours is insufficient to reach high conversion and high molecular weight considering the

mechanism of step growth polymerisation. Since DCM is a low boiling point solvent (boiling point 40 °C), it was not possible to investigate the effect of a higher temperature on the rate of the polymerisation reaction. As the reaction progresses, the number of reactive groups decreases and, therefore, the possibility for an acrylate end group of an oligomer to interact with an amine end group of a second oligomer decreases. Therefore, longer reaction times are needed to reach high conversion.

Because no reactions were performed at higher temperature using PEGDA with M_n 258 g/mol in DMSO or DCM, it is not possible to predict the influence of the temperature over the polymerisation of PEGDA M_n 258 g/mol with hexylamine carried out in these solvents.

The results reported in Table 2-5 for the polymerisations using PEGDA with M_n 700 g/mol showed that polymerisation conducted in DCM resulted in a much higher M_n (6260 g/mol, $DP_n=7-8$) than the co-polymer prepared in DMSO (1030 g/mol, $DP_n=1-2$) at 40 °C. The reason behind this result could be the enhanced solubility of the amine monomer in DCM compared to DMSO. The aliphatic amine is more soluble in less polar solvents (like DCM) than polar ones such as DMSO. The increased solubility of one of the monomers in the reaction mixture can favour the polymerisation, since the kinetics of step growth polymerisation is highly concentration dependent. Therefore, the molecular weight of the resulting co-polymer can reach higher values over a reaction time of 24 hours. Moreover, the co-polymer synthesised in DCM has a lower dispersity (1.9) than the co-polymer isolated from DMSO under the same reaction conditions (2.3). This could possibly be a consequence of the reactions between dimers/trimers to form longer chain oligomers in DCM solution. From the results summarised in Table 2-5 it would appear that the steric hindrance of the longer PEG chain has no impact on the M_n of the final co-polymer when the reaction is conducted in solution (6260 g/mol).

The use of a solvent with a high boiling point such as DMSO allowed us to study the variation of the M_n of the final co-polymers when the reaction is performed at higher temperatures (80 °C). The co-polymer isolated from the reaction conducted at 80 °C possessed a higher molecular weight (2940 g/mol, $DP_n=3-4$) than the co-polymer isolated in the same solvent at lower temperature (1030 g/mol, $DP_n=1-2$). Once more, the use of a higher temperature allowed the dimers/trimers formed to combine together into longer chains. The formation of a longer oligomer chain is also supported by the decrease in dispersity of the co-polymer isolated, from $\bar{D}=2.3$ (reaction at 40 °C) to $\bar{D}=2.0$ (reaction at 80 °C).

From the series of model reactions of PEGDA with hexylamine in solution it would appear that the best reaction conditions to perform the polymerisation between PEGDA and N-Boc-ethylenediamine are in DCM at 40 °C. Unfortunately, the use of this low boiling point solvent does not permit the use of reaction temperatures above 40 °C, thus to increase the reaction rate and diminish reaction times. The presence of a solvent during the polymerisation will, however allow the use of a PEGDA with longer PEG chains, thus the potential SRP product should theoretically have an enhanced affinity for the washing liquor due to the presence of a higher number of PEG repeating units.

2.3.3. Synthesis of a PEGDA-ethylenediamine-maltose co-polymer

In the case of the polymerisation of PEGDA with ethylenediamine, PEGDA possesses two reactive species (the two terminal diacrylate groups), while ethylenediamine possesses four reactive species, since each N-H bond can react with an acrylate group. Depending on the stoichiometry, the polymerisation of these two monomers in equal ratio to high conversion will lead to the formation

of a cross-linked material^[7]. Moreover, the second amine functionality may not be available to anchor the sugar moiety as shown in Figure 2.3.

To avoid this problem and retain the second amino functionality to anchor maltose, the commercially available mono-protected ethylenediamine N-Boc-ethylenediamine (Figure 2.4) was chosen for the polymerisation with PEGDA. The tert-butyloxycarbonyl protecting group (Boc) was preferred over fluorenylmethyloxycarbonyl (FMOC), since the latter is removed by basic reagents. Furthermore, the presence of the bulky fluorenyl group on FMOC might hinder the reaction between the free amino functionality of ethylenediamine with PEGDA. In contrast, the Boc protecting group possess a tert-butyl group, less bulky than three aromatic rings thus less likely to hinder the r

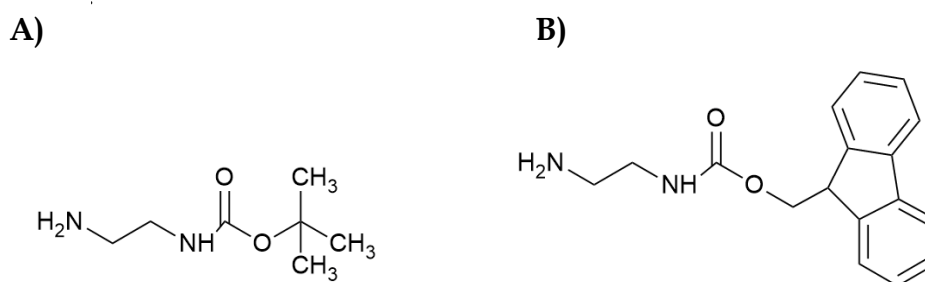
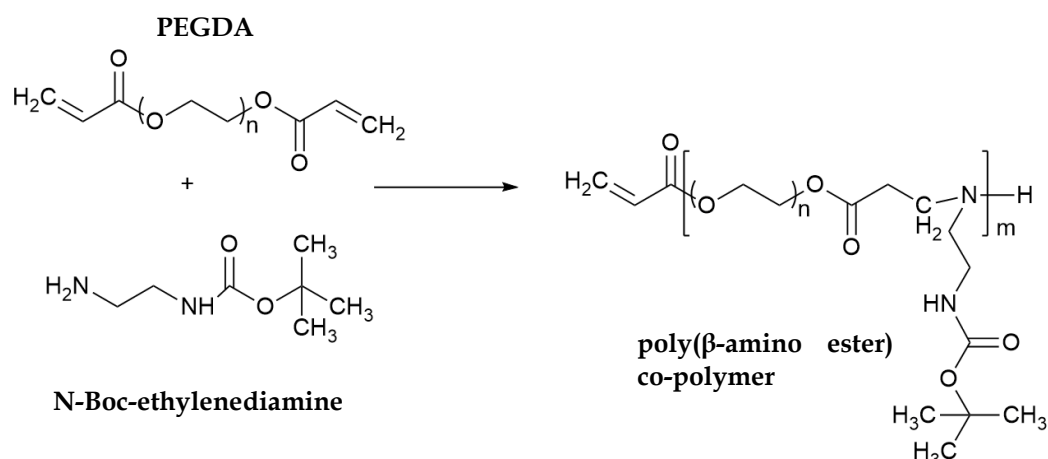


Figure 2.4. Structure of A) N-Boc-ethylenediamine and B) FMOC-ethylenediamine.

The step growth polymerisation of PEGDA with N-Boc-ethylenediamine occurs via a Michael addition mechanism and, therefore, there are no by-products to be isolated at the end of the reaction. The reaction scheme is shown in Scheme 2.2



Scheme 2.2. Step growth polymerization of PEGDA with N-Boc-ethylenediamine.

Upon synthesis of the co-polymer backbone, any remaining acrylate end groups were end-capped with N-Boc-ethylenediamine (Scheme 2.3) before proceeding with the de-protection of the second amine group of ethylenediamine (Scheme 2.4 and Scheme 2.5). The end-capping of the co-polymer backbone was important in order to retain the linear structure, thus avoiding cross-linking between co-polymer backbones. Indeed, if the de-protection of N-Boc-ethylenediamine is performed in the presence of unreacted terminal acrylates groups, the newly-formed amine functionalities may undergo Michael addition reactions with the remaining acrylates, thus forming links between co-polymer chains and losing linearity.

The final step toward the synthesis of the potential SRP involved the functionalisation of the co-polymer backbone with maltose units (Scheme 2.6). The pendant amine functionality of the PEGDA-ethylenediamine co-polymer were reacted with maltose via reductive amination in the presence of sodium cyanoborohydride (NaCNBH_3). The final co-polymer was then characterised by NMR spectroscopy and diffusion studies were conducted to confirm the presence of a bond between the co-polymer backbone and the sugar moiety.

In the following paragraphs, the synthesis of the co-polymer PEGDA-ethylenediamine-maltose will be discussed.

Following the results obtained from the preliminary model reactions, the first step toward the synthesis of a potential SRP for cotton surfaces involved the step growth polymerisation of PEGDA with N-Boc-ethylenediamine (Scheme 2.2).

As no significant steric impact was observed when increasing the PEG molecular weight, PEGDA (M_n 700 g/mol) was chosen for the reaction with N-Boc-ethylenediamine. Furthermore, the higher affinity of PEGDA M_n 700 g/mol with water, compared to PEGDA M_n 258 g/mol, should promote the desorption of the PEG-ethylenediamine-maltose-based SRP from the cotton surface. The reaction between the acrylate end group of PEGDA and the amino functionality of N-Boc-ethylenediamine is a Michael addition. The advantage of this type of reaction is the absence of by-products at the end, thus the purification procedure aims to separate any short chain oligomers from the longer chain ones. Moreover, the Michael addition (also called aza-Michael addition since it involves a nitrogen atom) does not require any catalyst to promote the reaction, since the amine plays the role of both the nucleophile and the base^[12].

The results of the model polymerisations suggested that in order to achieve a higher molecular weight of the resulting co-polymer, DCM should be used as solvent at 40 °C. These reaction conditions were, therefore, used for the initial experiments in this section.

2.3.3.1. Polymerisation in DCM

Using the reaction conditions (DCM/40 °C) described above, a poly(β -amino ester) oligomer with an average of around 7-8 repeat units is expected for the polymerisation of PEGDA (M_n 700 g/mol) and N-Boc-ethylenediamine. This will provide a co-polymer with a M_n of around 6800 g/mol (weight of repeat unit = 860 g/mol).

The progress of the polymerisation of PEGDA M_n 700 g/mol and N-Boc-ethylenediamine was followed using SEC in DMF by monitoring the increase in molecular weight. The reaction was continued at 40 °C until no further increase was observed and the final M_n of the poly(β -amino ester)s synthesised are reported in Table 2-6.

Table 2-6. SEC data for the polymerisation of PEGDA M_n 700 g/mol and N-Boc-ethylenediamine in DCM at 40 °C.

Time (h)	M_n^* (g/mol)	\bar{D}^*
26	2350	2.0
96	2720	2.6
192	3820	2.0

* Data collected using a refractive index detector and a calibration based on PEG standard

In contrast to the model reaction above, the M_n of the poly(β -amino ester) copolymers synthesised from PEGDA and N-Boc-ethylenediamine reached a DP_n of just 4 in 192 hours.

In an attempt to determine the reason for the low DP_n the 1H NMR spectrum of the oligomers was recorded and compared with the 1H spectra of the PEGDA and N-Boc-ethylenediamine starting materials as shown in Figure 2.5.

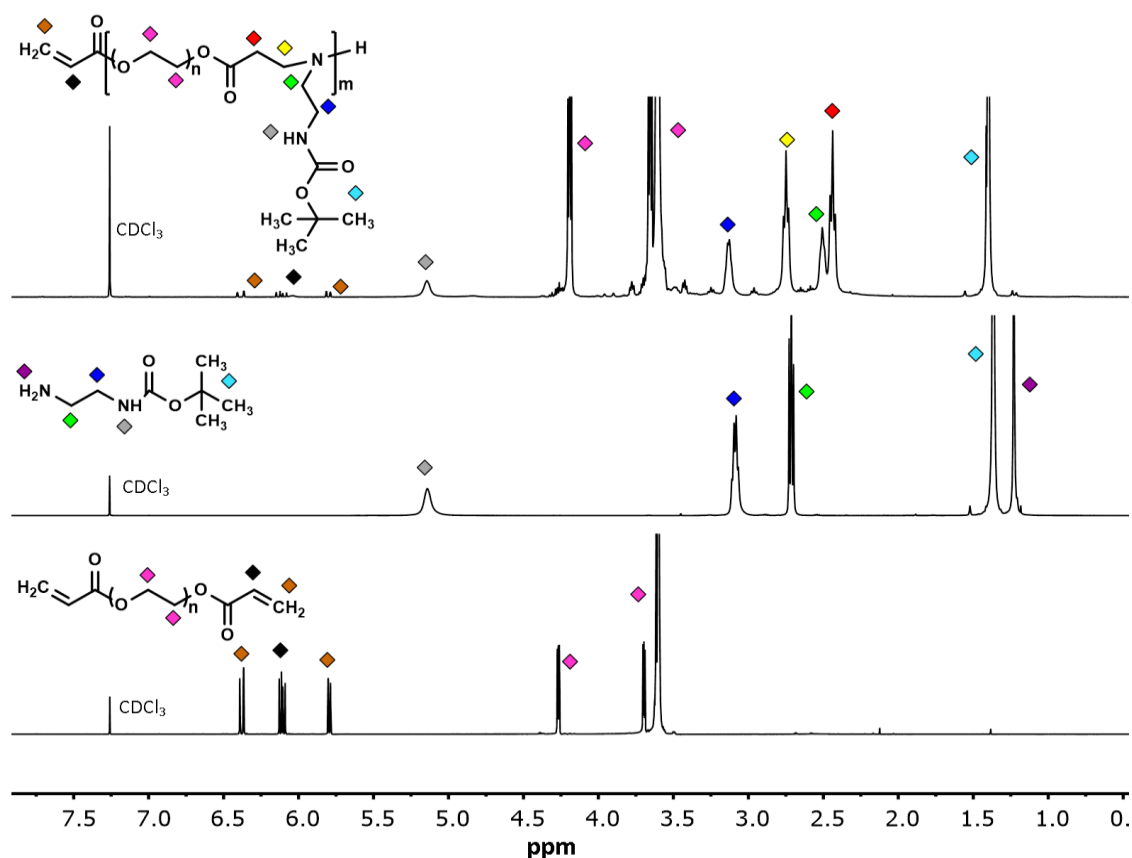


Figure 2.5. Comparison between ^1H NMR spectra of PEGDA-N-Boc-ethylenediamine poly(β -amino ester) co-polymer synthesised in DCM and the starting materials N-Boc-ethylenediamine and PEGDA. Spectra recorded at 700 MHz in CDCl_3 .

From the comparison in Figure 2.5 it is possible to notice the presence of new resonances at δ 2.49 (green diamond), δ 2.40 (red diamond) and δ 2.70 (yellow diamond), belonging to protons in α (green and yellow) and β (red) positions with respect to the amino end group. Furthermore, the signal at δ 1.20 (violet diamond), belonging to the primary amine group of N-Boc-ethylenediamine has disappeared, as a consequence of the polymerisation reaction. On the contrary, the resonances at δ 3.10 (blue diamond, CH_2 of N-Boc-ethylenediamine), δ 1.40 (turquoise diamond, CH_3 of Boc protecting group), δ 3.35-4.20 (purple diamonds, CH_2 of PEG chain) and δ 5.10 (grey diamond, proton of amino group Boc-protected) remained unchanged as they were not involved in the reaction. Despite the stoichiometric addition of each monomer

during the initial stages of the polymerisation, the presence of an intense signal of unreacted alkene end groups at $\delta 6.36$, $\delta 6.09$ and $\delta 5.78$ (brown and black diamonds) and the lack of the signal of unreacted N-Boc-ethylenediamine (violet diamond at $\delta 1.20$, amino group) suggests that there was an excess of acrylate groups in solution. Careful attention was made to the stoichiometry of the reaction starting materials, as the stoichiometry has a significant impact on the final molecular weight of the co-polymer. The lack of N-Boc-ethylene in the system could be explained by the difficulties of weighing out small quantities of reagents very accurately. Since the step growth polymerisation process is highly dependent of the concentration of the monomers involved (Equation 3.), the decrease of the concentration of N-Boc-ethylenediamine in solution would affect the molecular weight of the resulting poly(β -amino ester).

From the model reaction with hexylamine, it was observed that the use of DMSO instead of DCM as the reaction solvent caused the DP to drop from 7-8 to 1-2 (40 °C). Therefore the polymerisation of PEGDA and N-Boc-ethylenediamine was not repeated in a different solvent. However, in an attempt to increase the molecular weight of the resulting poly(β -amino ester) co-polymer it was decided to follow a procedure suggested by the literature^[10] and perform the reaction in bulk.

2.3.3.2. Reaction in bulk

The preliminary studies investigating the polymerisation of PEGDA and hexylamine in bulk (Table 2-4) suggested that the temperature had an effect on the final DP_n of the synthesised poly(β -amino ester) co-polymer. However, the lower boiling point of N-Boc-ethylenediamine (72 °C) compared with hexylamine (132 °C) does not allow the use of temperature as a way to improve the M_n of the resulting poly(β -amino ester). An impact on the final M_n of the co-polymer was also observed when the reaction time was doubled from 24 hours (1650 g/mol at 70 °C and 1770 g/mol at 100 °C) to 48 hours (2150 g/mol at 70 °C

and 2550 g/mol at 100 °C). Following the results previously described, the reaction of PEGDA and N-Boc-ethylenediamine was conducted in bulk at room temperature over a very long reaction time (30 days). This was to allow high conversion despite the high viscosity expected in the reaction mixture, and to prevent the evaporation of N-Boc-ethylenediamine.

The progress of the reaction in bulk was monitored using SEC in DMF. The molecular weight of the resulting poly(β -amino ester) co-polymer is reported in Table 2-7.

Table 2-7. SEC data for the polymerisation of PEGDA M_n 700 g/mol and N-Boc-ethylenediamine in bulk at room temperature.

Time (days)	M_n^* (g/mol)	\bar{D}^*
15	7800	2.0
30	8500	2.0

* Data collected using a refractive index detector and a calibration based on PEG standard

As expected, the M_n of the poly(β -amino ester) co-polymer synthesised in bulk for 30 days is significantly higher than the values obtained for the co-polymer synthesised in DCM at 40 °C in 24 hr. Moreover, the DP_n achieved is between 9-10, compared to a DP_n of between 7-8 from the reaction in solution. This proves that the reaction time has a great influence over the final size of the polymer and to reach high conversion it is necessary to allow very long reaction times, as suggested from the theory.

The poly(β -amino ester) co-polymer was also characterised by 1H and ^{13}C NMR spectroscopy in $CDCl_3$. 2D NMR spectra (1H - 1H COSY, 1H - ^{13}C HMBC, 1H - ^{13}C HSQC) were also recorded to facilitate the assignments of all the resonances. The comparison between the 1H NMR spectrum of the co-polymer synthesised in 30 days in bulk with the 1H NMR spectra of PEGDA M_n 700 g/mol and N-

Boc-ethylenediamine is shown in Figure 2.6. The ^{13}C spectrum recorded is shown in Appendix A.

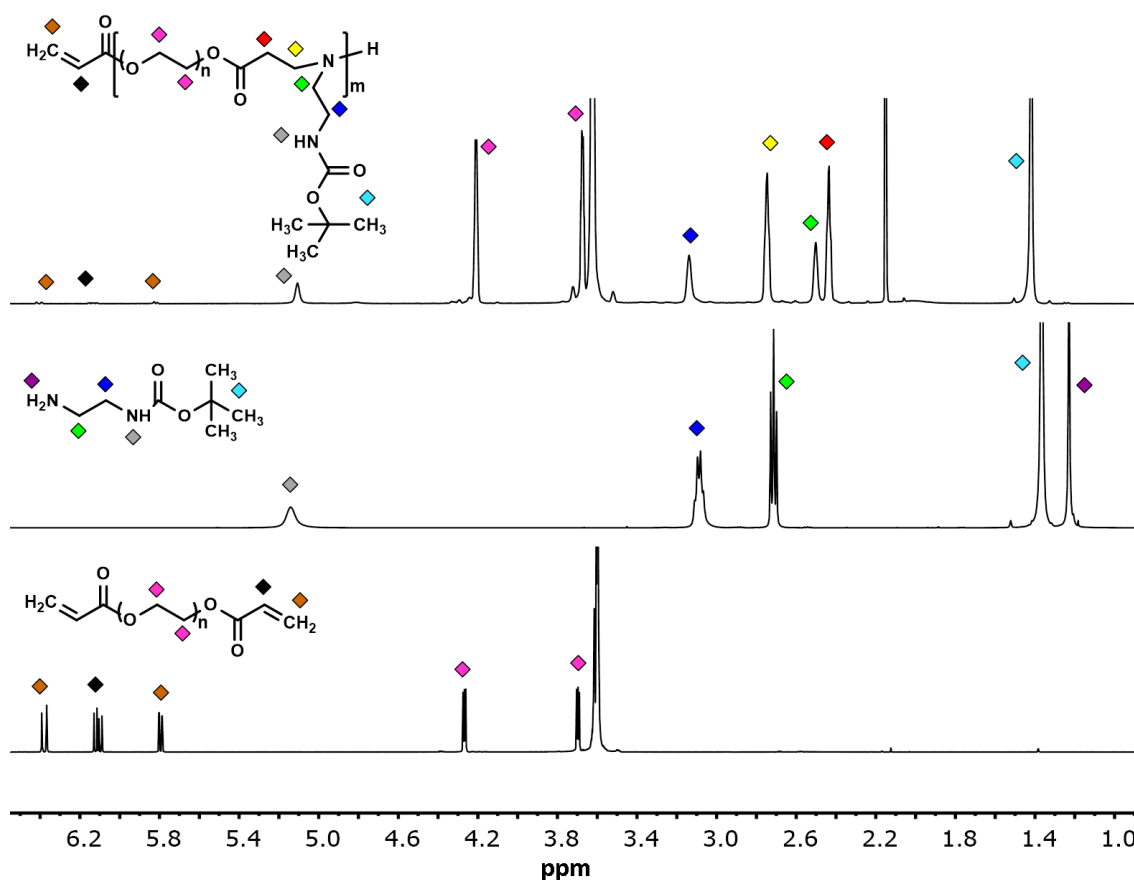


Figure 2.6. Comparison between ^1H NMR spectra of PEGDA-N-Boc-ethylenediamine poly(β -amino ester) co-polymer synthesised in bulk and the starting materials N-Boc-ethylenediamine and PEGDA. Spectra recorded at 700 MHz in CDCl_3 .

Once more, the resonances of the alkene protons of the acrylate groups (brown and black diamonds) have shifted from $\delta 6.36$ and $\delta 5.78$ to $\delta 2.73$ (brown diamonds to yellow diamond) and from $\delta 6.09$ to $\delta 2.43$ (black diamond to red diamond) as a consequence of the reaction. The resonances of the CH_2 of N-Boc-ethylenediamine monomer have also slightly shifted, from $\delta 2.71$ to $\delta 2.49$ (green diamond) and from $\delta 3.09$ to $\delta 3.14$ (blue diamond). The peak of the proton of the amide bond at $\delta 5.10$ (grey diamond), the peak of the CH_3 of the Boc protecting group at $\delta 1.43$ (turquoise diamond) and the peaks of the PEG repeating unit at

δ 3.63-4.19 (purple diamonds) did not move. The purple diamond at δ 4.19 corresponds to the protons of the PEG repeating unit adjacent to the ester bond. From the comparison of the data in Figure 2.6 it is possible to notice the complete disappearance of the signal of the primary amine functionality of N-Boc-ethylenediamine at δ 1.20 (violet diamond) in the ^1H NMR spectrum of the poly(β -amino ester) co-polymer, as a consequence of the high level of conversion of the starting material obtained in 30 days. Furthermore, the intensity of the peaks of the alkene protons of the acrylate groups (brown and black diamonds) are very weak, since most of these functional groups have reacted to form the co-polymer backbone.

The poly(β -amino ester) synthesised in bulk possessed a higher DP_n , therefore it was used for the next step in the synthesis of the potential SRP for cotton surfaces.

2.3.3.3. De-protection of PEGDA-N-Boc- ethylenediamine poly(β -amino ester) co-polymer

The expanded section of the ^1H NMR spectrum of the poly(β -amino ester) co-polymer synthesised in bulk by step growth polymerization between PEGDA M_n 700 g/mol and N-Boc- ethylenediamine showed the presence of some unreacted terminal alkene protons at δ 6.36, δ 5.78 and δ 6.09 (Figure 2.7)

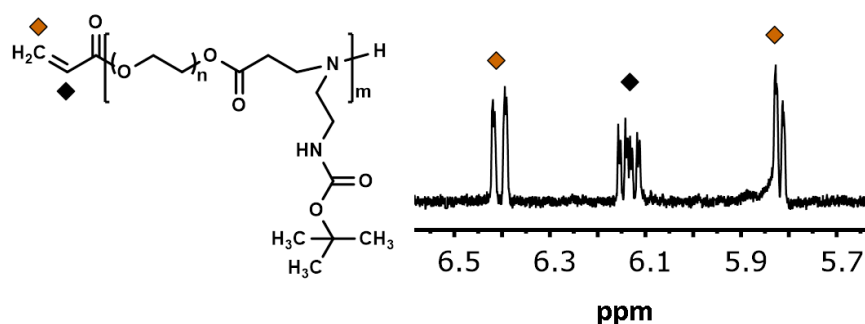
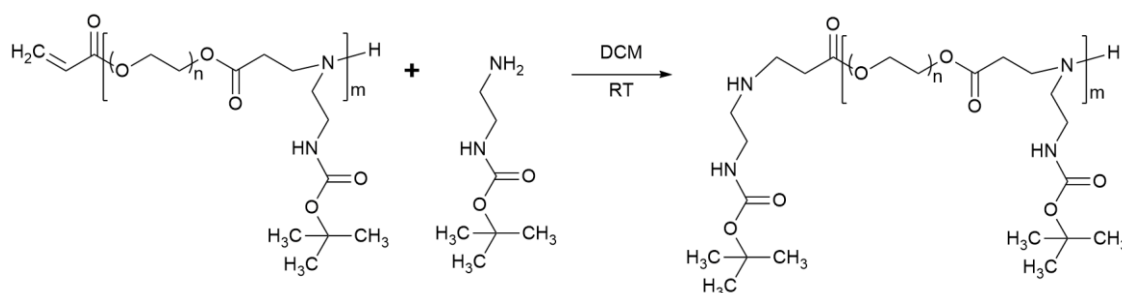


Figure 2.7. Enlargement of ^1H NMR spectrum of PEGDA-N-Boc-ethylenediamine poly(β -amino ester) co-polymer (Figure 2.6).

The intensity of these peaks is very weak, however, before proceeding with the de-protection of the second amine functional group, it is necessary to remove these alkene groups as shown in Scheme 2.3.



Scheme 2.3. End capping reaction of PEGDA-N-Boc-ethylenediamine co-polymer.

If these groups are not removed, the free amine released though deprotection may react with the vinyl group, resulting in the formation of cross-linked structure between co-polymer chains.

Therefore, the poly(β -amino ester) was end-capped with N-Boc-ethylenediamine. N-Boc-ethylenediamine was added until the resonance of the alkene protons at $\delta 6.36$, $\delta 5.78$ and $\delta 6.09$ in ^1H NMR spectrum of the poly(β -amino ester) disappeared (Figure 2.8).

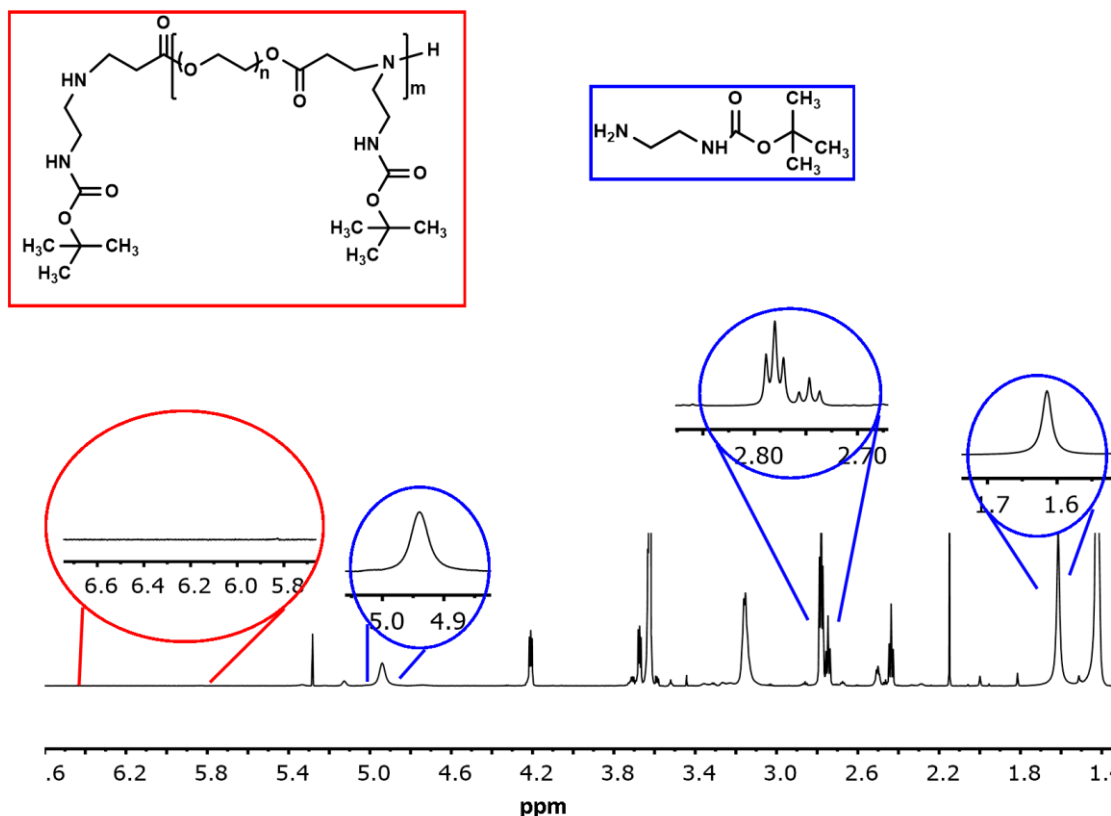
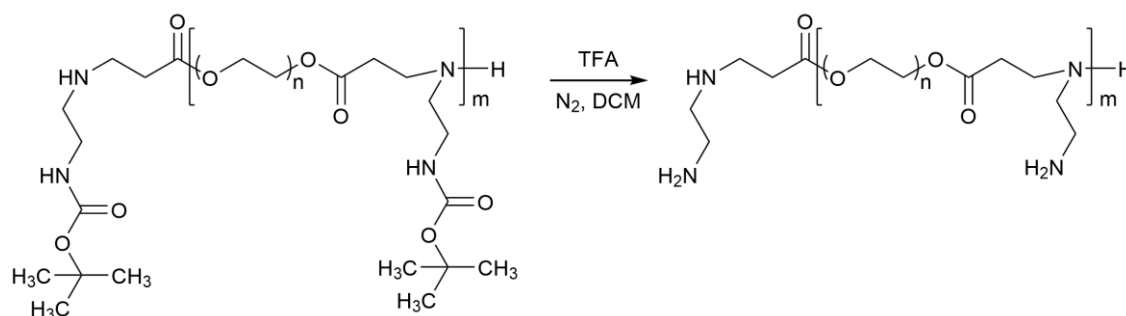


Figure 2.8. ^1H NMR spectrum of PEGDA-N-Boc-ethylenediamine co-polymer end capped with N-Boc-ethylenediamine. Spectrum recorded at 700 MHz in CDCl_3 .

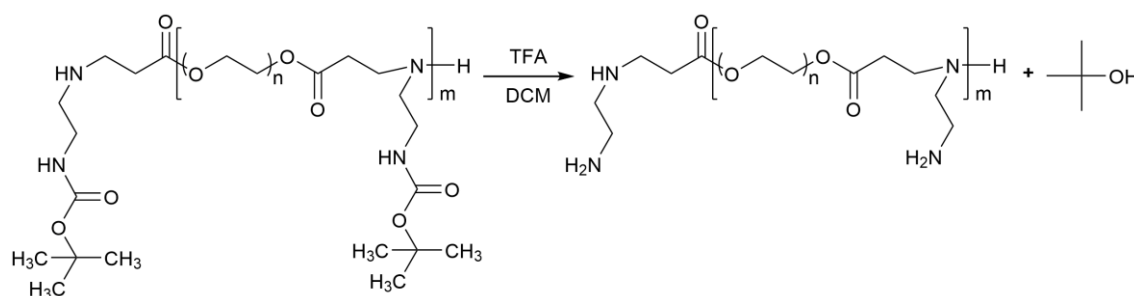
The expanded area between δ 5.8-6.6 in Figure 2.8 (red circle) shows that the peaks of the alkene end groups had disappeared as a consequence of the end-capping with N-Boc-ethylenediamine. Since an excess of mono-protected amine was used to end-capped the co-polymer backbone, the ^1H NMR of Figure 2.8 presents also the signals of unreacted N-Boc-ethylenediamine (blue enlargements) at δ 4.95 (NH amide), δ 2.78 (CH_2) and δ 1.62 (NH_2). The excess of amine was not removed prior the next step of the synthetic procedure.

The Boc protecting group was removed using trifluoroacetic acid (TFA), a specific de-protecting agent for tert-butyloxycarbonyl groups, under a flow of nitrogen. The reaction scheme is shown in Scheme 2.4



Scheme 2.4. De-protection of PEGDA-ethylenediamine poly(β -amino ester) under nitrogen flow.

By performing the reaction under anhydrous conditions, the side-products of the de-protection of the amino group with TFA (CO_2 and isobutylene) are volatile, thus are removed under the flow of nitrogen. Therefore, there was no requirement to further purify the unprotected poly(β -amino ester) before the next stage of the synthesis. However, if the reaction is not performed under nitrogen flow, water is introduced in the system and the de-protection reaction follows the scheme summarised in Scheme 2.5, with the formation of tert-butyl alcohol, which needs to be removed from the reaction mixture via evaporation prior to the next step.



Scheme 2.5. De-protection of PEGDA-ethylenediamine poly(β -amino ester) in presence of water.

The progress of the de-protection reaction was followed by the disappearance of the resonance of the tert-butyl group at $\delta 1.43$ in the ^1H NMR spectrum of the poly(β -amino ester) in CDCl_3 (Figure 2.9).

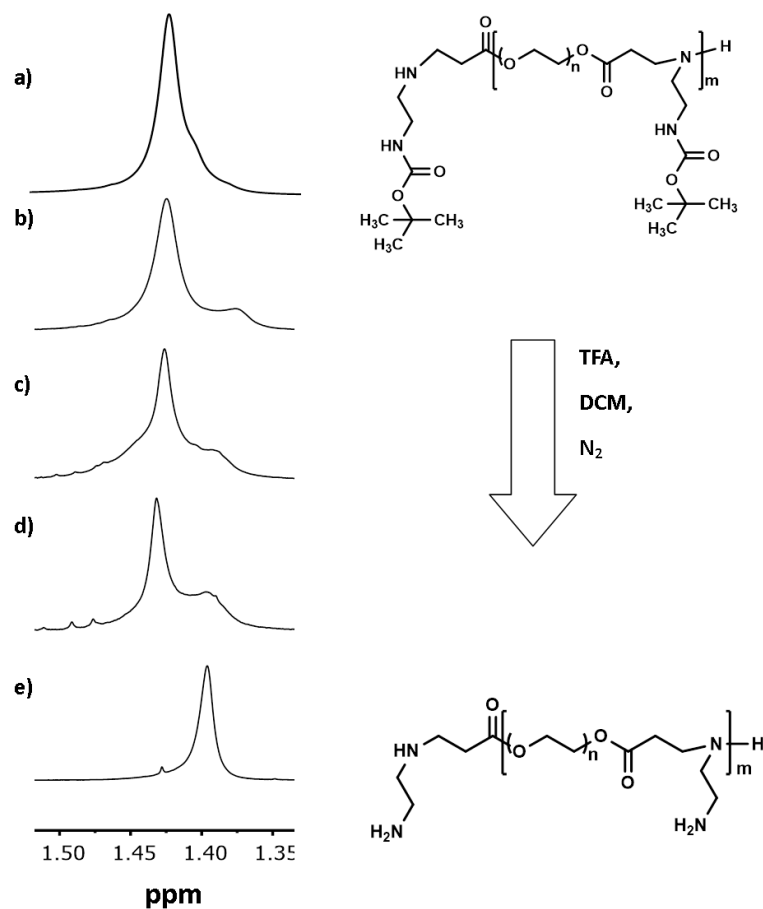


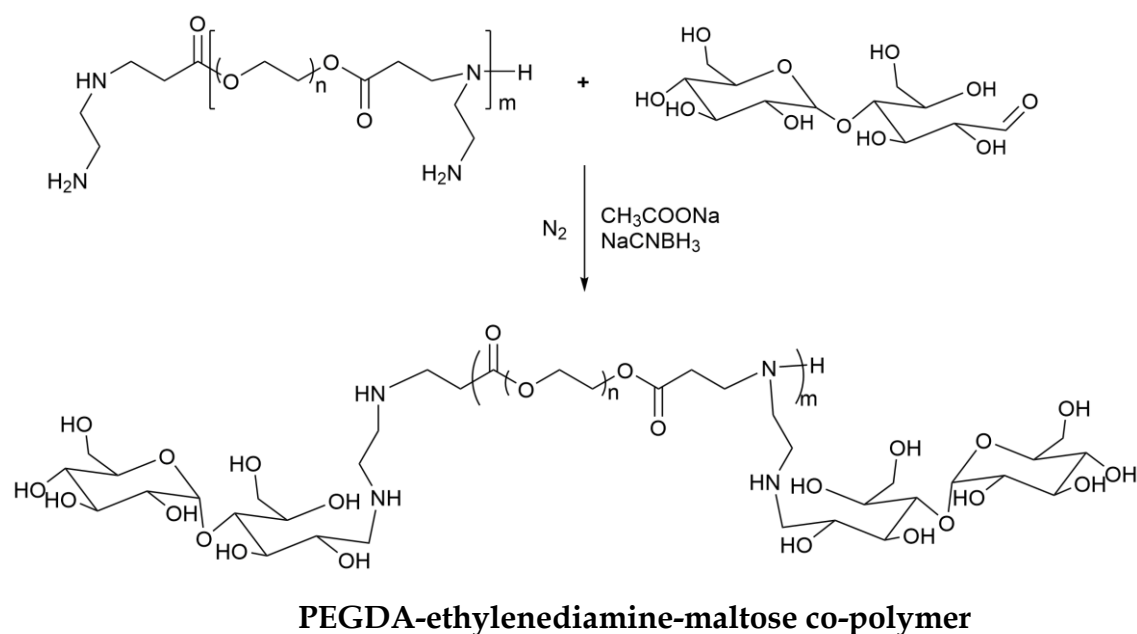
Figure 2.9. Progress of the de-protection of PEGDA-N-Boc-ethylenediamine copolymer with TFA. Spectra recorded after (b) 3 hours, (c) 24 hours, (d) 48 hours and (e) 72 hours in CDCl₃ (a-b-c) and D₂O (d) at 700 MHz.

From Figure 2.9 it is possible to observe that the peak of the tert-butyl group at δ 1.43 disappears as the reaction proceeds and simultaneously a new peak is formed at δ 1.40, belonging to the proton of the de-protected amine functionality.

The de-protected poly(β -amino ester) copolymer was then isolated from the reaction mixture and functionalised with maltose in the last step of the synthesis of the potential SRP for cotton surfaces.

2.3.3.4. Reductive amination between de-protected poly(β -amino ester) co-polymer and maltose

The last step toward the synthesis of a potential SRP (Figure 2.3) involved the addition of the maltose sugar moiety. The method used to attach the maltose group was reductive amination of the terminal amine groups of the side chains with the anomeric carbon of maltose. The reaction is shown in Scheme 2.6.



Scheme 2.6. Reductive amination between de-protected poly(β -amino ester) and maltose.

The reductive amination reaction takes advantage of the equilibrium between an open and closed ring forms of maltose (Figure 2.10). When open, the structure presents a free aldehyde group. This allows the potential for the reaction with the free amine of the poly(β -amino ester) co-polymer.

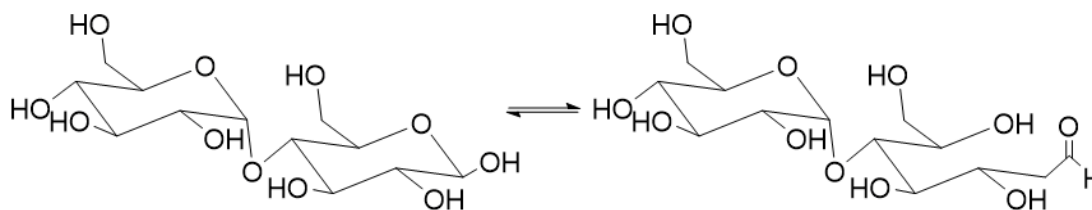


Figure 2.10. Equilibrium between open ring and closed ring forms of maltose in solution.

Unfortunately, the equilibrium described in Figure 2.10 is greatly shifted toward the ring-closed form, with the ring-opened form usually present in a concentration less than 1%. In order to promote the ring opening of the maltose structure, the amination reaction was performed in sodium acetate. The presence of sodium acetate pushes the equilibrium toward the open form of maltose by removing H^+ from the system^[13]. Although the presence of sodium acetate should increase the amount of maltose in the ring-opened form, the equilibrium will still favour the closed structure and therefore it is expected that the reductive amination reaction will proceed very slowly.

A second “obstacle” toward the formation of the bond between the anomeric carbon of maltose and the amine of the poly(β -amino ester) is the imine formed as an intermediate, since the reaction is reversible (Figure 2.11).

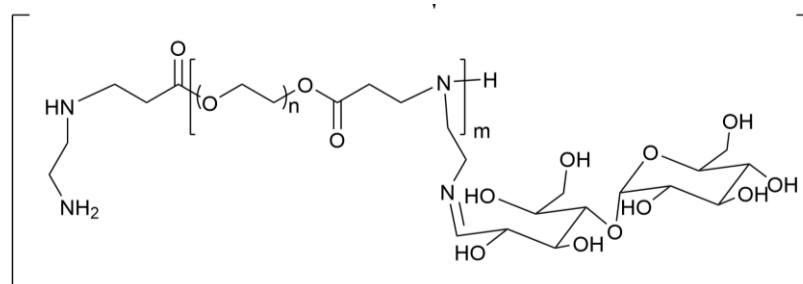


Figure 2.11. Imine intermediate of the reductive amination of de-protected poly(β -amino ester) co-polymer and maltose.

To overcome the possibility for a retro amination and decomposition of the imine intermediate back into the starting material, the use of NaCNBH_3 was fundamental. If the reducing agent NaCNBH_3 is present at high concentration in the system, the imine intermediate will be reduced to the more stable amine form as soon as it is produced, thus increasing the yield of the reaction.

The reaction of the de-protected poly(β -amino ester) with maltose was followed using TLC plates and ninhydrin as stain indicator. Since ninhydrin reacts with primary amines giving a deep purple coloration and with secondary amine giving a weak orange colour, the disappearance of the primary amine of poly(β -amino ester) could be easily followed via the change in colour of the spots on the TLC plate. The resulting PEGDA-ethylenediamine-maltose co-polymer was analysed using ^1H NMR spectroscopy (Figure 2.12). The ^{13}C NMR spectrum was also recorded and can be found in Appendix A.

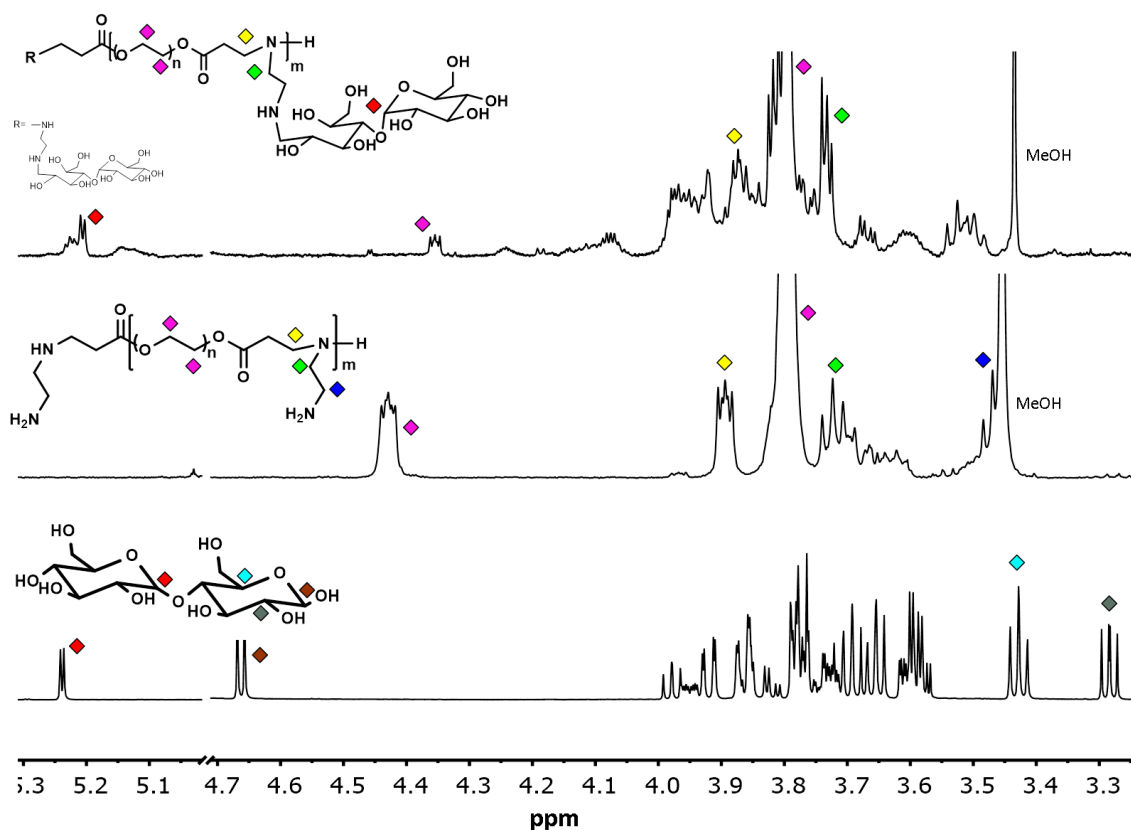


Figure 2.12. Comparison between ^1H NMR spectra of PEGDA-ethylenediamine-maltose co-polymer and the starting materials de-protected poly(β -amino ester) co-polymer and maltose. Spectra recorded in D_2O at 700 MHz.

From the ^1H NMR spectrum of the PEGDA-ethylenediamine-maltose co-polymer shown in Figure 2.12 it is possible to observe resonances due to the PEGDA-ethylenediamine co-polymer at $\delta 3.80\text{--}4.40$ (purple diamonds, PEG chain and PEG units closer to the ester bond respectively), $\delta 3.90$ and $\delta 3.73$ (yellow and green diamond respectively, CH_2 in α position with respect to the amine functionality of the co-polymer backbone). Furthermore, the resonance of the proton of the anomeric carbon of the second maltose ring ($\text{C1}'$, red diamond) is easily recognisable at $\delta 5.24$. This sugar ring is not involved in the reaction with the poly(β -amino ester) and, therefore, this resonance is left unchanged from the starting material. The signals in the ^1H NMR spectrum which are expected to change as a consequence of the reaction are the proton of the anomeric carbon (C1) of maltose (brown diamond at $\delta 4.67$), the protons of the first CH_2 group next to the amine group (blue diamond at $\delta 3.46$), the protons of the C2 next to the anomeric carbon (grey diamond at $\delta 3.28$) and the protons of the C5 next to the ring O (light blue diamond at $\delta 3.43$). Unfortunately, it is not possible to assign either of these resonances in the final spectrum, as they are located between $\delta 3.55\text{--}4.05$ and there is considerable overlap with the CH resonances of the sugar ring and the PEG chain at $\delta 3.80$.

The resonances observed in the ^1H NMR spectrum confirm the presence of both the PEG-ethylenediamine co-polymer and the maltose in the final mixture. Furthermore, the disappearance of the resonance of the proton of C1 at $\delta 4.67$ suggests that a reaction involving this centre happened. However, through this method alone it is not possible to determine whether the maltose and co-polymer are bound together.

In order to gain further information on the extent of binding, diffusion ordered spectroscopy (DOSY NMR) can be an important tool. In this work, 2D DOSY NMR spectroscopy was applied to estimate the diffusion coefficient of maltose in the system.

The diffusion coefficient D can be calculated as (Equation 4.)^[14]:

$$D = \frac{K * T}{6 * \pi * \eta * r}$$

Equation 4.

Where K is the Boltzman constant, T is the absolute temperature, η is the viscosity of the medium and r is the hydrodynamic radius of the species.

As the hydrodynamic radius of a species in solution increases, the diffusion coefficient will decrease, i.e. larger molecules will diffuse more slowly than smaller molecules. Diffusion spectra are usually represented as 2D plots, in which the chemical shifts of the nuclei analysed (in this case ^1H) are correlated with the value of diffusion coefficient D . If two protons with different resonances in the ^1H NMR spectrum are part of the same molecule, they will correlate with the same value of diffusion coefficient D , since a small single molecule can only have one diffusion behaviour. In contrast, if the two protons belong to two different molecules, their resonances in the ^1H NMR spectrum of the sample analysed will correlate with two different values of diffusion coefficient D , one for each molecule.

The extent of bonding between maltose and the de-protected poly(β -amino ester) can be investigated using the signal of the proton of the anomeric carbon of the second sugar ring of maltose ($\text{C1}'$) at $\delta 5.24$ as a target resonance for analysis. The choice to target this specific resonance was due to its position at higher ppm, making it easily identified and avoiding overlap with other resonances in the spectrum. Furthermore, this resonance is present in both the unreacted maltose and the maltose bound to the de-protected poly(β -amino ester), therefore it will help to determine whether maltose is bound or not.

If the maltose is fully bound to the de-protected poly(β -amino ester) co-polymer it is expected that only one diffusion coefficient will be associated with both the resonance of the $\text{C1}'$ ($\delta 5.24$) and the resonance of the protons of the PEG

repeating unit of the poly(β -amino ester) at δ 3.80. If the protons of the PEG chain and the proton of C1' possess the same diffusion coefficient it means that maltose and PEG are part of the same species, thus the resonances of maltose seen in the ^1H NMR spectrum of the PEGDA-ethylenediamine-maltose co-polymer must belong to maltose bound to the de-protected poly(β -amino ester) backbone.

The 2D DOSY NMR spectrum of the PEGDA-ethylenediamine-maltose co-polymer is shown in Figure 2.13.

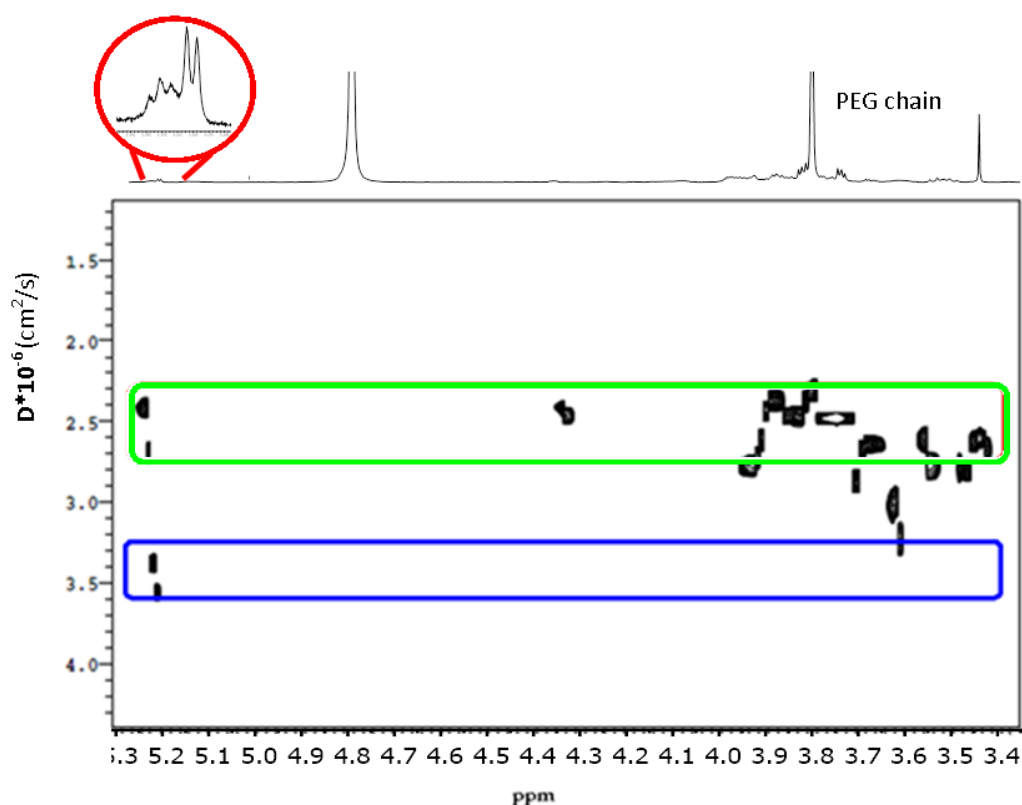


Figure 2.13. DOSY plot of the PEGDA-ethylenediamine-maltose co-polymer. The red circle shows the enlarged section of the ^1H NMR spectrum of the PEGDA-ethylenediamine-maltose co-polymer containing the C1' signal. The green rectangle highlights the resonances of the protons that belong to the PEGDA-ethylenediamine-maltose co-polymer. The blue rectangle highlights the resonances of the protons that belong to the maltose-ethylenediamine dimer. Data recorded in D_2O at 700 MHz.

To facilitate the identification of the target signal, the red circle of Figure 2.13 shows the enlarged section between $\delta 5.15$ - 5.30 of the ^1H NMR spectrum of the co-polymer. Since the sample analysed is disperse, the 2D DOSY NMR spectrum shows a distribution of diffusion coefficients instead of single peaks. From the 2D DOSY NMR spectrum of the PEGDA-ethylenediamine-maltose co-polymer, two diffusion coefficients can be identified for the resonance at $\delta 5.24$, thus there are two species in the system containing maltose. The blue and green rectangles of Figure 2.13 isolate the resonances of the protons that belong to each species. It is possible to notice that the species with the lower diffusion coefficient (green rectangle of Figure 2.13), thus possessing higher molecular weight, contains both PEG and maltose. The resonance at $\delta 5.24$ and the resonance of the protons of the PEG chain at $\delta 3.80$ correlate with the same diffusion coefficient D ($2.5 \times 10^{-6} \text{ cm}^2/\text{s}$). Therefore, maltose and PEG are part of the same compound. The resonances highlighted in the red rectangle belong to protons of in the PEGDA-ethylenediamine-maltose co-polymer.

Furthermore, Figure 2.13 shows that there is a second component containing maltose in the sample when analysed via 2D DOSY NMR. The second species (blue rectangle in Figure 2.13) possesses a diffusion coefficient higher than the co-polymer, indicating it has a lower molecular weight and lower hydrodynamic volume. The diffusion coefficient D of maltose in water is $4.8 \times 10^{-6} \text{ cm}^2/\text{s}$ ^[15], while the diffusion coefficient for the second species in Figure 2.13 (blue rectangle) is $3.5 \times 10^{-6} \text{ cm}^2/\text{s}$. Therefore, the second component containing maltose is not unreacted maltose. The lower value of diffusion coefficient suggests this second component has a higher molecular weight than maltose.

It is supposed that the second maltose containing species in the sample analysed could be a dimer formed between ethylenediamine and maltose. Upon de-protection of the second amine functionality of poly(β -amino ester) with TFA, the excess of N-Boc-ethylenediamine present in the mixture was also de-

protected. Therefore, in presence of NaCNBH_3 and an excess of maltose, ethylenediamine could have reacted to form a dimer. The structure of the maltose-ethylenediamine dimer is shown in Figure 2.14.

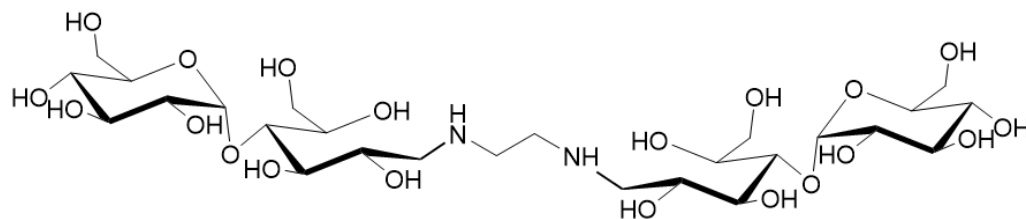


Figure 2.14. Structure of the dimer between ethylenediamine and maltose.

A possible way to remove the maltose dimer could be by dialysis, using a membrane that selectively separated the species with a molecular weight lower than the molecular weight of the dimer (712 g/mol).

2.4. Conclusions

In conclusion, the synthetic strategy discussed in this chapter led to the successful synthesis of a co-polymer between PEGDA-ethylenediamine-maltose with the potential application as SRP for cotton fibres in a three step process.

As the first step of the procedure involved the use of an expensive mono-protected amine, a model polymerisation with the cheaper hexylamine was conducted to investigate the best conditions for the step growth polymerisation between PEGDA and ethylamine. From this study it was found that the use of DCM as solvent for the reaction facilitates the step growth polymerisation reaction, possibly by enhancing the solubility of the amine monomer.

However, the optimal reaction conditions for the model reaction were not suitable for the polymerisation of PEGDA and N-Boc-ethylenediamine, as lower values of DP_n were achieved. It is possible that the difficulties in weighting small amount of material very accurately affected the outcome of the polymerisation reaction. Therefore, the step growth polymerisation of PEGDA and N-Boc-ethylenediamine was carried out in bulk. The poly(β -amino ester) synthesised in bulk from PEGDA M_n 700 g/mol and N-Boc-ethylenediamine possessed a M_n of 8500 g/mol and DP_n 10-11 and was used during the next step.

The second step involved the deprotection of the pendant amine functionality with TFA in DCM, upon end capping of the unreacted acrylate groups with N-Boc-ethylenediamine to avoid the formation of cross-linked structures.

The co-polymer PEGDA-ethylenediamine-maltose of Figure 2.3 was then obtained through reaction of the de-protected poly(β -amino ester) with maltose. The structure was confirmed via 1H , ^{13}C , and DOSY NMR spectroscopy.

Since the synthetic procedure for the synthesis of the PEGDA-ethylenediamine-maltose co-polymer comprised too many steps, the material is likely to be unfeasible for commercial applications. However, it demonstrated the possibility of producing efficiently functionalised amphiphilic co-polymers.

The next chapter will focus on the synthesis and characterisation of co-polymers comprising carboxymethyl cellulose (CMC) and PEG, in an attempt to yield a potential SRP for cellulosic surfaces.

2.5. References

1. McCall, E. R.; Jurgens, J. F. *Textile Research Journal* **1951**, 21, 19-21.
2. Zhou, Q.; Greffe, L.; Baumann, M. J.; Malmstrom, E.; Teeri, T. T.; Brumer III, H. *Macromolecules* **2005**, 38, 3547-3549.
3. Kargl, R.; Mohan, T.; Bracic, M.; Kulterer, M.; Doliska, A.; Stana-Kleinschek, K.; Ribitsch, V. *Langmuir: The ACS Journal of Surface and Colloids* **2012**, 28, (31), 11440-11447.
4. McIntyre, J. E.; Robertson, M. M. *Modifying Treatment of Shaped Articles Derived from Polyesters*. 1967.
5. Inoue, K. *Progress in Polymer Science* **2000**, 25, 453-571.
6. Lynn, D. M.; Langer, R. *Journal of American Chemical Society* **2000**, 122, 10761-10768.
7. Gao, C.; Tang, W.; Yan, D. *Journal of Polymer Science Part A: Polymer Chemistry* **2002**, 40, 2340-2349.
8. Chen, J.; Huang, S.-W.; Liu, M.; Zhuo, R.-X. *Polymer* **2007**, 48, (3), 675-681.
9. Safranski, D. L.; Lesniewski, M. A.; Caspersen, B. S.; Uriarte, V. M.; Gall, K. *Polymer* **2010**, 51, (14), 3130-3138.
10. Song, W.; Tang, Z.; Li, M.; Lv, S.; Yu, H.; Ma, L.; Zhuang, X.; Huang, Y.; Chen, X. *Macromolecular Bioscience* **2012**, 12, 1375-1383.
11. Anderson, D. G.; Lynn, D. M.; Langer, R. *Angewandte Chemie* **2003**, 42, (27), 3153-8.
12. Mather, B. D.; Viswanathan, K.; Miller, K. M.; Long, T. E. *Progress in Polymer Science* **2006**, 31, (5), 487-531.
13. Bigge, J. C.; Patel, T. P.; Bruce, J. A.; Goulding, P. N.; Charles, S. M.; Parekh, R. B. *Analytical Biochemistry* **1995**, 230, 229-238.
14. Johnson, C. S. J. *Progress in Nuclear Magnetic Resonance Spectroscopy* **1999**, 34, 203-256.
15. Uedaira, H.; Uedaira, H. *Bullettin of the Chemical Society of Japan* **1969**, 42, 2140-2142.

2.6. Appendix A

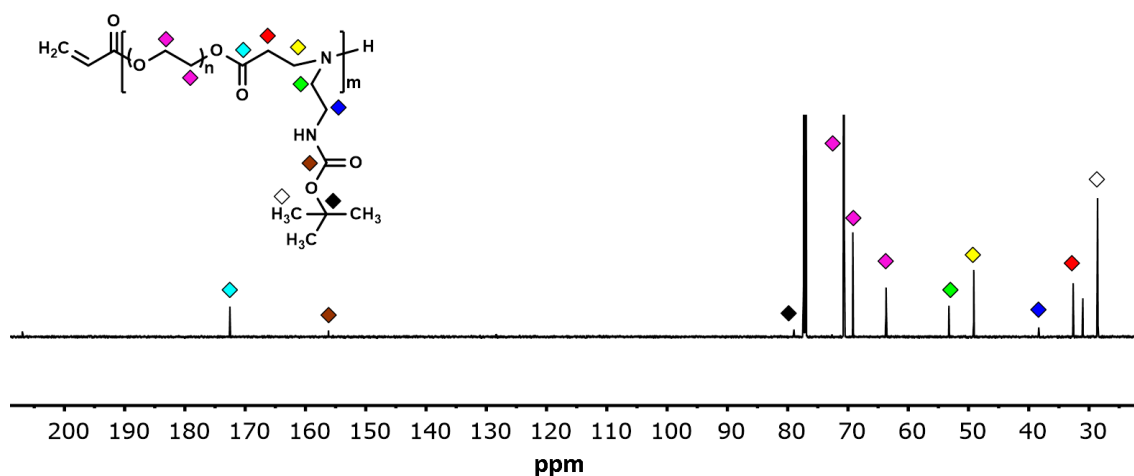


Figure 2.15. ^{13}C NMR spectrum of PEGDA-N-Boc-ethylenediamine poly(β -amino ester) co-polymer synthesised in bulk. Spectrum recorded at 700 MHz in CDCl_3 .

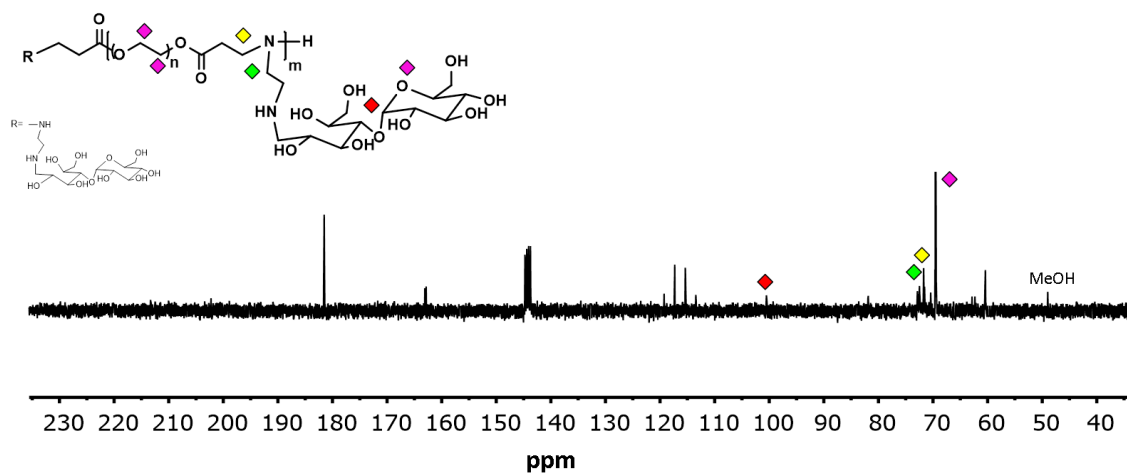


Figure 2.16. ^{13}C NMR spectrum of PEGDA-ethylenediamine-maltose co-polymer. Spectrum recorded in D_2O at 700 MHz.

3

Functionalization of carboxymethyl cellulose

3.1. Introduction

Upon removal of the stain from the fabric surface, promoted by the surfactants contained in the laundry detergent formulation, it is important that the stain does not re-deposit over the surface. The re-deposition of removed stains during a wash cycle leads to the greying of the textile surface over time. Sodium carboxymethyl cellulose (CMC) is currently used in laundry detergents as an anti-redeposition agent to prevent the redeposition of stains back onto a cotton surface during a wash cycle^[1].

CMC can adsorb onto a cotton surface due to affinity between the CMC polymer backbone and the cotton fabric (Chapter 1, sections 1.2 and 1.3). CMC is a non-toxic derivative of cellulose in which a proportion of the hydroxyl

groups on the polymeric backbone have been substituted with carboxymethyl groups (Figure 3.1).

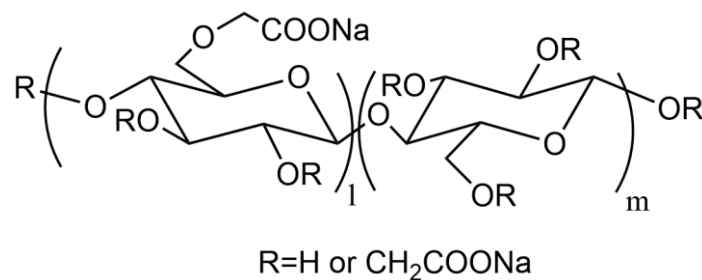


Figure 3.1. Structure of the sodium salt of carboxymethyl cellulose.

When dissolved in water during a wash cycle, the hydroxyl groups of the CMC backbone are partially deprotonated. Hence, upon adsorption of CMC, the surface of the fibre becomes negatively charged. Since the stains removed are usually surrounded by the anionic surfactants contained in the laundry detergent, the CMC layer adsorbed over cotton surface can prevent their re-deposition due to electrostatic repulsion^[1].

The adsorption of CMC onto cotton fibre is also promoted by the presence of surfactants during the wash cycle^[2]. The surfactants form aggregates with CMC, which have a higher affinity for cotton surface than the CMC alone. The interaction between the aggregates and the textile surface combined with the high structural affinity between CMC and cotton fibre prevents desorption of CMC from the fabric surface^[2]. Hence CMC can act only as an anti-redeposition agent and not a SRP.

Because the SRPs developed for synthetic fibres are not effective toward natural fibres^[3], a new class must be developed in order to apply the soil release technology to natural materials such as cotton. The interaction between CMC and cotton surfaces could be exploited to apply CMC as a potential SRP for cotton surfaces, however, the strength of this interaction must be modified to promote the desorption process. A possible way to tune the affinity of CMC for

cotton surface is to modify the polymer backbone. One approach could be the introduction of a component with affinity for the washing liquor, which should (in theory) promote desorption of the CMC from cotton surface. A possible candidate may be poly(ethylene glycol) (PEG). PEG is a water-soluble polymer with high compatibility with laundry detergents, low toxicity and a relatively low cost. By grafting PEG onto the CMC polymer backbone, the resulting modified CMC co-polymer may have improved affinity for the washing liquor, therefore promoting the desorption process and giving the polymer soil release properties.

In this chapter, the synthesis and characterization of CMC-g-PEG co-polymers will be discussed. A series of co-polymers have been synthesised via an amidation reaction between amino poly(ethylene glycol) methyl ether and CMC as the tetrabutylammonium salt. A series of co-polymers were synthesised by varying both the number of PEG chains grafted and the M_n of the PEG graft. Furthermore, the synthesis and characterisation of four amino poly(ethylene glycol) methyl ether precursor with increasing M_n will also be described.

Finally, in a preliminary study to quantify the amount of co-polymer adsorbed and desorbed during every washing cycle, two CMC-g-PEG co-polymers and two types of unmodified CMC were labelled with a fluorescent dye. The synthesis and the characterisation of the fluorescently labelled polymers will be discussed in this chapter. Moreover, the use of fluorescence spectroscopy allowed the determination of the degree of labelling of the polymeric backbone.

3.2. Experimental section

3.2.1. *Materials*

Poly(ethylene glycol) methyl ether (M_n 2000 g/mol, M_n 5000 g/mol and M_n 10000 g/mol), triphenylphosphine (purity \geq 95.0%), benzene (purity \geq 99.9%), dichloromethane (purity \geq 99.5%), tetrabromomethane (purity \geq 99%), chloroform (purity \geq 99.5%), magnesium sulphate (purity \geq 99.5%), diethyl ether (purity \geq 99.7%), dimethylformamide (anhydrous, purity \geq 99.8%), sodium azide (purity \geq 99.5%), toluene (purity \geq 99.8%), tetrabutylammonium hydroxide (purity \geq 98.0%), 2-chloro-1-methylpyridinium iodide (purity \geq 97%) and triethylamine (purity \geq 99.5%) were purchased from Sigma Aldrich and used as received unless specified below. CMC was supplied by P&G®. Deuterated chloroform (purity \geq 99.8%) and deuterated water (purity \geq 99.9%) were supplied by Goss Scientific. Poly(ethylene glycol) methyl ether and triphenylphosphine were azeotropically dried with benzene before use. Benzene and dichloromethane were dried over calcium hydride and stored under vacuum. Dimethylformamide was dried over molecular sieves (pellets, pore size 3 Å) and stored under nitrogen. Diethyl ether was dried over sodium wire and sodium benzophenone and stored under vacuum. Deuterated chloroform was stored over molecular sieves (pellets, pore size 3 Å).

3.2.2. *Analysis*

3.2.2.1. Potentiometric titration

The titration data were collected using a Jenway 3510 pH meter, equipped with a combined electrode.

The following procedure was used to determine the degree of substitution (DS) of CMC. The sodium salt of CMC was converted to the acidic form by an ion exchange resin (Dowex Monosphere 650C) overnight, freeze-dried into a white solid then dispersed in deionised water at 25 °C. The direct titration was conducted in the presence of a known amount of a 0.1 M NaCl and a 0.1 M solution of HCl. The HCl solution was previously standardised against Na₂CO₃ and used to determine the concentration of the solution of the titrant NaOH. The back titration was conducted with a 0.1 M solution of HCl in presence of an excess of NaOH. The system was allowed to stabilize for 2 hours before each titration and 10 minutes between each 0.2 mL addition of titrant.

3.2.2.2. ¹³C solid state NMR spectroscopy

Solid-state NMR spectra were recorded in collaboration with the EPSRC UK National Solid-state NMR Service at Durham.

The spectra were recorded at room temperature (25 °C) using a Varian VNMRS Spectrometer equipped with a 6 mm (rotor o.d.) magic-angle spinning probe. The frequency used for the ¹³C NMR spectra was approximately 100 MHz. The data were collected using a cross-polarisation with 5 or 10 recycle delay and 1 ms of contact time. The samples were spun at 6.8 kHz.

An external standard of tetramethylsilane was used as reference in the ¹³C spectra.

3.2.2.3. PFG NMR spectroscopy and ¹H gel state NMR spectroscopy

Gel-state NMR spectroscopy and Pulse field gradient NMR spectroscopy were carried out at the EPSRC UK National Solid-state NMR Service at Durham.

The experiments were carried out in D₂O at room temperature. Disposable rotor inserts were used to prepare the samples. The samples were prepared by adding approximately 1 mg of cellulose derivative (CMC or CMC-g-PEG co-polymer) to the insert and approximately 25 mg of D₂O.

The samples were spun at 4 kHz. The probe used was a 4 mm HR-MAS equipped with a deuterium lock. The gradient pulses were 4 ms in duration. An LED-bipolar sequence was used. The diffusion observation time was 200 ms, the recycle delay was 3 s. The 90° pulse width was 3.75 μs. A total of 128 data points were acquired in the PFG NMR experiments for each sample. The number of scans for each point was 48. For each CMC derivative analysed, three disposable rotor inserts were prepared.

3.2.2.4. ¹³C and ¹H NMR spectroscopy in solution

The ¹H NMR spectra were measured with a Varian VNMRS 700 MHz or Bruker DRX-400 MHz spectrometer using CDCl₃ as solvent.

3.2.2.5. Size exclusion chromatography (SEC)

The M_n values of the PEG-OH samples were determined by a conventional calibration created using poly(ethylene glycol) (PEG) standards (Polymer Labs). The chromatograms were recorded using a refractive index detector. Two PLgel 5 μm mixed B columns were used. The eluent was dimethylformamide (DMF) containing 0.1% of lithium bromide, the flow rate was 1.0 mL/min and the column was maintained at a temperature of 70 °C.

The CMC-g-PEG co-polymers were analysed using a triple detector calibration based on one polystyrene (PS) standard of M_n 66000 g/mol.

3.2.2.6. Fluorescence spectroscopy

The spectrofluorimeter used to measure the fluorescence of the washing liquor was a Molecular Device Spectramax M2. The fluorescence was measured at 5 nm intervals in the range of 500 nm to 700 nm. The excitation wavelength used was 494 nm.

3.2.3. Synthesis of poly(ethylene glycol) methyl ether bromide

Poly(ethylene glycol) methyl ether (PEG-OH) (21.95 g, 0.011 mol) and triphenylphosphine (PPh₃) (8.71 g, 0.033 mol) in a ratio of 1:3 with respect to the hydroxyls groups were azeotropically dried three times with benzene under vacuum in a round bottom flask. Then, the reaction mixture was dissolved in dry dichloromethane (DCM) (200 mL) and cooled to 0 °C in an ice bath. The subsequent addition of a solution of tetrabromomethane (CBr₄) (13.64 g, 0.041 mol) in dry DCM (20 mL) in a ratio of 1:3.75 with respect to the hydroxyls groups under vigorous stirrer resulted in a change of colour from pale yellow to orange. The reaction was allowed to proceed overnight, and the progress was checked by ¹H and ¹³C NMR spectroscopy in CDCl₃.

Upon completion of the reaction, the following purification procedure was used:

- For poly(ethylene glycol) methyl ether bromide 2000 g/mol (**1**), the DCM was removed by rotary evaporator and replaced with an equal volume of water (220 mL). Upon addition of water, PPh₃O precipitated as a white solid and was filtered out. The aqueous filtrate was extracted with chloroform (CHCl₃) (3x25 mL) in a separatory funnel. The organic fractions were collected and dried over MgSO₄. The solvent was

removed by rotary evaporator and the resulting product was characterized by ^1H and ^{13}C NMR spectroscopy in CDCl_3 .

(1) Yellow solid, ^1H NMR (CDCl_3 , 700 MHz): δ_{H} 3.36 (3H, s, $\text{H1}'$, $\text{H1}''$ and $\text{H1}'''$), 3.45 (2H, t, $J=7.0$ Hz, $\text{H6}'$ and $\text{H6}''$), 3.53 (2H, t, $J=5.6$ Hz, $\text{H2}'$ and $\text{H2}''$), 3.60-3.65 (180H, m, $\text{H3}'$, $\text{H3}''$, $\text{H4}'$, $\text{H4}''$, $\text{H4}'''$ and $\text{H4}''''$), 3.79 (2H, t, $J=7.0$ Hz, $\text{H5}'$ and $\text{H5}''$). ^{13}C NMR (CDCl_3 , 700 MHz): δ_{C} 30.3 (1C, s, C6), 58.9 (1C, s, C1), 70.5-70.7 (45C, m, C3, C4' and C4''), 71.2 (1C, s, C5), 71.9 (1C, s, C2). Yield=99%

- For poly(ethylene glycol) methyl ether bromide M_n 5000 g/mol **(2)** and 10000 g/mol **(3)**, the DCM was removed by rotary evaporator and replaced with an equal volume of water (220 mL). The aqueous phase was extracted with CHCl_3 (3x25 mL) in a separatory funnel. The organic layers were combined in one flask, dried over MgSO_4 and concentrated with a rotary evaporator. The polymer was precipitated three times from diethyl ether (3x500 mL) as a white solid and characterized by ^1H and ^{13}C NMR spectroscopy in CDCl_3 .

(2) Yellow solid, ^1H NMR (CDCl_3 , 700 MHz): δ_{H} 3.37 (3H, s, $\text{H1}'$, $\text{H1}''$ and $\text{H1}'''$), 3.46 (2H, t, $J=7.0$ Hz, $\text{H6}'$ and $\text{H6}''$), 3.54 (2H, t, $J=7.0$ Hz, $\text{H2}'$ and $\text{H2}''$), 3.60-3.65 (465H, m, $\text{H3}'$, $\text{H3}''$, $\text{H4}'$, $\text{H4}''$, $\text{H4}'''$ and $\text{H4}''''$), 3.80 (2H, t, $J=7.0$ Hz, $\text{H5}'$ and $\text{H5}''$). ^{13}C NMR (CDCl_3 , 700 MHz): δ_{C} 30.5 (1C, s, C6), 59.2 (1C, s, C1), 70.5-70.7 (226C, m, C3, C4' and C4''), 71.3 (1C, s, C5), 72.1 (1C, s, C2). Yield= 99%

(3) White solid, ^1H NMR (CDCl_3 , 700 MHz): δ_{H} 3.35 (3H, s, $\text{H1}'$, $\text{H1}''$ and $\text{H1}'''$), 3.44 (2H, t, $J=7.0$ Hz, $\text{H6}'$ and $\text{H6}''$), 3.50-3.53 (2H, m, $\text{H2}'$ and $\text{H2}''$), 3.60-3.65 (846H, m, $\text{H3}'$, $\text{H3}''$, $\text{H4}'$, $\text{H4}''$, $\text{H4}'''$ and $\text{H4}''''$), 3.78 (2H, t, $J=7.0$ Hz, $\text{H5}'$ and $\text{H5}''$). ^{13}C NMR (CDCl_3 , 700 MHz): δ_{C} 30.4 (1C, s, C6), 59.1 (1C, s, C1), 70.5-70.7 (423C, m, C3, C4' and C4''), 71.3 (1C, s, C5), 72.0 (1C, s, C2). Yield=99%

3.2.4. *Synthesis of poly(ethylene glycol) methyl ether azide*

Poly(ethylene glycol) methyl ether bromide (21.69 g, 0.011 mol) was added to a round bottom flask and azeotropically dried with benzene (3x20 mL). Dry DMF (140 mL) was added, then the reaction was stirred under nitrogen flow and heated at 50 °C with an oil bath before the addition of NaN₃ (2.89 g, 0.044 mol) in a ratio of 1:3 with respect to the bromide groups. The progress of the reaction was checked by ¹H and ¹³C NMR spectroscopy in CDCl₃.

Upon completion of the reaction, the following purification procedure was used:

- For poly(ethylene glycol) methyl ether azide 2000 g/mol (**1**), the DMF was distilled under vacuum and replaced with an equal volume of water (140 mL). The water phase was extracted with CHCl₃ (3x25 mL). The organic fractions were collected in one flask, dried over MgSO₄ and concentrated with rotary evaporator. The resulting product was characterized by ¹H and ¹³C NMR spectroscopy in CDCl₃.

(**1**) Yellow solid, ¹H NMR (CDCl₃, 700 MHz): δ_H 3.36 (3H, s, H1', H1'' and H1'''), 3.36-3.38 (2H, m, H6' and H6''), 3.52-3.54 (2H, m, H2' and H2''), 3.62-3.65 (185H, m, H3', H3'', H4', H4'', H4''', H4''', H5' and H5''). ¹³C NMR (CDCl₃, 700 MHz): δ_C 50.7 (1C, s, C6), 59.0 (1C, s, C1), 70.0 (1C, s, C5), 70.5-70.7 (89C, m, C3, C4' and C4''), 71.9 (1C, s, C2).
Yield= 98%

- For poly(ethylene glycol) methyl ether azide M_n 5000 g/mol (**2**), the DMF was distilled under vacuum and replaced with an equal volume of DCM (140 mL). The polymer was precipitated from diethyl ether (3x700 mL) as a white solid and characterized by ¹H and ¹³C NMR spectroscopy in CDCl₃.

(2) White solid, ^1H NMR (CDCl_3 , 700 MHz): δ_{H} 3.35 (3H, s, H1', H1'' and H1'''), 3.35-3.37 (2H, m, H6' and H6''), 3.51-3.53 (2H, m, H2' and H2''), 3.60-3.63 (486H, m, H3', H3'', H4', H4'', H4''', H4''''', H5' and H5''). ^{13}C NMR (CDCl_3 , 700 MHz): δ_{C} 50.6 (1C, s, C6), 59.0 (1C, s, C1), 69.9 (1C, s, C5), 70.4-70.7 (241C, m, C3, C4' and C4''), 71.9 (1C, s, C2). Yield= 98%

- For poly(ethylene glycol) methyl ether azide M_n 10000 g/mol (3), the polymer was precipitated from diethyl ether (3x700 mL) as a white solid. The solid was recovered, dissolved in DCM (100 mL) and precipitated a second time from diethyl ether (1 L). The resulting product was characterized by ^1H and ^{13}C NMR spectroscopy in CDCl_3 .

(3) White solid, ^1H NMR (CDCl_3 , 700 MHz): δ_{H} 3.31 (3H, s, H1', H1'' and H1'''), 3.31-3.33 (2H, m, H6' and H6''), 3.47-3.49 (2H, m, H2' and H2''), 3.56-3.60 (730H, m, H3', H3'', H4', H4'', H4''', H4''''', H5' and H5''). ^{13}C NMR (CDCl_3 , 700 MHz): δ_{C} 50.6 (1C, s, C6), 58.9 (1C, s, C1), 69.9 (1C, s, C5), 70.4-70.7 (363C, m, C3, C4' and C4''), 71.8 (1C, s, C2). Yield= 99%

3.2.5. *Synthesis of amino poly(ethylene glycol) methyl ether*

Poly(ethylene glycol) methyl ether azide (21.26 g, 0.011 mol) was dissolved in dry diethyl ether (150 mL) under a nitrogen flow in a three neck round bottom flask. The solution was cooled to 0 °C with an ice bath before the addition of PPh_3 (34.13 g, 0.13 mol) in a ratio of 1:12 with respect to the azide groups. The reaction was allowed to warm up at room temperature and left for 5 hours before the addition of water (30 mL) in a ratio of 3:1 with respect to the amount of diethyl ether. The progress of the reaction was checked by ^1H and ^{13}C NMR spectroscopy in CDCl_3 .

Upon completion of the reaction, the following purification procedure was used:

- For amino poly(ethylene glycol) methyl ether M_n 2000 g/mol (**1**), benzene was added (150 mL) in a ratio of 1:1 with respect to the amount of diethyl ether and the reaction was stirred overnight. The water phase was isolated, washed with toluene (3x100 mL) in a separatory funnel and freeze dried into the desired product. The product was characterized by ^1H and ^{13}C NMR spectroscopy in CDCl_3 .

(**1**) Yellow solid, ^1H NMR (CDCl_3 , 700 MHz): δ_{H} 2.98 (1H, t, $J = 7.0$ Hz, H6' and H6''), 3.35 (3H, s, H1', H1'' and H1'''), 3.51-3.53 (2H, m, H2' and H2''), 3.60-3.63 (187H, m, H3', H3'', H4', H4'', H4''', H4''', H5' and H5''). ^{13}C NMR (CDCl_3 , 700 MHz): δ_{C} 41.1 (1C, s, C6), 59.0 (1C, s, C1), 61.7 (1C, s, C5), 70.4-70.6 (92C, m, C4' and C4''), 71.9 (1C, s, C2).
Yield= 97%

- For the synthesis of amino poly(ethylene glycol) methyl ether M_n 5000 g/mol (**2**) and M_n 10000 g/mol (**3**), dry DCM (150 mL) was used as the solvent for the reaction instead of dry diethyl ether and the same procedure was followed. Upon completion of the reaction, benzene was added (150 mL) in a ratio of 1:1 with respect to the amount of DCM and the reaction was stirred overnight. The water and the organic phase were separated with a separatory funnel and treated separately to recover the polymer. The water phase was washed with toluene (3x100 mL) and freeze dried into a white solid. The organic phase was concentrated with a rotary evaporator and the polymer was precipitated from diethyl ether (500 mL) as a white solid. For further purification, the polymer was dissolved in CHCl_3 (25 mL) and precipitated from diethyl ether (3x250 mL). The polymer recovered from the water phase was combined

with the one recovered from the organic phase and characterized by ^1H and ^{13}C NMR spectroscopy in CDCl_3 .

(2) White solid, ^1H NMR (CDCl_3 , 700 MHz): δ_{H} 2.96 (2H, t, $J = 7.0$ Hz, $\text{H6}'$ and $\text{H6}''$), 3.35 (3H, s, $\text{H1}'$, $\text{H1}''$ and $\text{H1}'''$), 3.51-3.53 (2H, m, $\text{H2}'$ and $\text{H2}''$), 3.60-3.65 (469H, m, $\text{H3}'$, $\text{H3}''$, $\text{H4}'$, $\text{H4}''$, $\text{H4}'''$, $\text{H4}''''$, $\text{H5}'$ and $\text{H5}''$). ^{13}C NMR (CDCl_3 , 700 MHz): δ_{C} 41.3 (1C, s, C6), 59.0 (1C, s, C1), 70.4-70.7 (234H, m, C3, C4', C4'', C5), 71.9 (1C, s, C2). Yield= 98%

(3) White solid, ^1H NMR (CDCl_3 , 700 MHz): δ_{H} 3.32 (3H, s, $\text{H1}'$, $\text{H1}''$ and $\text{H1}'''$), 3.56-3.62 (880H, m, $\text{H2}'$, $\text{H2}''$, $\text{H3}'$, $\text{H3}''$, $\text{H4}'$, $\text{H4}''$, $\text{H4}'''$, $\text{H4}''''$, $\text{H5}'$ and $\text{H5}''$). ^{13}C NMR (CDCl_3 , 700 MHz): δ_{C} 58.9 (1C, s, C1), 70.4-70.8 (440C, m, C3, C4', C4'', C5), 71.9 (1C, s, C2). Yield= 98%

3.2.6. Synthesis of CMC-g-PEG co-polymers

Carboxymethyl cellulose sodium salt (CMC) (2.0 g, 7.38 mequ) was dissolved in deionized water (1% w/v solution) then Dowex monosphere 650C resin was added and the mixture was stirred overnight. The ion exchange resin was removed through a sieve and tetrabutylammonium hydroxide (5% w/v solution in deionized water) was added under vigorous stirring until pH 8-9 was attained. The reaction was carried out overnight at room temperature and the tetrabutylammonium salt of carboxymethyl cellulose (TBA-CMC) was recovered from the solution by lyophilisation.

The following general procedure was used for the synthesis of CMC-g-PEG samples.

TBA-CMC was dissolved in anhydrous DMF (180 mL) under vigorous stirring and flow of nitrogen. The solution was cooled to 0 °C using an ice bath before the addition of 2-chloro-1-methylpyridinium iodide (CMP-I) (114 mg, 0.446 mmol), the amount of which depended on the number of carboxymethyl

groups to be activated. The reaction was warmed up to room temperature before the addition of PEG-NH₂ (0.9 g, 0.45 mmol), in a ratio 1:1 with respect to the carboxymethyl groups activated, and triethylamine (10 mL).

Different reaction conditions were used for the synthesis of CMC-g-PEG co-polymers, in an attempt to improve the yield of amide formation.

Table 3-1. Reaction conditions for the synthesis of CMC-g-PEG co-polymers.

Sample code	Temperature (°C)	Time (h)	Yield (%)
CMC-g-PEG_2K_9.5	25	24	56
CMC-g-PEG_2K_23.7	25	4	58
CMC-g-PEG_2K_42.8	25	20	57
CMC-g-PEG_2K_50.4	25	96	60
CMC-g-PEG_2K_56.1	25	120	65
CMC-g-PEG_2K_62.5	25	144	70
CMC-g-PEG_5K_19.0	25	96	54
CMC-g-PEG_5K_51.1	25	144	59
CMC-g-PEG_5K_55.6	25	168	61
CMC-g-PEG_5K_63.7	25	7	65
CMC-g-PEG_10K_76.5 *	50	144	65
CMC-g-PEG_10K_84.5 *	50	144	68
CMC-g-PEG_10K_85.8 *	50	144	66

* PEG-NH₂10K was azeotropically dried three times with benzene and dissolved in a small volume of dried DMF before addition to the reaction.

The synthesised CMC-g-PEG co-polymer was recovered by precipitation from diethyl ether. The precipitate was filtered and purified by different procedures:

- Samples CMC-g-PEG_2K_42.8, CMC-g-PEG_5K_19.0, CMC-g-PEG_2K_50.4, CMC-g-PEG_2K_56.1 and CMC-g-PEG_5K_51.1 were purified by soxhlet extraction with chloroform for two days.
- Samples CMC-g-PEG_2K_9.5, CMC-g-PEG_2K_23.7, CMC-g-PEG_2K_62.5, CMC-g-PEG_5K_55.6, CMC-g-PEG_5K_63.7, CMC-g-PEG_10K_84.5, CMC-g-PEG_10K_76.5 and CMC-g-PEG_10K_76.5 were dialysed against a 0.1 M solution of NaCl at room temperature until no PEG-NH₂ was found in the dialysis liquor. The polymers were then recovered by lyophilisation.

All the samples were characterised by ¹³C solid state NMR spectroscopy, gel state ¹H NMR spectroscopy in D₂O, PFG NMR analysis and SEC in DMF.

¹³C NMR (100 MHz): δ_C 70.9 (92C, s, C9 and C10), 104.6 (2C, s, C1 and C1'), 63.7 (2C, s, C6 and C6'), 70.0-80.0 (10C, m, C2, C2', C3, C3', C4, C4', C5, C5', C7 and C7'), 171.7 (1C, s, C8), 177.9 (1C, s, C8').

N.B. C1-C8 belong to the glucose unit modified with PEG. C1'-C7' belong to carboxylated and non-carboxylated glucose units. The resonances reported above for sample CMC-g-PEG_2K_62.5 are also valid for all the CMC-g-PEG co-polymers synthesised.

3.2.7. Labelling of CMC and CMC derivative

The same procedure was used for the labelling of the unmodified CMCs samples and the labelling of the CMC-g-PEG co-polymers.

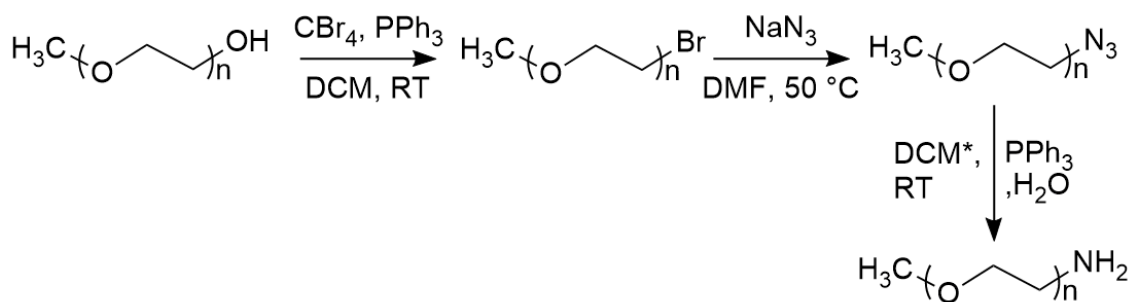
The cellulose derivative was dissolved in deionised water under vigorous stirring in order to obtain a 1% w/v solution. The pH was adjusted to 8 by addition of a 0.1 M solution of sodium hydroxide. 5-([4,6-dichlorotriazin-2-yl]amino)fluorescein (DTAF) was added and the reaction was allowed to proceed overnight, adjusting the pH to a value of 8. The polymer was purified by dialysis against a 0.1 M solution of NaCl until the dialysed liquor showed no fluorescence. The polymer was then recovered by lyophilisation.

3.3. Results and Discussion

3.3.1. Synthesis of amino poly(ethylene glycol) methyl ether

In order to graft PEG onto the CMC backbone via a reaction with the carboxymethyl groups, it was necessary to introduce a new functionality at the end of the commercially available PEG chain. NH_2 was chosen taking into account the stability of the resulting amide bond between CMC and PEG under the washing conditions, since the stability of the CMC-g-PEG co-polymer is fundamental in order to perform as a SRP. In particular, the pH of the washing liquor played an important role in the choice of the functional group to be introduced at the end of the PEG chain. The typical pH of a laundry detergent is around 8, therefore the subsequent formation of an amide bond through reaction between the amino group introduced to the PEG chain end with the carboxymethyl group of the CMC backbone should ensure a stable SRP at this basic pH.

Amino poly(ethylene glycol) methyl ether was synthesised in three steps from poly(ethylene glycol) methyl ether according to the procedure shown in Scheme 3.1^[4, 5].



Scheme 3.1. Multi-step procedure for the synthesis of amino poly(ethylene glycol) methyl ether. Step 1, yield >99%; step 2, yield >98 %; step 3, yield > 97%. Overall yield=94%. *Diethyl ether was used as solvent instead of dichloromethane (DCM) for poly(ethylene glycol) methyl ether azide M_n 2000 g/mol.

The terminal hydroxyl group of poly(ethylene glycol) methyl ether was first transformed into a bromide group via an Appel reaction in the first step. The subsequent reaction with sodium azide (NaN_3) allowed the introduction of an azide functionality at the end of the chain via an $\text{S}_{\text{N}}2$ mechanism. The azide end group was then reduced to an amine group via the Staudinger reaction during the last step of the process.

The PEG samples synthesised will be referred to with a code containing the end group and the molecular weight of the PEG chain as given by the supplier.

PEG - end group- M_n of the polymer chain given by supplier

For example, poly(ethylene glycol) methyl ether with M_n 2000 g/mol will be referred to as PEG-OH2K, while PEG-OH5K will be used for poly(ethylene glycol) methyl ether with M_n 5000 g/mol.

Prior to reaction, the starting materials PEG-OH were analysed using ^1H and ^{13}C NMR spectroscopy in CDCl_3 , size exclusion chromatography (SEC) in dimethylformamide (DMF) and MALDI spectrometry. Moreover, 2D NMR spectra COSY, HMBC and HSQC in CDCl_3 were also recorded to allow full characterization of the polymers.

The ^1H and ^{13}C NMR spectra for PEG-OH2K are shown in Figure 3.2 and Figure 3.3, respectively. The full ^1H and ^{13}C NMR spectra of PEG-OH5K and PEG-OH10K are reported in Appendix B.

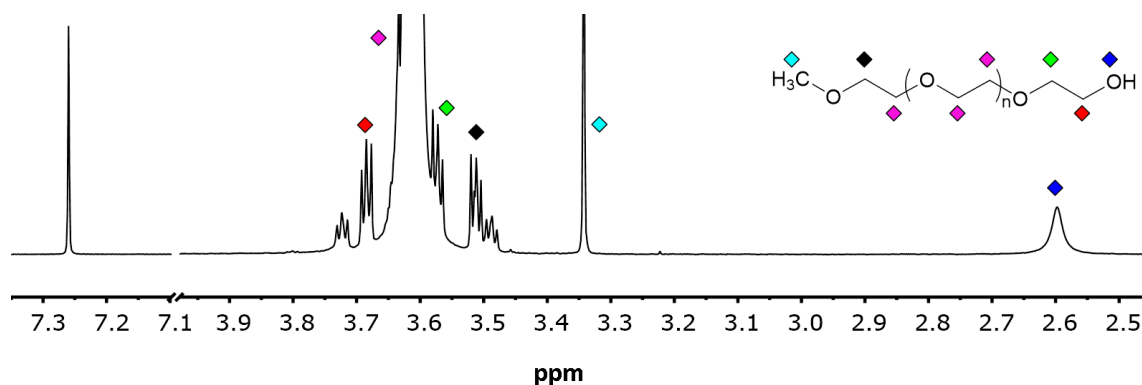


Figure 3.2. ^1H NMR spectrum of PEG-OH2K. Spectrum recorded at 700 MHz in CDCl_3 .

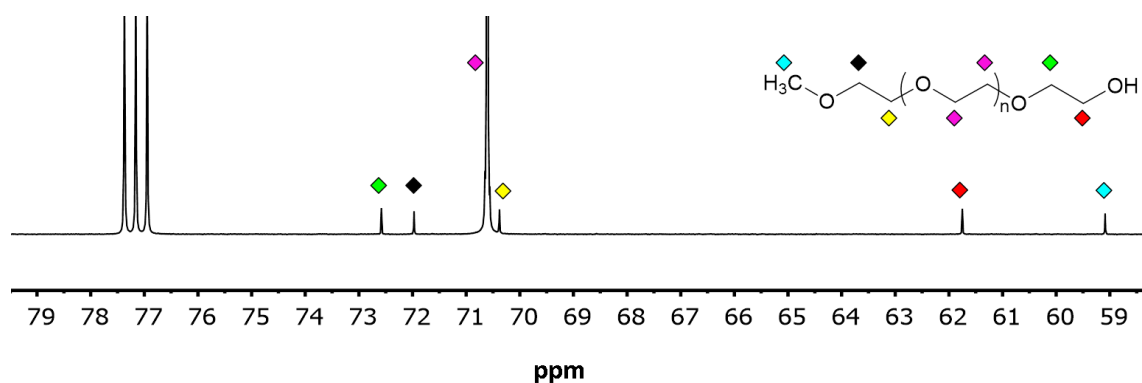


Figure 3.3. ^{13}C NMR spectrum of PEG-OH2K. Spectrum recorded at 700 MHz in CDCl_3 .

The assignment of each resonance of the ^1H and ^{13}C NMR spectra in Figure 3.2 and Figure 3.3 allows the key signals which change as a consequence of the reactions to be monitored.

The average molar mass of the PEG-OH starting materials was determined by ^1H NMR spectroscopy, MALDI mass spectrometry and size exclusion chromatography (SEC).

By ^1H NMR spectroscopy, the number-average mass M_n of the PEG-OH samples was calculated using the value of the integral of the proton resonance for the methyl end group as reference ($\delta 3.33$, turquoise diamond in Figure 3.2) and Equation 1, Equation 2 and Equation 3.

$$\text{Integral per proton} = \frac{\text{integral of end unit}}{n^{\circ} \text{ proton in end unit}}$$

Equation 1.

$$DP_n = \frac{\text{integral of chain} / n^{\circ} \text{ proton in repeating unit}}{\text{integral per proton}}$$

Equation 2.

$$M_n = \text{Sum of FW end groups} + \text{FW repeating unit} * DP_n$$

Equation 3.

Where “FW” is the weight formula of the end group and the repeating unit of the PEG chain respectively and “ DP_n ” is the degree of polymerisation.

By SEC in DMF, the M_n of the PEG-OH starting material was determined against a conventional calibration based on poly(ethylene glycol) standards. The traces obtained for the PEG-OH samples are shown in Figure 3.4.

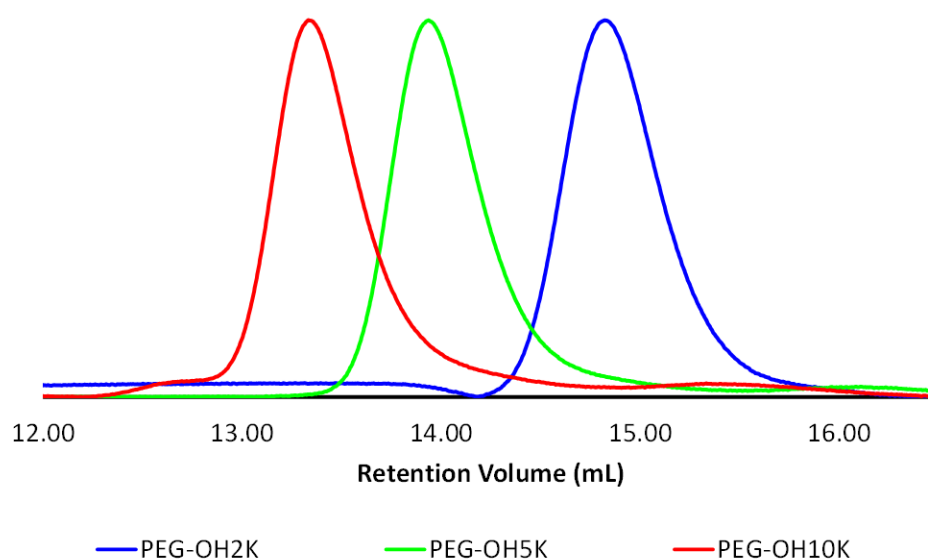


Figure 3.4. SEC traces of PEG-OH starting materials in DMF. Data recorded using a refractive index (RI) detector. The value of M_n was determined against a conventional calibration based on PEG standards.

The M_n values were also determined by MALDI mass spectrometry. The results of the M_n characterisations of the starting material PEG-OHs are summarised in Table 3-2 and show reasonable agreement with the values quoted by the supplier.

Table 3-2. Average M_n of PEG-OH starting materials.

Sample code	M_n (NMR) (g/mol)	M_n (SEC) (g/mol)	M_n (MALDI) (g/mol)
PEG-OH2K	2100	1800	1900
PEG-OH5K	5430	4800	5100
PEG-OH10K	9870	9700	9700

Full NMR analysis for the conversion of PEG-OH2K to PEG-NH₂2K is described in Figure 3.5 and Figure 3.6. The characterisation of PEG-NH₂5K and PEG-NH₂10K was conducted in the same manner and the assigned spectra are included in Appendix B. Through the use of 2D NMR data it was possible to

assign all the peaks in the ^1H NMR spectrum (Figure 3.5) and follow the conversion of the hydroxyl end group into amine. The most important observation to make is the shift of the resonance of the protons in the α and β position with respect to the hydroxyl end group (red and green diamond respectively) as a consequence of the reactions.

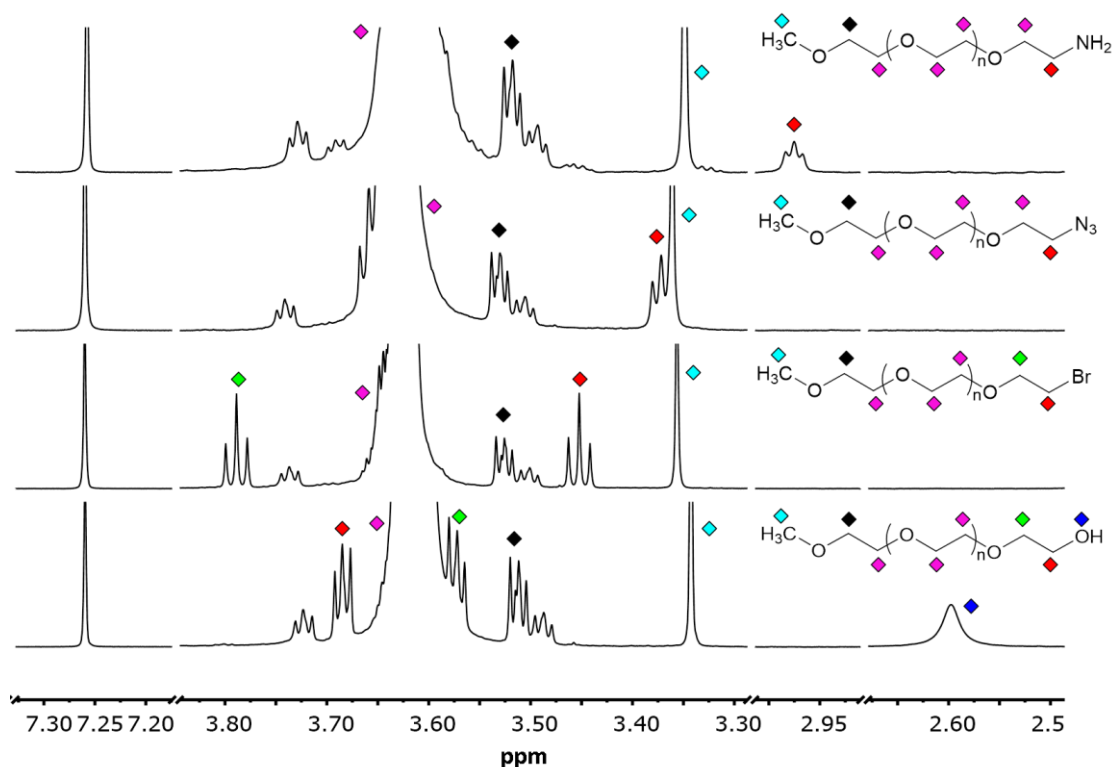


Figure 3.5. Comparison between ^1H NMR spectra of PEG-OH2K, PEG-Br2K, PEG-N₃2K and PEG-NH₂2K. Spectra recorded at 700 MHz in CDCl_3 .

During the first step, PEG-OH and tetrabromomethane (CBr_4) were reacted in dichloromethane (DCM) in the presence of triphenylphosphine (PPh_3) to produce poly(ethylene glycol) methyl ether bromide (PEG-Br). The resonance of the α -protons (red diamond) has shifted from $\delta 3.65$ to $\delta 3.45$, as the hydroxyl group is converted to a bromine group in PEG-Br2K. This shift is due to the lower electron withdrawing effect of the bromine compared with a hydroxyl group, hence the protons adjacent to the end group resonate at lower ppm. The protons in β -position (green diamond) shifted too, from $\delta 3.57$ to $\delta 3.79$.

Then, the bromide group of PEG-Br was converted into an azide functionality via S_N2 reaction with sodium azide in DMF to produce poly(ethylene glycol) methyl ether azide (PEG-N₃). The protons in α -position have shifted again from $\delta 3.45$ to $\delta 3.37$ in the ¹H NMR spectrum of PEG-N₃2K, as a consequence of the substitution reaction. Since the azide group is a nucleophile, it has the effect of pushing sigma electron density onto the hydrogens in the molecule. Moreover, this effect is greater for protons adjacent to the azide group (marked with a red and green diamond). The shift in the resonance of the protons in α and β position causes a merging of the signal of these protons with the resonance of the methyl chain end group ($\delta 3.33$, light blue diamond) and the resonance of the polymer chain ($\delta 3.63$, purple diamond) respectively.

In the final step of the synthesis of amino poly(ethylene glycol) methyl ether (PEG-NH₂), the azide functionality was reduced to amine group via the Staudinger reaction. Once again, the protons in α -position (red diamond) have shifted from $\delta 3.37$ to $\delta 2.97$ due to the reduction of the azide functionality to amine. The shift towards lower ppm is due to the amino group being a weaker electron withdrawing group than the azide group. The amino functionality pushes electron density onto the hydrogens in the molecule. Therefore, the hydrogens resonate at lower ppm. Moreover, this effect is greater for protons adjacent to the amino group (marked with a red diamond). The protons in β -position slightly shift toward higher ppm as the amino group is introduced at the end of the PEG chain.

The conversion from PEG-OH₂K to PEG-NH₂2K was also followed via ¹³C NMR spectra (Figure 3.6).

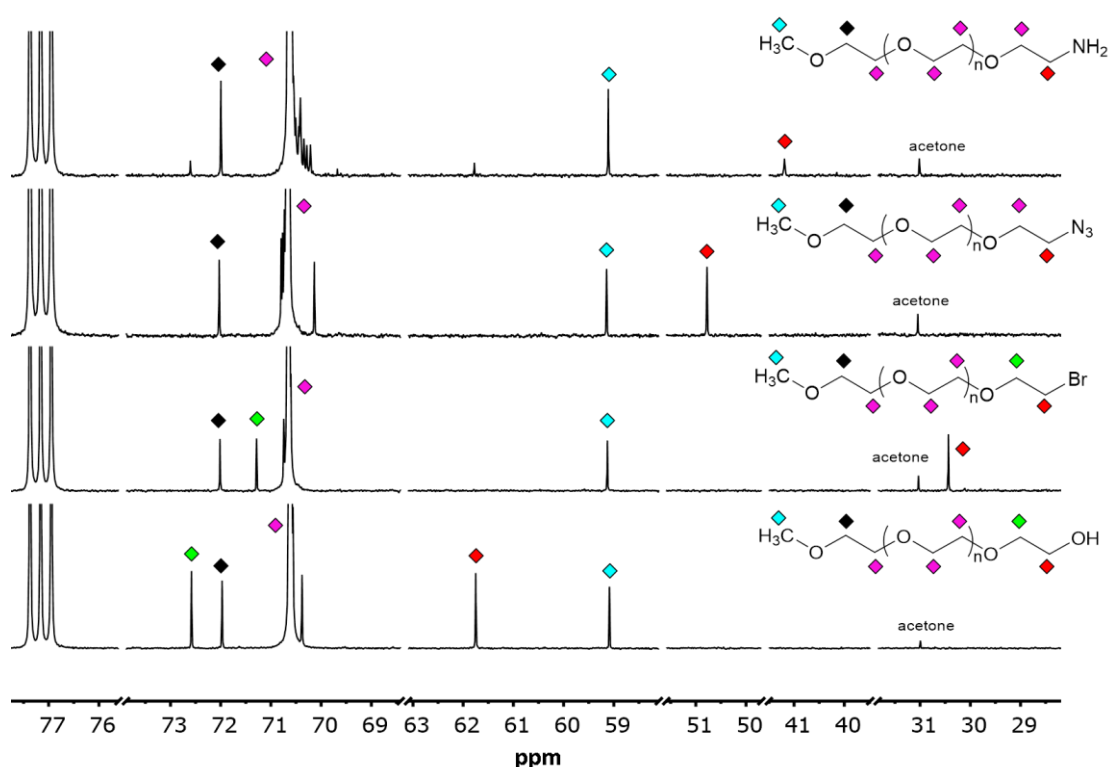


Figure 3.6. Comparison between ^{13}C NMR spectra of PEG-OH2K, PEG-Br2K, PEG-N₃2K and PEG-NH₂2K. Spectra recorded at 700 MHz in CDCl₃.

Once again, the use of 2D NMR data allowed assignment of all the peaks in the ^{13}C NMR spectra and allowed monitoring of the substitution of the terminal group from hydroxyl to amino. As predicted, the comparison between the ^{13}C NMR spectra of the starting material PEG-OH2K, PEG-Br2K, PEG-N₃2K and PEG-NH₂2K shows a shift in the resonance of both the carbons in α and β position as the end group is changed (red and green diamond respectively).

In particular, during the conversion of OH to Br, the resonance of the α -carbon (red diamond) is shifted from $\delta 61.7$ to $\delta 30.4$ due to the lower electron withdrawing effect of bromide compared to hydroxyl. The β -carbon (green diamond) is also shifted from $\delta 72.5$ to $\delta 71.2$. The complete disappearance of the signal at $\delta 61.7$ indicates full conversion of the hydroxyl end group into bromide (red diamond in PEG-OH2K).

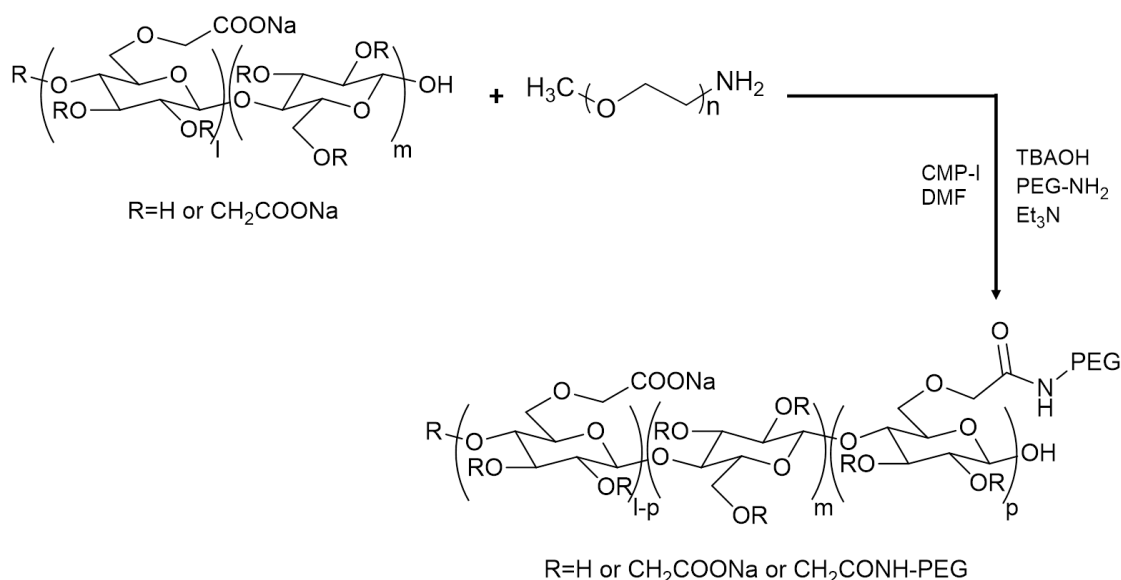
In the second step of the synthetic procedure describe in , the bromide group was converted in to an azide. Again, this resulted in a shift in the resonance of both the carbons in α and β position with respect to the bromide end group as a consequence of the reaction (red and green diamond respectively). The resonance of the α -carbon is shifted toward higher ppm, from $\delta 30.4$ to $\delta 50.8$ whilst the β -carbon is shifted toward lower ppm, from $\delta 71.2$ to $\delta 70.1$. The carbon in α -position being directly bonded to the azide group is affected more by the high electronegativity of the first nitrogen atom in the azide group than the overall nucleophilic effect of the functional group. Due to the high electronegativity of the nitrogen atom, the electron density is pulled away from the carbon in α -position. Therefore, the chemical shift of this carbon is located at higher ppm. On the contrary, the β -carbon is affected more by the overall high electron withdrawing effect of the azide group, thus the resonance is shifted toward higher ppm. Furthermore, the ^{13}C NMR spectrum indicate that the conversion of the bromide end group into azide is total, as the signal at $\delta 30.4$ of the α -carbon (red diamond in PEG-Br2K spectrum) completely disappears in the PEG-N₃2K spectrum.

Upon reduction of the azide functionality to amine, the resonance of both the carbons in α and β position (red and green diamond respectively) shifted once more. The resonance of the α -carbon (red diamond) is shifted toward lower ppm, from $\delta 50.8$ to $\delta 40.8$ whilst the β -carbon (green diamond) is shifted from $\delta 70.1$ to $\delta 69.7$. The carbon in α -position shifted more compared to the carbon in β -position because is it directly bonded to the amino group, therefore it is more affected by the electron donating nature of the amino group. The amino group pushes electron density onto the molecule, hence the carbons in α and β position adjacent to the amino group shift toward lower ppm since their nuclei are more shielded. The reduction of the azide end group into amino was total, as the signal at $\delta 50.8$ of the α -carbon (red diamond in PEG-N₃2K spectrum) completely disappears in the ^{13}C NMR spectrum of the product.

These products PEG-NH₂ synthesised were used without further purification for the synthesis of the CMC-g-PEG co-polymers.

3.3.2. Synthesis of CMC-g-PEG co-polymers

In order to produce a modified CMC with the possibility of reversible deposition to and from a cotton surface, the polymeric backbone of CMC was functionalised with PEG chains as shown in Scheme 3.2.



Scheme 3.2. Reaction scheme for the synthesis of CMC-g-PEG co-polymers using 2-chloromethylpyridinium iodide (CMP-I), tetrabutylammonium hydroxide (TBAOH), triethylamine and PEG-NH₂ in DMF.

PEG was chosen to graft onto the CMC backbone as it is a hydrophilic, non-toxic polymer which is compatible with laundry detergents. When PEG is grafted onto CMC, it was anticipated that the PEG would promote the desorption of the resulting co-polymer from the surface of cotton, hence giving the co-polymer the characteristic behaviour of a SRP.

The amidation reaction used to graft the PEG onto the CMC involves the carboxymethyl functionality of CMC and the amine group of PEG-NH₂. The use of a mono functionalised PEG derivative prevents the possibility of crosslinking. If an amino group was present at both end of the PEG chain, intra-molecular or inter-molecular crosslinks could occur through reaction of the bis-amino PEG with two carboxymethyl groups.

The CMC-g-PEG samples synthesised in this study are named throughout using a code which includes the M_n of the PEG-NH₂ polymer and the weight percentage of PEG bound to the CMC backbone. The actual weight percentage used in the sample code should not be confused with the target weight percentage of PEG bound.

CMC-g-PEG _ M_n PEG-NH₂ _weight percentage of PEG bound

Therefore, a CMC-g-PEG co-polymer synthesised using PEG-NH₂ with M_n 5000 g/mol as given by the supplier and containing 18.3% weight percentage of PEG bound will be referred to as CMC-g-PEG_5K_18.3.

In this chapter, the synthesis and characterisation of CMC-g-PEG co-polymers will be discussed, as well as the characterisation of the CMC starting material. Various reaction conditions have been explored in an attempt to improve the yield of the amidation (PEGylation) reaction, and a range techniques were adopted to recover the resulting co-polymer. The characterisation of the materials in this study proved to be a significant challenge, as several conventional techniques used to characterise polysaccharide- derivatives, such as solution NMR, Fourier transform infrared spectroscopy (FTIR) and elemental analysis, could not be adopted. Solution NMR analysis could not be applied to the characterisation of the CMC-g-PEG compounds due to the difficulties with dissolving sufficient material in a deuterated solvent to acquire a good quality NMR spectrum. Analysis using FTIR could not be used to distinguish the different CMC-g-PEG co-polymers, as the peaks present were seen consistently

in all the spectra. Whilst elemental analysis could be used to determine the presence of PEG in the mixture, it would not provide any information regarding the binding of PEG to the CMC backbone. Therefore, the characterisation of the CMC-g-PEG samples was performed using ^{13}C solid state NMR spectroscopy, pulse field gradient NMR spectroscopy (PFG NMR) and ^1H gel state NMR spectroscopy. Size exclusion chromatography in DMF (SEC) was also used in an unconventional way to characterise the CMC-g-PEG co-polymers. The combined use of ^{13}C solid state NMR spectroscopy and ^1H gel state NMR spectroscopy in D_2O enabled the structural identification of the co-polymer and determination of the weight percentage of PEG bound to the CMC backbone. Through SEC and PFG NMR spectroscopy it was possible to collect information about the purity of the sample in terms of residual unbound PEG.

3.3.2.1. Characterization of sodium carboxymethyl cellulose (CMC)

In order to characterise the CMC starting material, ^{13}C solid state NMR spectroscopy and potentiometric titrations were used.

Solid state NMR spectroscopy was used to characterise the CMC backbone instead of solution NMR spectroscopy due to the physical properties of CMC. The CMC used for the synthesis of the CMC-g-PEG co-polymers could only be solubilised in water and due to the swelling of CMC in water^[6-9], it was not possible to dissolve the necessary amount of CMC material in D_2O required to record a good quality NMR spectrum. Indeed, above a 1% w/v concentration of CMC in D_2O , the solution became very viscous, creating a gel which could not be transferred to an NMR tube for analysis.

A typical solid state NMR spectrum is very different from its analogous solution NMR spectrum. The most noticeable difference is the broadness of the peaks of the nuclei analysed as a consequence of the presence of anisotropic

interactions of the molecule with the magnetic field during the experiment. In solution NMR these anisotropic interactions are averaged in all directions due to the rapid movement of the molecules in solution – isotropic tumbling. In the case of solid state NMR, the molecules are static. Hence, the presence of these anisotropic interactions complicates solid state NMR analysis resulting in a loss of resolution (i.e. broadening of the signals) in the final spectrum^[10].

The ^{13}C solid state NMR spectrum of CMC as sodium salt is shown in Figure 3.7.

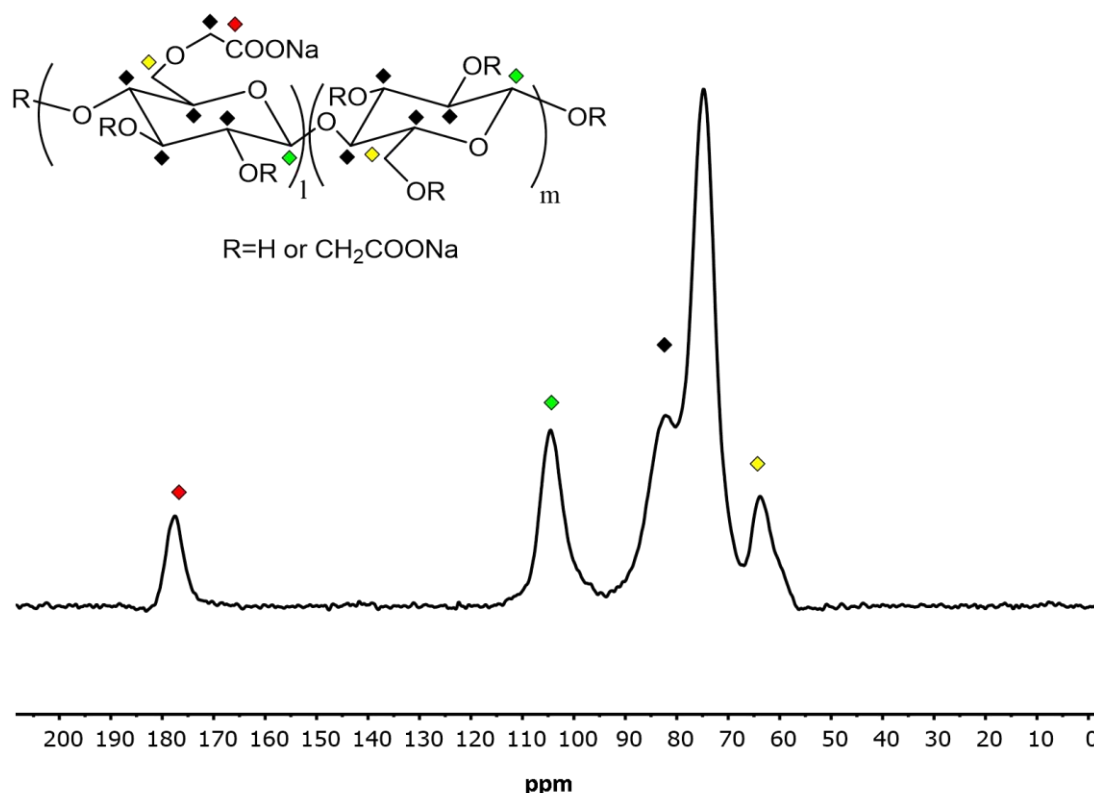


Figure 3.7. ^{13}C solid state NMR spectrum of CMC as sodium salt. Spectrum recorded at 100 MHz.

^{13}C solid state NMR spectroscopy was preferred to ^1H solid state NMR spectroscopy for the characterisation of the CMC starting material. The chemical shifts of the protons of the glucose repeating unit of CMC are usually between $\delta 3-4$ in a solution NMR spectrum. The CMC characterised in this

chapter has a M_n of 180 000 g/mol, thus there were an average of 1000 glucose repeat units per polymer chain. The high number of repeat units combined with the broadness of the signals in solid state NMR causes the resonance of the protons to all merge together in one single broad peak, making it impossible to discern the individual resonances. As an example, the ^1H solid state NMR spectrum of CMC as sodium salt is reported in Appendix B.

The ^{13}C NMR spectrum in Figure 3.7 was referenced using tetramethylsilane (TMS) as internal standard.

The most important (and useful) resonance identifiable from Figure 3.7 is due to the COO^- moiety of the carboxymethyl functionality which can be seen at $\delta 177.9$ (red diamond of Figure 3.7). The identification of this resonance is fundamental because it enables monitoring of the PEGylation reaction between the carboxyl group of CMC and PEG- NH_2 , through a shift of the resonance resulting from the formation of an amide bond. All the remaining signals of Figure 3.7 belong to the glucose ring and will remain unchanged during the reaction with PEG- NH_2 . In particular, the signal at $\delta 104.6$ is assigned to the anomeric carbon (C1, green diamond of Figure 3.7), the signal at $\delta 63.7$ to the C6 of the glucose unit (yellow diamond of Figure 3.7) and the signals between $\delta 70$ -80 to the C2, C3, C4 and C5 carbons in the glucose ring (black diamond of Figure 3.7).

In a CMC backbone, the number of hydroxyl units substituted with carboxymethyl groups per glucose unit is referred to as the “degree of substitution” (DS). The highest value of DS achievable is 3, as there are only 3 hydroxyl groups per glucose repeat unit. The DS of the CMC starting material used in this study was determined by conducting a potentiometric titration^[11, 12]. The use of a potentiometric titration instead of a direct acid/base titration is necessary because of the weak acidic nature of CMC. In a direct titration, the equivalence point of the titration curve corresponds to a variation of the pH of the solution. This variation becomes smaller as the acid/base strength of the molecule titrated reduces. CMC is a very weak acid, therefore, the variation of

pH associated with the equivalence point of the titration curve with a base will be very small. In a potentiometric titration the variation of the potential of the system corresponds to the end point of the titration, not to the equivalence point. The end-point of the titration corresponds to a volume of titrant higher than the amount needed to titrate the titrate. The actual equivalence point is calculated mathematically from the second derivative of the titration curve. Therefore, even if the variation of potential is small (e.g. titration of weak acids/bases) the mathematical approach allows clear identification of the equivalence point of the curve^[13].

The results obtained by the potentiometric titration of CMC are plotted in Figure 3.8.

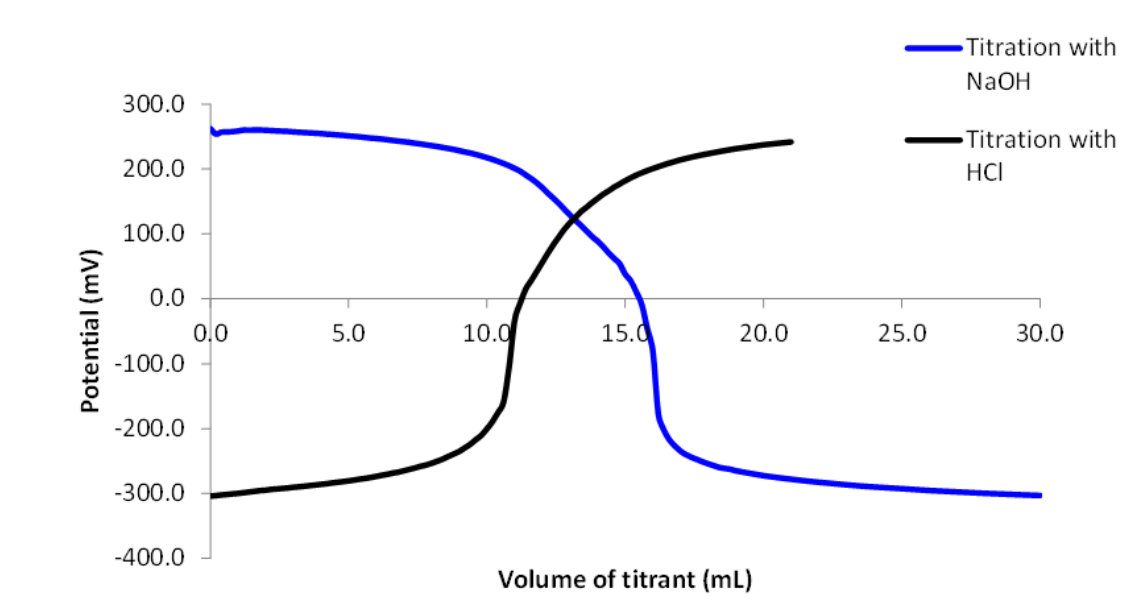


Figure 3.8. Titration profiles for the potentiometric titration of CMC with 0.1 M NaOH (blue curve) and 0.1 M HCl (black curve). Data recorded at 25 °C using a glass combined electrode.

The graph in Figure 3.8 shows the variation of potential registered during the addition of sodium hydroxide (NaOH, blue curve of Figure 3.8) and hydrochloric acid (HCl, black curve of Figure 3.8) to a solution of CMC in water. Prior to analysis, CMC was converted overnight to its acidic form using

an ion exchange resin (DOWEX Monoshere 650C). Moreover, to ensure that all the carboxymethyl functionalities of the CMC backbone were protonated, the titration with NaOH was conducted in the presence of a known amount of HCl. The ionic strength of the environment must be kept constant during the potentiometric titration because it can affect the activity of the titrate at low concentrations, and hence influence the dissociation of weak acids like CMC and interfere with the detection of the end point. Therefore, a known amount of a 0.1 M solution of sodium chloride (NaCl) was added to the system during the analysis.

During the titration with NaOH (blue curve of Figure 3.8) the potential decreased up to the complete neutralization of the HCl added. When a strong and a weak acid are in the same solution, the dissociation of the strong acid suppresses the dissociation of the weak acid, thus the first to be titrated by NaOH is the HCl. The second end point, which corresponds to the titration of the COOH group of the carboxymethyl functionalities of the CMC backbone, was not visualised during the titration with NaOH, even if the delay between each addition of titrant was increased and the volume of titrant added was reduced. This was due to the fact that in acidic form, the structure of CMC is uncharged^[6], hence the structure is very compact, making it difficult for NaOH to react with the COOH groups.

To visualise the titration of the COOH groups, an excess of base was added to the system. The addition of an excess of base allowed the complete titration of the COOH groups of CMC into COO⁻ groups. The negative charges located onto the backbone cause inter- and intra- molecular electrostatic repulsion, thus causing the structure of CMC to expand and expose the negative groups. This excess of NaOH was then back-titrated with 0.1 M HCl (black curve of Figure 3.8). During the back titration, the first end point corresponded to the titration of the excess of NaOH and resulted in a clearly visible variation of the potential. As we would expect, the second end point resulted in a very small variation of

the potential, almost not visible from the plot in Figure 3.8. In order to identify the end point for the titration of the COO^- groups with NaOH, the mathematical approach was adopted^[13].

Mathematically, the equivalence point corresponds to the inflexion of the titration curve, therefore it is the point at which the second derivative of the titration curve is equal to zero (Equation 4).

$$\frac{\partial(\partial\text{potential})}{\partial\text{Volume}^2} = 0$$

Equation 4.

The flex point of the titration curve can be visualised graphically by plotting the function $\partial(\partial\text{potential})$ Vs ∂Volume^2 and interpolate the curve obtained with the x-axis. The titration curve obtained from the titration of the COO^- groups of CMC with 0.1 M HCl in presence of an excess of NaOH is shown in .

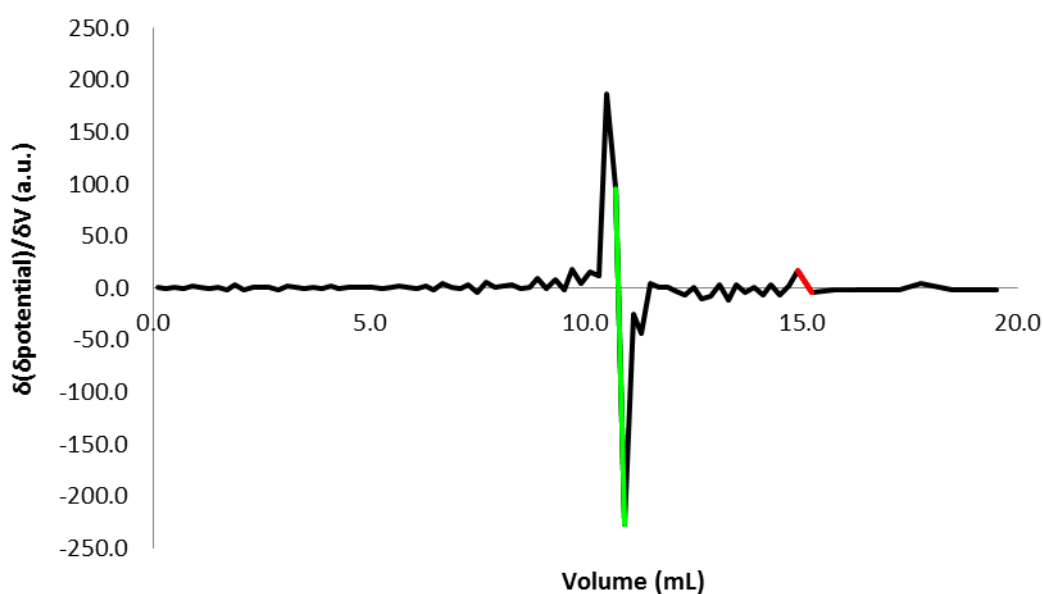


Figure 3.9. Second derivative of the titration curve of the potentiometric titration of CMC with HCl in presence of an excess of NaOH (black). The first equivalence point is identified by the first instance of crossing of the data with the x-axis (green), while the second equivalent point is identified by the second crossing of the data with the x-axis (red).

The second derivative of the titration curve (black curve of) crosses the x-axis twice, thus identifying the two equivalence points. The first equivalence point corresponds to the titration of excess of NaOH by HCl, while the second equivalence point corresponds to the titration of the COO⁻ groups of the CMC backbone. The value of DS was determined using Equation 5 and Equation 6^[14]:

$$A = \frac{(b - c) * M}{n}$$

Equation 5.

Where A are the milli-equivalents of total carboxyl units per gram of sample, b is the volume of titrant in millilitres used for the second equivalence point, c is the volume of titrant in millilitres used for the first equivalence point, M is the concentration of the titrant expressed as molarity and n is the amount of CMC used for the titration in grams.

$$DS = \frac{0.162 * A}{1 - (0.058 * A)}$$

Equation 6.

Where 0.162 is the molecular weight of the anhydroglucose unit of cellulose divided by 1000 and 0.058 corresponds to the increase in weight of the anhydroglucose unit for each carboxymethyl group substituted divided by 1000^[14]. The potentiometric titration of the CMC starting material was repeated three times, in order to determine the error associated with the measurement. The DS of the CMC starting material for the synthesis of the CMC-g-PEG copolymer as determined by potentiometric titration was (0.81 ± 0.05).

Alongside the degree of substitution (DS) for the CMC polymer backbone is the “degree of blockiness” (DB), which refers to the distribution of the substituted

glucose units on the polymer backbone. If the substituted sugar units are evenly distributed on the CMC backbone, the polysaccharide is characterised by a low DB, while if the substituted units are localised in “blocks” the polysaccharide will have a high DB^[15].

The CMC provided by P&G and used for the synthesis of the CMC-g-PEG copolymer had a high DB. The reaction of CMC with a high DB with PEG-NH₂ should result in the formation of PEGylated areas of the CMC backbone alternated with areas of unmodified CMC (Figure 3.10) i.e. equally blocky.

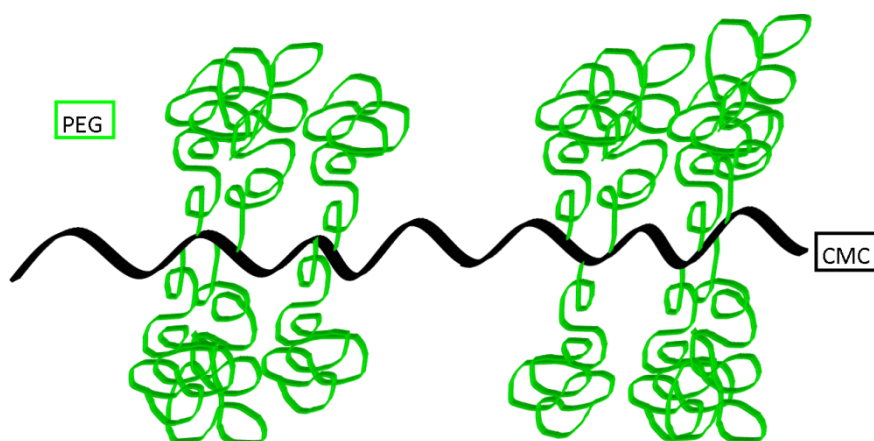
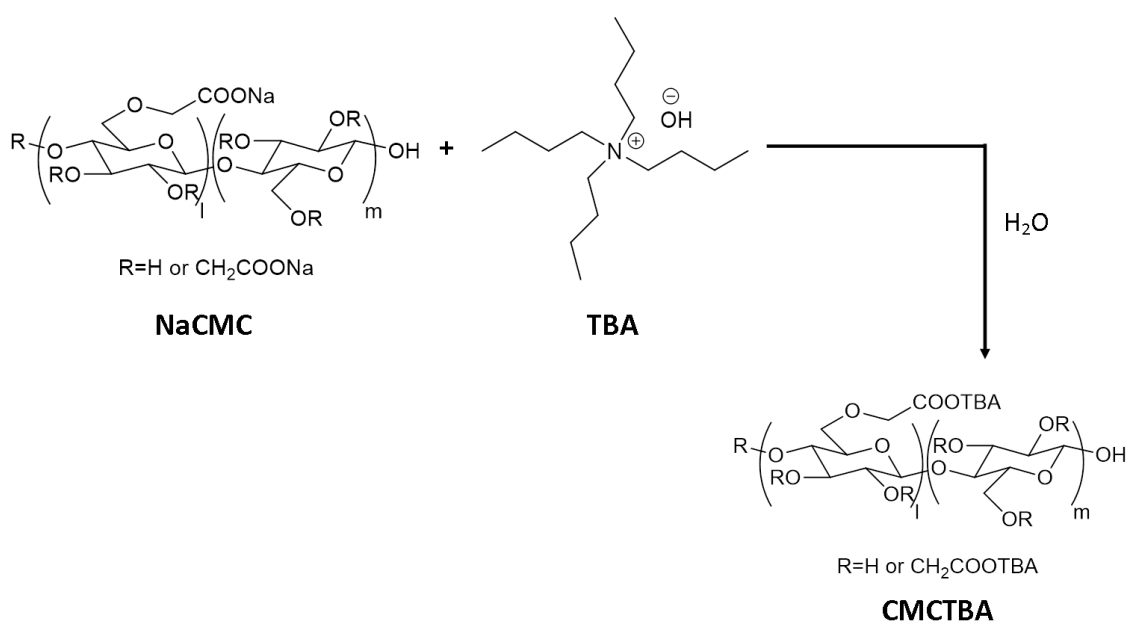


Figure 3.10. Idealised picture showing formation of PEGylated area on to a CMC backbone with high DB upon reaction with PEG-NH₂.

The DB can be determined using a procedure described in the literature^[15], which determines the ratio between the unsubstituted sugar units directly and not directly linked to substituted sugar units. In this work, the DB of the CMC used for the synthesis of CMC-g-PEG co-polymers was not determined as it was not relevant for the synthetic procedure. The value given by the supplier (DB = 0.7) was adopted.

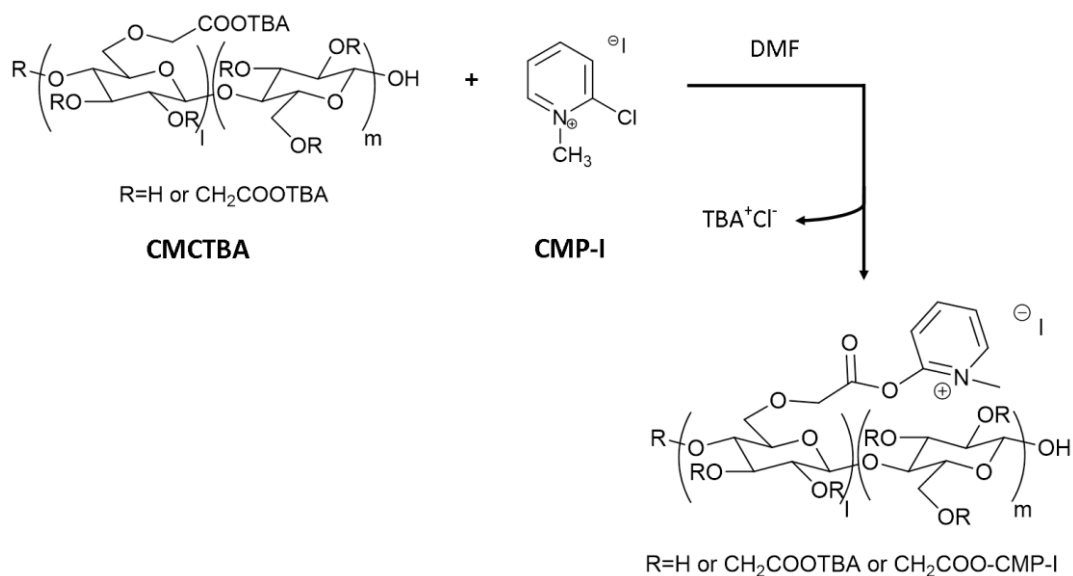
3.3.2.2. Synthesis of CMC-g-PEG co-polymers

The first step of the synthesis of the CMC-g-PEG co-polymers, summarized in, involved the transformation of the CMC starting material from a sodium salt to a tetrabutylammonium salt (TBA) via an ion exchange resin as shown in . This transformation was necessary in order to solubilize the CMC starting material in DMF, the amidation reaction solvent, since CMC as sodium salt cannot be dissolved in organic solvents.



Scheme 3.3. Synthesis of CMCTBA

As a proof of the success of the ion exchange, the material isolated was soluble in DMF. Subsequently the carboxymethyl groups of the CMC backbone were converted in to a more reactive species via a nucleophilic attack by 2-chloro-1-methylpyridinium iodide (CMP-I), with release of TBACl salt (Scheme 3.4)^[6].



Scheme 3.4. Activation of the carboxymethyl group of CMCTBA with CMP-I in DMF.

The reaction with CMP-I “activated” the carboxylic groups of CMC toward the amidation reaction by introducing a good leaving group (1-methyl-2-pyridone). The addition of CMP-I was performed at 0 °C to avoid the formation of inter chain ester bonds that would interfere with the amidation reaction by creating a hydrogel (Figure 3.11). The activated carboxymethyl group could react with the hydroxyls group of the CMC backbone^[16] to form esters. By adding the activating agent CMP-I at low temperature and using diluted systems, it is possible to prevent this side reaction.

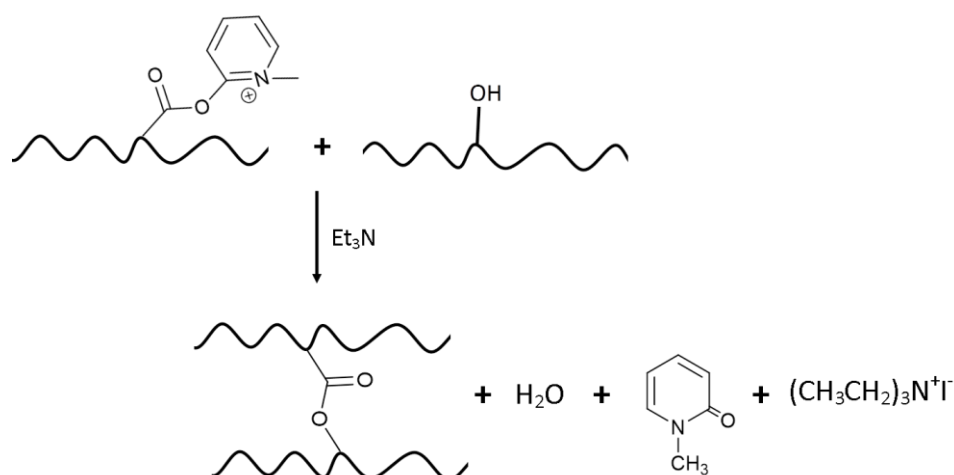
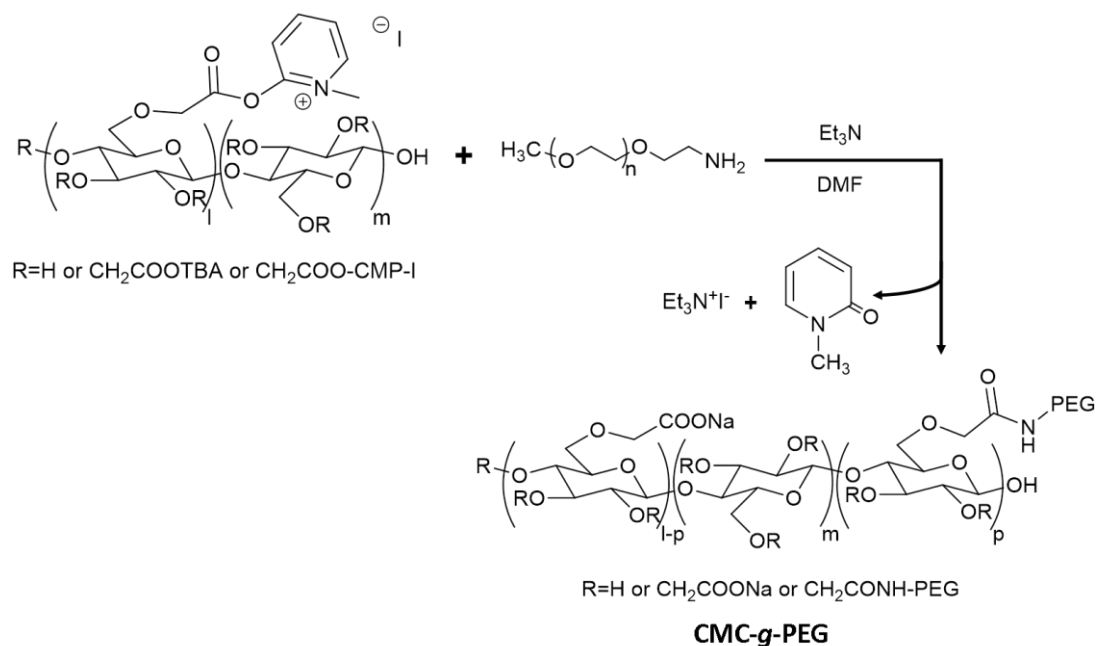


Figure 3.11. Inter chain ester bond between CMC backbones.

The following step of the synthesis of the CMC-g-PEG co-polymers involves the addition of PEG-NH₂ together with triethylamine (Scheme 3.5).



Scheme 3.5. Reaction between the activated carboxymethyl groups of the CMC backbone with PEG-NH₂ in presence of triethylamine in DMF.

Amides are usually formed by reaction between a carboxylic acid and an amine with release of water^[6]. However, the equilibrium of this reaction is

unfavourable for the formation of the amide, thus the removal of water is essential to drive the equilibrium toward the formation of the amide. The amidation reaction shown in Scheme 3.2 was carried out under anhydrous conditions in a nitrogen atmosphere to prevent hydrolysis of the ester bond of the activated carboxymethyl group. As PEG-NH₂, triethylamine and CMP-I are all hygroscopic compounds, these materials were dried in vacuum oven overnight prior to use in the reaction. An exception was made with PEG-NH₂10K which may possess a higher water content compared with the other PEG-NH₂ samples due to the higher weight fraction of PEG units in the polymer backbone. Hence, drying overnight in the vacuum oven may not be enough to remove completely the water adsorbed. Therefore, PEG-NH₂10K was azeotropically dried with benzene prior to its use in the amidation reaction.

A series of CMC-g-PEG co-polymers were synthesised with the aim of varying the graft density of PEG chains and the M_n of the PEG-NH₂ component used. The complete list of samples is summarised in Table 3-3. Different weight percentages of PEG bound were targeted in order to investigate the impact of PEG graft density on the soil release properties of the co-polymers and the M_n of the PEG chain.

The first co-polymer synthesised was CMC-g-PEG_2K_23.7 which followed a literature procedure^[8] for the synthesis of amidic derivatives of CMC. This procedure allowed careful control of the degree of substitution of the resulting material by varying the ratio between the CMP-I added and the amount of amine derivative. As the synthetic strategy described by Barbucci et al. was very successful, it was decided to adapt it for the synthesis of CMC-g-PEG co-polymers.

During the first attempt of the synthesis of a CMC and PEG-NH₂ co-polymer, a weight percentage of PEG bound of 99% was targeted. The characterisation of CMC-g-PEG_2K_23.7 (described in the following paragraphs) showed that sample isolated after 4 hours of reaction only contained 23.7% in weight of PEG

bound, despite the addition of CMP-I and PEG-NH₂2K in a stoichiometric ratio with respect to the carboxymethyl group to react. Therefore, the reaction was allowed to proceed for a longer time for the synthesis of the remaining copolymers, in an attempt to increase the weight percentage of PEG bound.

Table 3-3. List of CMC-g-PEG samples synthesised by amidation reaction in DMF between CMC and PEG-NH₂.

Sample	M _n PEG-NH ₂ * (g/mol)	Weight PEG target (%)	Reaction time (hours)	Weight PEG achieved** (%)
CMC-g-PEG_2K_9.5	2000	80	24 hours	9.5±0.3
CMC-g-PEG_2K_23.7	2000	99	4 hours	23.7±0.5
CMC-g-PEG_2K_42.8	2000	65	20 hours	42.8±0.2
CMC-g-PEG_2K_50.4	2000	65	4 days	50.4±0.2
CMC-g-PEG_2K_56.1	2000	80	5 days	56.1±0.6
CMC-g-PEG_2K_62.5	2000	90	6 days	62.5±0.8
CMC-g-PEG_5K_19.0	5000	85	4 days	19.0±0.4
CMC-g-PEG_5K_51.1	5000	90	6 days	51.1±0.4
CMC-g-PEG_5K_55.6	5000	90	7 days	55.6±0.6
CMC-g-PEG_5K_63.7	5000	95	7 days	63.7±0.8
CMC-g-PEG_10K_76.5	10000	85	6 days	76.5±0.3
CMC-g-PEG_10K_84.5	10000	95	6 days	84.5±0.2
CMC-g-PEG_10K_85.8	10000	99	6 days	85.8±0.3

*Value given by the supplier.

** Value determined through the combined use of size exclusion chromatography, pulse field NMR spectroscopy and ¹H gel state NMR spectroscopy techniques. For details see sections 3.3.2.4., 3.3.2.5 and 3.3.2.6.

As a higher weight percentage of PEG bound was targeted, an increased quantity of PEG-NH₂ was added to the reaction mixture. In addition, the reaction time was also increased in order to allow a larger quantity of PEG-NH₂ to bind to the CMC backbone. Due to the blocky nature of CMC, the longer reaction times should help to overcome the increased steric hindrance experienced with a larger number of chains (Figure 3.10). However, even if the reaction was allowed to proceed for longer, the actual weight percentage of PEG bound achieved (as determined from the characterisation of the copolymers) was lower than the targeted value for each experiment. A possible reason behind the low conversion of the carboxymethyl groups achieved during the amidation reaction of CMC with PEG-NH₂ could be the steric hindrance of the PEG-NH₂ chain. In solution, PEG-NH₂ assumes the conformation of a random coil, thus an increase in chain length might be expected to result in reduced accessibility of the amino functionality and reducing the rate of the reaction (Figure 3.12). This effect may be further enhanced due to the high flexibility of the PEG chain.

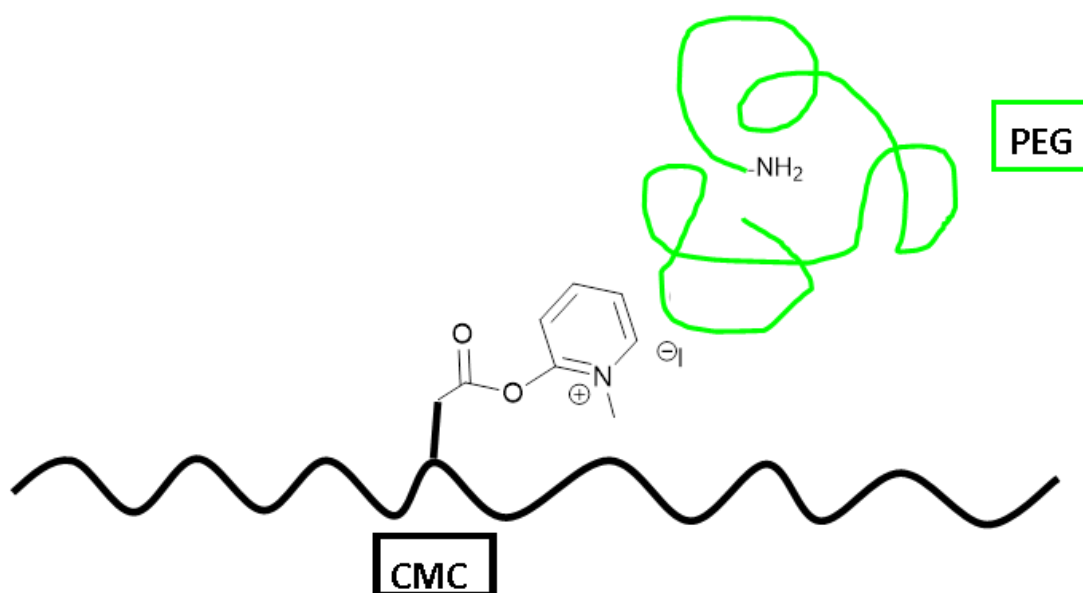


Figure 3.12. Interference of the random coil conformation of PEG-NH₂ in solution upon the speed of the amidation reaction.

Furthermore, upon the successful grafting of a PEG chain to the CMC backbone, the steric bulk of the grafted PEG chain may also hinder the adjacent carboxymethyl group, thus making the grafting of a subsequent chain harder and slowing the amidation reaction (Figure 3.13).

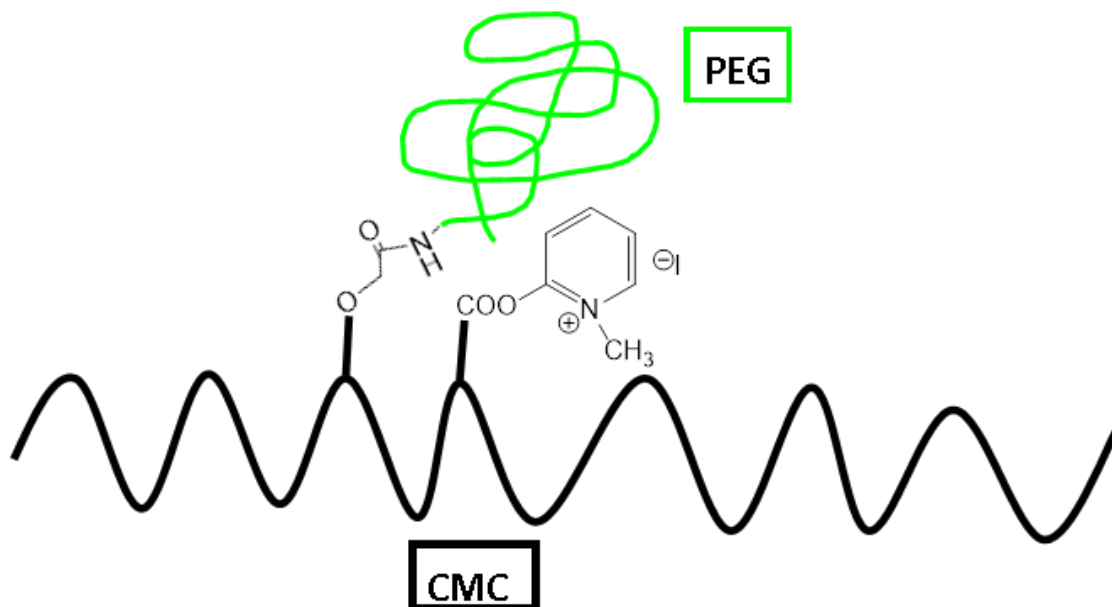


Figure 3.13. Sterical hindrance of a grafted PEG chain on the grafting of a second PEG chain to the CMC backbone.

This steric effect becomes more pronounced as the M_n of the grafted PEG-NH₂ increases. For example, due to the high steric bulk of the PEG-NH₂10K polymer chains, all the CMC-g-PEG_{10K} co-polymers possess a smaller proportion of chains of PEG bound compared to the other co-polymers based on lower M_n PEG-NH₂ (Table 3-3), despite longer reaction times and higher temperatures being used for their syntheses. Furthermore, as the graft density increases, the grafting of the subsequent PEG chain becomes thermodynamically unfavourable, since the grafted chains would need to undergo chain stretching to alleviate the steric bulk and allow more PEG chain to be bound^[17].

Due to the long purification procedure required to isolate the CMC-g-PEG co-polymers from unreacted PEG-NH₂, it was not practical to follow the progress of the reaction. Hence, the reaction was stopped at an arbitrary time.

The co-polymers listed in Table 3-3 were recovered from the reaction vessel by precipitation in diethyl ether, a non-solvent for PEG-NH₂. Upon precipitation, the co-polymers were initially purified by dialysis against sodium chloride (NaCl) as solvent, as suggested from the literature^[6]. However, due to the swelling of the CMC moiety of the co-polymer in water, the complete removal of unreacted PEG-NH₂ with this technique was difficult. Extended times were required for dialysis due to the trapping of unreacted PEG-NH₂ in the swollen structure of the CMC-g-PEG co-polymer. In an attempt to improve the speed of the purification process, a Soxhlet extraction (of unreacted PEG-NH₂) in chloroform (CHCl₃) was chosen as purification procedure for the CMC-g-PEG co-polymers. The choice of CHCl₃ as solvent for the soxhlet extraction was made due to the high solubility of PEG-NH₂ in this solvent, allowing any residual PEG-NH₂ to be easily removed. On the contrary, the CMC-g-PEG co-polymers are insoluble in this solvent, hence they are not removed by this technique. Unreacted PEG-NH₂ is collected in the still pot, while the CMC-g-PEG co-polymer can be recovered from the thimble. The temperature of the Soxhlet extraction was set at 70 °C, above the boiling point of CHCl₃ to ensure a vigorous reflux of the solvent. A vigorous reflux of the solvent in the Soxhlet extraction allows the extraction of the unreacted PEG-NH₂ to occur more rapidly because more extractions with hot solvent can be performed in a shorter period of time.

The CMC-g-PEG co-polymers listed in Table 3-3 were characterised using several analysis techniques. ¹³C solid state NMR spectroscopy was used to investigate the structure of the resulting co-polymers (see paragraph 3.3.2.3. for full discussion). Using a combination of size exclusion chromatography (SEC,

paragraph 3.3.2.4.) in DMF and pulse field NMR spectroscopy (PFG NMR, paragraph 3.3.2.6.) the purity of the samples was determined by analysis of the percentage of unreacted PEG. Furthermore, ^1H gel state NMR spectroscopy (paragraph 3.3.2.5.) was used to evaluate the weight percentage of PEG bound in the CMC-g-PEG co-polymers.

3.3.2.3. Solid state NMR spectroscopy

Solid state NMR spectroscopy was preferred to solution state NMR spectroscopy to characterize the CMC-g-PEG samples due to the physical properties of the co-polymers. Despite attempts (with varying success) to graft PEG-NH₂ to the CMC backbone, the resulting products were insoluble in all common organic solvents and could only be swollen in water. Hence, it was impossible to disperse the necessary amount of CMC-g-PEG material in D₂O required to record a good quality solution NMR spectrum.

By way of an example of the ^{13}C solid state NMR spectrum of the products of the amidation reaction, a comparison between the ^{13}C solid state NMR spectra of CMC-g-PEG_2K_62.5 (product) and PEG-NH₂2K and CMC (TBA salt, starting material) is reported in Figure 3.14. All of the CMC-g-PEG co-polymers prepared in this work were characterised in the same manner and the ^{13}C solid state NMR spectra can be found in Appendix B. For simplicity, only the main resonances of the CMC-g-PEG product are highlighted in Figure 3.14.

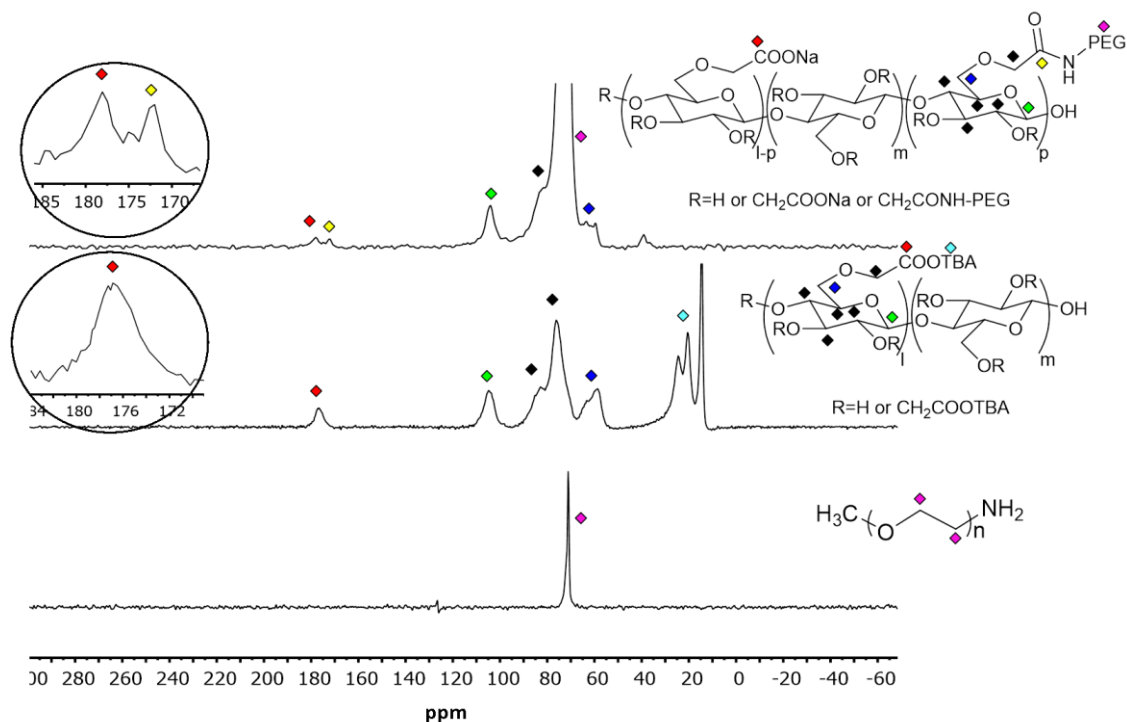


Figure 3.14. Comparison between ^{13}C solid state NMR of CMC-g-PEG_2K_62.5, CMC as TBA salt and PEG-NH₂K. The expanded region on the left highlights the presence of the resonance of the amide functionality. Spectra recorded at 100 MHz.

From the comparison between the ^{13}C solid state NMR spectra of CMC-g-PEG_2K_62.5 and PEG-NH₂K in Figure 3.14, it is possible to identify the resonance at $\delta 70.9$ due to the $-\text{CH}_2$ carbons of the PEG chain (purple diamonds) in the finished product. This is possible despite the partial merging of the resonance with that of the carbons of the CMC repeating unit (black diamonds). Through the comparison between the ^{13}C solid state NMR spectra of CMC-g-PEG_2K_62.5 and the CMC-TBA starting material it is possible to recognize the resonance at $\delta 9.2\text{--}23.8$ typical of the TBA cation (turquoise diamond). Furthermore, a close look at the expanded region between $\delta 170\text{--}180$ in the spectrum of CMC-g-PEG_2K_62.5 in Figure 3.14 demonstrate a resonance corresponding to both the carboxylic group of the carboxymethyl functionality at $\delta 177.9$ (red diamond) and a second signal at $\delta 171.7$ typical of the carbonyl carbon of an amide functional group (yellow diamond). The presence of this

resonance at $\delta 171.7$ suggests the presence of an amide bond and therefore the partially successful grafting of PEG-NH₂ to the CMC backbone.

From the ¹³C solid state NMR spectrum of CMC-g-PEG_2K_62.5 it is not possible to distinguish whether the resonance at $\delta 70.9$ belongs to PEG which is bound to CMC backbone or unreacted PEG or a mixture of the two of them. Determination of the amount of unreacted PEG left in a mixture is important in order to evaluate the weight percentage of PEG bound to the CMC backbone achieved during the reaction. The value of the weight percentage of PEG is fundamental to correlate the structure of the co-polymer shown with its soil release properties for the industrial tests.

The weight percentage of PEG bound was, therefore, evaluated through the combined use of ¹H gel state NMR spectroscopy, SEC in DMF and PFG NMR spectroscopy. Through the use of a calibration curve based on the resonance of the protons of the PEG chain in a ¹H gel state NMR spectrum, the total amount of PEG contained in the sample could be determined. The percentage of unreacted PEG left in a mixture with CMC-g-PEG was then determined using both SEC and PFG NMR spectroscopy. The actual amount of PEG grafted to CMC was calculated as the difference between the amount of total PEG in the sample and the amount of unreacted PEG. Finally, the weight percentage of PEG was estimated by the ratio between the weight of PEG bound and the weight of the CMC-g-PEG sample.

3.3.2.4. Size Exclusion Chromatography (SEC)

It is clear from the results in Table 3-3 that in all cases, the target and actual weight percentage of PEG bound were not in good agreement, although in many cases the weight percentage of PEG was still quite reasonable. However, in order to evaluate the performance of the resulting CMC-g-PEG co-polymers

as SRPs it is important to purify the co-polymers and to ensure that all unreacted/unbound PEG-NH₂ is removed from the co-polymer. Purification was achieved either by dialysis against a 0.1 M solution of sodium chloride or by Soxhlet extraction in chloroform, as previously described. Moreover, to accurately calculate the weight percentage of PEG bound (i.e. the weight fraction of PEG in a CMC-g-PEG sample) it was necessary to establish that all the PEG was actually grafted to the CMC backbone and did not remain in a mixture as unbound PEG. If any unbound PEG did remain, it would be important to know exactly how much so that this could be taken into consideration.

The amount (if any) of unbound PEG-NH₂ in each sample of CMC-g-PEG co-polymer was determined by SEC using DMF as the eluent. The CMC-g-PEG co-polymers were dissolved in DMF to give an approximate concentration of 1 mg/ml; the exact concentration of each solution was recorded. Although CMC (as TBA salt), the CMC-g-PEG and unreacted PEG-NH₂ were all soluble in DMF, it was anticipated that the CMC-g-PEG might not elute due to interactions between the highly functionalised polymer backbone and the column. As it turned out, any ungrafted CMC starting material and the CMC-g-PEG co-polymer were retained by the SEC system, probably within the guard column, and the only species to elute was the unbound PEG. It was possible to confirm that the eluting species was indeed the unreacted PEG-NH₂ by comparison with a sample of pure PEG-NH₂.

The triple detection SEC system (with right angle laser light scattering (RALLS)) was calibrated with a solution of polystyrene (PS) standard of known molecular weight and concentration. The concentration of unbound PEG-NH₂ was obtained from the area under the concentration curve (refractive index detector) using a dn/dc for polyethylene glycol of 0.044 dL/g.

The results of the SEC analysis are summarised in Table 3-4.

Table 3-4. Percentage of purity of the CMC-g-PEG co-polymers determined by SEC in DMF.

Sample	Purification technique	PEG-NH ₂ unbound* (%)	Purity ** (%)
CMC-g-PEG_2K_9.5	Dialysis	5.2±0.2	94.8±0.2
CMC-g-PEG_2K_23.7	Dialysis	8.9±0.4	91.1±0.4
CMC-g-PEG_2K_42.8	Soxhlet***	1.5±0.2	98.5±0.2
CMC-g-PEG_2K_50.4	Soxhlet***	3.2±0.5	96.8±0.5
CMC-g-PEG_2K_56.1	Soxhlet***	8.5±0.8	95.5±0.8
CMC-g-PEG_2K_62.5	Dialysis	3.6±0.4	96.4±0.4
CMC-g-PEG_5K_19.0	Soxhlet***	0.9±0.1	99.1±0.1
CMC-g-PEG_5K_51.1	Soxhlet***	1.1±0.6	98.9±0.6
CMC-g-PEG_5K_55.6	Dialysis	4.5±0.3	95.5±0.3
CMC-g-PEG_5K_63.7	Dialysis	16.7±0.5	83.3±0.5
CMC-g-PEG_10K_76.5	Dialysis	20.4±0.9	79.6±0.9
CMC-g-PEG_10K_84.5	Dialysis	30.5±0.3	69.5±0.3
CMC-g-PEG_10K_85.8	Dialysis	13.5±0.4	86.5±0.4

*Percentage of PEG recovered estimated by the software as comparison between the area underneath the peak of PEG-NH₂ with the area underneath the peak of PS from a PS solution in DMF of known concentration. Three repetitions were recorded for each sample. Data collected using a triple detector calibration based on PS standard of M_n 66350 g/mol and Đ 1.025.

**Purity of sample calculated as difference between the percentage of PEG recovered estimated by the software and the total sample injected.

*** Soxhlet extraction performed in CHCl₃ at 70 °C.

From the results outlined above, it would appear that the use of Soxhlet extraction in CHCl₃ instead of dialysis against NaCl 0.1 M allows a slightly higher level purity of the co-polymer to be reached. The co-polymers purified

by Soxhlet extraction (CMC-g-PEG_2K_42.8, CMC-g-PEG_2K_50.4, CMC-g-PEG_2K_56.1, CMC-g-PEG_5K_19.0 and CMC-g-PEG_5K_51.1) contain about 3% or less of unbound PEG-NH₂ with the exception of CMC-g-PEG_2K_56.1 which contain about 8%. A possible reason for this exception could be the entanglement of PEG-NH₂2K unbound chains in the CMC-g-PEG_2K_56.1 structure due to the high graft density of the co-polymer, which leads to a lower amount of PEG unbound removed upon extraction.

In contrast, the co-polymers purified by dialysis contain a percentage of unbound PEG in the range of 1 to 30%, with the value increasing with the M_n of PEG. A possible reason for this difference could be entrapment of residual of PEG-NH₂ in the gel structure of the swollen CMC in water, which makes the removal of PEG-NH₂ more difficult by preventing it from crossing the dialysis membrane, especially as the M_n of PEG increases. From the results of Table 3-4, it would appear that the removal of unreacted PEG-NH₂10K from the CMC-g-PEG_10K co-polymers by dialysis is not very effective at all. The percentages of residual PEG-NH₂10K estimated by SEC are much higher than the corresponding values for PEG-NH₂2K and PEG-NH₂5K. It is likely that PEG-NH₂10K is not efficiently removed by dialysis because of a combined effect of the swelling of CMC and the M_n of PEG-NH₂10K being close to the M_n cut-off of the dialysis membrane - 14,000 g/mol. Polymer chains with a M_n which is lower than the M_n cut-off of the dialysis member will easily pass through the membrane while polymer chains with a M_n higher than the cut-off will be retained. Despite the dispersity (\mathcal{D}) of the PEG-NH₂10K sample being relatively narrow (1.1) it is likely that a significant portion of the PEG-NH₂10K has a M_n which is equal or higher than the cut-off M_n , hence it might be partially retained by the membrane. Therefore, the percentage of PEG-NH₂10K residual estimated by SEC in DMF is significantly higher than for any other PEG-NH₂ starting material.

With the knowledge of the percentage of unbound PEG present in the CMC-g-PEG co-polymers, it is now possible to evaluate the exact weight percentage of PEG in the co-polymers by ^1H gel state NMR spectroscopy which determines the overall quantity of PEG in the mixture –bound and unbound.

3.3.2.5. Gel state NMR spectroscopy

Gel state NMR spectroscopy (also called “gel-phase NMR spectroscopy”) is a solid state NMR technique for the analysis of solvent swollen solids^[18]. It is usually applied to the study of solid phase organic reactions^[19] because it enables the investigation of the structure of intermediates or products without separation from the support. The main advantages associated with this technique are the short time required to record a good quality spectrum and the small amount of material necessary for the analysis^[20]. Moreover, the sample investigated by gel state NMR spectroscopy does not require preliminary treatment, in contrast to solution NMR spectroscopy in which the compound for analysis must be dissolved in a deuterated solvent prior to use. A series of factors influence the quality of the spectra recorded for the swollen material^[19]. In particular, the type of solvent plays an important role. The solvent chosen for the analysis must provide a good swelling of the material, hence it has to match the polarity of the molecule to be examined^[19].

In this work, ^1H gel state NMR spectroscopy was used to calculate the total amount of PEG present in each sample and therefore estimate the actual weight percentage of PEG of each CMC-g-PEG co-polymers by subtracting the amount of unbound PEG calculated by SEC. In order to obtain quantitative data, the acquisition of a ^1H NMR spectrum was carried out instead of a ^{13}C NMR spectrum. Because previous analysis by solid state ^1H NMR (APPENDIX B) showed only one broad signal for all the protons in the CMC backbone and in the PEG chain, and it was not possible to dissolve enough CMC-g-PEG material

in D₂O to record a solution ¹H NMR spectrum with good resolution, a gel state ¹H NMR spectrum was a suitable compromise for quantitative analysis. The solvent used to swell the co-polymers was D₂O, as it interacts with both the CMC backbone and the PEG-NH₂ moiety of the co-polymers, thus allowing a better quality ¹H gel state NMR spectra to be recorded.

In order to estimate the weight percentage of PEG of the CMC-g-PEG co-polymers, it was first necessary to quantify the total amount of PEG contained in the sample (i.e. the amount of bound and unbound PEG). Since the weight percentage of PEG of the CMC-g-PEG co-polymers refers to the proportion of PEG in a CMC-g-PEG sample, the peak of the protons of the PEG chain in the ¹H gel state NMR spectrum of the co-polymers was chosen as the key signal for the evaluation of the total amount of PEG.

The analysis of five samples of gel, of varying and known concentrations, of PEG-NH₂ in D₂O enabled the construction of calibration profiles relating peak integration to PEG concentration, allowing the integral of the peak corresponding to the protons of the PEG chains present in the co-polymer samples to be correlated with the amount of PEG present in the gel. Figure 3.15 shows an example of the calibration profile obtained for PEG-NH₂2K.

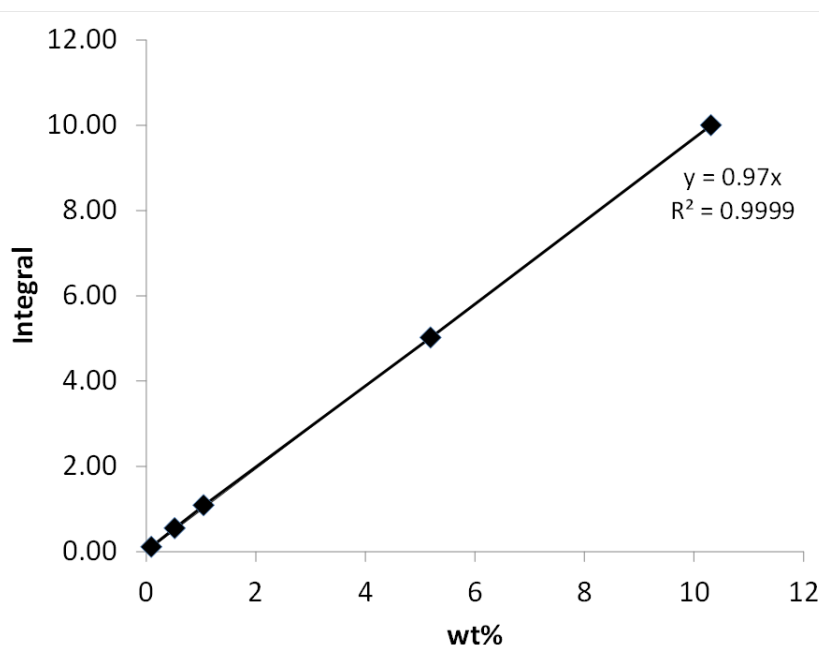


Figure 3.15. Calibration profile for PEG-NH₂K correlating the peak integral of the protons of the PEG chain with the weight percentage of PEG in the sample.

Then, the peak integral of the protons of the PEG chain in the CMC-g-PEG copolymer ¹H gel state NMR spectrum was cross-referenced to the calibration profile and the total amount of PEG-NH₂ present in the sample was estimated. Since several co-polymers were synthesised with varying M_n values for the PEG component, a calibration profile was recorded for each PEG-NH₂. The weight percentage of PEG could then be estimated using Equation 7.

$$\text{weight \% } PEG_{\text{bound}} = \frac{\text{mass } PEG_{\text{bound}}}{\text{mass copolymer}} \times 100$$

Equation 7.

The proportion of bound PEG was calculated using Equation 8 and Equation 9, which takes into account the percentage of PEG unbound estimated via SEC, and the total amount of PEG was evaluated through the interpolation of the peak integral of PEG chain with the calibration curve based on the same M_n PEG.

$$\text{mass PEG}_{\text{bound}} = \text{mass PEG}_{\text{total}} - (\text{mass PEG}_{\text{unbound}})$$

Equation 8.

$$\text{mass PEG}_{\text{unbound}} = \text{mass of PEG}_{\text{total}} \times \% \text{ PEG}_{\text{unbound}}$$

Equation 9.

An example of the procedure to evaluate the weight percentage of PEG bound is shown in Figure 3.16.

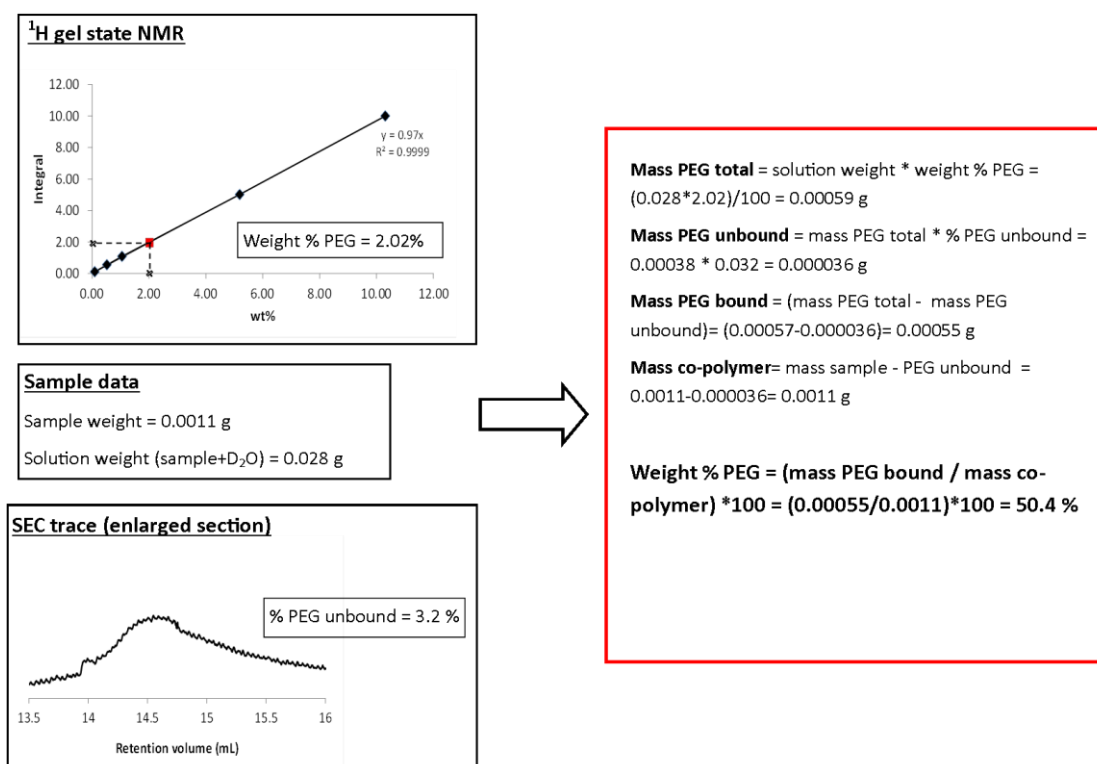


Figure 3.16. Example of the procedure to calculate the weight percentage of PEG bound of CMC-g-PEG_2K_50.4 co-polymer.

The results of the ^1H gel state NMR analysis and the weight percentage of PEG bound of each co-polymer are summarised in Table 3-5.

Table 3-5. Weight percentage of PEG bound in the CMC-g-PEG co-polymers.

Sample	Integral (a.u.)	PEG-NH ₂ bound* (%)	PEG bound target (%)
CMC-g-PEG_2K_9.5	0.60	9.5±0.3	80
CMC-g-PEG_2K_23.7	0.14	23.7±0.5	99
CMC-g-PEG_2K_42.8	1.79	42.8±0.2	65
CMC-g-PEG_2K_50.4	1.99	50.4±0.2	65
CMC-g-PEG_2K_56.1	2.11	56.1±0.6	80
CMC-g-PEG_2K_62.5	3.18	62.5±0.8	90
CMC-g-PEG_5K_19.0	1.00	19.0±0.4	85
CMC-g-PEG_5K_51.1	2.63	51.1±0.4	90
CMC-g-PEG_5K_55.6	2.64	55.6±0.6	90
CMC-g-PEG_5K_63.7	3.29	63.7±0.8	95
CMC-g-PEG_10K_76.5	0.38	76.5±0.3	85
CMC-g-PEG_10K_84.5	0.39	84.5±0.2	95
CMC-g-PEG_10K_85.8	0.37	85.8±0.3	99

*Percentage of PEG-NH₂ bound to the CMC backbone express as weight percentage of PEG-NH₂ in the CMC-g-PEG sample. Three repetitions were recorded for each sample.

The results summarised in Table 3-5 showed that as the M_n of the grafted PEG chain increases, the weight percentage of PEG bound achieved is much lower compared to the target value, even if the reaction was allowed to proceed for a longer time. As previously hypothesised (section 3.3.2.2.), it is possible that the conformation assumed by the PEG chain in solution hinders the amino end group, thus slowing the rate of the reaction (Figure 3.12). Moreover, as the graft

density increases, the accessibility of the carboxymethyl groups of the CMC backbone is reduced due to steric bulk of PEG chains grafted, as described in Figure 3.13.

3.3.2.6. Pulse field gradient NMR analysis (PFG NMR)

Pulse field-gradient (PFG) NMR (also called “pulsed field gradient spin-echo NMR”) is a technique that probes of the self-diffusion of components of a system. The term “self-diffusion” refers to the diffusion of a species in a system at chemical potential gradient of zero, hence when no reaction is occurring involving the species under investigation. PFG NMR analysis can be applied to polymer systems to study self-diffusion of a polymer and even to obtain information about the structure of the polymer, such as M_n and molecular weight distribution (\mathcal{D})^[21]. The nucleus investigated by this technique is usually ^1H , due to its abundance and because it has a high magnetogyric ratio (γ), hence it has a high sensitivity for diffusion. During a PFG experiment, a sequence of two electromagnetic pulses at 90° and 180° is applied to the sample and the NMR signal is recorded. After the second electromagnetic pulse is applied, the system refocuses and loses intensity (decay) due to relaxation. If the molecule under investigation does not move in space during the time (t) between the two consecutive electromagnetic pulses, the loss of intensity of the NMR signal is only due to relaxation processes. On the contrary, if the molecule moves (self-diffusion) in the time between the two consecutive pulses, a loss in the decay intensity can be noticed and the system does not refocus completely at $2t$.

The intensity of the NMR signal (I) is related to the magnitude of the magnetic field-gradient (G) applied to the nucleus by Equation 10.

$$I(b) = I_0 e^{-D\gamma^2 G^2 \delta^2 (t - \frac{\delta}{\epsilon})}$$

Equation 10.

Where D is the self-diffusion coefficient of the molecule, I_0 is the intensity of the NMR signal at G zero, γ is the magnetogyric radius γ , t is the time between pulses and δ is the duration of the electromagnetic pulse. D is a measure of the mobility of the self-diffusing species^[21].

In the current work, PFG NMR was applied to the study of the self-diffusion of PEG in a 1% w/v gel of CMC-g-PEG co-polymers in D₂O. Through the self-diffusional behaviour of PEG it will be possible to obtain some information regarding the structure of the co-polymers, and thus determine whether the PEG is bound to the CMC backbone or not. The self-diffusional behaviour of PEG will be different when it is bound to the CMC backbone compared to when it is unbound. If we assume that the PEG component identified from ¹³C solid state NMR spectrum of the CMC-g-PEG co-polymers (Figure 3.14) is not actually bound to the CMC backbone but just in a mixture with CMC, we would expect the self-diffusion behaviour of the unbound PEG chains in the sample to be similar to the self-diffusion behaviour of unreacted PEG-NH₂. On the contrary, if the PEG component identified from the ¹³C solid state NMR spectrum of the CMC-g-PEG co-polymers (Figure 3.14) is actually bound to the CMC backbone, then the CMC backbone would have a significant influence on the self-diffusion behaviour of the bound PEG chains. In this event, since the PEG and CMC are covalently connected, the bound PEG chains would self-diffuse together with the CMC moiety as one species and therefore, the rate of self-diffusion of the PEG bound to the CMC will be slower than the rate of self-diffusion of unbound PEG. If, however, some of the PEG chains are bound and some are unbound, the analysis of the self-diffusion of PEG chains will show two different self-diffusion behaviours for the two types of PEG chain. Thus it

will be possible to identify whether the PEG chains present are bound to CMC and in theory, estimate what proportion of the PEG chains are bound.

The samples for the PFG NMR analysis were prepared according to the procedure described in section 3.2.2.3. A concentration of 1% w/v was chosen due to the low solubility of the co-polymer in D₂O. A 1% w/v gel in D₂O was very viscous and the use of a higher concentration might interfere with the analysis by inhibiting the self-diffusion of PEG. Furthermore, this choice of concentration allowed a comparison of the results obtained by the PFG NMR analysis with results from a previous study conducted by Nydén et al.^[22] on the self-diffusion of PEG in a ethyl(hydroxyethyl)cellulose (EHEC) gel. The target signal for the PFG NMR analysis was the ¹H resonance of the CH₂O of the PEG chain, since this signal is very intense and easily identified.

The results of the PFG NMR analysis of the CMC-g-PEG co-polymers prepared using PEG-NH₂2K are shown in Figure 3.17.

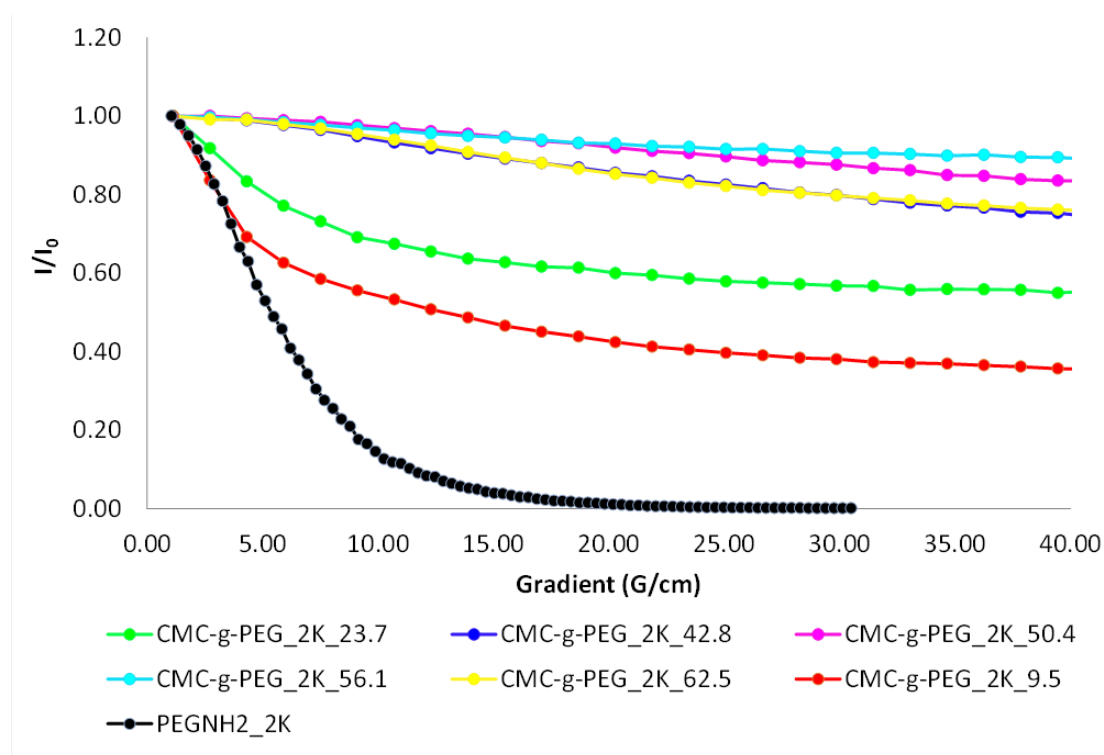


Figure 3.17. Plot of I/I_0 Vs the magnetic field-gradient applied (G) for the study of the self-diffusion behaviour of the PEG component of the CMC-g-PEG_{2K} co-polymers and unbound PEG.

The plot represented in Figure 3.17 shows the variation of the normalised intensity of the NMR signal (I/I_0) of the protons of the PEG chain versus the magnitude of the magnetic field-gradient (G) applied to the sample. The intensity I of the decay for the samples was normalised to I_0 , which is the intensity of the decay of the ^1H NMR resonance of the protons of the PEG chain in a 1% w/v gel of CMC-g-PEG_2K in D_2O when G applied is zero. The value of I_0 was calculated for each sample individually. This was because the decay of the resonance of the protons of the PEG chain varied in each case. The different characteristics of the samples investigated (i.e. different percentage of bound PEG and unbound PEG) can influence the self-diffusion behaviour of the PEG moiety, hence the value of I_0 changes from sample to sample.

In order to allow a comparison with unbound PEG and CMC, a control experiment was conducted on a physical mixture of the two materials, under the same conditions -i.e. 1% w/v gel of CMC in D_2O with added PEG (black dashed line of Figure 3.17). The decay profile for unbound PEG initially decreases linearly with an increase of the applied magnetic field-gradient (G), in accordance with the self-diffusional behaviour of a hard sphere in solution^[23]. Then as G increases, the slope of the curve changes, deviating from the ideal model due to the dispersity of PEG and the small obstruction to diffusion created by the CMC in solution^[22]. This decay profile agrees with the expected decay of the NMR signal of a linear polymer able to freely diffuse through the gel.

The slope of the decay curve for the samples CMC-g-PEG_2K_9.5 (red curve) and CMC-g-PEG_2K_23.7 (green curve) changes as the applied magnetic field-gradient (G) increases. Therefore, the decay curve could be divided into two parts:

- a first part where the decay of the NMR signal of the PEG chain decreases linearly with the increase of G , thus the self-diffusion behaviour of PEG in the sample is similar to the self-diffusion behaviour

of PEG in a physical mixture with CMC, as during the control experiment (black dashed line)

- a second part where the decay of the NMR signal of the PEG chain tends to a constant value as G increases, indicating that the PEG in the sample self-diffuses very slowly.

The presence of an initial steep fall in the decays of the NMR signal of the PEG chain (red and green curves) followed by a plateau in the curve suggest the presence of both bound and unbound PEG in the co-polymer samples. The unbound PEG showing a rapid self-diffusion and steep decay curve whilst the grafted PEG, being part of a much larger molecule is limited in its ability to self-diffuse due to its attachment to the bulky CMC backbone.

In some cases it is not clearly possible to identify two PEG components in the system. For the co-polymers CMC-g-PEG_2K_56.1 (turquoise curve), CMC-g-PEG_2K_62.5 (yellow curve), CMC-g-PEG_2K_42.8 (blue curve) and CMC-g-PEG_2K_50.4 (purple curve) the change is barely visible from this representation.

The self-diffusion coefficient (D) of the slow diffusing species in the CMC-g-PEG_2K co-polymers can be evaluated from Figure 3.17 using Equation 10. Moreover, the plot represented in Figure 3.17 allows an estimate of the proportion of the slow (bound) and fast (unbound) self-diffusing species in the co-polymer sample analysed. The values of intensity ratio to which the decay curve tends to at higher G represent the relative amounts of PEG bound, i.e. the slow self-diffusing species in the sample. Thus, by difference, the remaining percentage refers to the fast self-diffusing species containing PEG. As an example, if the decay curve tends to a value of 0.65, the percentage of the slow self-diffusing species in the sample analysed will be 65%, and the percentage of the fast self-diffusing species in the sample will be 35%.

The estimated proportion of bound PEG is directly related to the purity of the CMC-g-PEG_2K co-polymers synthesised. This percentage features the amount of PEG that self-diffuses slowly due to a bond with the CMC backbone. Hence it represents indirectly the amount of CMC-g-PEG co-polymer in the sample analysed.

The estimated purity of the CMC-g-PEG_2K co-polymers evaluated by PFG NMR analysis and the self-diffusing coefficient (D) of the slow self-diffusing bound PEG in the co-polymer samples are summarised in Table 3-6.

Table 3-6. Self-diffusion coefficient (D) and purity of the CMC-g-PEG_2K co-polymers synthesised.

Sample	D (m ² /s)	Purity % * (PFG NMR)	Purity % * (SEC)
CMC-g-PEG_2K_9.5	5.18×10^{-11}	40.2±0.8	94.8±0.2
CMC-g-PEG_2K_23.7	5.25×10^{-11}	61.2±0.6	91.1±0.4
CMC-g-PEG_2K_42.8	4.14×10^{-11}	79.9±0.7	98.5±0.2
CMC-g-PEG_2K_50.4	1.82×10^{-11}	92.4±0.9	96.8±0.5
CMC-g-PEG_2K_56.1	5.00×10^{-11}	94.5±0.1	95.5±0.8
CMC-g-PEG_2K_62.5	3.33×10^{-11}	79.8±0.9	96.4±0.4

* Three repetitions were recorded for each sample.

The results reported in Table 3-6 show that the purities estimated by PFG NMR technique for samples CMC-g-PEG_2K_23.7, CMC-g-PEG_2K_9.5, CMC-g-PEG_2K_42.8 and CMC-g-PEG_2K_62.5 is lower than the purities evaluated by SEC in DMF, whilst for samples CMC-g-PEG_2K_50.4 and CMC-g-PEG_2K_56.1 the values determined are almost in agreement.

A possible reason for this difference could be that whilst the movement of the whole PEG chain is restricted due to bonding to the CMC backbone, the PEG

chain end will still have a high degree of freedom in solution. As a result the data observed may be skewed by fast diffusion of the PEG chain end away from the CMC backbone. The graph then levels off as no further diffusion away from the CMC occurs.

The fast self-diffusion of the PEG chain end could also be observed graphically. For the purpose of the explanation, the diffusion behaviour of CMC-g-PEG_2K_9.5 co-polymer was chosen.

Theoretically, the variation to the diffusional behaviour of the species in solution should correspond to a very sharp change in the decay curve, with the curve then reaching a plateau immediately, as shown from Figure 3.18 (blue trace). Although the change in the slope of the decay curve for CMC-g-PEG_2K_9.5 (red curve) at $G = 4.7$ G/cm is sharp, the second part of the decay curve reaches a plateau only at higher values of G applied ($G = 28.8$). The portion of the decay curve between the sharp change in the slope and the plateau point probably refers to the diffusion of the free chain end of PEG bound to the CMC backbone (Figure 3.18).

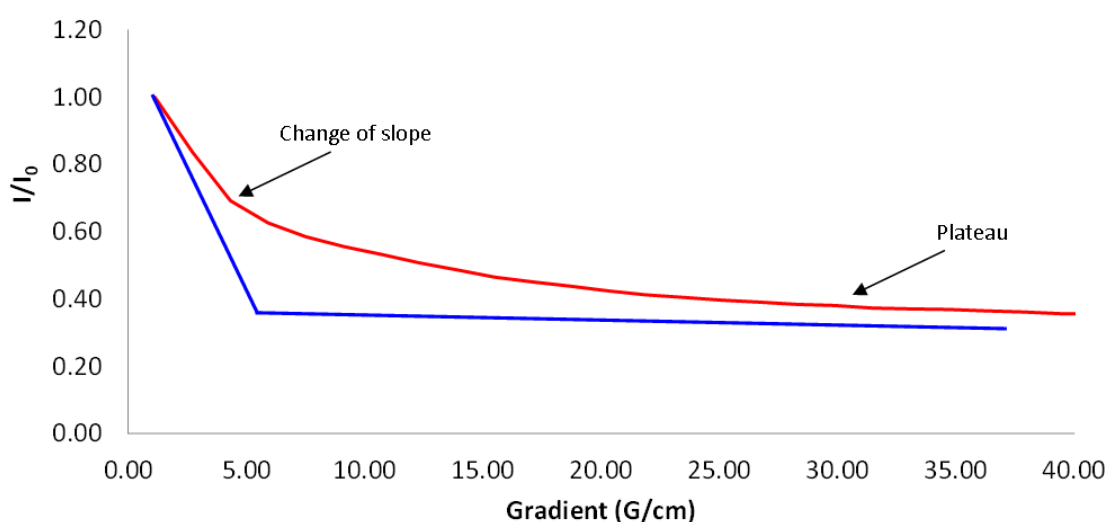


Figure 3.18. Example of the percentage of unbound PEG in CMC-g-PEG_2K_9.5 determined by the software.

The CMC-g-PEG co-polymers containing PEG-NH₂5K were also analysed via PFG NMR and the results obtained are shown in Figure 3.19.

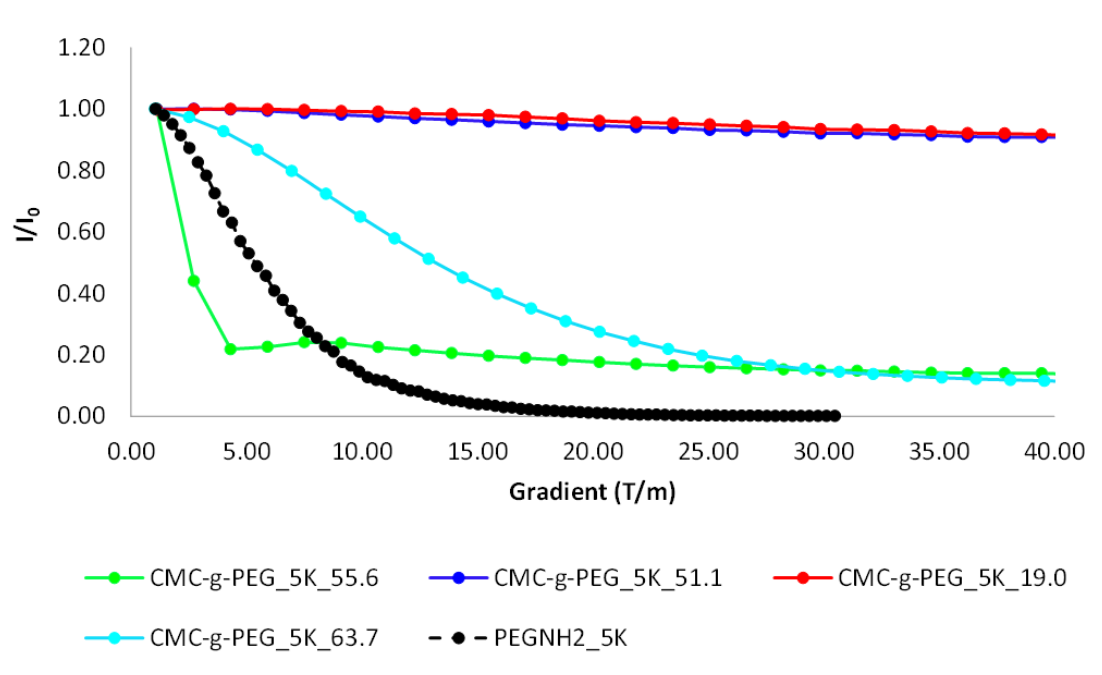


Figure 3.19. Plot of I/I_0 Vs the magnetic field-gradient applied (G) for the study of the self-diffusion behaviour of the PEG component of the CMC-g-PEG_{5K} co-polymers.

As for the previous plots, the black dashed line of Figure 3.19 shows the decay (I/I_0) of the intensity of the ¹H NMR resonance of the protons of the PEG chain for PEG in a physical mixture with CMC in D₂O. The observed decay for the black curve is the same as Figure 3.17. The initially decrease is followed by a deviation from the ideal model as the G applied increased.

Once again, two PEG components can be identified in the system for sample CMC-g-PEG_{5K}_{55.6} (green curve) and CMC-g-PEG_{5K}_{63.7} (turquoise curve), as the slope of the decay curve changes. The fast self-diffusing PEG component corresponds to unbound PEG present in a mixture with the CMC-g-PEG_{5K} co-polymer, whilst the second slow self-diffusing component containing PEG corresponds to PEG grafted to the CMC backbone. For sample

CMC-g-PEG_5K_19.0 (red curve) and CMC-g-PEG_51.1 (blue curve) it is not possible to notice a variation in the slope of the curve from Figure 3.19.

Equation 10 and Figure 3.19 can be used in the same way to calculate D of the slow self-diffusing species and the relative percentages of both the fast and slow self-diffusing species in the CMC-g-PEG_5K co-polymers. The results are summarised in Table 3-7.

Table 3-7. Self-diffusion coefficient (D) and purity of the CMC-g-PEG_5K co-polymers synthesised.

Sample	D (m ² /s)	Purity % * (PFG NMR)	Purity % * (SEC)
CMC-g-PEG_5K_19.0	1.48×10^{-13}	98.5±0.5	99.1±0.1
CMC-g-PEG_5K_51.1	2.21×10^{-13}	97.8±0.6	98.9±0.6
CMC-g-PEG_5K_55.6	3.04×10^{-12}	13.2±0.9	95.5±0.3
CMC-g-PEG_5K_63.7	3.87×10^{-12}	11.0±0.3	83.3±0.5

* Three repetitions were recorded for each sample.

Once more, from Table 3-7 it is possible to notice that the purity estimated by PFG NMR technique for some of the samples (CMC-g-PEG_5K_55.6 and CMC-g-PEG_5K_63.7) is significantly lower than the purity evaluated by SEC in DMF, while for others (CMC-g-PEG_5K_19.0 and CMC-g-PEG_5K_51.1) the purity estimated by these two techniques is very similar. As outlined before, it is possible that the self-diffusion of the PEG chain end could affect the observed diffusional behaviour, thus leading to overestimate the relative proportion of unbound PEG. Furthermore, if the M_n of the PEG chain grafted to the CMC backbone increases, it would be expected that the PEG chain end could self-diffuse more before being slow down by the bulky CMC. Thus, the overestimates of the relative proportion of unbound PEG would be even higher.

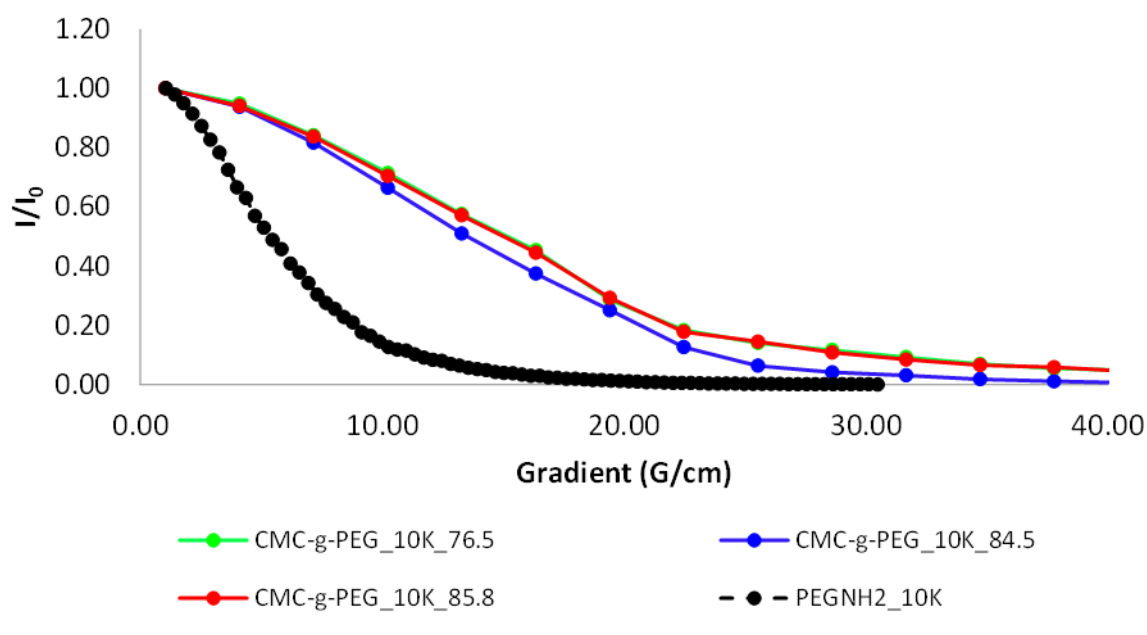


Figure 3.20. Plot of I/I_0 Vs the magnetic field-gradient applied (G) for the study of the self-diffusion behaviour of the PEG component of the CMC-g-PEG_{10K} co-polymers.

Table 3-8. Self-diffusion coefficient (D) and purity of the CMC-g-PEG_{10K} co-polymers synthesised.

Sample	D (m^2/s)	Purity %* (PFG NMR)	Purity %* (SEC)
CMC-g-PEG _{10K} _{76.5}	3.33×10^{-11}	4.7 ± 0.9	79.6 ± 0.9
CMC-g-PEG _{10K} _{84.5}	4.22×10^{-11}	1.3 ± 0.5	69.5 ± 0.3
CMC-g-PEG _{10K} _{85.8}	3.35×10^{-11}	4.5 ± 0.7	79.6 ± 0.9

* Three repetitions were recorded for each sample.

Once more, the purity estimated by PFG NMR technique for all the co-polymers containing PEG-NH₂10K is significantly lower than the purity evaluated by SEC in DMF. As discussed before, it would appear that as the M_n of the PEG chain increases, PFG NMR fails to account for the limitation to self-diffusion of long PEG chains due to the bond with CMC. Thus in the case of PEG-NH₂10K the

long PEG chain self-diffuses as unbound PEG-NH₂10K even when it is bound to CMC.

Through PFG NMR technique it was possible to confirm the presence of a bond between the PEG chains and the CMC backbone in CMC-g-PEG co-polymers containing PEG-2K and PEG-5K due to a difference in the self-diffusion behaviour of the PEG chain present in the sample. Furthermore, the relative proportions of bound and unbound PEG were estimated, which allowed to determine the purity of the co-polymer samples analysed. A comparison with the value of unbound PEG measured by SEC in DMF showed that in some cases there was a close agreement between the two techniques (e.g. CMC-g-PEG_2K_50.4, CMC-g-PEG_2K_56.1, CMC-g-PEG_5K_19.0 and CMC-g-PEG_5K_51.1), while in other cases there was a large overestimation of the proportion of unbound PEG (e.g. CMC-g-PEG_2K_62.5, CMC-g-PEG_2K_42.8, CMC-g-PEG_5K_19.0, CMC-g-PEG_5K_55.6, CMC-g-PEG_10K_84.5, CMC-g-PEG_10K_85.8 and CMC-g-PEG_10K_76.5) with PFG NMR. Several repeats of the PFG NMR analysis might be necessary to increase the accuracy of the results obtained. Therefore, the purity of the CMC-g-PEG co-polymer estimated through SEC in DMF was used throughout the entire work.

3.3.3. Fluorescent Labelling of CMC-g-PEG co-polymers

In order to evaluate and in an attempt to quantify the adsorption/desorption process of the CMC-g-PEG co-polymers during a wash cycle and compare it with the behaviour of unmodified CMC, two CMC-g-PEG co-polymers and two unmodified samples of CMC were labelled with 5-([4,6-dichlorotriazin-2-yl]amino)fluorescein (DTAF). DTAF was chosen as fluorescent label because the reaction between DTAF and the CMC backbone can be performed in water (Figure 3.21).

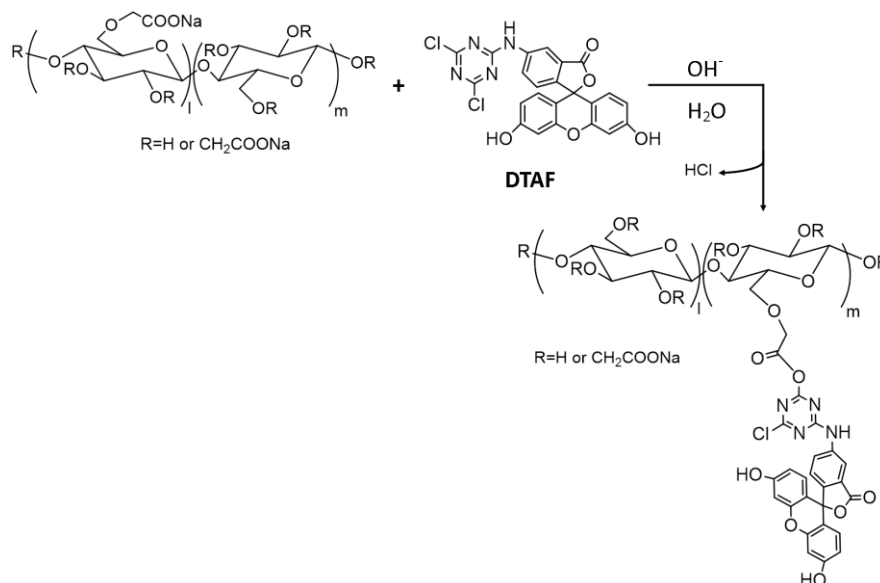


Figure 3.21. Labelling of CMC with DTAF in water at pH 8.

The displacement of one of the two residual chloride groups on the cyanuric chloride moiety of DTAF by a hydroxyl group on the CMC backbone by nucleophilic substitution allows the fluorescent dye to be covalently bound to the polymeric backbone. The reaction is performed under basic conditions (pH = 8), so as to neutralise the HCl formed.^[24]

A fluorescent dye was used instead of a non-fluorescent dye to minimise the necessary modification to the polymeric backbone. The fluorescent signal is intense even at low concentrations of fluorophore, while a non-fluorescent dye would have required a much higher extent of labelling to have a detectable signal. Furthermore, a low level of labelling was preferred in order to reduce the risk of changing the interactions between the polymeric backbone and the fabric during the wash cycle.

Two types of unmodified CMC were labelled with the fluorescent dye:

- Finnifix V, which is the same type of CMC used for the synthesis of the CMC-g-PEG co-polymers

- Finnifix DK, which has a lower degree of blockiness (DB) than Finnifix V but the same degree of substitution (DS). The DS refers to the proportion of hydroxyl groups substituted with carboxymethyl groups per glucose ring, while the DB refers to the distribution of the carboxymethyl groups in the CMC backbone. A high value of DB means that the carboxymethyl groups are localised in “blocks”.

Through the labelling of two different types of unmodified CMC it was possible to investigate the effect of the DB over the adsorption/desorption process. Due to a lack of material, only two of the CMC-g-PEG co-polymers were labelled with DTAF and their adsorption/desorption properties were investigated in Chapter 4.

The labelled CMC-g-PEG co-polymer and labelled unmodified CMCs samples will be referred to from now on with a * next to their code name.

The extent of labelling of the unmodified CMCs* and the CMC-g-PEG* co-polymers was evaluated by means of a calibration curve based on solutions of known concentration of the fluorophore DTFA in water. The results are summarised in Table 3-9.

Table 3-9. Extent of labelling of the Finnifix V*, Finnifix DK* and CMC-g-PEG* co-polymers.

Sample	Degree of labelling (mg DTAF/g polymer)
Finnifix V*	0.11
Finnifix DK*	0.24
CMC-g-PEG_5K_51.1*	0.0019
CMC-g-PEG_5K_19.0*	0.007

The extent of labelling achieved through the reaction between CMC-g-PEG co-polymers and DTAF is much lower than obtained with unmodified CMC, despite the same reaction conditions and stoichiometry being used. Moreover, the sample containing the higher weight percentage of PEG bound has the lower degree of labelling. A possible reason for this difference could be the presence of grafted PEG on the CMC backbone. The steric hindrance of the grafted PEG chain could inhibit the carboxymethyl groups of the CMC backbone from reacting with DTAF as shown in Figure 3.22.

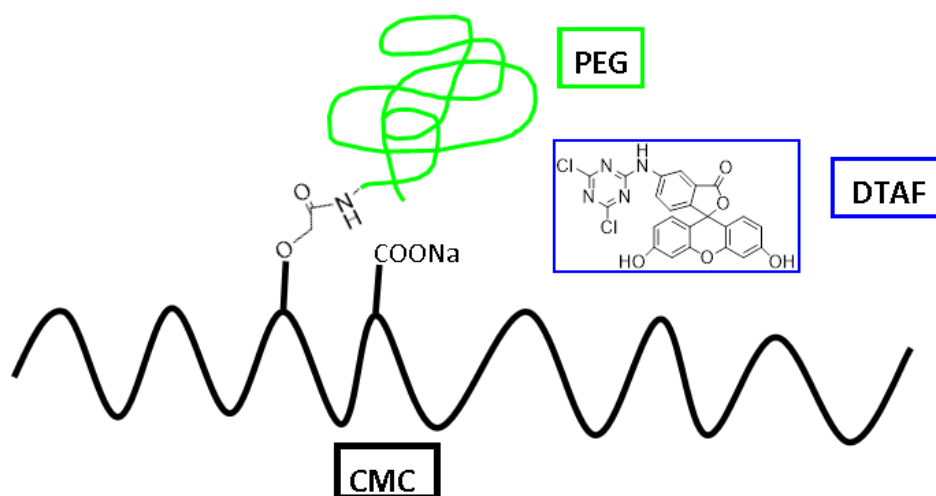


Figure 3.22. Steric hindrance of PEG grafted on to the CMC backbone to the reaction with DTAF.

With the knowledge of the amount of DTAF per gram of co-polymer, it should be possible to quantify the adsorption of the CMC-g-PEG co-polymers and unmodified CMC over cotton surface by assessing the difference in the fluorescence emission before and after the wash cycle (see Chapter 4, section 4.4.1 for the discussion).

3.4. Conclusions

In conclusion, the PEGylation reaction of activated CMC in DMF was discussed as a strategy for the synthesis of potential SRPs for cotton surfaces. The reaction was found to be influenced by the steric hindrance of the PEG chain, which limits the accessibility of the terminal amino group of PEG in solution.

The synthesised co-polymers were characterised through a series of techniques, such as ^{13}C solid state NMR, ^1H gel state NMR, SEC in DMF and PFG NMR. From ^{13}C solid state NMR the structure of the co-polymers was confirmed. The strong peak at $\delta 70.9$ proved the presence of PEG chain in the sample, while the presence of a new signal at $\delta 171.7$ in the carbonyl region demonstrated the formation of an amide bond. Whilst the weight percentage of PEG bound was evaluated through the SEC data and ^1H gel state NMR spectrum. Through SEC in DMF, it was possible to evaluate the concentration of unbound PEG present in the mixture from the area underneath the concentration curve, using a triple detector calibration. Whilst the total amount of PEG in the co-polymers (bound and unbound) was estimated through ^1H gel state NMR spectrum. Through cross-referencing of the peak integral of PEG in CMC-g-PEG co-polymers with a calibration curve and following the procedure described in Figure 3.16 it was possible to obtain the total concentration of PEG and therefore by difference with the SEC data the weight percentage of PEG bound was evaluated.

The relative proportions of bound and unbound PEG were also estimated via PFG NMR analysis. The decay curves obtained for the CMC-g-PEG co-polymers it confirmed that all the samples synthesised contained a proportion of PEG bound to CMC backbone. The proportion of unbound PEG, evaluated from PFG NMR, was higher than the value measured via SEC for most of the samples, possibly due to a faster self-diffusion of the PEG chain end compared to the whole PEG chain bound to the CMC backbone, which led to an overestimation of the overall amount of PEG unbound.

In readiness to study the adsorption/desorption of the co-polymers through fluorescence spectroscopy, two CMC-g-PEG co-polymer and two different types of CMC were successfully labelled with DTAF.

The next chapter will focus on the evaluation of the soil release properties of the synthesised CMC-g-PEG co-polymers, and the discussion of the results of a preliminary study on the adsorption/desorption ability of the co-polymers.

3.5. References

1. Lang, F. P.; Morschhauser, R. *SOWT-Journal* **2006**, 132, 24-34.
2. Hoffmann, I.; Theile, M.; Gratz, S.; Scholz, J.; Barreleiro, P.; Von Rybinski, W.; Gradzielski, M. *Langmuir : The ACS Journal of Surfaces and Colloids* **2012**, 28, (31), 11400-11409.
3. Lang, F. P. *Chimica Oggi* **1998**, 16, (9).
4. Agostini, S.; Hutchings, L. R. *European Polymer Journal* **2013**, 49, (9), 2769-2784.
5. Cameron, D. J. A.; Bissessur, R.; Dahn, D. C. *European Polymer Journal* **2012**, 48, 1525-1537.
6. Barbucci, R.; Leone, G.; Monici, M.; Pantalone, D.; Fini, M.; Giardino, R. *Journal of Materials Chemistry* **2005**, 15, (22), 2234.
7. Bao, Y.; Ma, J.; Sun, Y. *Carbohydrate Polymers* **2012**, 88, (2), 589-595.
8. Barbucci, R.; Magnani, A.; Consumi, M. *Macromolecules* **2000**, 33, 7475-7480.
9. Chang, C.; Zhang, L. *Carbohydrate Polymers* **2011**, 84, (1), 40-53.
10. Apperley, D.; Harris, R. K.; Hodgkinson, P., *Solid State NMR : Basic Principles and Practice*. Momentum Press: 2012.
11. Aggerlyd, I.; Olin, A. *Talanta* **1985**, 32, 645-649.
12. Hoodgendam, C. W.; Keizer, A. d.; Cohen Stuart, M. A.; Bijsterbosch, B. H. *Macromolecules* **1998**, 31, 6297-6309.
13. Gran, G. *Analyst* **1952**, 77, (920), 661-671.
14. Eyley, R. W.; Klug, E. D.; Diephuis, F. *Analytical Chemistry* **1947**, 19, 24-27.
15. Lant, N. Laundry composition. Patent number EP2135933A1, 2009.
16. Saigo, K.; Usui, M.; Kikuchi, K. *Bulletin of the Chemical Society of Japan* **1977**, 50, 1863-1866.
17. Kopf, A.; Baschnagel, J.; Wittmer, J.; Binder, K. *Macromolecules* **1996**, 29, 1433-1441.

18. Sternlicht, H.; Kenyon, G. L.; Packer, E. L.; Sinclair, J. *Journal of the American Chemical Society* **1971**, 93, (1), 199-208.
19. Braunshier, C.; Hametner, C. *QSAR & Combinatorial Science* **2007**, 26, (8), 908-918.
20. Cipriani, G.; Salvini, A.; Dei, L.; Macherelli, A.; Cecchi, F. S.; Giannelli, C. *Journal of Cultural Heritage* **2009**, 10, (3), 388-395.
21. Walderhaug, H.; Söderman, O.; Topgaard, D. *Progress in Nuclear Magnetic Resonance Spectroscopy* **2010**, 56, (4), 406-25.
22. Nydén, M.; Söderman, O.; Karlström, G. *Macromolecules* **199**, 32, 127-135.
23. Johansson, L.; Elvingson, C. *Macromolecules* **1991**, 24, 6024-6029.
24. Belder, A. N.; Granath, K. *Carbohydrate Research* **1973**, 30, 375-378.

3.6. Appendix B

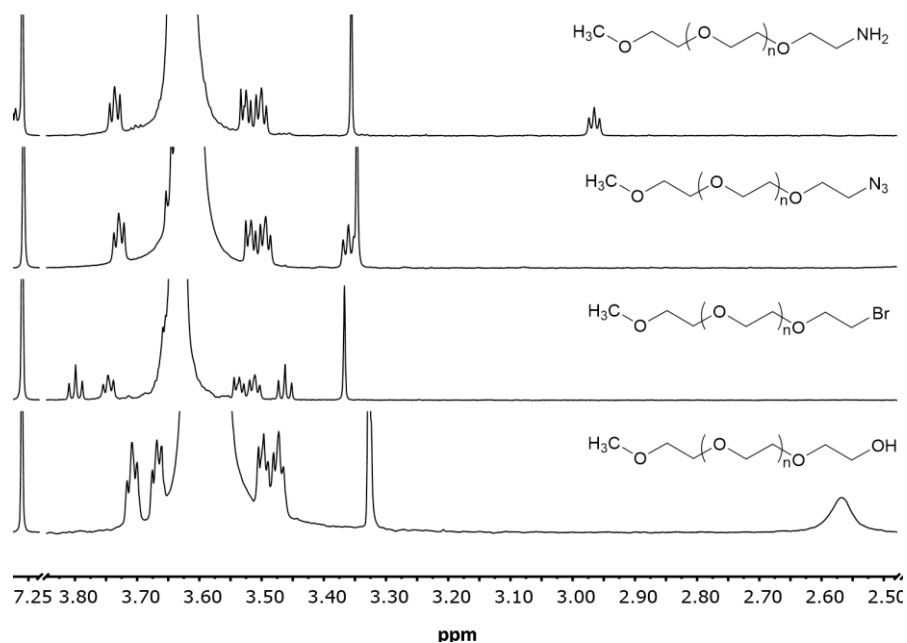


Figure 3.23. Comparison between ^1H NMR spectra of PEG-OH5K, PEG-Br5K, PEG-N₃5K and PEG-NH₂5K. Spectra recorded at 700 MHz in CDCl_3 .

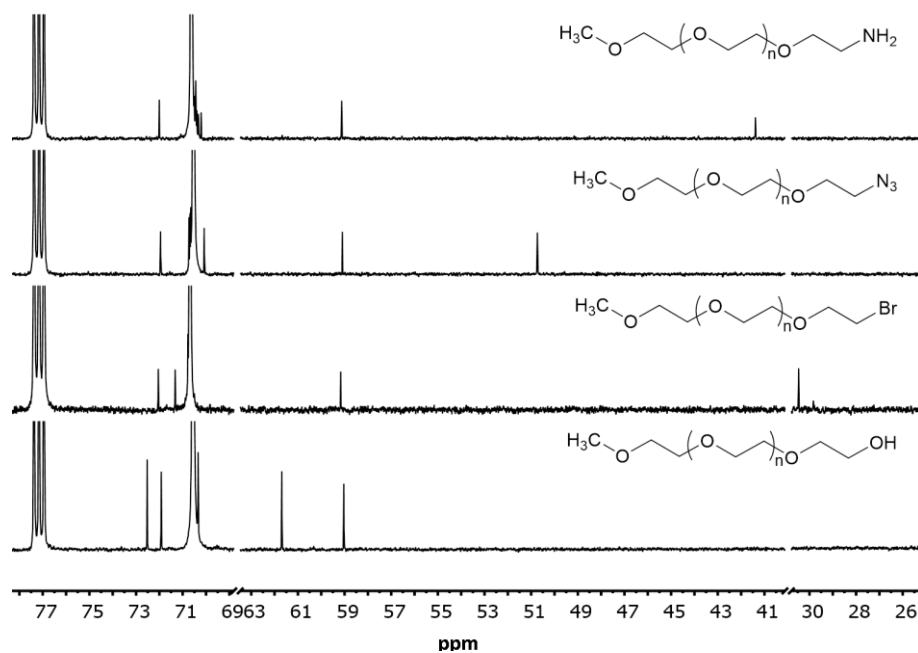


Figure 3.24. Comparison between ^{13}C NMR spectra of PEG-OH5K, PEG-Br5K, PEG-N₃5K and PEG-NH₂5K. Spectra recorded at 700 MHz in CDCl_3 .

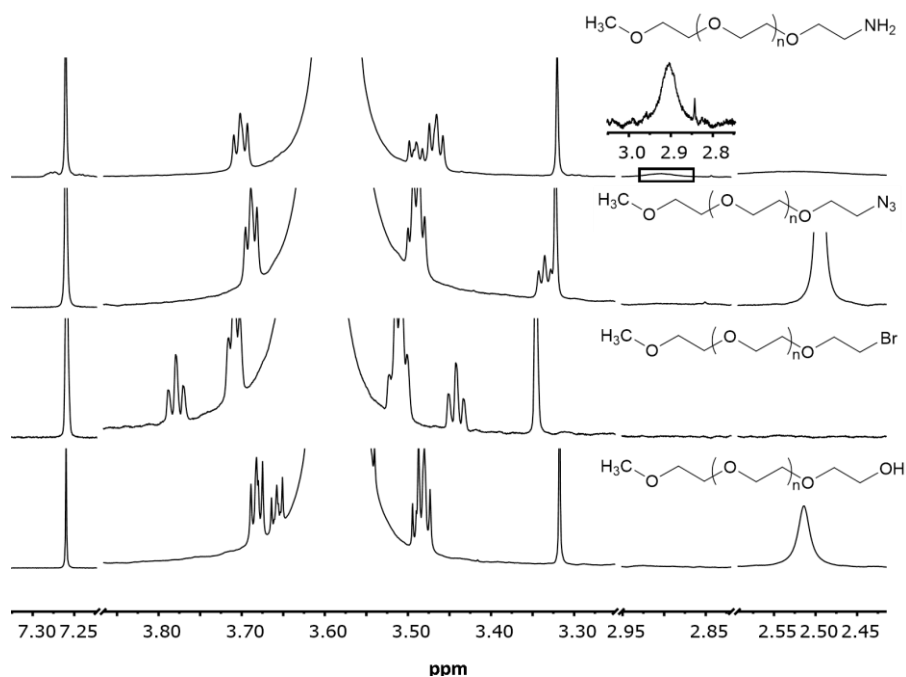


Figure 3.25. Comparison between ^1H NMR spectra of PEG-OH10K, PEG-Br10K, PEG-N₃10K and PEG-NH₂10K. Spectra recorded at 700 MHz in CDCl₃.

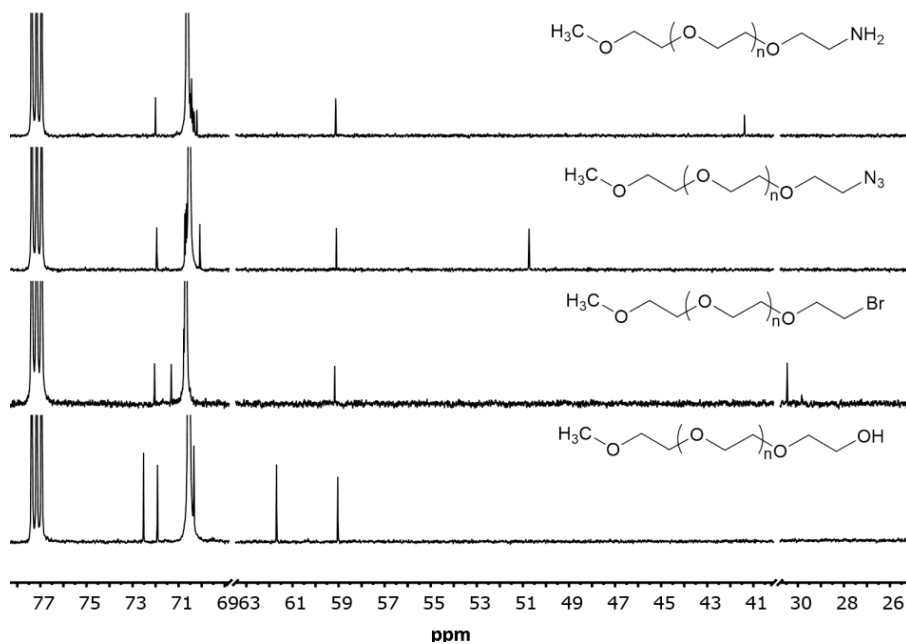


Figure 3.26. Comparison between ^{13}C NMR spectra of PEG-OH10K, PEG-Br10K, PEG-N₃10K and PEG-NH₂10K. Spectra recorded at 700 MHz in CDCl₃.

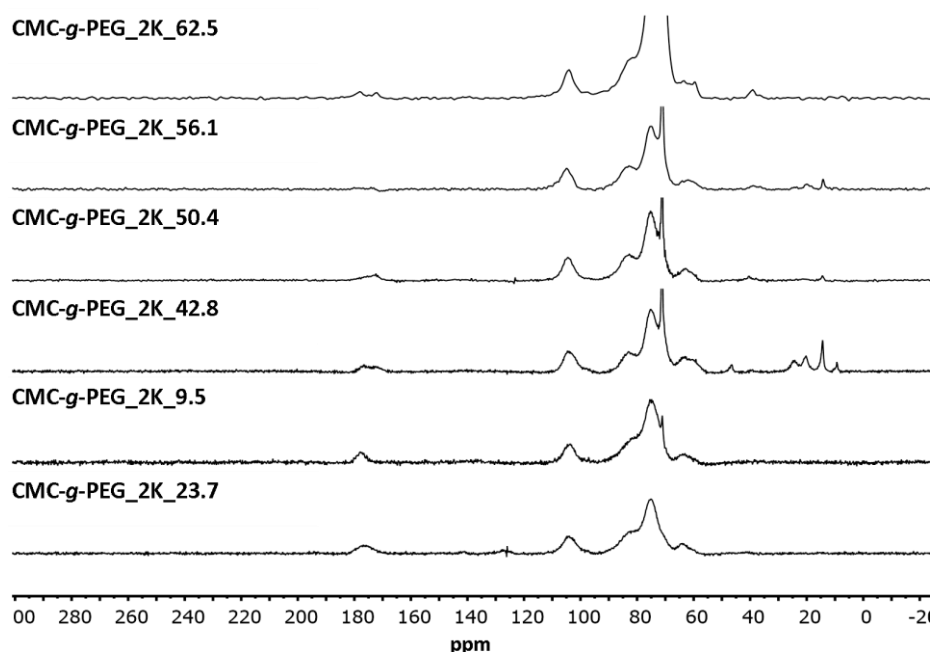


Figure 3.27. ^{13}C solid state NMR spectra of CMC-g-PEG_2K co-polymers. Spectra recorded at 100 MHz.

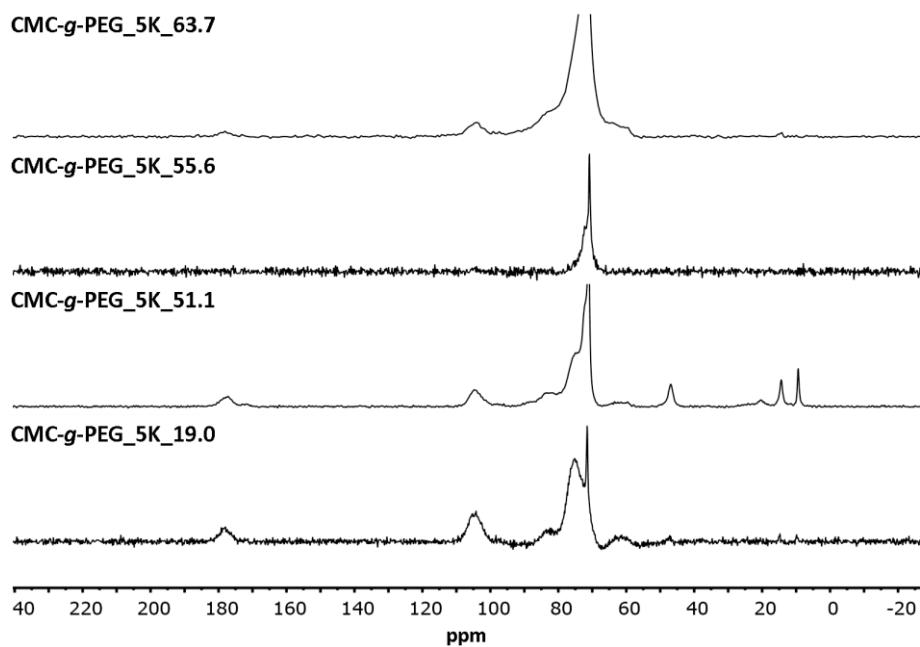


Figure 3.28. ^{13}C solid state NMR spectra of CMC-g-PEG_5K co-polymers. Spectra recorded at 100 MHz.

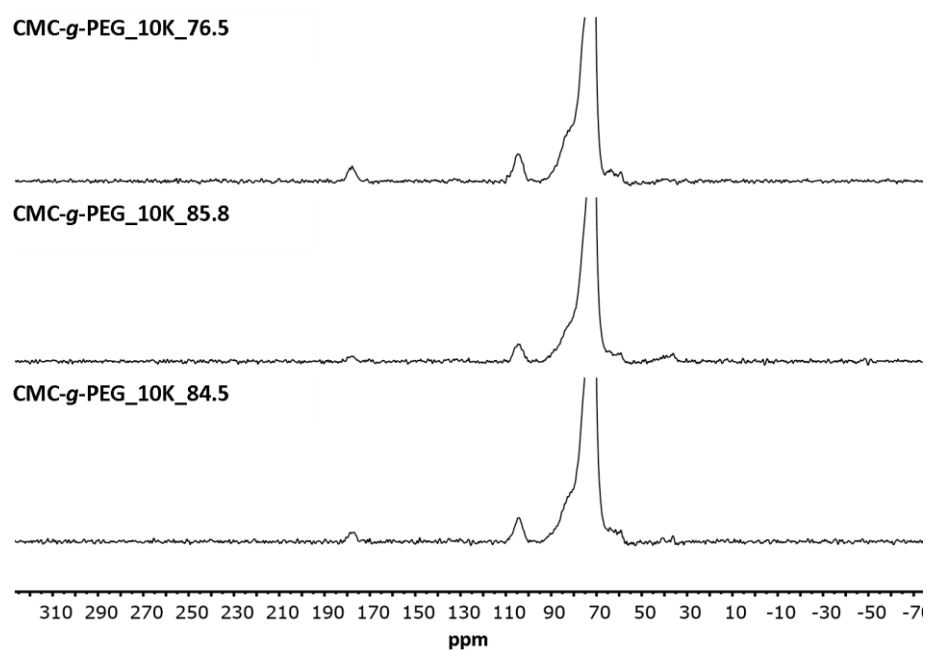


Figure 3.29. ^{13}C solid state NMR spectra of CMC-g-PEG_10K co-polymers. Spectra recorded at 100 MHz.

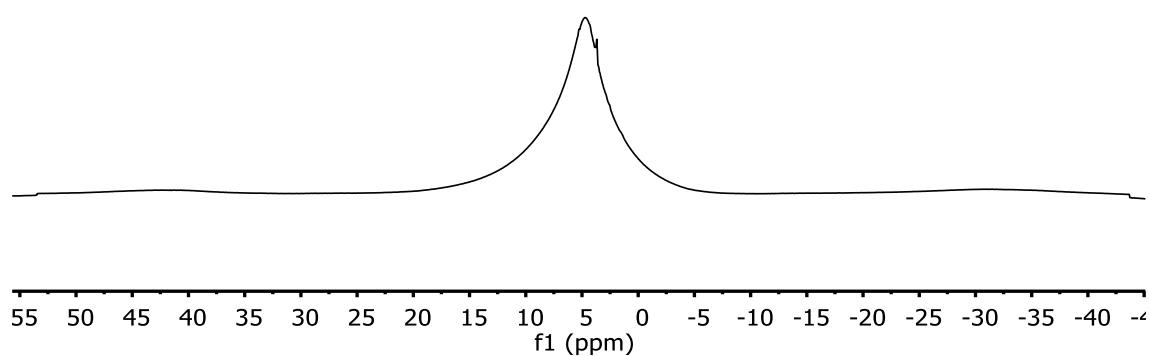


Figure 3.30. Example of ^1H solid state NMR spectrum of CMC. Spectrum recorded at 100 MHz in cross-polarisation.

4

Evaluation of the washing properties of CMC-*g*-PEG copolymers

4.1. Introduction

In order to evaluate the efficacy of a potential soil release polymer (SRP) to remove stains from fabric surfaces, a test was developed in 1969 by the American Association of Chemists and Colourists^[1] called the “*soil release test*”. This test consists of three stages: prewash, staining and rinsing (Figure 4.1).

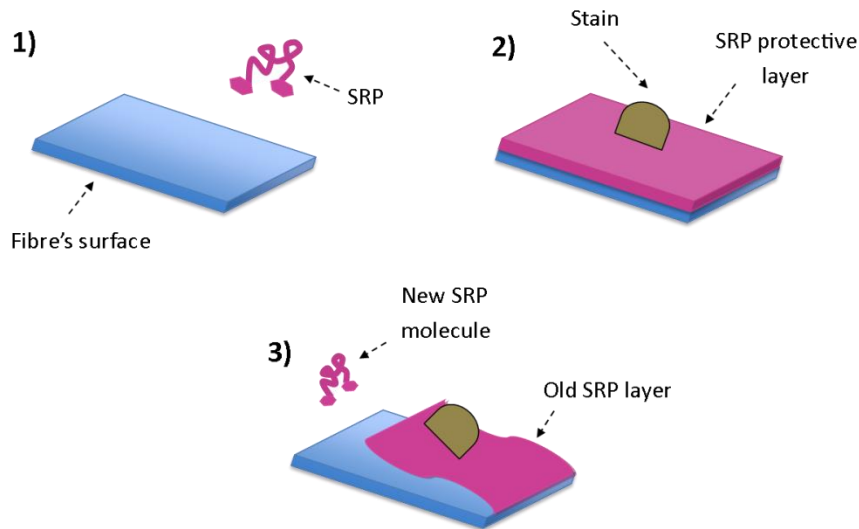


Figure 4.1. Soil release test stages. 1) Prewash stage. 2) Staining stage. 3) Rinsing stage.

During the first stage, small pieces of fabric called “swatches” are washed with a laundry detergent containing the SRP to be analysed. This allows a build-up of a layer of SRP over the surface of the fabric and guarantees optimal coverage by the polymer. The number of prewashes necessary to build-up such a layer depends on several parameters, such as the affinity of the SRP for the substrate, the number of swatches used, the concentration of SRP in the formulation, the temperature adopted during the wash cycle and the wash time^[2].

The second “*staining*” stage involves the deposition of the stain over the fabric. Stubborn stains, for example lipstick, motor oil or fat are typically used in this step. The use of these stubborn stains allows the most accurate evaluation of the action of the SRP. In contrast, common stains such as coffee and mascara are easily removed by the surfactants contained in a regular laundry detergent and so the relevant efficacy of the SRP cannot be assessed. The presence of a specific SRP product is necessary to remove stubborn stains and hence the removal of a stubborn stain by a laundry detergent containing a SRP proves the activity of the SRP in the formulation.

Prior to performing the final “*rinsing*” stage, the reflectance of the fabric surface must be measured using a spectrophotometer. The result is expressed either as percentage of reflectance of the surface or as a numerical value which corresponds to a point in the 3D colour space^[1]. The final stage of the process then comprises a simple wash cycle with a laundry detergent that does not contain an SRP in the formulation. The performance of the SRP can then be evaluated as the difference between the reflectance (or colour) of the swatch’s surface before and after the rinse cycle. A successful SRP would desorb during this final stage, simultaneously removing the stain.

When conducting a washing cycle using a laundry detergent, a common problem encountered is the redeposition of removed stains back on to the garments. This results in the greying of the fabric surface over time. To prevent this, sodium carboxymethyl cellulose (NaCMC) is added to laundry detergents in order to act as an anti-redeposition agent. In more recent formulations, the enzyme amylase has been included to remove starch-like stains. Unfortunately, the structure of NaCMC is similar to starch, therefore amylase enzyme cannot distinguish between them, meaning that the two cannot be used in combination.

The incompatibility of amylase with NaCMC led to the necessity for other anti-redeposition agents to be developed^[1]. The main property of an anti-redeposition agent is the ability to adsorb over the target surface. Since SRPs are designed to specifically interact with a textile surface, they could be applied as potential anti-redeposition agents^[3]. Although the adsorption in the case of SRPs is reversible, for the anti-redeposition agents it is not, the SRP layer is constantly renewed during each wash cycle. Furthermore, due to the mechanism of action of the SRPs, the removed stain is wrapped in a shell constituting the SRP itself^[1], hence it is prevented from re-depositing on the fabric due to electrostatic repulsion between the two layers of SRPs.

The performance of a SRP as an anti-redeposition agent is evaluated using a Whiteness test. In this test, a set of fabric swatches is washed in the presence of carbon black using a laundry detergent containing a SRP. Simultaneously, a second set of swatches are washed without SRP in the formulation. The difference between the reflectance of these two sets of swatches as measured using a spectrophotometer indicates the efficacy of the SRP as anti-redeposition agent. Carbon black is used as the stain in this test because of its colour. The dark colour of carbon black effectively mimics the visible greying of the textile's surface detected by human sight due to redeposition of stains.

In this chapter the soil release and anti-redeposition properties of the CMC-g-PEG co-polymers synthesised in this study will be evaluated and discussed. Moreover, the results from a preliminary study on the amount of CMC-g-PEG co-polymer adsorbed over the surface of cotton fabric will be discussed.

4.2. Experimental section

4.2.1. *Material*

All the described tests were conducted at P&G Newcastle Innovation Centre. The test fabric swatches used for the tests were approximately 5 cm x 5 cm in size, made of white knitted cotton and supplied by Warwick Equest. The soils used were lard (with added SV13-DYE) and carbon black, both supplied by Warwick Equest. The water used for the washing test had a hardness of approximately 200 mg/L. The laundry detergent used was TIDE®.

4.2.2. *Instruments*

The soil release and whiteness tests were performed in a tergotometer. This equipment reproduces the action of a domestic washing machine on a smaller scale. The tergotometer comprises ten small 'washing machines' (1 L capacity), known as pots, in series. Each pot features a temperature control, a mechanical stirrer and a lid to avoid external contamination during service and to allow control of the washing conditions. The tergotometer used for the analysis was proprietary to P&G.

The spectrophotometer used to measure the brightness of the swatches was model Jenway 6850, equipped with a UV/Vis filter, calibrated with daylight illuminant D65 standard (mimics the light in Western Europe/Northern Europe at midday).

The spectrofluorimeter used to measure the fluorescence of the washing liquor was a Molecular Devices Spectramax M2. The fluorescence was measured at 5 nm intervals in the range of 500 nm to 700 nm. The excitation wavelength used was $\lambda_{\text{ex}} = 495 \text{ nm}$.

4.2.3. Analysis

4.2.3.1. Fluorescence Microscope

Microscope images of the swatches were recorded using a Nikon Eclipse ME600, equipped with a B-2A filter and a mercury lamp. The excitation wavelength used was $\lambda_{\text{ex}} = 495 \text{ nm}$.

4.2.3.2. ^{13}C solid state NMR analysis

^{13}C solid state NMR spectra were recorded in collaboration with the EPSRC UK National Solid-state NMR Service at Durham.

The spectra were recorded at room temperature (25 °C) using a Varian VNMR5 Spectrometer equipped with a 6 mm (rotor o.d.) magic-angle spinning probe. The frequency used for the ^{13}C NMR spectra was approximately 100 MHz. The data were collected using cross-polarisation with a 5 or 10 recycle delay and a 1 ms contact time. The samples were spun at 6.0 kHz.

4.2.4. Soil release test

The following procedure was used to determine the effectiveness of the CMC-g-PEG co-polymer as a SRP.

A stock solution of each of the CMC-g-PEG co-polymers was prepared by dispersing approximately 0.2 g of co-polymers in high purity water (50 mL).

The wash cycle was performed as follows. In a tergotometer pot, TIDE® (2.0 g) laundry detergent was dissolved in water at 25 °C (average hardness of the water 200 mg/L) and stirred at 200 rpm for 1 min before the addition of 5 mL of the stock solution of the co-polymer under analysis. The amount of co-polymer

added was equal to 1% in weight of the laundry detergent composition. The solution in the tergotometer pot was stirred for further 2 minutes before the addition of the white knitted cotton swatches (approximately 33 g). The swatches were washed at 25 °C for 20 minutes, rinsed for 5 minutes with fresh water (average hardness of the water 200 mg/L) and drained.

The wash cycle was repeated four times, before the swatches were dried in a tumble dryer at 150 °C for 1 hour. In the meantime, lard SV13-DYE was melted at 70 °C through the use of a hot plate. Upon drying, the swatches were stained with lard (200 µL) using a micropipette. The stain was allowed to dry overnight. Then, the brightness of the surface of each swatch was measured by a spectrophotometer at 460 nm (D65/10°).

During the final stage, the stained swatches were washed at 25 °C for 20 minutes, without the addition of the CMC-g-PEG co-polymer solution. Once the swatches were dried, the brightness of the surfaces were measured again and the soil release index (SRI) was calculated as the difference between the brightness of the surface before and after the last wash cycle (sections 4.3.2., 4.3.3. and 4.3.4.).

4.2.5. Whiteness test

The following procedure was used to determine the efficacy of the CMC-g-PEG co-polymer as an anti-redeposition agent.

A stock solution of each of the CMC-g-PEG co-polymers was prepared by dispersing the co-polymer (approximately 0.2 g) in high purity water (50 mL). Carbon black (0.04 g) was dispersed in high purity water (5 mL) and sonicated for 20 minutes before addition to the wash cycle.

The wash cycle was performed as follows. In a tergotometer pot, TIDE® (2.0 g) laundry detergent was added to water at 25 °C (average hardness of the water 200 mg/L) and stirred at 200 rpm for 1 min before the addition of 2.5 mL of the stock solution of the co-polymer under analysis. The amount of co-polymer added was equal to 0.5% in weight of the laundry detergent composition. After 1 minute, carbon black (0.04 g dispersed in 5 mL of high purity water via sonication bath for 20 minutes) was added to the tergotometer pot. The mixture in the tergotometer pot was stirred for further 2 minutes before the addition of the white knitted cotton swatches (approximately 33 g). The swatches were washed at 25 °C for 20 minutes, rinsed for 5 minutes with fresh water (average hardness of the water 200 mg/L) and drained.

The wash cycle was repeated four times, then the swatches were allowed to dry naturally overnight. Upon drying, the brightness of the surface of each swatch was measure by a spectrophotometer at 460 nm (D65/10°). The CIE whiteness was then calculated as difference between the brightness of the surface before and after the washing cycles (sections 4.3.2., 4.3.3. and 4.3.4.).

4.2.6. Quantitative analysis of deposition using fluorescently labelled CMC

The following procedure was used to determine the amount of CMC-g-PEG* co-polymer adsorbed over the surface. The analysis were repeated using three different concentrations of CMC-g-PEG* (1 %, 0.5 % and 0.3 % in weight with respect to the amount of laundry detergent used) as described below.

A stock solution of each of the fluorescently labelled CMC-g-PEG* co-polymers was prepared by dispersing the co-polymer (approximately 0.2 g) in high purity water (50 mL).

The fluorescence of the washing liquor was measured by a spectrofluorimeter ($\lambda_{\text{exc}} = 495 \text{ nm}$, $\lambda_{\text{em}} = 400\text{-}700 \text{ nm}$) equipped with a mercury vapour lamp. The samples were filtered through a $0.45 \mu\text{m}$ nylon filter and analysed in quartz cuvettes.

A new laundry detergent was prepared specifically for this analysis, having the same composition as TIDE® but omitting the optical brighteners. A solution of linear alkylbenzene sulphonate surfactants (LAS) in high purity water was added at each wash cycle (section 4.4.1.).

4.2.6.1. 1% CMC-g-PEG co-polymer in weight in the laundry detergent composition

The wash cycle was performed as follows. In a tergotometer pot, the powder laundry detergent (1.8 g) and the LAS solution (10 mL) were dissolved at $25 \text{ }^\circ\text{C}$ in water (average hardness of the water 200 mg/L) and stirred at 200 rpm for 1 min before the addition of the stock solution of the fluorescently labelled co-polymer to analyse (5 mL). The solution in the tergotometer pot was stirred for further 2 minutes. A sample of the washing liquor (5 mL) was taken before the addition of the un-brightened white knitted cotton swatches (approximately 33 g). The swatches were washed at $25 \text{ }^\circ\text{C}$ for 20 minutes. A second sample of the washing liquor (5 mL) was taken before rinsing the swatches for 5 minutes with fresh water (average hardness of the water 200 mg/L) and draining.

The wash cycle was repeated four times without taking any sample of the washing liquor. Then the swatches were allowed to dry naturally overnight and the surface was analysed by fluorescence microscopy and surface NMR techniques (section 4.4.1.).

4.2.6.2. 0.5% CMC-g-PEG co-polymer in weight in the laundry detergent composition

The wash cycle was performed exactly as described above, except that 2.5 mL of the stock solution of the fluorescently labelled co-polymer was added.

4.2.6.3. 0.3% CMC-g-PEG co-polymer in weight in the laundry detergent composition

The wash cycle was performed exactly as previously described, except that 1.25 mL of the stock solution of the fluorescently labelled co-polymer was added.

4.3. Soil release and anti-redeposition properties of the CMC-g-PEG co-polymers

In order to evaluate the efficacy of the CMC-g-PEG co-polymers synthesised in this study as soil release agents, soil release tests were conducted using lard as a stain. To visualise the deposition of the stain over the fabric, lard was dyed with 1-hydroxy-4-(p-tolylamino)-anthraquinone, also known as SV13-DYE, to achieve a deep purple colouration. The structure of the dye is shown in Figure 4.2.

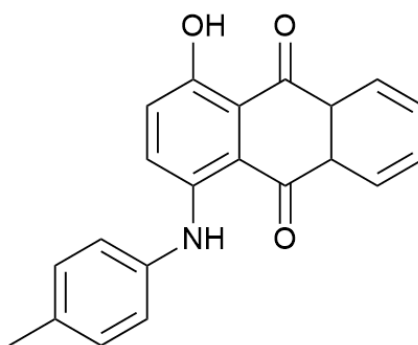


Figure 4.2. Structure of 1-hydroxy-4-(p-tolylamino)-anthraquinone (SV13-DYE).

SV13-DYE is specifically used to dye hydrocarbon compounds. Since lard is a triglyceride containing three hydrocarbon chains derived from stearic and oleic acid, SV13-DYE can dissolve into it, highlighting the presence of lard.

The stain was positioned at the very centre of the cotton swatch to mimic the behaviour of a stain on a garment, and avoid edge effects.

Thermodynamically, a stain is removed from a fabric surface if the force of adhesion between the stain and the fabric is smaller than the affinity between the stain and the washing liquor^[4] as expressed in Equation 1.

$$W = \gamma_{CF} + \gamma_{SC} - \gamma_{SF}$$

Equation 1.

Whereby W is the adhesion, γ_{CF} is interfacial tension between the cleaning solution (C) and the fabric (F), γ_{SC} is the interfacial tension between the stain (S) and the cleaning solution and γ_{FP} is the interfacial tension between the stain and the fabric. Therefore, if the value of the adhesion force W is below zero, the stain can desorb from the textile surface. If a film of SRP is present between the fabric and the stain, as seen during the soil release test, Equation 1 will be modified as follows^[4]:

$$W = \gamma_{CF} + \gamma_{SC} + \gamma_{CP} + \gamma_{SP} + \gamma_{FP} - \gamma_{SF}$$

Equation 2.

This introduces the interfacial tension between the cleaning solution and the film (P) (γ_{CP}), the stain and the film (γ_{SP}) and the fabric and the film (γ_{FP}). When the values of γ_{CP} , γ_{SP} and γ_{FP} decrease, the interaction of the stain with the SRP is increased and the removal of the stain is promoted.

The anti-redeposition properties of the CMC-g-PEG co-polymers were investigated through the use of whiteness tests. During the whiteness test, swatches of fabric are washed in presence of a known amount of the SRP under analysis. At each wash cycle, carbon black was added. Carbon black was dispersed in water and sonicated before being added to the system, in order to facilitate the deposition over the fabric. Four wash cycles were run before

measuring the brightness of the surface, in order to achieve the best possible coverage of the fabric^[2]. The brightness of the surface is measured as “CIE whiteness”. CIE stands for the French “International Commission on Illumination”, which means that the value of brightness of the surface is measured against standard illuminants and it is internationally recognised. The standard used for these whiteness tests is a daylight illuminant D65, which mimics the amount of light in Western Europe/Northern Europe at midday^[5].

The soil release tests and the whiteness tests were conducted using a tergotometer. Washing conditions including temperature, amount of detergent used, amount of SRP added and wash-cycle timings were kept constant during the several repeats of the test. However, the hardness of the water used in the wash cycle changed on a daily basis, as general supply water was used. The change in hardness of the water can affect the removal of the stain. In hard water, the sodium soaps contained in the laundry detergent formulation react with calcium and magnesium ions from the water, producing insoluble calcium/magnesium soaps^[6]. Therefore the amount of sodium soap left to clean the fabric is lower than the amount actually added. For this reason it is not possible to directly compare the results for CMC-g-PEG co-polymers run on different days.

In light of the large number of samples, the CMC-g-PEG co-polymers were divided into three groups and analysed on different days. For each group, soil release and whiteness tests were performed.

In order to compare the action of the CMC-g-PEG co-polymers as SRPs/anti-redeposition agents with the performance of unmodified CMC and to normalise the data collected on different days, three types of unmodified CMC were tested, each day, under the same conditions. The unmodified samples of CMC used were:

- Finnifix V, abbreviated as “V” - a blocky CMC with degree of substitution (DS) of 0.81.
- Finnifix DK, abbreviated as “DK” - a CMC with the same (DS) as Finnifix V but lower degree of blockiness (DB = 0.4). The term “degree of substitution” (DS) refers to the number of hydroxyl groups substituted with carboxymethyl groups per glucose unit, while the term “degree of blockiness” (DB) refers to the distribution of the carboxymethyl groups on the polymer backbone. A high DB means that the carboxymethyl groups are distributed in clusters, rather than randomly, along the CMC backbone.
- CMC BDA, abbreviated as “BDA” - the CMC currently used as anti-redeposition agent in laundry detergents. The carboxymethyl groups are randomly distributed along the polymer backbone.

Therefore, each set of samples analysed included the unmodified CMC samples, the CMC-g-PEG co-polymers and a nil sample. The nil sample was introduced to allow comparison of the benefit deriving from the presence of a SRP during the wash cycle against a wash cycle where no SRP was used.

4.3.1. Possible shortcomings of soil release test and whiteness test

Several parameters can have an impact on the outcome of the soil release test, thus leading to a high error associated with the measurements of SRI.

From the visual observation of the test, the swatches added in the pot tended to stick together during the wash cycle, due to the large amount of fabric (33 g) present in the pot (1 L volume) and the spin force of the stirring. If the swatches stick together, the adsorption of CMC-derivative over the surface will not be uniform, as only the exposed area of the swatches would be able to interact

with the washing liquor. A uniform distribution of co-polymer over the textile surface is fundamental in order to investigate the potential of the co-polymer as a SRP. If the surface is not uniformly coated, it is possible that the stain deposited during the soil release test penetrates into the fabric, thus its removal would be harder. A similar problem can be encountered if the swatches fold on themselves during the wash cycle.

The stain used during the test could also have an impact on the outcome of the test. Lard, for example, was melted at 70 °C with a hot plate prior to deposition onto the fabric through a micropipette. The small difference in temperature between the hot lard melt in the container and the tip of the micropipette could be enough to decrease the temperature of the melted lard. Since the temperature is related to the viscosity, the effective amount of stain deposited over the surface might be lower or different in each swatch, as a residue of lard would be left in the micropipette tip. A lower amount of lard might result “easier” to remove, thus the performance of the co-polymer investigated might be altered.

The variability of the hardness of the water can affect the results of the soil release test/whiteness test, as it influences the amount of surfactant in solution. The concentration of surfactants in solution during the wash cycle can impact the adsorption of CMC^[7] over cotton surfaces to the point that if the concentration is too low, it could possibly inhibit the deposition of CMC during the wash cycle.

Different strategies are here suggested that could be used to overcome these problems. For example, the folding of the swatches during the wash cycle could be prevented by using only one swatch of fabric per pot, thus scaling down the quantities of washing powder and SRP used during the test. In this way, the probability of the swatch to fold would be reduced, and the formation of a uniform layer of co-polymer could be favoured.

Warming up the tip of the micropipette used to deposit the melted lard stain on to the swatch surface could favour the deposition of the same amount of stain on each swatch, thus reducing the impact on the final performance of the co-polymer analysed.

Due to the large number of factors affecting the outcome of the soil release test/whiteness test, the reproducibility and the accuracy of these tests should be questioned before drawing any conclusion on possible correlation between structure of the co-polymer in analysis and soil release benefit/anti-redeposition properties.

4.3.2. Soil release and whiteness properties of CMC-g-PEG_{2K}_{23.7}, CMC-g-PEG_{2K}_{9.5}, CMC-g-PEG_{2K}_{42.8} and CMC-g-PEG_{5K}_{19.0}

The CMC-g-PEG co-polymers were designed to reversibly adsorb and desorb from cotton surface. The strong affinity of the CMC backbone for cotton fibres that promotes adsorption could be reduced upon grafting of PEG chains to the backbone, thus promoting desorption of the co-polymer from the fabric surface. In theory the adsorption/desorption process could be finely tuned by changing the weight percentage of PEG, the graft density of PEG (i.e. the number of PEG chains grafted to the CMC backbone) and the length of the PEG chains. If two co-polymers, for example, contain different weight percentages of PEG, the CMC-g-PEG with the higher proportion of PEG is expected (in theory) to desorb better from cotton surface, due to an increased affinity for the washing liquor. However, if two co-polymers possess the same weight percentage of PEG but different graft density or length of the PEG chain, it is not possible to predict the optimal distribution of PEG that would promote desorption from the cotton surface. The graft density and the length of the PEG chains grafted to

the CMC backbone should be carefully balanced as they will likely also have an impact on the adsorption process. If the affinity for the washing liquor is too high, it is possible that the co-polymer will not adsorb onto the fabric surface because the structural affinity of the CMC backbone for the textile surface is overcome by the affinity of the PEG moiety for the washing liquor. Furthermore, the steric impact of the PEG chain could prevent adsorption (Figure 4.3), thus a high number of short chains would be expected to inhibit adsorption more than few longer chains.

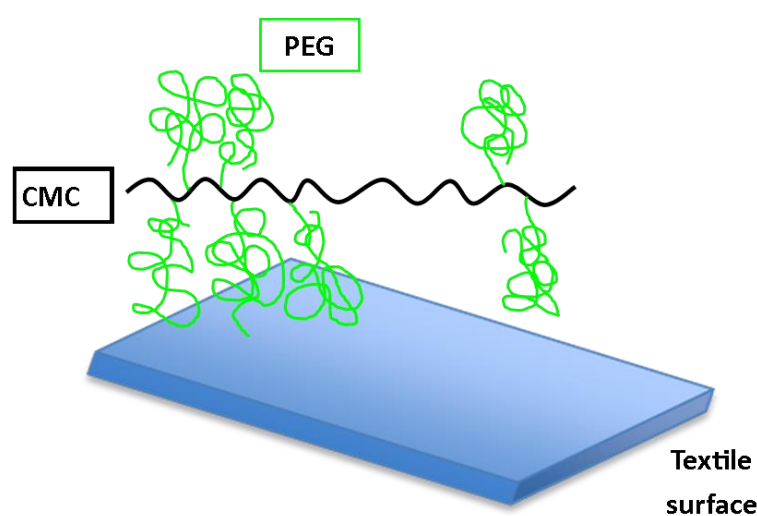


Figure 4.3. Steric interference of grafted PEG chains on adsorption of CMC-g-PEG co-polymer onto a cotton surface.

The purpose of a soil release test is to measure the increment in brightness of the target surface upon removal of a stain during a wash cycle. The increment is referred to as *soil release index* (SRI). The value of SRI correlates with the ability of the soil release agent to remove the stain under examination. The higher the value of the SRI, the bigger the difference in brightness of the surface before and after the wash cycle, hence the stain is removed better.

On the contrary, the whiteness test aims to evaluate the anti-redeposition properties of a polymeric additives by measuring the decrease in brightness of

the surface after several wash cycles in the presence of carbon black. The decrease in brightness is referred to as CIE whiteness, as it is based on the use of a CIE standard daylight illuminants D65.

The characteristics of the first group of CMC-g-PEG co-polymers analysed are summarised in Table 4-1.

Table 4-1. Properties of the CMC-g-PEG analysed via soil release test and whiteness test.

Sample	M _n PEG grafted (g/mol)	Weight % PEG* (%)	Test code
CMC-g-PEG_2K_9.5	2000	9.5±0.3	2K_9.5
CMC-g-PEG_2K_23.7	2000	23.7±0.5	2K_23.7
CMC-g-PEG_2K_42.8	2000	42.8±0.2	2K_42.8
CMC-g-PEG_5K_19.0	5000	19.0±0.4	5K_19.0

* Weight of PEG in the CMC-g-PEG samples expressed as percentage (Chapter 3, section 3.3.2.4, 3.3.2.5. and 3.3.2.6.).

The co-polymers listed in Table 4-1 as well as three samples of unmodified CMC and a nil sample were subjected to the soil release test and whiteness test. The results are summarised in Figure 4.4 and Figure 4.5 respectively.

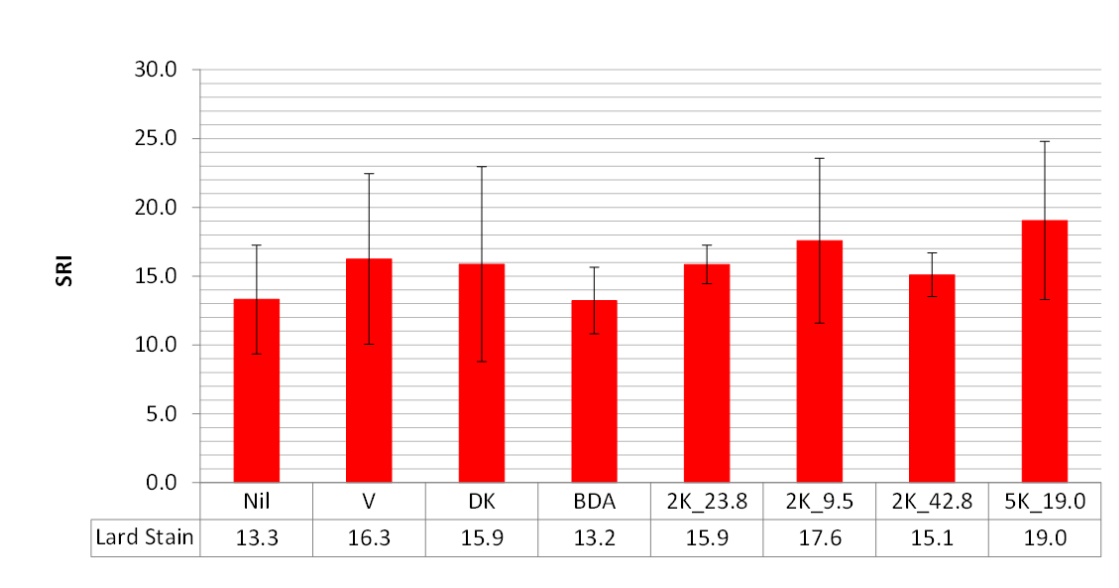


Figure 4.4 Comparison between soil release index (SRI) of unmodified CMC (sample V, DK and BDA) and CMC-g-PEG co-polymers (sample 2K_23.8, 2K_9.5, 2K_42.8 and 5K_19.0) as measured using the spectrophotometer at 460 nm. Error calculated as standard deviation.

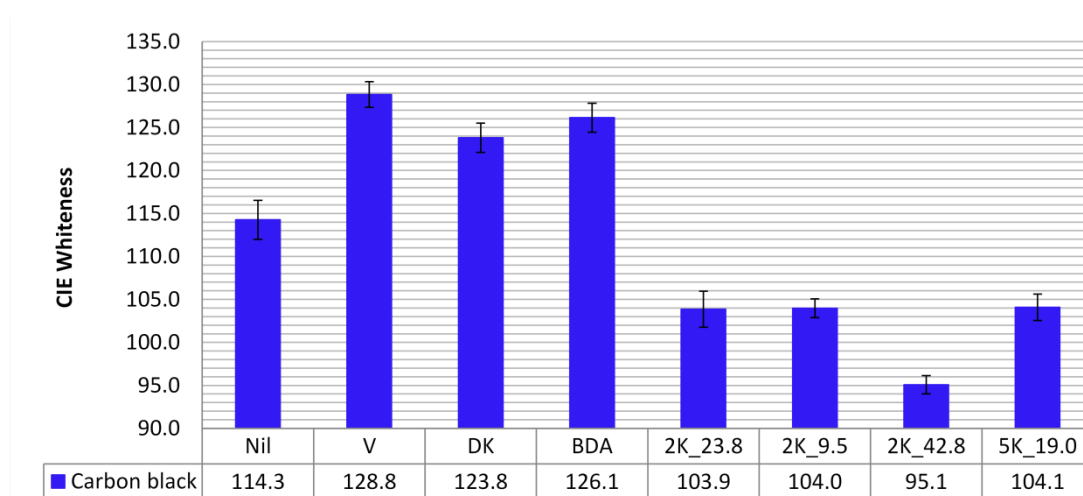


Figure 4.5. Comparison between CIE whiteness (y-axis) of unmodified CMC (sample V, DK and BDA) and CMC-g-PEG co-polymers (sample 2K_23.8, 2K_9.5, 2K_42.8 and 5K_19.0) as measured by the spectrophotometer at 460 nm. Error calculated as standard deviation.

From Figure 4.4, it is possible to observe that the error associated with the measurement of SRI is very high, possibly due to the complexity of the test and the relatively low number of cotton swatches analysed. The test is based on the

formation of a uniform layer of co-polymer over the entire surface of the cotton swatches, which may be difficult to obtain consistently. An industrial standard test was used whereby the total number of swatches used in each wash cycle weighted approximately 33 g, in order to maintain the optimal 33:1 ratio between the amount of cotton used and the liquid in the pot (1 L). Of the total number of swatches of white knitted cotton used for the test, only 5 swatches (corresponding to 3.3 g approximately) were stained and analysed. Increasing the number of swatches of cotton stained and analysed for each SRP could be a way to reduce the error associated with the measurements.

A statistical analysis of the results from the soil release test (Figure 4.4) shows that all the value of SRI determined are within the standard deviation of each other. Therefore, it is not possible to affirm that any of the co-polymer samples analysed show a significant improvement in the detachment of lard stain from cotton fabric.

Considering the thermodynamics of stain removal (Equation 2), the presence of a SRP film contributes to a reduction in $\gamma_{CF}^{[4]}$. Unmodified CMC has a strong affinity for cotton surface, therefore the interface tension γ_{FP} is very low and the adsorption is irreversible. It had been expected that the grafting of PEG on to the CMC backbone would reduce γ_{CP} interfacial tension, due to the hydrophilicity of PEG. Therefore, two parameters should be considered in order to predict the affinity of the resulting co-polymer for water: the graft density of PEG chains and the length of the PEG chain grafted. Long PEG chain and high graft density would be expected to increase the affinity of the co-polymer for water, thus the γ_{CP} interfacial tension becomes smaller, promoting a better removal of the stain.

In light of these assumptions, it was expected to observe a difference between the SRI of the co-polymers, the unmodified CMC samples and the nil sample. As the unmodified CMC samples do not desorb from cotton surface, the SRI associated with sample V, DK and BDA was expected to be lower than the SRI

associated with the co-polymers. Moreover, the SRI associated with co-polymers was anticipated to be different from the SRI of the nil sample, due to the potential benefit deriving from the presence of a SRP during a wash cycle observed for synthetic fibres^[1]. Among the co-polymers, sample 2K_42.8 possess the highest amount of PEG (42.8% by weight), therefore was expected to show a higher SRI. The high PEG content should have increased the affinity of the co-polymer for the washing liquor, thus promoting co-polymer desorption and simultaneous removal of the stain. Based on the amount of PEG present in the co-polymer, it was expected sample 2K_23.8 (23.8% in weight of PEG) to possess the second higher SRI, followed by sample 5K_19.0 and 2K_9.5.

The results from this soil release test (Figure 4.4) seems to suggest any improvement conveyed by the presence of PEG grafted onto the CMC backbone on the removal of lard is marginal at best.

The results obtained from the whiteness test are displayed in Figure 4.5. In order to visualise the variation of the CIE whiteness for the samples, the y-axis starts at a value of CIE whiteness of 90 instead of 0. The error associated with these measurements is much lower than the error calculated for the soil release tests, as a result of the higher number of swatches analysed and the protocol used for the test. According to the industrial standard procedure followed, the carbon black powder used at each wash cycle was dispersed in 5 mL of high purity water prior to addition to the tergotometer pots. This allowed a more uniform deposition of the carbon black powder over the swatches surface, thus reducing the error associated with the brightness measurements. Furthermore, the higher number of swatches analysed in comparison with the soil release test (10 swatches for the whiteness test instead of 5) may have contributed to a reduction in the error on the CIE whiteness measurements by increasing the amount of data collected.

Samples V, DK and BDA are all different types of unmodified CMC. The use of a CMC during a wash cycle improves the brightness of the surface^[5] compared

to a sample in which no CMC was used. Since CMC can prevent the redeposition of a removed stain back onto the textile surface^[8], it was used as anti-redeposition agent in laundry detergents^[1]. Due to the adsorption of the CMC layer during the wash cycles of the whiteness test, the surface of the swatches is negatively charged. The carbon black particles in solution are negatively charged too, since they are dispersed by the surfactants. Hence, the electrostatic repulsion between them does not allow the carbon black particles to deposit over cotton surface. From Figure 4.5 it is possible to observe the benefit of the presence of an anti-redeposition agent during the wash cycle by comparing the CIE whiteness of the unmodified CMC samples (V, DK, BDA, values of CEI respectively 128.8, 123.8 and 126.1) with the nil sample (CEI = 114.3). In the nil sample, the carbon black particles accumulates over the swatches surface at each wash cycle, thus leading to a darkening of the fabric. On the contrary, the surface of the swatches treated in the presence of V, DK and BDA is brighter (higher value of CIE whiteness), due to the anti-redeposition properties of samples V, DK and BDA.

A close look at the results for the CMC-g-PEG co-polymers in Figure 4.5 shows that not only do all the co-polymer samples perform worse than the unmodified CMC (especially in comparison with the CIE whiteness for sample V), they are also worse than the nil sample. It is possible that the PEG chains grafted onto the CMC backbone have an affinity for the carbon black particles in the washing liquor, thus leading to a darkening of the swatch surfaces. The surface of carbon black is decorated with hydroxyl and carboxylic acid groups ^[9] due to the manufacturing conditions. These hydrogen bond donor groups can interact with the ether oxygen (H-bond acceptors) atoms in the PEG chains

The statistical analysis of the CIE whiteness of the co-polymers in Figure 4.5 shows that co-polymer samples 2K_23.8, 2K_9.5 and 5K_19.0 possess almost the same value of CIE whiteness (around 104.0) within error, while sample 2K_42.8 has a value of CIE whiteness significantly lower. The lower value of CIE

whiteness registered for sample 2K_42.8 is likely due to the higher amount of PEG grafted to the CMC backbone. Sample 2K_42.8 contains a 42.8% weight of PEG, while sample 5K_19.0 has 19.0% of PEG, sample 2K_9.5 9.5% and sample 2K_23.7 contains 23.7% in weight of PEG. As the percentage of grafted PEG increases, more carbon black will be retained by the PEG chain, thus the swatches surface is expected to become darker and the CIE whiteness parameter decrease.

The results from this whiteness test suggest that the grafting of PEG onto the CMC backbone transforms the co-polymers into “soil magnets” capable to capture carbon black dispersed in the washing liquor.

4.3.3. Soil release and whiteness properties of CMC-g-PEG_2K_50.4, CMC-g-PEG_2K_56.1, CMC-g-PEG_5K_51.1 and CMC-g-PEG_5K_55.6

The characteristics of the second group of CMC-g-PEG co-polymers analysed are listed in Table 4-2.

Table 4-2. Properties of the CMC-g-PEG analysed via soil release test and whiteness test.

Sample	M _n PEG grafted (g/mol)	Weight % PEG*	Test code
CMC-g-PEG_2K_50.4	2000	50.4±0.2	2K_50.4
CMC-g-PEG_2K_56.1	2000	56.1±0.6	2K_56.1
CMC-g-PEG_5K_51.1	5000	51.1±0.4	5K_51.1
CMC-g-PEG_5K_55.6	5000	55.6±0.6	5K_55.6

* Weight of PEG in the CMC-g-PEG samples expressed as percentage (Chapter 3, section 3.3.2.4, 3.3.2.5. and 3.3.2.6.).

Since the hardness of the water used for the tests changes on a daily base, three unmodified CMC samples (V, DK and BDA) and a nil sample were tested again together with the co-polymers listed in Table 4-2. The results of the soil release test and whiteness test of this second group of compounds are summarised in Figure 4.6 and Figure 4.7 respectively.

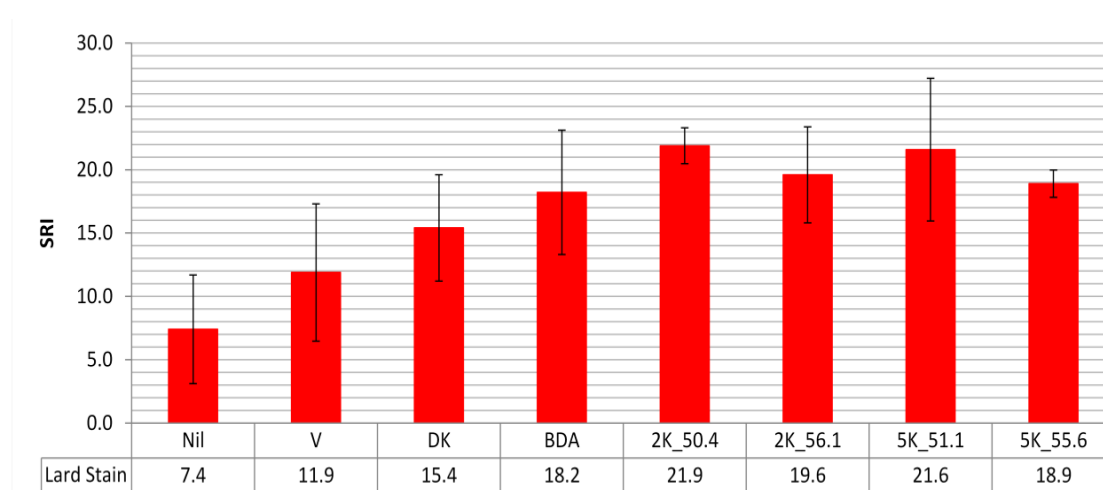


Figure 4.6. Comparison between soil release index (SRI) of unmodified CMC (sample V, DK and BDA) and CMC-g-PEG co-polymers (sample 2K_50.4, 2K_56.1, 5K_51.1 and 5K_55.6) as measured by the spectrophotometer at 460 nm.

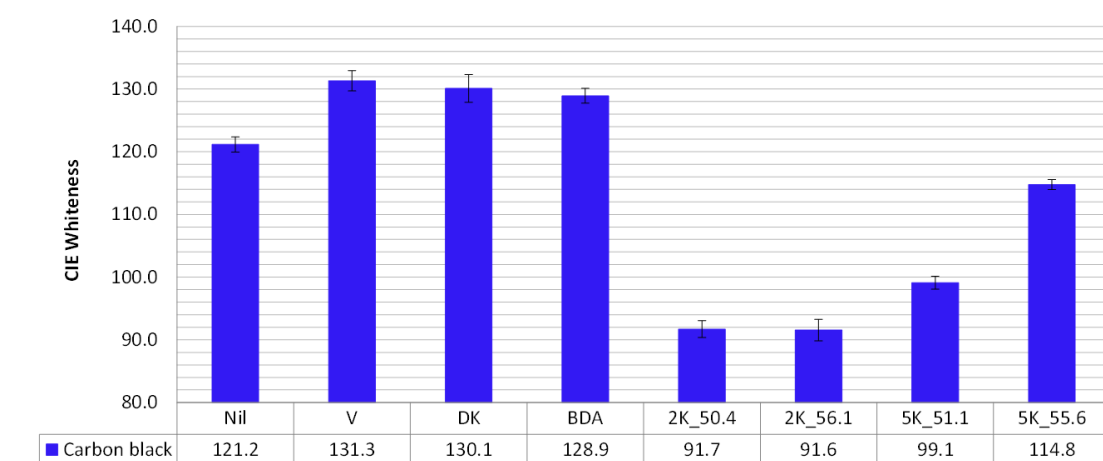


Figure 4.7. Comparison between CIE whiteness (y-axis) of unmodified CMC (sample V, DK and BDA) and CMC-g-PEG co-polymers (sample 2K_50.4, 2K_56.1, 5K_51.1 and 5K_55.6) as measured by the spectrophotometer at 460 nm.

Once more, the error associated with the measurement of SRI (Figure 4.6) is very high, even if a larger number of swatches were tested and analysed compared to the previous group (10 swatches instead of 5). It is possible that the large errors arise from the poor uniformity of the layer of co-polymer adsorbed over the swatch surfaces.

The statistical analysis of the data represented in Figure 4.6 shows that most of the values of SRI determined via soil release test are within one standard deviation of each other. For example, although the unmodified CMC samples V and DK gave apparently different (higher) values of SRI compared to the nil sample, given the magnitude of the associated errors, means that any claims of significant benefits toward the removal of lard stain should be treated with caution. However, sample BDA (the CMC currently used in laundry detergents) with an SRI value of 18.2 does seem to display a significant improvement in brightness of the surface in this set of data compared to the nil sample (SRI = 7.4), reaffirming its proven behaviour as an anti-redeposition agent.

It might also be argued that a slight improvement of the removal of lard stain from cotton surface is achieved when a co-polymer based on PEG-NH₂2K or PEG-NH₂5K is added during the wash cycle. From Figure 4.6 it is possible to observe that the SRI value for samples 2K_50.4, 2K_56.1, 5K_51.1 and 5K_55.6 is similar for each sample (with SRI values between 18.9 and 21.9) and significantly higher than the nil sample (SRI = 7.4), hence stain removal is improved in the presence of these co-polymers. The improved removal of the stain is likely due to the high amount of PEG contained in these co-polymers. The weight percentage of PEG is 50.4%, 56.1%, 51.1% and 55.6% respectively, thus it could (in theory) be high enough to favour the desorption of the co-polymer from the surface.

As the backbone of the co-polymers is constituted of CMC Finnifix V, the soil release properties of the CMC-g-PEG co-polymers will be compared with the

results for sample V when possible. Thus the SRI value measured for the co-polymers 2K_56.1 and 5K_51.1 (19.6 and 21.6 respectively) are both substantially higher than the value for sample V (SRI = 11.9), but given the large error especially associated with sample V, it is not possible to state with absolute certainty that these substantial differences are statistically significant.

However, samples 2K_50.4 and 5K_55.6 possess values of SRI (21.9 and 18.9 respectively) that are significantly higher than the corresponding value of sample V (SRI = 11.9). Therefore, it is possible to affirm that sample 2K_56.1 and sample 5K_51.1 show a significant improvement in the detachment of lard stain from cotton fabric. The improvement in performance of samples 2K_56.1 and 5K_51.1 compared to sample V is likely due to the presence of a high amount of PEG grafted to the CMC backbone (above 50% in weight). The grafting of PEG, a hydrophilic polymer, could increase the affinity of the co-polymer for the washing liquor, thus favouring the desorption process with simultaneous removal of the stain.

The comparison between the SRI of the co-polymers based on PEG-NH₂2K (2K_50.4 and 2K_56.1, values of SRI 21.9 and 19.6 respectively) and PEG-NH₂5K (5K_51.1 and 5K_55.6, values of SRI 21.6 and 18.9 respectively) with sample BDA (SRI = 18.2) shows that the average value of SRI obtained for the co-polymers is higher than the corresponding value for sample BDA. However, as the error associated with the measurements is high, it is not possible to confirm any statistical significance among the behaviours of the co-polymers 2K_50.4, 2K_56.1, 5K_51.1 and 5K_55.6 and sample BDA.

From the results of the analysis of the second group of co-polymers, it would appear that there is no evidence of actual desorption for the co-polymers based on PEG-NH₂2K and PEG-NH₂5K.

Figure 4.7 summarises the results of the whiteness test performed on the co-polymers listed in Table 4-2. To better visualise the variation of the CIE whiteness for the samples, the y-axis starts at a value of 80 instead of 0.

Once more, the results of the whiteness test shows that the brightness of the surface increases, in comparison to the nil result, if an anti-redeposition agent like sample V, DK and BDA is used during the wash cycle. However, the CIE whiteness values for all the CMC-g-PEG co-polymers (CEI between 91.7 and 114.8) tested are significantly lower than both the nil sample (CEI = 121.2) and all the unmodified CMC samples (V, DK and BDA; values of CEI 131.3, 130.1 and 128.9 respectively) possibly as consequence of the presence of PEG chains grafted to the CMC backbone. The PEG chains could potentially bind carbon black via H-bonding with the functional groups present on the surface of particles, as outlined for the previous group of co-polymers, thus turning the surface darker.

The comparison of the values of CIE whiteness obtained for the co-polymers seems to show that the brightness of the swatches depends upon two parameters: the amount of PEG grafted and the length of the PEG chains. If the whiteness of the swatches was influenced only by the amount of PEG grafted, the results of the test would have been different. Sample 2K_56.1 and sample 5K_55.6 would have been expected to possess the lowest CIE whiteness values, since they contain the higher amount of grafted PEG (56.1% and 55.6% in weight respectively).

However, the results plotted in Figure 4.7. are different. The value of CIE whiteness increases from samples 2K_56.1 (CEI = 91.6) and 2K_50.4 (CEI = 91.7), to sample 5K_51.1 (CEI = 99.1) and sample 5K_55.6 (CEI = 114.8). It is clear that the amount of PEG grafted is not the only factor to have an impact of the brightness of the swatches. The length of the PEG chains, thus the M_n of the PEG-NH₂ used during the synthesis, also has an influence on the results of the whiteness test. The influence of the length of the PEG chains can be observed by

comparing the CIE whiteness obtained for the co-polymers based on PEG-NH₂5K with the results for the co-polymers containing PEG-NH₂2K. Sample 2K_56.1 has similar amount of PEG grafted as sample 5K_55.6, but lower CIE whiteness. The same pattern is observed for sample 2K_50.4, which possesses similar amount of PEG grafted as sample 5K_51.1 but considerably lower CIE whiteness value. Despite each co-polymer having a comparable weight fraction of PEG grafted, both the samples based on PEG-NH₂5K possess a higher value of CIE whiteness than the samples based on PEG-NH₂2K. It is possible that the presence of shorter PEG chains grafted to the CMC backbone act as a stronger soil magnet to the carbon black.

The results of this whiteness test suggest that the co-polymers are capable to behave as soil magnets for carbon black particles in solution, since in all cases the CEI whiteness was lower than the nil sample.

4.3.4. Soil release and whiteness properties of CMC-g-PEG_2K_62.5, CMC-g-PEG_5K_63.7, CMC-g-PEG_10K_84.5, CMC-g-PEG_10K_85.8 and CMC-g-PEG_10K_76.5

The characteristics of the third and last group of CMC-g-PEG co-polymers analysed are listed in Table 4-3.

Table 4-3. Properties of the CMC-g-PEG analysed via soil release test and whiteness test.

Sample	M _n PEG grafted (g/mol)	Weight % PEG*	Test code
CMC-g-PEG_2K_62.5	2000	62.5±0.8	2K_62.5
CMC-g-PEG_5K_63.7	5000	63.7±0.8	5K_63.7
CMC-g-PEG_10K_76.5	10000	76.5±0.3	10K_76.5
CMC-g-PEG_10K_84.5	10000	84.5±0.2	10K_84.5
CMC-g-PEG_10K_85.8	10000	85.8±0.3	10K_85.8

* Weight of PEG in the CMC-g-PEG samples expressed as percentage (Chapter 3, section 3.3.2.4, 3.3.2.5. and 3.3.2.6.).

The three unmodified CMC samples (V, DK and BDA) were tested again together with the co-polymers listed in Table 4-3 to allow comparison of the soil release properties of the co-polymers with unmodified CMC. The results of the soil release and whiteness tests of the third group of compounds are summarised in Figure 4.8 and Figure 4.9 respectively.

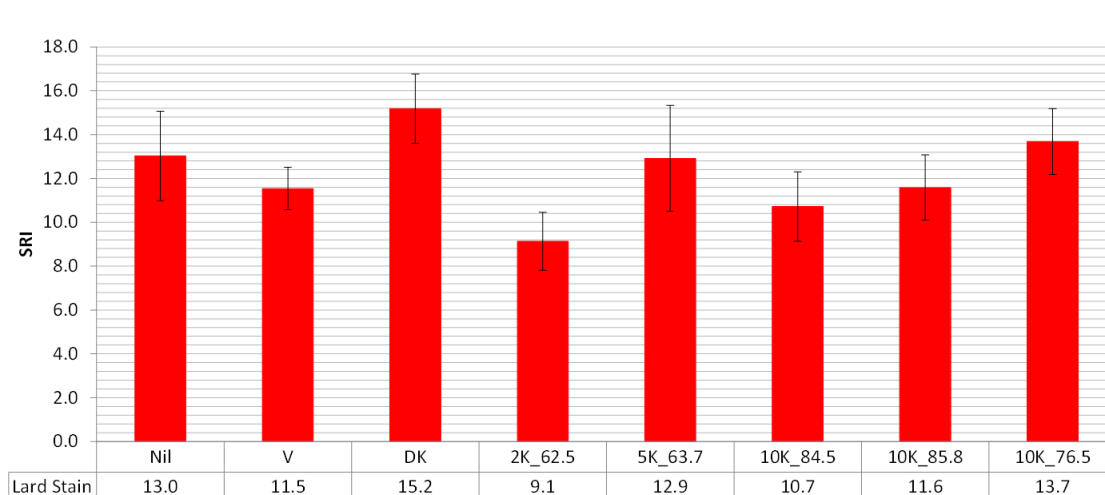


Figure 4.8. Comparison between soil release index (SRI) of unmodified CMC (sample V and DK) and CMC-g-PEG co-polymers (sample 2K_62.5, 5K_63.7, 10K_76.5, 10K_84.5 and 10K_85.8) as measured by the spectrophotometer at 460 nm.

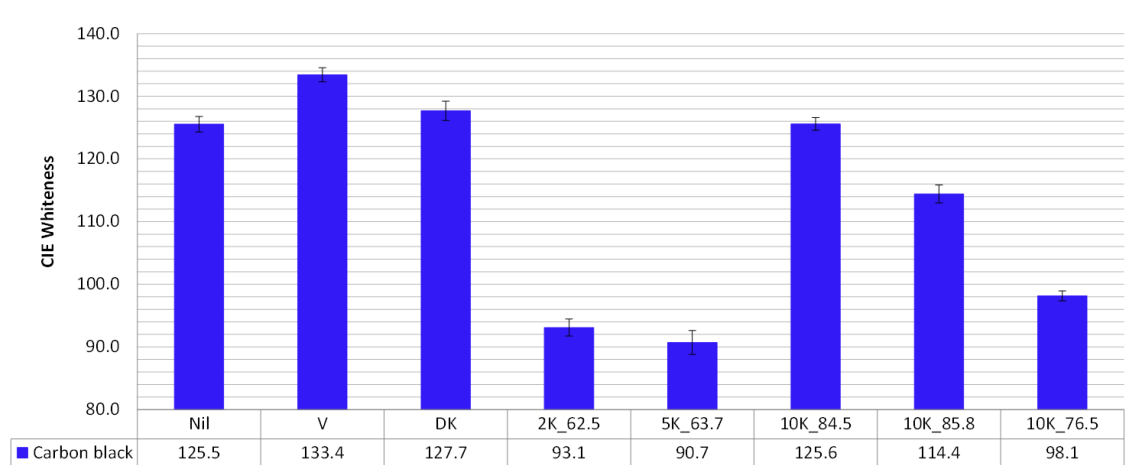


Figure 4.9. Comparison between CIE whiteness (y-axis) of unmodified CMC (sample V and DK) and CMC-g-PEG co-polymers (sample 2K_62.5, 5K_63.7, 10K_76.5, 10K_84.5 and 10K_85.8) as measured by the spectrophotometer at 460 nm.

The errors associated with the measurements of SRI for the unmodified CMC samples, the co-polymers and the nil sample are very high. As outlined before, it is possible that the formation of a uniform layer of co-polymer adsorbed over the surface of each swatch is difficult to achieve consistently, therefore the final value of SRI obtained is spread across a wide range of values. Probably

increasing the number of swatches analysed might contribute to further reduce the standard deviation.

A statistical analysis of the data represented in Figure 4.8 shows that due to the large error associated with the measurement of SRI, most of the values of SRI determined are still within the standard deviation of each other. The SRI values observed for the unmodified CMC samples (V and DK, SRI values 11.5 and 15.2 respectively) are the same within error as the nil samples (SRI = 13.0), thus it would appear that no benefit derives from the presence of a sample of unmodified CMC during the wash cycle toward removal of a lard stain, in contrast to the implications of the previous set of data in Figure 4.4 and Figure 4.6.

With the exception of sample 2K_62.5, all the co-polymers listed in Table 4-3 possess an SRI value which is not significantly different to the nil sample (SRI = 13.0), thus it would appear that they do not display any improvement toward the detachment of lard stains. Sample 2K_62.5 (SRI = 9.1) performs slightly worse than the nil sample, which is unexpected and in contradiction with the data of Figure 4.6 and inconsistent with any hypothesis outlined so far. It would appear that despite sample 2K_62.5 containing 62.5% of PEG grafted by weight, the co-polymer does not improve the removal of lard stains. This sample was expected to show an improvement toward stain removal due to the high PEG content and because sample 2K_56.1 analysed in the previous group seemed to do so. Performing a soil release test on sample 2K_56.1, sample 2K_62.5 and a nil sample at the same time could help to investigate the unusual behaviour observed for sample 2K_62.5 by direct comparison with a sample containing the same PEG but at a lower level.

As the co-polymers backbone is formed by Finnifix V, the comparison between the value of SRI for the unmodified CMC sample V and the co-polymers is necessary to investigate the improvement of the soil release properties deriving from the grafting of PEG onto the CMC backbone. The comparison between the

value of SRI of sample V (SRI = 11.5) and the co-polymers (SRI between 9.1 and 13.7) shows that, once more, there seems to be no difference in soil removal upon grafting of PEG to the CMC backbone, since the SRI observed are the same, within error, as sample V.

Unfortunately, it is not possible to comment on the difference in SRI observed for the co-polymers as results of the presence of different amounts of PEG grafted, since the SRI values measured for the samples are within statistical error of each other.

The results obtained for the third group of co-polymers are inconsistent with previous observations based on the results observed for the previous group of co-polymers and on the influence of PEG upon the mechanism of action of the SRPs. It was assumed that the co-polymers containing the highest amount of PEG would show the higher SRI in comparison with both sample V and the nil sample. Due to the hydrophilic nature of PEG, it was hypothesised that the presence of PEG grafted would promote desorption over adsorption. As a consequence of the presence of PEG, the interfacial tension γ_{CP} (Equation 2) for the co-polymers should be lower than the corresponding value for the unmodified CMC, since the presence of PEG would increase the affinity for the washing liquor. On the contrary, γ_{FP} is expected to increase, as the affinity of the co-polymer for the fabric surface should (in theory) decrease upon grafting of PEG. γ_{SP} is also anticipated to be different to the value for unmodified CMC, although it is not possible to predict whether it would be higher or lower. Due to the influence of the amount of PEG grafted, it was expected that sample 10K_85.8 would possess the higher value of SRI compared to the other co-polymers analysed. It was thought that the high amount of long PEG chains present in sample 10K_85.8 (85.8% in weight of PEG with M_n 10000 g/mol) would have been enough to allow the desorption of the co-polymer from the surface of the fabric, thus enhancing the stain removal. For the same reason, the second best SRP was expected to be sample 10K_84.5, because it contains an

amount of PEG comparable with sample 10K_85.8 (84.5% in weight). Then, in decreasing order, samples 10K_76.5, sample 5K_63.7 and sample 2K_62.5.

The results from the soil release test conducted on the last set of data seems to suggest there is no improvement to the soil release properties due to the presence of PEG grafted onto the CMC backbone, as there is no evidence to suggest that any of these samples deliver a significant SRP benefit.

The CMC-g-PEG co-polymers listed in Table 4-3 were also analysed via whiteness test, together with three samples of unmodified CMC and a nil sample. The results are summarised in Figure 4.9. To help visualise the variation of CIE whiteness, the y-axis starts at a value of 80 instead of 0.

For the CMC-g-PEG co-polymers listed in Table 4-3 the results of the whiteness test is a lower value of CIE whiteness than the nil sample. The co-polymers containing the lower M_n PEG (sample 2K_62.5 and sample 5K_63.7) possess the lowest CIE whiteness (62.5 and 90.7 respectively), as result of the high amount of carbon black bound and retained over the surface of the swatches. Among the co-polymers containing PEG-NH₂10K, sample 10K_84.5 is the only one that possesses the same value of CEI whiteness (125.6) as the nil sample (CEI = 125.5) within error.

From the comparison with the results obtained for the previous set of co-polymers analysed via whiteness test, it was expected that an increase of the amount of PEG grafted would have increased the proportion of carbon black retained, thus reducing the CEI index. Furthermore, sample 5K_63.7 was expected to possess a higher CEI index than sample 2K_62.5 due to the longer PEG chain grafted.

However, it is possible that the presence of a high density of long PEG chains grafted to the CMC backbone may sterically affect the adsorption by creating a barrier around the CMC backbone as shown in Figure 4.3. In this case, the co-

polymer may be inhibited from adsorption over the textile surface, thus the amount of carbon black retained could be comparable to the nil sample.

From the results of the whiteness test plotted in Figure 4.9 it would appear that none of the co-polymers analysed desorb from cotton surface and the low CIE whiteness index observed suggests an affinity between the carbon black and PEG chains.

4.4. Quantitative analysis of deposition using fluorescently labelled CMC

In an attempt to further investigate the adsorption and to quantify the amount of CMC-g-PEG co-polymer adsorbed onto the cotton surface, two of the co-polymers were labelled with the fluorescent tag 5-([4,6-Dichlorotriazin-2-yl]amino)fluorescein (DTAF). The accurate characterisation of the labelled co-polymers (from now on referred to with a * next to their name) via fluorescence spectroscopy, as described in Chapter 3, allowed us to establish the amount of dye bound to the polymer backbone per gram of polymer. With this knowledge it should be possible to correlate the intensity of the fluorescence signal with the amount of co-polymer adsorbed onto the cotton.

The amount of co-polymer adsorbed was evaluated by measuring the difference in the intensity of the fluorescence emission signal of the washing liquor before and after one single wash cycle, as describe in the experimental section. The use of only one wash cycle was to avoid alteration of the fluorescence signal from co-polymers already adsorbed over cotton. According to the industrial procedure followed (and described in the experimental section), the fluorescence of the washing liquor was measured before the addition of the fabric to the tergotometer pot and after washing in the presence of laundry detergent before rinsing the swatches with fresh water. If the fluorescence signal of the wash liquor was evaluated after two wash cycles, part of the CMC-g-PEG* adsorbed onto cotton during the first wash cycle may desorb in a second wash cycle, contributing to an increase of the fluorescence intensity of the washing liquor. In that case it would not be possible to correlate the difference in fluorescence measured with the amount of co-polymer adsorbed. The swatches were also tested using different concentration of CMC-g-PEG* in order to investigate the influence of the CMC-g-PEG* concentration on the adsorption process.

If the CMC-g-PEG* co-polymer in question is adsorbed onto the cotton surface during the wash cycle, the concentration of CMC-g-PEG* in the wash liquor at the end of the cycle will be diminished and a concomitant decrease in fluorescence intensity will be observed. The change in the fluorescence intensity might be very small, therefore contamination by internal and external agents can be an issue with this type of measurement. In an attempt to avoid contamination from external sources, the pots of the tergotometer were rinsed three times with fresh water and brushed to remove any residue of washing powder from previous tests before the analysis. Residues of TIDE® washing powder can alter the result of this analysis because the fluorescence signal of the optical brighteners contained in the formulation coincides with the fluorescence emission peak of DTAF. For this reason a new formulation of TIDE® washing powder was prepared (which omits optical brighteners) and used for these analysis. Unbrightened white knitted cotton swatches were used as the target substrate to avoid potential contamination of the fluorescence signal of the washing liquor by the optical brighteners which may have been adsorbed onto the surface of the swatches and to enable subsequent examination of the surface of the swatches by fluorescence microscopy.

To visualise the build-up of the protective layer of CMC-g-PEG* on the cotton surface, the swatches of unbrightened cotton were washed four times in presence of different concentration CMC-g-PEG* in the formulation. The surface of the swatches were then analysed by solid state NMR spectroscopy^[10] and fluorescence microscopy.

Through solid state NMR spectroscopy, it should be possible to identify the presence of any CMC-g-PEG* co-polymers by detecting the ¹³C NMR signal of the PEG chain. This signal was chosen because the PEG repeating unit gives a very intense peak at $\delta 70.9$.

The use of fluorescence microscopy should enable the visualisation of any adsorbed CMC-g-PEG* co-polymer on the surface of the cotton and allow qualitative evaluation of the distribution of the co-polymer adsorbed.

Finnifix V and Finnifix DK samples were also labelled with DTAF to allow comparison of the adsorption properties of the CMC-g-PEG* co-polymers with unmodified CMC.

4.4.1. Fluorescence measurements

Only two of the CMC-g-PEG co-polymers synthesised in this study were fluorescently labelled with DTAF and subsequently investigated due to the lack of residual material in the case of the other co-polymers synthesised, after the soil release and whiteness tests were performed.

The set of samples analysed is summarised in Table 4-4.

Table 4-4. CMC-g-PEG* co-polymers analysed during the quantitative test.

Sample	Degree of labelling (mg DTAF/g polymer)	Quantitative analysis code
Finnifix V	0.11	V*
Finnifix DK	0.24	DK*
CMC-g-PEG_5K_51.1*	0.019	5K_51.1*
CMC-g-PEG_5K_19.0*	0.07	5K_19.0*

The quantitative analysis of polymer adsorption by fluorescence intensity measurements of the wash liquor was initially performed using a concentration of 0.3% of unmodified CMC* or CMC-g-PEG* during the wash cycle and the results are shown in Figure 4.10. This low concentration was chosen according

to the industrial protocol followed and reported in the experimental section. Adsorption of the fluorescently labelled polymer should result in decrease in fluorescence intensity of the wash liquor as the concentration of the labelled polymer is depleted. In each case below, only one measurement was made for each sample so it was not possible to calculate the error associated with the measurements.

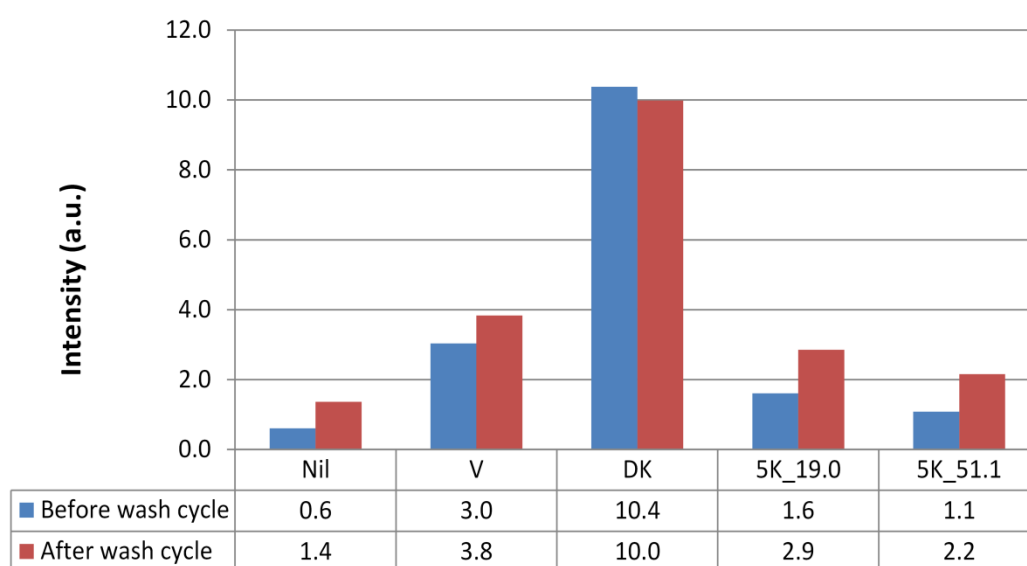


Figure 4.10. Fluorescence emission intensity of the wash liquor before and after wash cycle with 0.3% concentration of unmodified CMC* or CMC-g-PEG* co-polymers.

The samples of wash liquor were filtered before measuring the fluorescence intensity to remove any residue of undissolved laundry detergent or lint of fabric which could alter the result of the analysis due to light scattering, hence increasing the amount of light that reaches the detector.

Each sample of wash liquor taken before the addition of fabric contained exactly the same concentration of CMC-g-PEG* or unmodified CMC*. However, the data in Figure 4.10 show that the relative fluorescent intensity of each sample is different, reflecting the different degree of labelling for each co-polymer. Sample DK, for example, possessed a much higher degree of labelling

than any other compound listed in Table 4-4, thus even if the concentration of the polymer in solution was the same as any other sample, the intensity of the fluorescence signal was higher because of the presence of a higher amount of fluorophore. However, the relative intensities of the samples are not in agreement. For instance, based on the degree of labelling, the intensity of the fluorescent signal for sample 5K_19.0 before the addition of the fabric was expected to be proportionally higher than the signal for sample 5K_51.1, since a higher proportion of fluorophore was attached to the CMC backbone. It is possible that these discrete points are not representative of the sample, thus a statistical analysis of the samples would enable a more conclusive comparison.

In contrast to expectations, Figure 4.10 shows that the intensity of the fluorescence signal *increases* after the washing cycle. The only exception being sample DK, where the fluorescence intensity of the solution after the wash cycle is slightly lower than before. A likely and logical explanation to these unusual results is that despite all best efforts, the system was contaminated during the wash cycle. The data collected before the wash cycle (blue columns, Figure 4.10) were obtained after the dissolution of the laundry detergent and the fluorescent sample, but before the addition of the fabric swatches. While data collected after the wash cycle (red columns, Figure 4.10), was obtained just before rinsing the swatches with fresh water. Hence, the only change to the system that occurred between measurements was the addition of the fabric. It is possible that a small residue of optical brightener was adsorbed over the surface of the unbrightened swatches, and was subsequently released into the wash liquor during the wash cycle. The source of such contamination is not immediately obvious but it is possible that optical brightener contamination could originate from the manufacturing factory (since the same company supplied brightened cotton swatches). Another possible source of contamination is the test laboratory, since other tests were run at the same time using TIDE® containing optical brighteners.

A second possible source of contamination of the system might have been the tergotometer itself. The nil sample of Figure 4.10 was washed without the addition of any fluorescently labelled polymer. Since the washing liquor of the nil sample showed fluorescence properties even before the addition of the fabric, it is possible that there was a low level of contaminants left from previous use of the tergotometer.

Any minor contamination is likely to play a significant role with such low concentrations of fluorescently labelled co-polymer and the initial results shown in Figure 4.10 would appear to suggest that a low level contamination of the system results in an increase in intensity which, masks completely any difference in fluorescence intensity due to the adsorption of fluorescently labelled polymer onto the cotton swatches. It is also possible that the amount of CMC-g-PEG* or unmodified CMC* adsorbed in one wash cycle at 0.3% of concentration is very low. However, a more detailed analysis would be necessary to effectively evaluate the amount of fluorescent material adsorbed. For these reasons the tests were repeated with higher concentrations of labelled co-polymer.

The set of samples listed in Table 4-4 were subsequently tested using a concentration of 0.5% of unmodified CMC* or CMC-g-PEG* during the wash cycle. This concentration was chosen to mimic the conditions adopted during the whiteness test and the results are summarised in Figure 4.11. Once again, only one measurement was made for each sample, thus it was not possible to determine the error associated with the measurements of fluorescence.

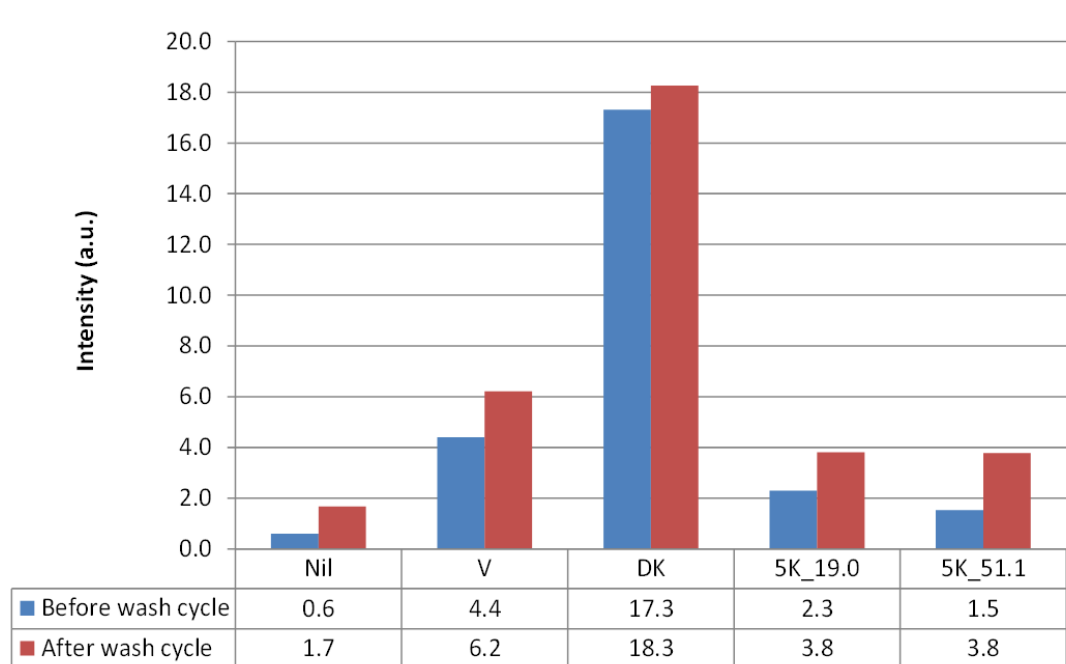


Figure 4.11. Fluorescence emission intensity of the wash liquor before and after wash cycle with 0.5% concentration of unmodified CMC* or CMC-g-PEG* copolymers.

The same problem of contamination appeared in this set of data. Indeed the wash liquor of the nil sample again is fluorescent even though no fluorescent material was used during the test. Furthermore, the intensity of the fluorescent signal for all the samples after the wash cycle is higher, while it should have been lower due to adsorption of CMC* material over the swatches surfaces. It would appear that contamination must be the cause of these results and that the origin of the contamination has two possible sources. Firstly it is possible that the swatches used possessed some residual of optical brighteners adsorbed over the surface and secondly the tergotometer used for the test was not perfectly clean.

The absolute value of intensity of the fluorescence signal in Figure 4.11 is higher than the absolute value observed for the previous washing conditions (Figure 4.10), since a higher concentration of fluorescent material was used. Therefore,

more CMC-g-PEG* or unmodified CMC* polymers were dissolved in the washing liquor.

Once more, it would appear that the level of contamination is enough to overpower any decrease in intensity of the fluorescence signal due to adsorption of the CMC-g-PEG* or unmodified CMC* polymers onto the cotton surface.

In light of the results above a third set of quantitative test was performed using the same set of polymers samples described in Table 4-4. The concentration of CMC-g-PEG* or unmodified CMC* added during the wash cycle was increased to 1%. The choice to use this concentration was also convenient since it reproduces the conditions adopted during the soil release test. The results are plotted in Figure 4.12.

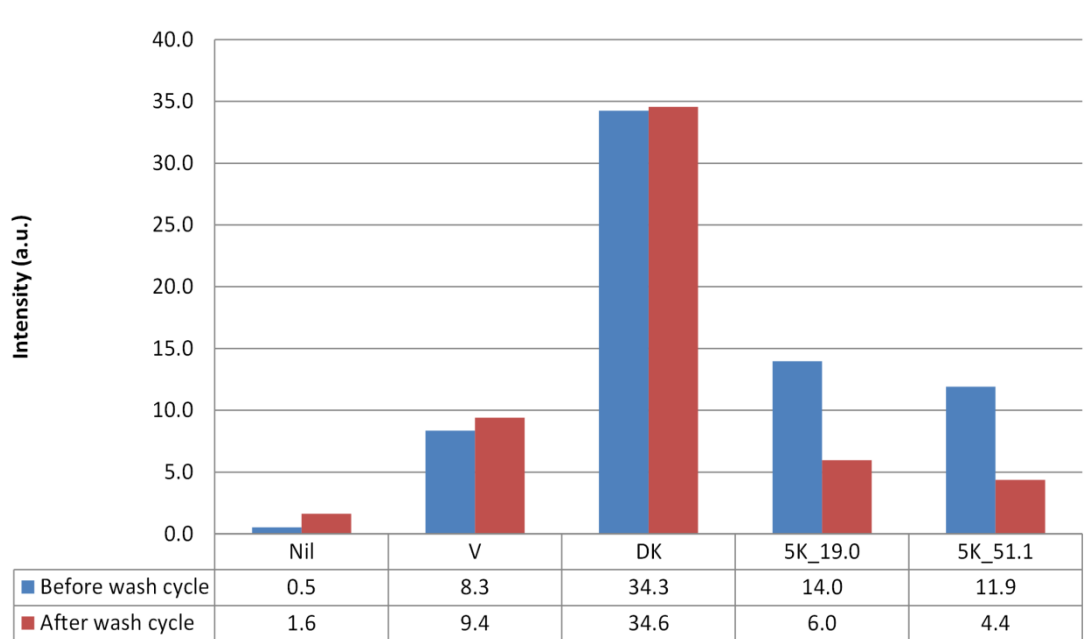


Figure 4.12. Fluorescence emission intensity of the wash liquor before and after wash cycle with 1% concentration of unmodified CMC* or CMC-g-PEG* copolymers.

The data shown in Figure 4.12 require careful interpretation and conclusions are tentative. Firstly the effect of the contamination on the fluorescence signal

can also be seen in this set of data. The intensity of the fluorescence signal of the wash liquor after the wash cycle seems to be slightly higher than before the cycle for the unmodified CMC* samples (V* and DK*). However, due to their ability to irreversibly adsorb over cotton surfaces, a significant drop in intensity was expected for the unmodified CMC* samples. The analysis of the washing liquor of the nil sample before and after the wash cycle suggests the presence of fluorescent material despite the fact that no fluorescently labelled polymer was added in that pot. It would appear that the pots containing the CMC-g-PEG* co-polymers samples were either not contaminated during the wash cycle, enabling a realistic and quantitative assessment of the impact of adsorption or that the higher concentration of CMC-g-PEG* allows the adsorption of enough fluorescent material to overcome or mask any contamination.

Ignoring any possible impact of contamination, the amount of co-polymer adsorbed over the surface of the fabric could be calculated according to Equation 3.

$$co - polymer\ adsorbed = \frac{mass\ fluorophore\ adsorbed}{degree\ of\ labelling\ x\ weight\ fabric}$$

Equation 3.

The mass of fluorophore can be determined by interpolation of the value of the fluorescence intensity observed for the washing liquor with a calibration curve based on fluorescence intensity of solutions of the fluorophore at known concentrations.

For the purpose of the calculation, the difference in fluorescence intensity of the washing liquor for the CMC-g-PEG* co-polymers observed in Figure 4.12 was assumed to be due to the adsorption of fluorescent material over the swatch surfaces, and the possibility of contamination is ignored. The cross-referencing of the values of fluorescence intensity of the wash liquor before and after the

wash cycle with the calibration curve (Figure 4.13), enabled the amount of fluorophore “depleted” from the washing liquor to be estimated as the difference between the amount of fluorophore present before and after the wash cycle in the washing liquor.

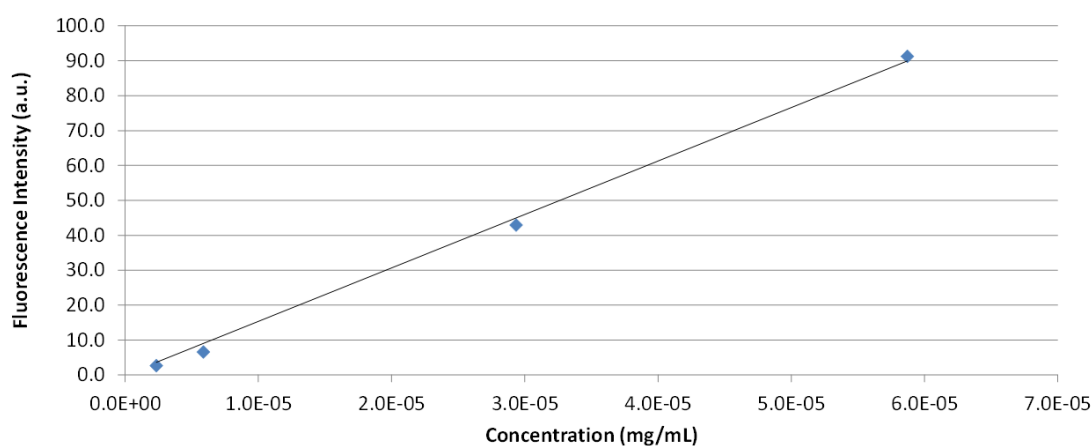


Figure 4.13. Calibration curve for DTAF fluorophore in water.

Then, the amount of CMC-g-PEG* co-polymers adsorbed over one wash cycle was calculated through Equation 3. The results are summarised in Table 4-5.

Table 4-5. Amount of CMC-g-PEG* co-polymer adsorbed in one wash cycle over cotton fabric.

Sample	Co-polymer adsorbed* (g co-polymer/g fabric)
CMC-g-PEG_5K_51.1*	7.5×10^{-6}
CMC-g-PEG_5K_19.0*	2.2×10^{-6}

* Value calculated through Equation 3.

The amount of co-polymer adsorbed per gram of fabric over one wash cycle is almost negligible. For this reason, it would be necessary to perform several prewashes in order to create a film of co-polymer adsorbed over the surface. Moreover, it must be repeated that these results are to be treated with caution

since contamination to the system may have occurred during the test. Furthermore, only one data set was collected per sample, so the confidence and accuracy of these results are low. More tests should be run in future, collecting more data in order to mitigate these problems.

4.4.2. Fluorescence microscopy

It should be possible to visualise the distribution of the CMC-g-PEG* co-polymers adsorbed over the fabric surface through the use of a fluorescence microscope. By illuminating the surface of the swatches with light at 495 nm, the presence of any fluorescently labelled SRP adsorbed onto the surface should be identified. This specific wavelength was chosen because it corresponds to the wavelength of maximum adsorption of the fluorophore DTAF used to label the CMC-g-PEG co-polymers. Any areas covered by the CMC-g-PEG* co-polymer will emit fluorescence in the green region, as the peak in emission of the fluorophore is at 516 nm.

Through images of the swatch surfaces it should be possible to investigate whether the distribution of the CMC-g-PEG* co-polymers is homogeneous or not. In the case of a homogenous distribution over the fabric surface, each single fibre will be coated with the co-polymer, hence one would expect uniform green fluorescence. On the other hand, if the distribution is not uniform, the use of a fluorescently labelled co-polymer will allow visualisation of the formation of deposits of SRP* between the yarns or the presence of clusters of CMC-g-PEG* over the surface.

Fluorescence microscope images of the swatch surfaces were taken after four wash cycles in the presence of 1% of CMC-g-PEG* in the formulation. The washing conditions adopted were the same as for the quantitative analysis of deposition and for the soil release tests. Four wash cycles were used in an

attempt to reproduce the results of the soil release tests. Moreover, from previously published studies it was discovered that the best coverage of the fabric surface occurs after four washes in the presence of SRP^[2].

Figure 4.14 shows the microscope images of the swatches surface.

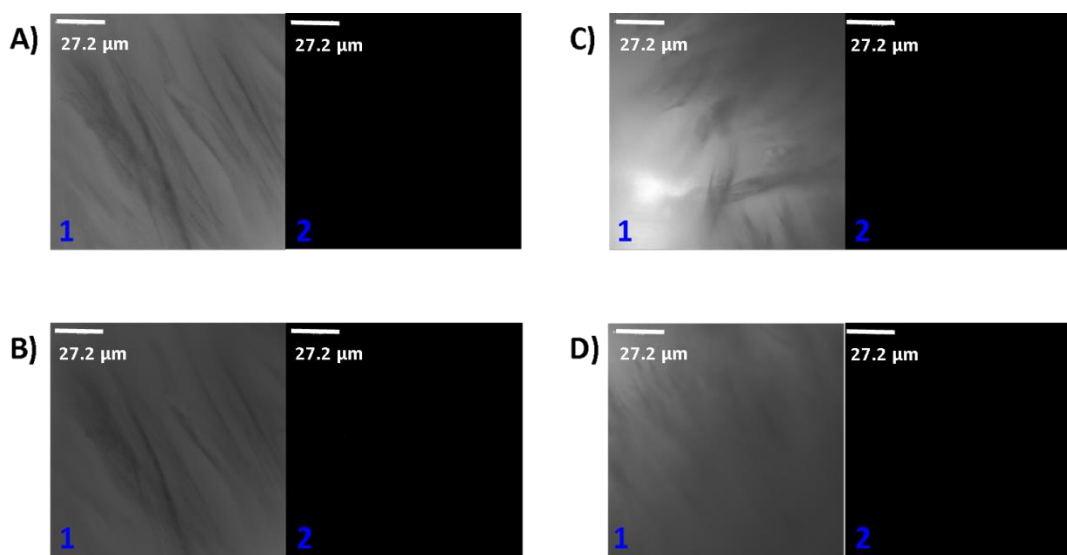


Figure 4.14. Microscope images of the swatches surfaces under transmitted light (1) and using a fluorescence filter (2). Scale Bar 27.2 μm . A) Finnifix V. B) Finnifix DK. C) CMC-g-PEG*_{5K_19.0}. D) CMC-g-PEG*_{5K_51.1}. $\lambda_{\text{ex}} = 495 \text{ nm}$, $\lambda_{\text{em}} = 516 \text{ nm}$.

One swatch of unbrightened cotton was analysed for each fluorescently labelled polymer investigated. The photos in Figure 4.14 marked with the number “1” show the surface of the fabric under transmitted light. It is possible to notice the weaving of the yarn of cotton (photo C1) and single fibres of cotton (especially from photo A1). The series of photos in Figure 4.14 marked with the number “2” show the fabric surface using a fluorescent filter. In stark contrast to our expectations none of the swatches analysed showed any evidence of fluorescence, suggesting that no labelled polymer was adsorbed onto the surface.

In an attempt to investigate the unexpected results of the fluorescence microscopy images of the swatches, a control experiment was conducted

reproducing the conditions of a wash cycle in the tergotometer. Finnifix V* was chosen as the material for this study, as it is known to irreversibly adsorb onto cotton surfaces^[11]. One single swatch of unbrightened cotton was added to a 250 mL beaker containing deionised water (100 mL) and a stock solution of Finnifix V* (0.5 mL, Figure 4.15, image on the left-hand side), prepared according to the procedure described in the experimental section for the soil release test (section 4.2.4.). The swatch was stirred at room temperature (21 °C) for 20 minutes. Then, the swatch was extracted from the solution, positioned under the UV lamp and exposed to UV radiation. Pictures of the swatch and of the “washing liquor” are shown in Figure 4.15.

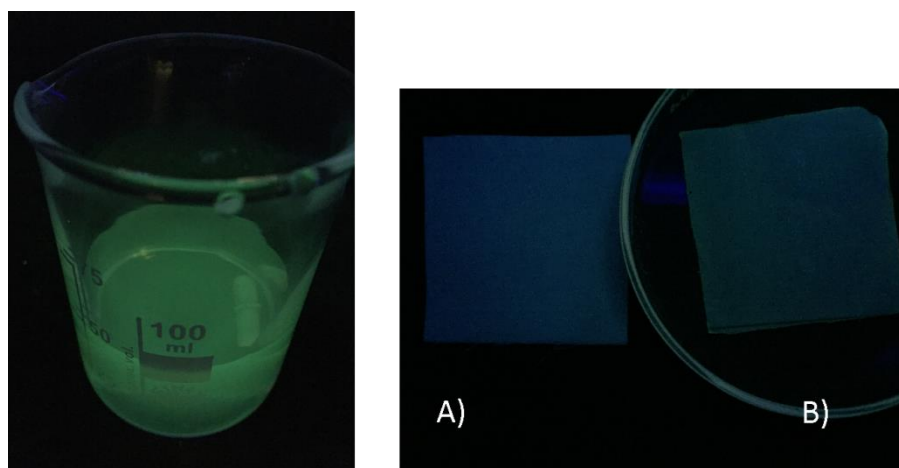


Figure 4.15. Image of a 0.02% w/v solution of Finnifix V* in deionised water (left, washing liquor of the control experiment) and comparison between a swatch of unbrightened cotton (A) and the swatch washed in the control experiment (B).

From Figure 4.15 it is clearly visible that the solution of Finnifix V* is fluorescent, and from a visual observation, the fluorescence signal seems to be very intense. Furthermore, through comparison between a swatch of unbrightened cotton (A) and the swatch washed in the presence of Finnifix V* (B) (image on the right hand-side of Figure 4.15) it is possible to notice that while the colour of the unbrightened cotton surface has a blue shade, the surface of the swatch B appears green. This difference in the colour of the

surface confirms that Finnifix V* should have been adsorbed over the surface of the unbrightened cotton swatches during the wash cycle in the tergotometer.

A possible explanation as to why the fluorescently labelled co-polymers and the unmodified CMC samples did not appear to adsorb during the test conducted in the tergotometer could be that upon rinsing of the fabric with fresh water (last stage of the wash cycle), the adsorbed CMC*/CMC-g-PEG* material is actually removed. During the control experiment, the swatch was not rinsed after the “wash cycle”, but simply shaken to remove the excess of water and dried in open air. Other works reported in the literature^[12] [ENREF_12](#) regarding the study of the adsorption of SRPs over textile surfaces omit the rinsing phase of the wash cycle. Thus it is possible that by exposing the swatch to fresh water and simultaneously stirring vigorously (as in the tergotometer), the newly adsorbed fluorescent polymer is removed, either by desorption or by mechanical action.

Alternatively, it is possible that the new formulation of TIDE® used for the study of fluorescence did not favour the adsorption of CMC and CMC derivatives onto cotton surfaces. Hoffmann et al.^[7] demonstrated that the amount of CMC adsorbed over cotton is related to the amount of surfactant in solution. If the concentration of surfactant is higher than the critical micellar concentration, the adsorption of CMC is promoted, because the CMC-surfactant aggregates formed in solution possess a higher affinity for cotton fibre than the CMC alone, thus they adsorb better on the surface. During the four wash cycles performed to allow the build-up of the SRP* layer over the swatches surface, it is possible that the amount of surfactant available in solution was below the critical micellar concentration, hence the unmodified CMC* and the CMC-g-PEG* co-polymers did not adsorb.

4.4.3. ^{13}C solid state NMR spectroscopy analysis

The presence (or otherwise) of CMC-g-PEG* co-polymers adsorbed onto the surface of the swatches was further investigated by ^{13}C solid state NMR spectroscopy. By targeting the ^{13}C signal of the PEG chains grafted to CMC backbone it should be possible to identify the presence of any SRP adsorbed onto cotton. If the co-polymer is adsorbed, from the solid state NMR spectrum of the surface it would be possible to identify a peak at 70.9 ppm, typical of the PEG chain and a weak and broad peak around 177.9 ppm typical of the carboxymethyl group of the CMC backbone. Moreover, it might be possible to identify any residual of surfactants adsorbed over the surface.

Figure 4.16 shows the results for the ^{13}C solid state NMR analysis.

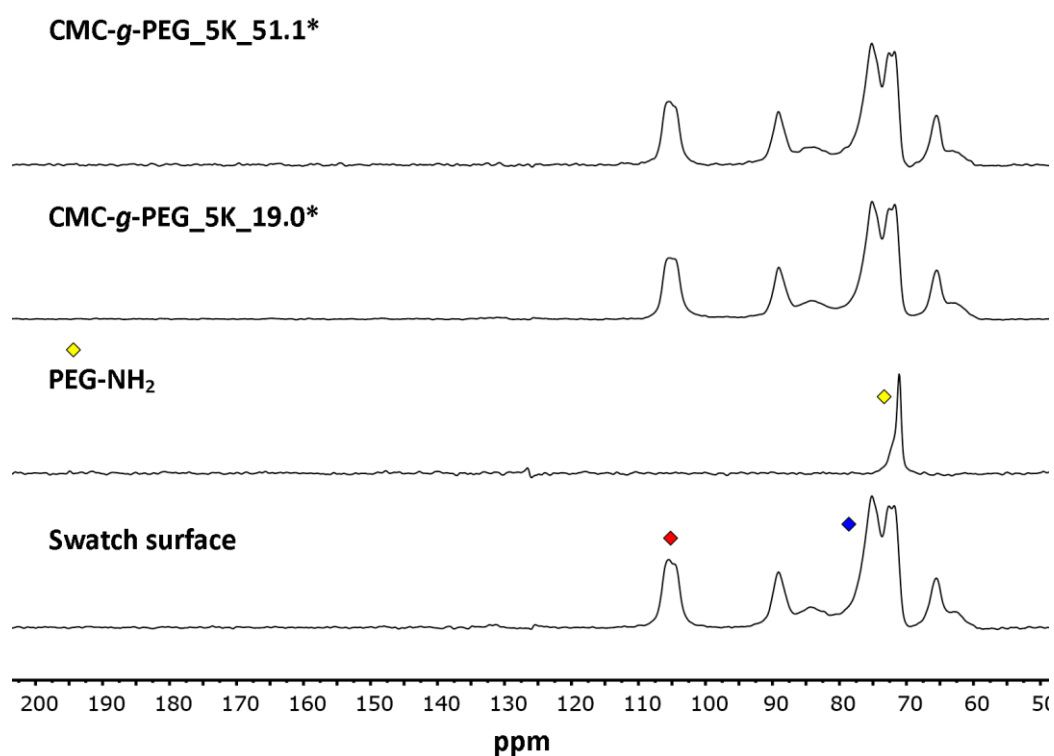


Figure 4.16. ^{13}C solid state NMR spectra of an unbrightened cotton swatch, PEGNH₂, a swatch treated with CMC-g-PEG_5K_19.0* and a swatch treated with CMC-g-PEG_5K_51.1*. Data recorded at 100 MHz in cross-polarization.

From Figure 4.16, it is possible to observe that the NMR spectrum of the swatch surface of unbrightened cotton prior to the wash cycles shows the signals of glucose, the repeating unit of cotton. It is possible to notice the resonance at δ 104 typical of the anomeric carbon (C1, red diamond) of a glucose unit and the signals between δ 70-80 typical of carbons that belong to a glucose unit (C2-C6, blue diamond).

The comparison of the spectra of swatches treated in presence of CMC-g-PEG_5K_19.0* and CMC-g-PEG_5K_51.1* with the spectrum of the untreated swatch seems to suggest that no CMC-g-PEG* co-polymer was adsorbed during the four wash cycles, as the signal of the repeating unit of the PEG chain grafted to the CMC backbone at δ 70.9 (yellow diamond) is missing. However, it is possible that the intensity of the resonance of the PEG chain (correlated with the presence of CMC-g-PEG* adsorbed) is either below the detection limit of the technique, or it is masked by the signal of the background in the same region.

4.5. Conclusions

In conclusion, the potential for application as SRP for cotton surfaces of the CMC-g-PEG copolymers synthesised in Chapter 3 was evaluated through soil release and whiteness tests.

The values of SRI evaluated through soil release test are affected by a very large error, as a consequence of the complexity of the tests performed and the variety of parameters that can impact the outcomes. The large statistical error causes an overall uncertainty in the SRI data, as demonstrated through the values of SRI measured for the unmodified CMC samples and the nil sample. The nil sample and the unmodified CMC analysed were expected to give the same value (within error) of SRP at each repetition of the test. However, the value of SRI for these samples varied each time, proving that the protocol followed for the evaluation of the soil release properties is inconsistent. As a consequence of the large error associated with the SRI data it is not possible to draw any substantial conclusions correlating the amount and M_n of the PEG grafted with the performance as SRP. Of the samples tested, only two (sample 2K_56.1 and sample 5K_51.1) showed a significant improvement upon removal of lard stain compared to Finnifix V, perhaps due to the high percentage of bound PEG present in these co-polymers. On the contrary, the comparison with sample BDA shows that none of the samples tested seemed to improve the removal of lard stain.

The results of the CEI whiteness test showed that the co-polymers seem to act more like “soil magnets” for carbon black dispersed in solution, probably due to interactions between the functional groups on the surface of carbon black particles and the PEG chain.

The preliminary fluorescence spectroscopy investigations on the adsorption of the CMC-g-PEG co-polymers were rather inconclusive and highly affected by

possible contamination. No fluorescence was observed from the fluorescence microscopy images of the swatches surfaces treated in the tergotometer, thus it would appear that no fluorescent CMC/CMC-g-PEG material was adsorbed. In contrast, the control experiment (conducted under the same conditions) demonstrated that the unmodified Finnifix V* sample adsorbs over cotton, as expected from the literature.^[11] A possible reason for the unexpected behaviour of CMC noted during the tests performed in the tergotometer could be the desorption (or mechanical removal) of any adsorbed fluorescent material during the rinsing cycle, as this stage of the wash cycle was not performed during the control experiment. The ¹³C solid state NMR technique did not allow to demonstrate the presence of any PEG adsorbed nor its absence.

4.6. References

1. Lang, F. P.; Morschhauser, R. *SOWT-Journal* **2006**, 132, 24-34.
2. Lang, F. P. *Chimica Oggi* **1998**, 16, (9).
3. O'Lenick, A. J. J. *Journal of Surfactants and Detergents* **1999**, 2, (4), 553-557.
4. Calvimontes, A.; Dutschk, V.; Koch, H.; Voit, B. *Tenside Surfactants Detergents* **2005**, 42, (4), 210-216.
5. Lant, N. Laundry composition. patent number EP2135933A1, 2009.
6. Kaurav, M. S., *Engineering Chemistry with Laboratory Experiments*. PHI Learning; 2011.
7. Hoffmann, I.; Theile, M.; Gratz, S.; Scholz, J.; Barreleiro, P.; Von Rybinski, W.; Gradzielski, M. *Langmuir : the ACS Journal of Surfaces and Colloids* **2012**, 28, (31), 11400-11409.
8. Johnson, G. A.; Lewis, K. E. *Journal of Applied Chemistry* **1967**, 17, 283-287.
9. Arico, A. S.; Antonucci, V.; Minutoli, M.; Giordano, N. *Carbon* **1989**, 27, (3), 337-347.
10. Blum, F. D. *Colloid-Polymer Interactions* **1999**, 207-223.
11. Kargl, R.; Mohan, T.; Bracic, M.; Kulterer, M.; Doliska, A.; Stana-Kleinschek, K.; Ribitsch, V. *Langmuir: The ACS Journal of Surface and Colloids* **2012**, 28, (31), 11440-11447.
12. Hasan, B. M. M.; Calvimontes, A.; Dutschk, V. *Journal of Surfactants and Detergents* **2009**, 12, (4), 285-294.

5

Conclusions and future works

5.1. Conclusions

In this thesis, the synthesis of functional carbohydrate-based materials with potential applications as soil release polymers for cellulosic surfaces was investigated. The synthetic strategies proposed took advantage of the affinity of polysaccharides for cellulosic surfaces and applied it to the modification of cotton textile in order to increase the removal of stains at low temperatures (below 30 °C).

In chapter 2, the synthesis of a co-polymer between PEGDA-ethylenediamine-maltose with the potential application as SRP for cotton fibres was achieved in a three step process.

The first stage of the procedure involved the reaction between PEGDA and N-Boc-ethylenediamine via step growth polymerisation to yield a poly(β -amino ester) co-polymer. Due to the high cost of the amine monomer, a model reaction

with the cheaper hexylamine was conducted to investigate the best conditions for the polymerisation. The polymerisations conducted in the presence of solvent resulted in a higher DP_n in a shorter time than the reaction in bulk. Of the solvent tested, DCM seemed to favour the step growth polymerisation possibly due to an enhanced solubility of the hexylamine in a non-polar solvent.

Despite the results obtained from the model polymerisation of PEGDA with hexylamine, the polymerisation of PEGDA and N-Boc-ethylenediamine conducted in the same reaction conditions did not achieve similar results, likely due to the difficulties in weighing small amounts of material very accurately. Therefore, in an attempt to synthesise the co-polymer backbone, the polymerisation of PEGDA and N-Boc-ethylenediamine was conducted in bulk. The poly(β -amino ester) synthesised in bulk from PEGDA M_n 700 g/mol and N-Boc-ethylenediamine resulted in a M_n of 8500 g/mol and DP_n 10-11, and this material was carried forward to the next steps toward the synthesis of a potential SRP.

The second step of the synthetic procedure involved the de-protection of the second amine functionality of N-Boc-ethylenediamine using TFA in DCM. Prior to de-protection, any remaining acrylate groups of the poly(β -amino ester) were end-capped with N-Boc-ethylenediamine to avoid possible cross-links between co-polymers chains upon de-protection.

The successfully de-protected poly(β -amino ester) was then reacted with maltose via a reductive amination reaction to yield the co-polymer PEGDA-ethylenediamine-maltose of Figure 2.3. The final structure of the co-polymer was confirmed via 1H , ^{13}C , and DOSY NMR spectroscopy.

Due to the synthetic procedure involving too many steps, the co-polymer was not considered commercially viable for a SRP. However, it was proved that the material could be prepared and the synthetic strategy described could

potentially be applied toward the synthesis of functionalised amphiphilic co-polymers.

In chapter 3, PEG chains were successfully grafted onto the CMC backbone via amidation reaction (PEGylation) in DMF to yield CMC-g-PEG co-polymers for application as potential soil release polymers (SRPs) for cotton surfaces.

Prior to reaction, a variety of PEG-NH₂ (M_n 2000 g/mol, M_n 5000 g/mol and M_n 10000 g/mol) were synthesised following a literature procedure^[1], and the structure of the CMC starting material was confirmed through ¹³C solid state NMR. Moreover, the proportion of carboxymethyl groups per glucose unit (DS) of CMC, evaluated via potentiometric titration, was found to be in agreement with the value given by the supplier.

The PEGylation reaction of the CMC appeared to be influenced by steric hindrance, as a result of the PEG chain. To overcome the limited accessibility of the terminal amino group of PEG in solution, the reaction was allowed to proceed for a long time. High weight percentages of PEG bound were achieved, although the target value was never actually met.

The synthesised co-polymers were characterised through ¹³C solid state NMR, ¹H gel state NMR, SEC in DMF and PFG NMR, because the most common techniques used to characterise polysaccharide-derivatives (e.g. solution NMR, IR and elemental analysis) could not be applied to these materials.

From ¹³C solid state NMR it was possible to confirm the structure of the co-polymers. The strong peak at δ 70.9 proved the presence of PEG chain in the sample, while the presence of a new signal at δ 171.7 in the carbonyl region proved the formation of an amide bond. However, it was not possible to determine the actual amount of PEG bound to the CMC backbone from these data.

Hence, the weight percentage of PEG bound was evaluated through the combined used SEC data and ^1H gel state NMR spectrum. Through SEC in DMF, the concentration of unbound PEG present in the mixture was estimated from the area underneath the concentration curve, using a triple detector calibration. The total amount of PEG in the co-polymers (bound and unbound) was evaluated through ^1H gel state NMR spectroscopy. A calibration profile was built, correlating the peak integrals of the protons of the PEG chain with the amount of PEG present in the gel. Then, the peak integrals of the PEG in the CMC-g-PEG spectra were cross-referenced with the calibration profile to obtain the total concentration of PEG. By subtracting the proportion of PEG unbound to the total amount of PEG in each sample, the weight percentage of bound PEG was evaluated.

The relative proportions of bound and unbound PEG were also estimated via PFG NMR analysis. The self-diffusion behaviour of PEG is different when it is bound to the CMC backbone, and thus part of a large species, as opposed to when it is unbound, and thus free to diffuse without constrictions. From the decay curves obtained for the CMC-g-PEG co-polymers it was possible to confirm that all the samples synthesised contained a proportion of PEG bound to CMC backbone. Furthermore, the proportion of PEG unbound evaluated from PFG NMR was higher than the values measured via SEC for most of the samples. It is possible that the differences between the techniques are related to the faster self-diffusion of the PEG chain end compared to the whole PEG chain bound to the CMC backbone, which led to an overestimation of the overall amount of PEG unbound.

In light of the potential application of these co-polymers as SRP for cotton surface, two CMC-g-PEG co-polymer and two different types of CMC were successfully labelled with DTAF to allow the study of their adsorption/desorption from cotton surface through fluorescence spectroscopy.

In chapter 4, the CMC-g-PEG copolymers synthesised and characterised in Chapter 3 were evaluated as potential SRPs for cotton surfaces through soil release and whiteness tests.

The industrial protocols followed for these tests (and described in the experimental section) seemed to be affected by several factors, which ultimately led to a very large error associated with the measurements of SRI (especially) and CEI, and to an overall uncertainty in the data. The nil sample and the unmodified CMC analysed were expected to give the same value (within error) of SRP/CEI whiteness at each repetition of the tests. However, at each analysis the values of SRI and CEI for these samples varied. Regarding the result of the soil release test for the CMC-g-PEG samples, the large error associated with the data does not allow us to draw any firm conclusions correlating the structure of the co-polymer (in particular the amount and M_n of the PEG grafted) with the performance as SRP. Among the co-polymers tested only sample 2K_56.1 and sample 5K_51.1 showed a significant improvement upon removal of lard stain compared to the unmodified CMC Finnifix V, possibly due to the high percentage of bound PEG. On the contrary, none of the samples tested seemed to show any improvement of the removal of lard stain when compared with sample BDA, the unmodified CMC currently used in laundry detergent formulations.

From the results of the CEI whiteness tests, it would appear that the co-polymers act more like “soil magnets” for carbon black dispersed in solution, probably due to interactions between the functional groups on the surface of carbon black particles and the PEG chain.

The fluorescence spectroscopy investigations on the adsorption of the CMC-g-PEG co-polymers were rather inconclusive and highly affected by possible contamination. The fluorescence microscopy images of the swatches surfaces (treated in the tergotometer) seemed to suggest that no fluorescent CMC/CMC-g-PEG material was adsorbed, while the control experiment conducted under

the same conditions proved that at least the unmodified Finnifix V* sample should adsorb over cotton. A tentative explanation of this unexpected behaviour could be the desorption (or mechanical removal) of any adsorbed fluorescent material during the rinsing cycle, as the omission of this stage in the control experiment resulted in a fluorescence surface. The ^{13}C solid state NMR spectra did not prove the presence or absence of any PEG adsorbed over the surface of the swatches treated in the tergotometer.

5.2. Future Work

Possible future work could be outlined for the development of a soil release polymer for cellulosic surfaces based on the two approaches discussed in this thesis.

Regarding the potential SRP comprising PEGDA, ethylenediamine and maltose, future works could involve the synthesis of a library of compounds based on the synthetic procedure described. Indeed, by changing the length of both the PEG chain and the sugar moiety it should be possible to modulate the interaction of this new class of potential SRP with cotton fabrics to achieve a reversible adsorption/desorption. The use of long polysaccharide chains, as previously reported in the literature^[2], should ensure the adsorption of the potential SRP onto cellulosic surfaces. Polysaccharides with linear as well as branched structures may be worth investigating, as their potential for interaction with cellulosic surfaces has previously been proven^[3].

Upon synthesis, the stability of these potential SRPs in the washing conditions (pH, temperature, laundry detergent composition) will be investigated, as well as their life-shelf and their eco-toxicity in light of possible commercial applications.

The synthesis of a series of CMC-g-PEG co-polymers containing a variety of M_n of PEG and weight percentages of PEG bound could be investigated in the future, to evaluate the impact of the length of the PEG chain and the amount of PEG grafted upon the adsorption process.

The CMC-g-PEG co-polymers structure could also be developed to target a specific class of stains. Indeed, the results of the whiteness tests (Chapter 4) showed that the presence of PEG chains grafted onto the CMC backbone led to the binding of carbon black particles dispersed in the washing liquor during the wash cycle. The use of block co-polymers comprising PEG and a hydrophobic

moiety could, for example, promote the affinity of the SRPs for lard-type of stains, and thus improving the anti-redeposition properties.

Furthermore, the protocols of analysis followed to evaluate the soil release properties of CMC-g-PEG samples and the adsorption of CMC-g-PEG over cotton surface probably need to be revised and improved, in order to enhance the reproducibility of the data and decrease the contamination, following to record consistent data. The suggestions outlined in Chapter 4 could be adopted. For example the use of a lower proportion of swatches per wash cycle, to prevent folding of the swatches and to promote the formation of a uniform layer of adsorbed SRP.

Ensuring that the viscosity of the stain does not change during the deposition phase of the soil release test as a consequence of a drop in the temperature, to allow for a better comparison of the performance of the SRPs; the use of high purity water while performing the wash cycle in the tergotometer instead of city water, to reduce the problems associated with the variability of the hardness of the water (as discussed in Chapter 4).

The improvement of the soil release testing protocol (and thus the whiteness test protocol) would ensure a more accurate measurement of the co-polymers ability as SRPs. Furthermore, it would allow the identification of the key co-polymer properties, the knowledge of which is vital for the design of new SRPs.

5.3. References

1. Agostini, S.; Hutchings, L. R. *European Polymer Journal* **2013**, 49, (9), 2769-2784.
2. Kamel, S. *eXPRESS Polymer Letters* **2008**, 2, (11), 758-778.
3. Stiernstedt, J.; Brumer III, H.; Zhou, Q.; Teeri, T. T.; Rutland, M. W. *Biomacromolecules* **2006**, 7, 2147-2153.